Optosensor Based on Nanocomposite Sensing Probes and Composite Adsorbents for the Determination of Trace Organic Compounds in Foods and Beverages

Naphatsakorn Orachorn

A Thesis Submitted in Partial Fulfillment of the Requirements for the Degree of Doctor of Philosophy in Chemistry (International Program)
Prince of Songkla University
2023

Optosensor Based on Nanocomposite Sensing Probes and Composite Adsorbents for the Determination of Trace Organic Compounds in Foods and Beverages

Naphatsakorn Orachorn

A Thesis Submitted in Partial Fulfillment of the Requirements for the Degree of Doctor of Philosophy in Chemistry (International Program)
Prince of Songkla University
2023

Thesis Title	Optosensor Based on Nanocomposite Sensing Probes and Composite Adsorbents for the Determination of Trace Organic Compounds in Foods and Beverages
Author	Miss Naphatsakorn Orachorn
Major Program	Chemistry (International Program)

Major Advisor

……
(Assoc. Prof. Dr. Opas Bunkoed)

Examining Committee:

……..……...Chairperson
(Asst. Prof. Dr. Piyaluk Nurerk)

……..…….Committee
(Assoc. Prof. Dr. Opas Bunkoed)

……..…….Committee
(Assoc. Prof. Dr. Warakorn Limbut)

……..…….Committee
(Asst. Prof. Dr. Nararak Leesakul)

……..…….Committee
(Asst. Prof. Dr. Apichai Phonchai)

……..…….Committee
(Assoc. Prof. Dr. Pongsaton Amornpitoksuk)

The Graduate School, Prince of Songkla University, has approved this thesis as partial fulfillment of the requirements for the Doctor of Philosophy Degree in Chemistry (International Program)

……..……
(Asst. Prof. Dr. Thakerng Wongsirichot)
Acting Dean of Graduate School

This is to certify that the work here submitted is the result of the candidate's own investigations. Due acknowledgement has been made of any assistance received.

……..……..……Signature
(Assoc. Prof. Dr. Opas Bunkoed)
Major Advisor

……..……..……Signature
(Miss Naphatsakorn Orachorn)
Candidate

I hereby certify that this work has not been accepted in substance for any degree, and is not being currently submitted in candidature for any degree.

……..……..……Signature
(Miss Naphatsakorn Orachorn)
Candidate

ชื่อวิทยานิพนธ์ เซนเซอร์ทางแสงโดยใช้ตัวตรวจวัดนาโนคอมโพสิทและตัวดูดซับคอมโพสิทสำหรับการวิเคราะห์สารอินทรีย์ปริมาณน้อยในอาหารและเครื่องดื่ม

ผู้เขียน นางสาวนภัสกร อรชร

สาขาวิชา เคมี (นานาชาติ)

ปีการศึกษา 2565

บทคัดย่อ

วิทยานิพนธ์นี้มีวัตถุประสงค์เพื่อพัฒนาเซนเซอร์ทางแสงโดยใช้ตัวตรวจวัดคอมโพสิทและตัวดูดซับคอมโพสิทสำหรับตรวจวิเคราะห์สารอินทรีย์ปริมาณน้อยในตัวอย่างอาหารและเครื่องดื่ม ซึ่งประกอบด้วย 2 ส่วนคือ เซนเซอร์ทางแสง และเทคนิคการเตรียมตัวอย่าง โดยแบ่งออกเป็น 4 งานวิจัยย่อย

ส่วนแรกเป็นการพัฒนาเซนเซอร์ทางแสงโดยใช้ตัวตรวจวัดนาโนคอมโพสิท โดยวัดสัญญาณฟลูออเรสเซนต์ที่ลดลงของพอลิเมอร์ลอกแบบโมเลกุลคอมโพสิทร่วมกับควอนตัมดอทสำหรับตรวจวิเคราะห์สารอินทรีย์ ได้แก่ โลมีฟล็อกซาซิน เมฟีไนด์ และซัลฟิโซซาโซล โดยสังเคราะห์พอลิเมอร์ลอกแบบโมเลกุลผ่านกระบวนการโซลเจลพอลิเมอไรเซชัน โดยใช้สารที่ต้องการวิเคราะห์เป็นโมเลกุลแม่แบบ 3-อะมิโนโพรพิลไตรเอทอกซีไซเลนเป็นมอนอเมอร์ และเตตระเอทิลออร์โธซิลิเกตเป็นสารเชื่อมขวาง หลังจากกำจัดโมเลกุลแม่แบบออกจากชั้นพอลิเมอร์ทำให้เกิดช่องการจดจำที่จำเพาะเจาะจงต่อสารที่ต้องการวิเคราะห์ทั้งหมู่ฟังก์ชัน รูปร่าง และขนาด ในงานวิจัยแรกเป็นการพัฒนาตัวตรวจวัดทางแสงฟลูออเรสเซนต์ที่ประกอบด้วยพอลิเมอร์ลอกแบบโมเลกุลที่มีความจำเพาะเจาะจง แคดเมียมเทลลูไรด์ควอนตัมดอทที่มีความไววิเคราะห์สูง และพอลิอะนิลีนร่วมกับแกรฟีนออกไซด์ที่มีประสิทธิภาพในการจับกับสารโลมีฟล็อกซาซิน สัญญาณฟลูออเรสเซนต์ของตัวตรวจวัดทางแสงที่พัฒนาขึ้นลดลงเมื่อความเข้มข้นของโลมีฟล็อกซาซินเพิ่มขึ้น ซึ่งให้ช่วงความเป็นเส้นตรงตั้งแต่ 0.10 ถึง 50.0 ไมโครกรัมต่อลิตร และมีขีดจำกัดการตรวจวัดเท่ากับ 0.07 ไมโครกรัมต่อลิตร เซนเซอร์ทางแสงที่พัฒนาขึ้นสามารถประยุกต์ใช้ในการตรวจวิเคราะห์โลมีฟล็อกซาซินในตัวอย่างนม เนื้อไก่ และไข่ โดยให้ค่าร้อยละการได้กลับคืนอยู่ในช่วง 81.5 ถึง 99.6 และมีค่าร้อยละเบี่ยงเบนมาตรฐานสัมพัทธ์ต่ำกว่า 7 งานวิจัยที่สองเป็นการพัฒนาตัวตรวจวัดทางแสงแม่เหล็กคอมโพสิทแบบคู่โดยการประยุกต์ใช้ควอนตัมดอทสองชนิดคือ แกรฟีนควอนตัมดอท และแคดเมียมเทลลูไรด์ควอนตัม

ดอทคอมโพสิทร่วมกับพอลิเมอร์ลอกแบบโมเลกุลแบบแม่เหล็กและวัสดุโครงข่ายโลหะอินทรีย์สำหรับการเพิ่มความเข้มข้นและตรวจวัดเมฟีไนด์และซัลฟิโซซาโซลได้ในเวลาเดียวกัน ซึ่งตัวตรวจวัดทางแสงแบบคู่นี้สามารถตรวจวัดสารที่ต้องการวิเคราะห์สองชนิดได้พร้อมกัน เนื่องจากตัวตรวจวัดให้สัญญาณการเปล่งแสงฟลูออเรสเซนต์แตกต่างกันที่ 435 และ 572 นาโนเมตร ภายใต้สภาวะที่เหมาะสมพบว่าสัญญาณฟลูออเรสเซนต์ของตัวตรวจวัดทางแสงลดลงเมื่อมีสารเมฟีไนด์และซัลฟิโซซาโซลเพิ่มขึ้น ให้ช่วงความเป็นเส้นตรงตั้งแต่ 0.10 ถึง 25.0 ไมโครกรัมต่อลิตร และขีดจำกัดการตรวจวัดเท่ากับ 0.10 ไมโครกรัมต่อลิตร ตัวตรวจวัดทางแสงที่พัฒนาขึ้นสามารถตรวจวัดเมฟีไนด์และซัลฟิโซซาโซลปริมาณน้อยในตัวอย่างนม โดยมีค่าร้อยละการได้กลับคืนอยู่ในช่วง 80.4 ถึง 97.9 และมีค่าร้อยละเบี่ยงเบนมาตรฐานสัมพัทธ์ต่ำกว่า 5 นอกจากนี้เมื่อนำเซนเซอร์ทางแสงที่พัฒนาขึ้นมาทดสอบเปรียบเทียบกับเทคนิคโครมาโทกราฟีของเหลวสมรรถนะสูง พบว่าผลการวิเคราะห์จากสองวิธีนี้มีความสอดคล้องกัน แต่เซนเซอร์ทางแสงให้ค่าความไววิเคราะห์ที่สูงกว่า แสดงว่าเซนเซอร์ทางแสงที่พัฒนาขึ้นเป็นวิธีที่มีความน่าเชื่อถือและมีประสิทธิภาพสำหรับการตรวจวิเคราะห์โลมีฟล็อกซาซิน เมฟีไนด์ และซัลฟิโซซาโซลปริมาณน้อยในตัวอย่างอาหารและเครื่องดื่ม นอกจากนี้เซนเซอร์ทางแสงที่พัฒนาขึ้นมีคุณสมบัติที่โดดเด่นคือ มีความจำเพาะเจาะจงต่อสารที่ต้องการวิเคราะห์ มีความไววิเคราะห์สูง สามารถสังเคราะห์ได้ง่าย ตรวจวิเคราะห์ได้รวดเร็ว ใช้งานง่าย และราคาถูก

ในส่วนที่สองเป็นการพัฒนาตัวดูดซับคอมโพสิทสำหรับการสกัดและเพิ่มความเข้มข้นสารอินทรีย์หลายชนิดพร้อมกัน ได้แก่ กลุ่มพทาเลตเอสเทอร์ และกลุ่มยาต้านอักเสบชนิดที่ไม่ใช่สเตียรอยด์ ร่วมกับการวิเคราะห์ด้วยเทคนิคทางด้านโครมาโทกราฟี งานวิจัยที่สามเป็นการพัฒนาตัวดูดซับคอมโพสิทแกรฟีนออกไซด์ วัสดุโครงข่ายโลหะอินทรีย์ และอนุภาคแม่เหล็กเคลือบด้วยซิลิกาที่กักอยู่ในเส้นใยอัลจิเนตไฮโดรเจลสำหรับสกัดเพิ่มความเข้มข้นและตรวจวิเคราะห์สารกลุ่มพทาเลตเอสเทอร์สี่ชนิด ได้แก่ ไดบิวทิลพทาเลต บิส(2-เอทิลเฮกซิล)พทาเลต เบนซิลบิวทิลพทาเลต และไดนอร์มอลออกทิลพทาเลต โดยอัลจิเนตไฮโดรเจลถูกนำมาใช้เป็นวัสดุหลักในการสังเคราะห์ตัวดูดซับ เนื่องจากมีข้อดีคือ ไม่เป็นพิษ ย่อยสลายได้ง่าย ออกแบบรูปทรงได้หลากหลาย และสามารถคอมโพสิทกับวัสดุดูดซับอื่นๆได้ง่าย แกรฟีนออกไซด์และวัสดุโครงข่ายโลหะอินทรีย์สามารถดูดซับสารกลุ่มพทาเลตเอสเทอร์ได้ด้วยพันธะไฮโดรเจน อันตรกิริยาแบบไฮโดรโฟบิค และอันตรกิริยาแบบ π-π นอกจากนี้อนุภาคแม่เหล็กเคลือบด้วยซิลิกาที่กักอยู่ในเส้นใยไฮโดรเจลช่วยให้สามารถแยกตัวดูดซับออกจากสารละลายตัวอย่างได้อย่างรวดเร็วโดยการใช้แท่งแม่เหล็กภายนอก ตัวดูดซับคอมโพสิทเส้น

ใยอัลจิเนตไฮโดรเจลที่ประยุกต์ใช้สำหรับสกัดสารกลุ่มพทาเลตเอสเทอร์ และตรวจวิเคราะห์ด้วยเทคนิคโครมาโทกราฟีของเหลวสมรรถนะสูง ให้ช่วงความเป็นเส้นตรงตั้งแต่ 5.0 ถึง 250.0 ไมโครกรัมต่อลิตร สำหรับบิส(2-เอทิลเฮกซิล)พทาเลตและไดนอร์มอลออกทิลพทาเลต และ 3.0 ถึง 250.0 ไมโครกรัมต่อลิตร สำหรับเบนซิลบิวทิลพทาเลตและไดบิวทิลพทาเลต มีขีดจำกัดการตรวจวัดอยู่ในช่วง 3.0 ถึง 5.0 ไมโครกรัมต่อลิตร วิธีที่พัฒนาขึ้นสามารถประยุกต์ใช้สำหรับสกัดและตรวจวิเคราะห์สารกลุ่มพทาเลตเอสเทอร์ในตัวอย่างชา น้ำ และน้ำผลไม้ โดยให้ค่าร้อยละการได้กลับคืนที่ยอมรับได้อยู่ในช่วง 80.7 ถึง 89.9 และมีค่าร้อยละเบี่ยงเบนมาตรฐานสัมพัทธ์ต่ำกว่า 8 นอกจากนี้ตัวดูดซับคอมโพสิทไฮโดรเจลมีเสถียรภาพที่ดี ซึ่งสามารถนำกลับมาใช้ซ้ำได้ถึง 16 ครั้ง งานวิจัยที่สี่เป็นการพัฒนาตัวดูดซับคอมโพสิทที่ประกอบด้วยแกรฟีนควอนตัมดอท อนุภาคแม่เหล็กเคลือบด้วยซิลิกา คาร์บอนรูพรุนระดับเมโซ และพอลิเมอร์ลอกแบบโมเลกุล สำหรับสกัด เพิ่มความเข้มข้นและตรวจวิเคราะห์สารกลุ่มยาต้านอักเสบชนิดที่ไม่ใช่สเตียรอยด์สามชนิด พอลิเมอร์ลอกแบบโมเลกุลสามารถเพิ่มความจำเพาะเจาะจงของตัวดูดซับได้ เนื่องจากมีช่องการจดจำที่จำเพาะเจาะจงต่อสารที่ต้องการวิเคราะห์ นอกจากนี้แกรฟีนควอนตัมดอทและคาร์บอนรูพรุนระดับเมโซช่วยเพิ่มประสิทธิภาพในการดูดซับระหว่างตัวดูดซับคอมโพสิทและสารกลุ่มยาต้านอักเสบชนิดที่ไม่ใช่สเตียรอยด์โดยเกิดอันตรกิริยาแบบ π-π อันตรกิริยาแบบไฮโดรโฟบิค และพันธะไฮโดรเจน หลังจากสกัดด้วยตัวดูดซับคอมโพสิทที่พัฒนาขึ้นได้วิเคราะห์ยาต้านอักเสบชนิดที่ไม่ใช่สเตียรอยด์ด้วยเทคนิคโครมาโทกราฟีของเหลวสมรรถนะสูง ภายใต้สภาวะการสกัดที่เหมาะสมให้ช่วงความเป็นเส้นตรงตั้งแต่ 0.5 ถึง 100.0 ไมโครกรัมต่อลิตรสำหรับไดฟลูนิซอลและเมเฟนามิค แอซิด และ 1.0 ถึง 100.0 ไมโครกรัมต่อลิตรสำหรับเฟอร์บิโพรเฟน และมีขีดจำกัดการตรวจวัดอยู่ในช่วง 0.5 ถึง 1.0 ไมโครกรัมต่อลิตร ตัวดูดซับคอมโพสิทที่พัฒนาขึ้นสามารถนำไปประยุกต์ใช้สำหรับสกัดสารกลุ่มยาต้านอักเสบชนิดที่ไม่ใช่สเตียรอยด์ในตัวอย่างนม โดยให้ค่าร้อยละการได้กลับคืนที่ยอมรับได้อยู่ในช่วง 81.4 ถึง 93.7 และมีค่าร้อยละเบี่ยงเบนมาตรฐานสัมพัทธ์ต่ำกว่า 7 นอกจากนี้ตัวดูดซับคอมโพสิทที่พัฒนาขึ้นสามารถนำกลับมาใช้ในการสกัดซ้ำอย่างมีประสิทธิภาพได้ถึง 6 ครั้ง ข้อดีที่โดดเด่นของตัวดูดซับคอมโพสิทที่พัฒนาขึ้นเหล่านี้คือ มีประสิทธิภาพในการสกัดสูง สามารถเตรียมได้ง่าย ใช้ปริมาณตัวทำละลายอินทรีย์น้อย และมีความสามารถในการทำซ้ำและใช้ซ้ำที่ดี

โดยสรุปผลการศึกษาแสดงให้เห็นว่าเซนเซอร์ทางแสงและเทคนิคการเตรียมตัวอย่างที่พัฒนาขึ้นในวิทยานิพนธ์นี้สามารถนำไปประยุกต์ใช้สำหรับตรวจวิเคราะห์สารอินทรีย์ปริมาณน้อยใน

อาหารและเครื่องดื่มได้อย่างมีประสิทธิภาพ วิธีที่พัฒนาขึ้นมีข้อดีคือ สังเคราะห์ได้ง่าย มีความไว วิเคราะห์และความจำเพาะเจาะจงสูง ความเป็นพิษน้อย ใช้งานง่ายและราคาถูก ซึ่งสามารถนำไปปรับใช้เป็นกลยุทธ์ทางเลือกสำหรับตรวจวิเคราะห์สารอินทรีย์ชนิดอื่นในตัวอย่างที่มีความซับซ้อนต่างๆได้

Thesis Title Optosensor Based on Nanocomposite Sensing Probes and Composite Adsorbents for the Determination of Trace Organic Compounds in Foods and Beverages

Author Miss Naphatsakorn Orachorn

Major Program Chemistry (International Program)

Academic Year 2022

Abstract

This thesis aimed to develop optosensor using composite sensing probes and composite adsorbents for the determination of trace organic compounds in food and beverage samples. This thesis is composed of two parts including the optosensor and sample preparation method, which are divided into four sub-projects.

The first part focused on the development of optosensor using nanocomposite probes based on the fluorescence quenching of molecularly imprinted polymer (MIP) composited with quantum dots (QDs) for the detection of organic compounds including lomefloxacin, mafenide and sulfisoxazole. Molecularly imprinted polymer was synthesized via a sol-gel polymerization method consisting of template molecules (lomefloxacin, mafenide and sulfisoxazole), a functional monomer (3-aminopropyltriethoxysilane) and a cross-linker (tetraethyl orthosilicate). After template removal from MIP layer, the specific imprinted cavities are generated that are complementary to the templates in terms of functional groups, shape and size. For the first sub-project, the fabricated fluorescent probe combined the high selectivity of molecularly imprinted polymer, excellent sensitivity of cadmium telluride quantum dots (CdTe QDs) and high adsorption ability of polyaniline (PANI) and graphene oxide (GOx). The nanocomposite PANI-GOx-MIP-CdTe QDs probe was successfully fabricated and employed for the detection of lomefloxacin. The fluorescence emission of the developed fluorescent probe was linearly reduced with increasing concentrations of lomefloxacin from 0.10 to 50.0 μg L^{-1}, and the developed probe provided a low detection limit of 0.07 μg L^{-1}. The developed optosensor can be utilized to detect lomefloxacin in milk, chicken meat and egg samples, and the obtained recoveries ranged from 81.5 to 99.6% with relative standard deviations (RSDs) below 7%. For the second sub-project, dual magnetic composite fluorescent probes were developed and

fabricated by incorporating metal organic framework (MIL-101) with graphene quantum dots (GQDs) or cadmium telluride quantum dots into a magnetic molecularly imprinted polymer (MMIP) for the enrichment and simultaneous detection of mafenide and sulfisoxazole. The dual MIL101-MMIP-GQDs and MIL101-MMIP-CdTe QDs probes can detect mafenide and sulfisoxazole at the same time since their fluorescence emission intensities were different at 435 and 572 nm, respectively. Under optimal condition, the emission intensities of dual fluorescent probes were linearly decreased with increasing mafenide and sulfisoxazole concentrations ranging from 0.10 to 25.0 $\mu g\ L^{-1}$ with low detection limits of 0.10 $\mu g\ L^{-1}$. The developed dual probes successfully detected ultra-trace levels of mafenide and sulfisoxazole in milk with satisfactory recoveries of 80.4 to 97.9% and RSDs lower than 5%. In addition, the accuracy of these developed optosensors was confirmed by comparing with that of the high performance liquid chromatography (HPLC) technique. The analytical results produced by the developed optosensor not only agreed well with HPLC method but also exhibited superior sensitivity. The developed optosensor of both sub-projects is a reliable and effective method for the determination of trace lomefloxacin, mafenide and sulfisoxazole in food and beverage samples. The outstanding properties of the developed optosensor are high selectivity, good sensitivity, simple fabrication, short analysis time, uncomplicated measurement and cost-effectiveness.

The second part focused on the development of composite adsorbents for the simultaneous extraction and enrichment of multiple target compounds including phthalate esters and nonsteroidal anti-inflammatory drugs (NSAIDs) coupled with chromatographic analysis. For the third sub-project, a composite adsorbent of graphene oxide, metal organic framework and silica-modified magnetite (Fe_3O_4-SiO_2) incorporated into alginate hydrogel fiber was fabricated and utilized as dispersive magnetic solid-phase extraction (D-MSPE) adsorbent for the extraction, enrichment and determination of four phthalate esters including dibutyl phthalate (DBP), bis(2-ethylhexyl) phthalate (DEHP), benzyl butyl phthalate (BBP) and di-n-octyl phthalate (DNOP). Alginate hydrogel was employed as a non-toxic and biodegradable supporting material, which can be created in various shapes and readily entrap other composite materials. GOx and MIL-101 were utilized as the primary adsorption materials to adsorb phthalate esters through hydrogen bonding, hydrophobic and π-π interactions.

The Fe_3O_4-SiO_2 nanoparticles incorporated in hydrogel fiber facilitated rapid isolation of adsorbent from sample solution using an external magnet. The applied composite GOx/MIL-101/Fe_3O_4-SiO_2 alginate hydrogel fiber for the extraction of phthalate esters and quantitative analysis by HPLC method exhibited wide linear response in the range of 5.0 to 250.0 μg L^{-1} for DEHP and DNOP and 3.0 to 250.0 μg L^{-1} for BBP and DBP. The limit of detections were achieved in the range of 3.0 to 5.0 μg L^{-1}. The developed method was successfully utilized to extract and determine phthalate esters in tea, water and juice samples, and the acquired recoveries were satisfactory in the range of 80.7 to 89.9% with RSDs below 8%. In addition, the developed composite hydrogel adsorbent had excellent stability which can be reused up to 16 times. The fourth sub-project was a composite magnetic adsorbent of graphene quantum dots, silica-modified magnetite and mesoporous carbon (MPC) embedded into a molecularly imprinted polymer for the extraction of NSAIDs. The composite GQDs/Fe_3O_4-SiO_2/MPC/MIP adsorbent was successfully fabricated and applied as D-MSPE adsorbent for the extraction, enrichment and determination of three NSAIDs. The selectivity of the adsorbent can be enhanced with MIP, which produced specific imprinted cavities for NSAIDs. In addition, GQDs and MPC enabled increasing adsorption ability between the composite adsorbent and NSAIDs via π-π stacking, hydrophobic interaction and hydrogen bonding. The extracted NSAIDs were identified and determined by HPLC. Under optimal condition, the developed method exhibited good linearity with ranges of 0.5 to 100.0 μg L^{-1} for diflunisal and mefenamic acid and 1.0 to 100 μg L^{-1} for flurbiprofen. The limit of detections were acquired from 0.5 to 1.0 μg L^{-1}. The satisfactory recoveries of composite magnetic MIP adsorbent for NSAIDs extraction in milk samples were achieved from 81.4 to 93.7% with RSDs lower than 7%. Furthermore, the fabricated GQDs/Fe_3O_4-SiO_2/MPC/MIP adsorbent can be effectively used to extract NSAIDs up to 6 cycles. The distinctive advantages of the developed composite adsorbents are high extraction efficiency, simple preparation, low solvent consumption, good reproducibility and reusability.

In conclusion, the developed optosensor with composite fluorescent probes and the developed D-MSPE with composite adsorbents in this thesis were successfully applied for the determination of trace organic compounds in foods and

beverages with good analytical performances. The developed methods have numerous advantages including simple fabrication, good sensitivity, high selectivity, low toxicity, ease of use and cost-effectiveness. In addition, they can be adapted as alternative strategies for the determination of other organic compounds in a variety of complex samples.

Acknowledgements

The accomplishment of this thesis would be impossible without the assistance and support of many people. I desire to express my gratitude to those who have contributed to the achievement of this thesis:

I wish to express my sincere gratitude and appreciation to my advisor, Assoc. Prof. Dr. Opas Bunkoed for all of his support, assistance, suggestion and advice throughout the entire duration of this thesis. The acquired instruction and scientific spirit will be beneficial to my career in the future and my whole life.

I would like to thank the financial support from the Science Achievement Scholarship of Thailand (SAST), Center of Excellence for Innovation in Chemistry (PERCH-CIC), Graduate School, Division of Physical Science, Faculty of Science, Prince of Songkla University for the scholarship and research funding.

I would like to express my gratitude to the members of the Analytical Chemistry for Environmental and Food Safety (ACEFs) research group for their assistance, support and encouragement.

Finally, I would like to express my sincere gratitude and appreciation to my family and my dear friends for their love, encouragement, help and support throughout my life, especially my mother who is always beside me**.**

Naphatsakorn Orachorn

The Relevance of the Research Work to Thailand

The aim of this Doctor of Philosophy Thesis in Chemistry is to develop and increase the analytical performance of optosensor and sample preparation methods for the determination of trace organic compounds in foods and beverages. The developed optosensor is based on molecularly imprinted polymer composited with quantum dots, which exhibited excellent sensitivity, good selectivity, cost-effectiveness, ease and convenience of use. It can be employed for the determination of lomefloxacin, mafenide and sulfisoxazole in chicken meat, milk, and egg samples. The developed composite adsorbents used in the sample preparation procedure provided high extraction efficiency, simple operation, environmental friendliness and cost-effectiveness. They can be utilized for the extraction, enrichment and determination of phthalate esters and nonsteroidal anti-inflammatory drugs in beverage samples including mineral water, vitamin water, juice, tea and milk. Furthermore, both developed methods can be used as alternative strategies for the determination of multiple organic compounds in several government agencies and the private sector in Thailand.

Contents

Contents (Continued)

Contents (Continued)

List of Tables

List of Figures

List of Figures (Continued)

List of Abbreviations

AOAC	Association of Official Analytical Chemists
APTES	3-aminopropyltriethoxysilane
BBP	Benzyl butyl phthalate
CA	Cysteamine
CdS	Cadmium sulfide
CdSe	Cadmium selenide
CdTe QDs	Cadmium telluride quantum dots
DAD	Diode array detector
DBP	Dibutyl phthalate
DEHP	Bis(2-ethylhexyl) phthalate
D-MSPE	Dispersive magnetic solid-phase extraction
DNOP	Di-n-octyl phthalate
EU	European Union
Fe_3O_4	Magnetite
GOx	Graphene oxide
GQDs	Graphene quantum dots
GSH	Glutathione
HPLC	High performance liquid chromatography
ICH	International Conference of Harmonization
IF	Imprinting factor
InP	Indium phosphide
LLME	Liquid-liquid microextraction
LOD	Limit of detection
LOQ	Limit of quantification
MCL	Maximum contaminant level
MIL-101	Materials of Institute Lavoisier-101
MIP	Molecularly imprinted polymer
MMIP	Magnetic molecular imprinted polymer
MOF	Metal organic framework
MPA	Mercaptopropionic acid

List of Abbreviations (Continued)

MPC	Mesoporous carbon
MRLs	Maximum residue limits
MSA	Mercaptosuccinic acid
NIP	Non-imprinted polymer
NSAIDs	Nonsteroidal anti-inflammatory drugs
PAEs	Phthalate esters
PANI	Polyaniline
PbS	Lead sulfide
PbSe	Lead selenide
ppb	Parts per billion
QDs	Quantum dots
R^2	Coefficient of determination
RSD	Relative standard deviation
SBSE	Stir bar sorptive extraction
SEM	Scanning electron microscopy
SiO_2	Silica
SPE	Solid-phase extraction
SPME	Solid-phase microextraction
TEM	Transmission electron microscopy
TEOS	Tetraethyl orthosilicate
TGA	Thioglycolic acid
US EPA	United States Environmental Protection Agency
UV	Ultraviolet
ZnS	Zinc sulfide
ZnSe	Zinc selenide

List of Publications

This thesis is conducted in two parts comprising the optosensor based on molecularly imprinted polymer composited with quantum dots and the development of composite adsorbents for the determination of trace organic compounds in foods and beverages. Roman numerals in the text represent the order of publications.

Paper I **Orachorn, N.**, Bunkoed, O., A nanocomposite fluorescent probe of polyaniline, graphene oxide and quantum dots incorporated into highly selective polymer for lomefloxacin detection. ***Talanta*** 203 (2019), 261-268.

Paper II **Orachorn, N.**, Bunkoed, O., Nanohybrid magnetic composite optosensing probes for the enrichment and ultra-trace detection of mafenide and sulfisoxazole. ***Talanta*** 228 (2021), 122237.

Paper III **Orachorn, N.**, Klongklaew, P., Bunkoed, O., A composite of magnetic GOx@MOF incorporated in alginate hydrogel fiber adsorbent for the extraction of phthalate esters. ***Microchemical Journal*** 171 (2021), 106827.

Paper IV **Orachorn, N.**, Bunkoed, O., A composite adsorbent of graphene quantum dots, mesoporous carbon, and molecularly imprinted polymer to extract nonsteroidal anti-inflammatory drugs in milk. ***Microchimica Acta*** 189(12) (2022), 446.

Reprints were made with permission from the publisher

Paper I

Reprinted with permission of Elsevier

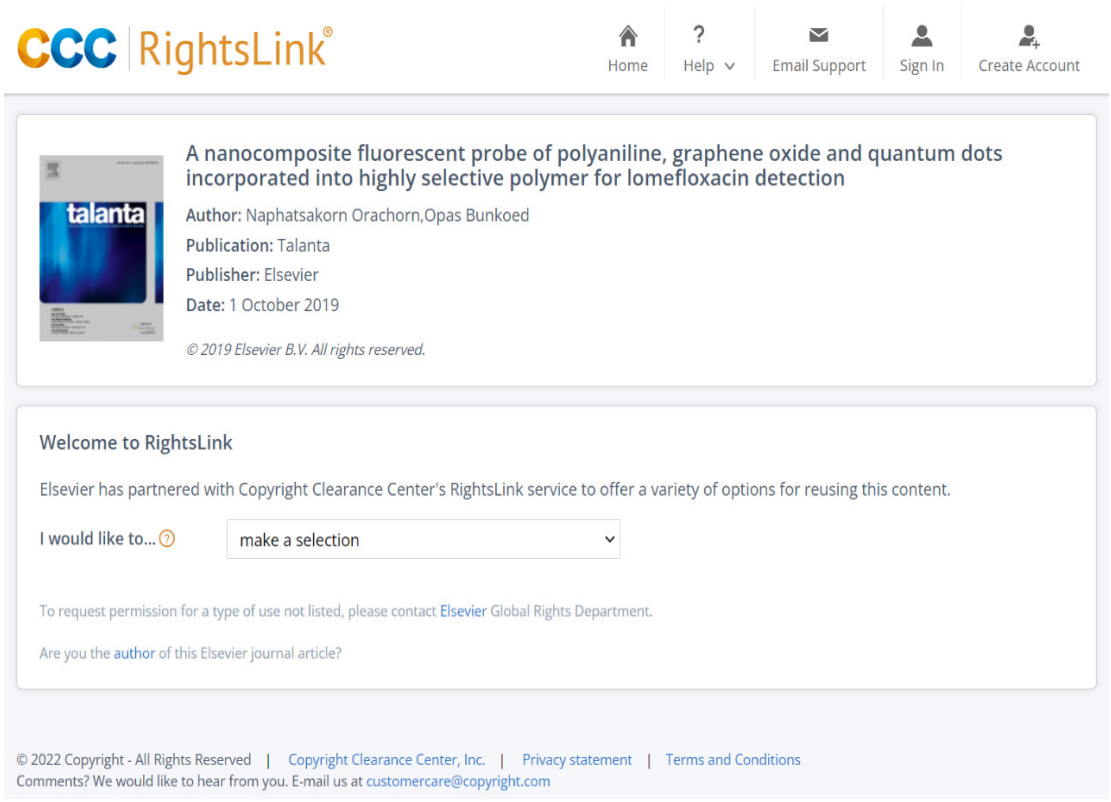

Paper II

Reprinted with permission of Elsevier

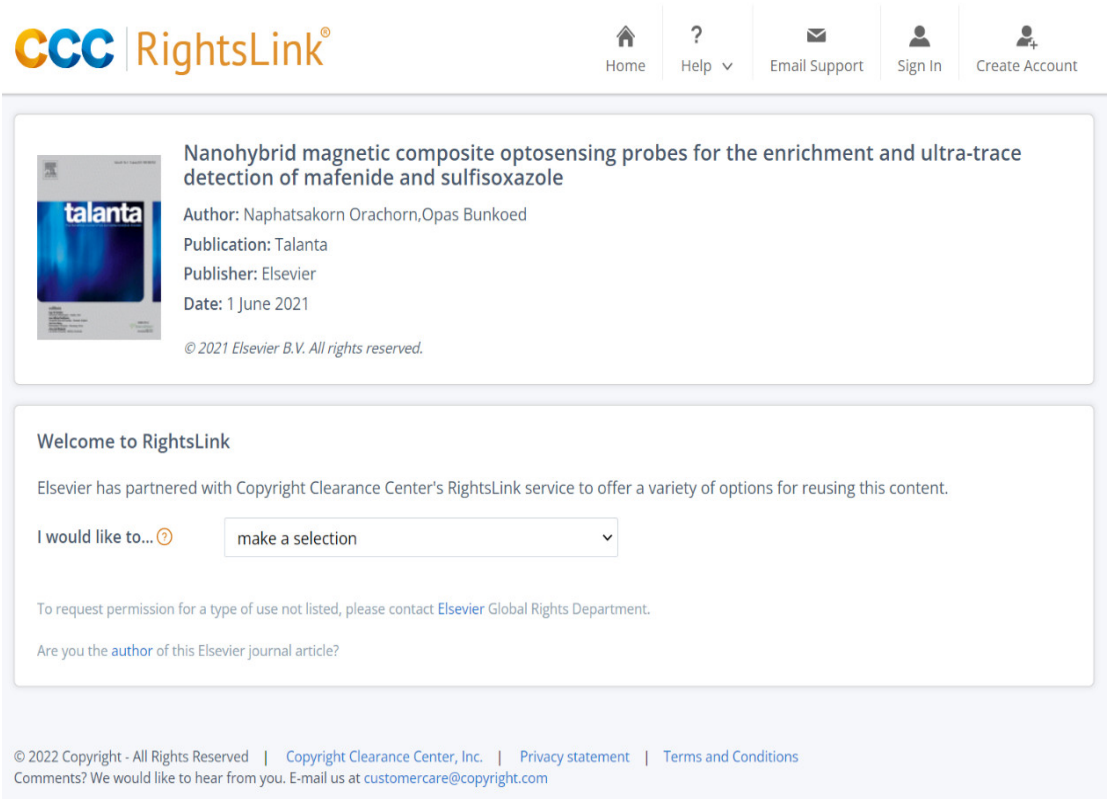

Paper III

Reprinted with permission of Elsevier

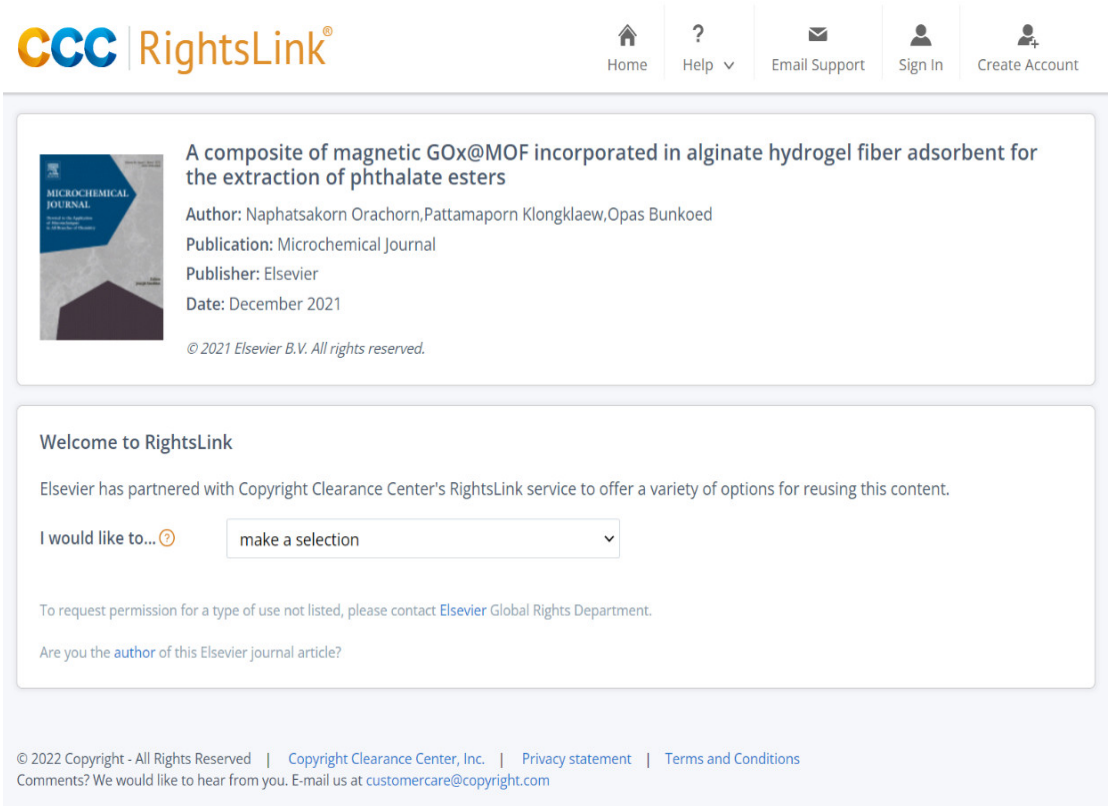

Paper IV

Reprinted with permission of Springer Nature

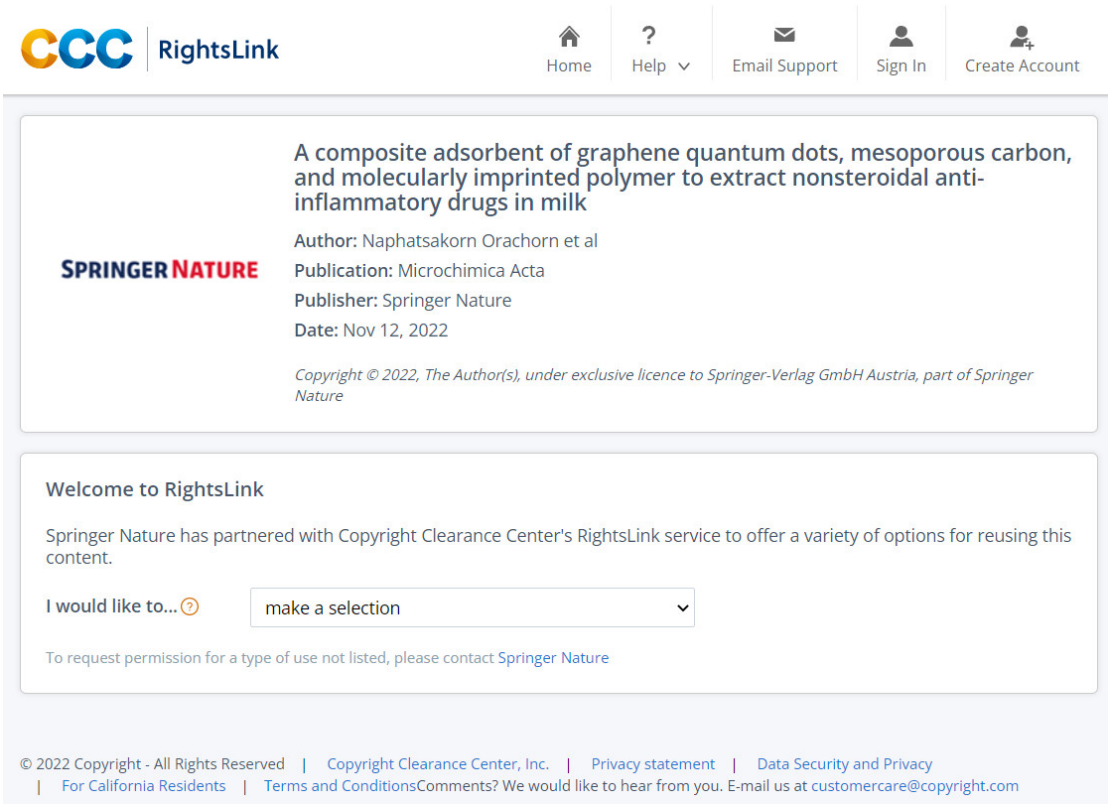

1. Introduction

1.1 Background and rationale

Antibiotic drugs and nonsteroidal anti-inflammatory drugs (NSAIDs) are dramatically attracted to use for treating diseases, preventing infections, relieving persistent pains and promoting growth in both humans and animals (Baile *et al*., 2019; Wise *et al*., 1999). However, the excessive use of antibiotics and NSAIDs in livestock contributes to the residue of them in animal tissues, and they can adversely affect consumers.

Among antibiotics, fluoroquinolones and sulfonamides have been pervasively utilized because of their broad-spectrum activity. Lomefloxacin is an antibiotic drug classified in the group of fluoroquinolones and popularly used to heal respiratory tract diseases, bronchitis, and infections of skin and urinary tracts (Klimberg *et al*., 1998; Lu *et al*., 2007; Saenz-Aguirre *et al*., 1992). Accumulation of lomefloxacin in the human body can cause side effects such as headache, diarrhea, drug resistance and carcinogenesis (Lietman, 1995; Yi *et al*., 2011). In addition, mafenide and sulfisoxazole, sulfonamide antibiotic drug are widely employed as veterinary medicine to cure bacterial infections and serve growth in animals. Both mafenide and sulfisoxazole residuals in animal products can transfer to humans through the food chain and may result in endocrine disorders, drug tolerance and allergic reactions (Liu *et al*., 2020).

Some NSAIDs including mefenamic acid, diflunisal and flurbiprofen are difficult degradation and low solubility in aqueous solution leading to health problems in humans such as gastrointestinal hemorrhage, cardiovascular hazard and kidney damage (Golzari Aqda *et al*., 2018; Tanwar *et al*., 2015). To certify food safety and prevent consumer health, the maximum residue limits (MRLs) defined by the European Union (EU) have been set at 100 μg kg^{-1} for fluoroquinolones in chicken meat and milk, at 100 μg kg^{-1} for sulfonamides in animal tissues and milk, and at 0.1 μg kg^{-1} for NSAIDs in milk (EU, 2010).

Phthalate esters (PAEs) are multipurpose reagents utilized as polymer additives or plasticizers in plastic manufacture for improving the elasticity, softness and durability of plastic products (Adenuga *et al*., 2020). However, chemical interactions

occurring between PAEs and polymer chains are unstable, and PAEs can subsequently bind other compounds (Li *et al*., 2020). Furthermore, PAEs can be simply released from plastic wares to foods or beverages, and the residue of PAEs in the human body leads to endocrine disorders, mutagenicity, reproductive hazards and teratogenicity (Wu *et al*., 2020). The United States Environmental Protection Agency (US EPA) has defined some PAEs consisting of dibutyl phthalate (DBP), bis(2-ethylhexyl) phthalate (DEHP), benzyl butyl phthalate (BBP) and di-n-octyl phthalate (DNOP) as priority environmental pollutants and it has imposed the maximum contaminant level (MCL) at 6.0 μg L^{-1} for DEHP in drinking water (EPA, 2017). Therefore, it is important to develop an efficient and credible method for monitoring antibiotics, NSAIDs and PAEs in foods and beverages.

A variety of analytical methods have been reported for the determination of antibiotics, NSAIDs and PAEs such as electrochemical method (Annamalai *et al*., 2020; Bourais *et al*., 2017; Saghatforoush *et al*., 2012), capillary electrophoresis (Jeong *et al*., 2021; Wu *et al*., 2019), fluorescence spectroscopy (El-Hamshary *et al*., 2019; Silpcharu *et al*., 2020; Zhou *et al*., 2017) and high performance liquid chromatography (HPLC) (El-Sheikh *et al*., 2019; Li *et al*., 2015; Urraca *et al*., 2014; Wu *et al*., 2021).

Among these techniques, fluorescence spectroscopy is an interesting alternative method for the analysis and determination of single or two target analytes due to its rapidity, uncomplicated measurement procedure and cost-effectiveness (Feng *et al*., 2019; Xia *et al*., 2012). The quantitative analysis of the target analytes is usually operated by measuring the quenching of fluorescence emission when the chemical formation between fluorescent probes and target analytes occurs (Chullasat *et al*., 2018).

For the determination of ultra-trace levels, the improvement of the sensitivity and selectivity of fluorescence spectroscopy can be achieved using nanocomposite fluorescent probes. Among sensing materials, quantum dot (QD) nanoparticles have been considerably attracted due to their distinctive optical characteristics, consisting of size-dependent emission, narrow and symmetric shape of emission spectra, good photostability, high fluorescence intensity and good dispersibility in aqueous solution (Wei *et al*., 2016; Wu *et al*., 2018). Among various types of QDs, cadmium telluride quantum dots (CdTe QDs) are extensively employed

as sensing materials owing to their easy preparation and high fluorescence response (Choudhary *et al*., 2019; Tall *et al*., 2021). However, fluorescent probe utilizing mere QDs still lacks selectivity. A molecularly imprinted polymer (MIP) is an outstanding polymeric material that can generate molecular cavities with high specificity to templates in the MIP layer (Arabi *et al*., 2020). The specific recognition cavities of MIP layer are formed through sol-gel copolymerization procedure using three components of templates (target analytes), a functional monomer and a cross-linker (Gui *et al*., 2019). In the last step of the process, a suitable solvent is utilized to remove templates from MIP layer to leave unique imprinted cavities complementary in functional groups, shape and size to the templates (Chullasat *et al*., 2018). Other advantages of MIP are good stability, simple preparation and low cost (Arabi *et al*., 2020). The selectivity improvement of optical probes can be performed by incorporating QDs into the MIP. The use of high affinity materials composited with a selective fluorescent probe can also improve the adsorption ability between the fluorescent probe and target analytes. Polyaniline (PANI) is a conductive polymer that has acquired significant attention to be used as an affinity material. It has various advantages including low cost, easy preparation, huge surface area, environmentally friendly and good chemical stability (Sadeghi *et al*., 2018; Zhang *et al*., 2018). PANI comprises aromatic rings with amino groups that play an important role in strong π-π interaction with aromatic compounds and can form hydrogen bonding (Razavi *et al*., 2018; Sadeghi *et al*., 2018). To further increase the kinetic adsorption of target analyte to a fluorescent probe, graphene oxide (GOx) is a noticeable carbon-based material used as an additional adsorption material due to it has a large π-conjugated structure and significant functional groups of hydroxyl, carboxyl and epoxy (Naing *et al*., 2016; Wu *et al*., 2015). Thus, a nanocomposite fluorescent probe consisting of PANI, GOx and CdTe QDs incorporated into a MIP (PANI-GOx-MIP-CdTe QDs) was created and utilized to efficiently detect lomefloxacin **(Paper I)**. The fabricated PANI-GOx-MIP-CdTe QDs fluorescent probe interacts with lomefloxacin through π-π interaction and hydrogen bonding as illustrated in **Figure 1**.

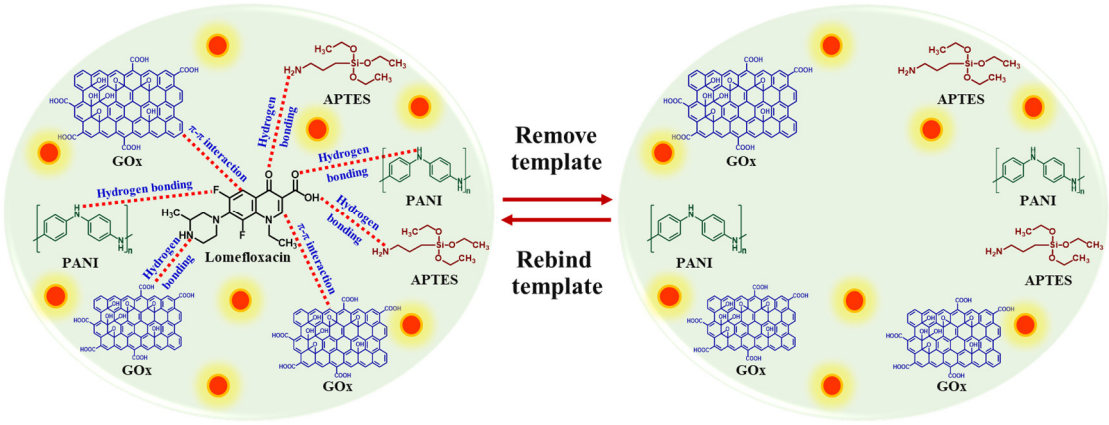

Figure 1 The interaction between the PANI-GOx-MIP-CdTe QDs fluorescent probe and lomefloxacin (Orachorn *et al*., 2019)

To further improve sensitivity and facilitate isolation of the fluorescent probe, the magnetization of the fluorescent probe has earned incremental attention by compositing of magnetite (Fe_3O_4) nanoparticles with MIP to fabricate magnetic molecularly imprinted polymer (MMIP) (Dinc *et al*., 2019; Fu *et al*., 2021; Lin *et al*., 2016). However, bare Fe_3O_4 nanoparticles are not popularly utilized as a core material in MIP due to their easy agglomeration, low stability and poor dispersibility in aqueous solution (Arabi *et al*., 2020; Dinc *et al*., 2019). The surface of Fe_3O_4 is generally improved by modification with supporting materials such as silica (SiO_2) (Banan *et al*., 2022; Fan *et al*., 2015; Kaewsuwan *et al*., 2017), polyethylene glycol (Bagheri *et al*., 2019; Mukhopadhyay *et al*., 2012), polydopamine (Socas-Rodríguez *et al*., 2015) and dextran (Hong *et al*., 2008; Sakaguchi *et al*., 2019). Among the above supporting materials, magnetite nanoparticles encapsulated with silica (Fe_3O_4-SiO_2) are a good choice because they are not only easily prepared but also can improve the weaknesses of bare Fe_3O_4 (Fan *et al*., 2015; Kaewsuwan *et al*., 2017). The improvement of the sensitivity and selectivity of an analytical method for the simultaneous detection of two target analytes, the composite fluorescent probe can be fabricated by incorporating two sensing materials into MMIP. Another type of QDs called graphene quantum dots (GQDs) is also a great sensing material that can be combined with CdTe QDs for the determination of two analytes because they exhibit different emission wavelengths from CdTe QDs (Chullasat *et al*., 2019). In addition, GQDs have strong fluorescence emission, low environmental toxicity and excellent stability (Mehrzad-Samarin *et al*.,

2017). The adsorption ability between a magnetic composite fluorescent probe and target analytes can be enhanced by compositing an adsorption material with a fluorescent probe. Metal organic framework (MOF) is a class of crystalline hybrid porous materials created by inorganic metal ions and organic ligands via coordinate covalent bonds (Li *et al*., 2022; Zheng *et al*., 2022). One type of MOFs called materials of institute Lavoisier-101 (MIL-101) has received more attention as an adsorption material constructed from chromium and terephthalic acid ligands because it has a large surface area, adjustable pore size and good stability (Hou *et al*., 2020; Jia *et al*., 2020; Mertsoy *et al*., 2021). Moreover, strong interactions of π-π and hydrophobic occur between MIL-101 and target analytes (Huo *et al*., 2012). Therefore, dual magnetic nanocomposite fluorescent probes were fabricated by incorporating MIL-101 with GQDs or CdTe QDs into MMIP (MIL101-MMIP-GQDs and MIL101-MMIP-CdTe QDs) for the simultaneous determination of mafenide and sulfisoxazole at ultra-trace levels **(Paper II)**. The possible binding of nanocomposite MIL101-MMIP-GQDs and MIL101-MMIP-CdTe QDs probes toward mafenide and sulfisoxazole is based on hydrogen bonding and π-π and hydrophobic interactions as demonstrated in **Figure 2 and 3**.

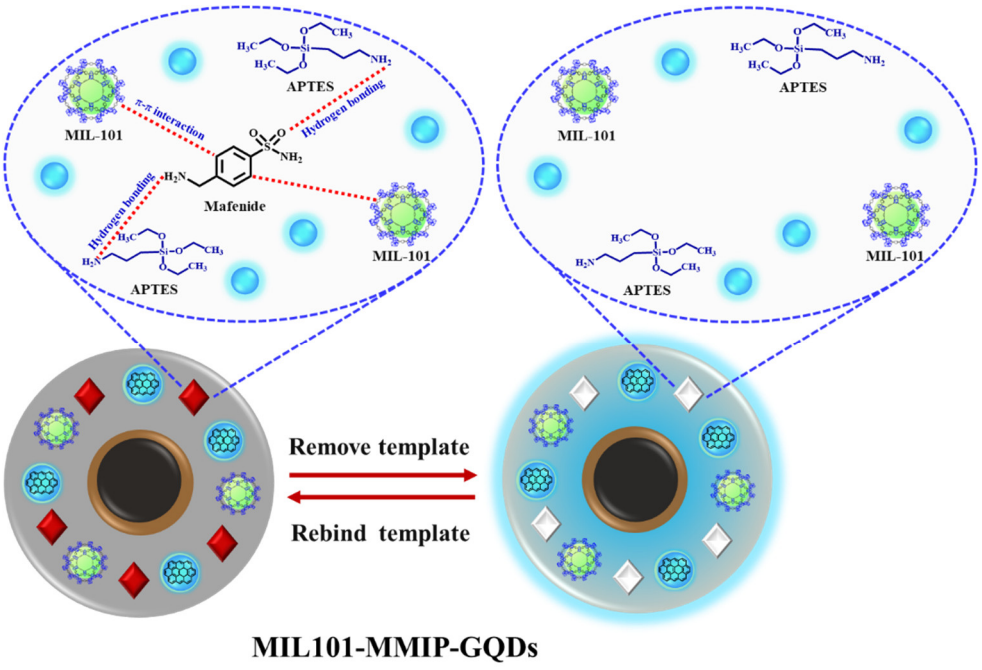

Figure 2 The interaction of the nanocomposite MIL101-MMIP-GQDs toward mafenide (Orachorn *et al*., 2021)

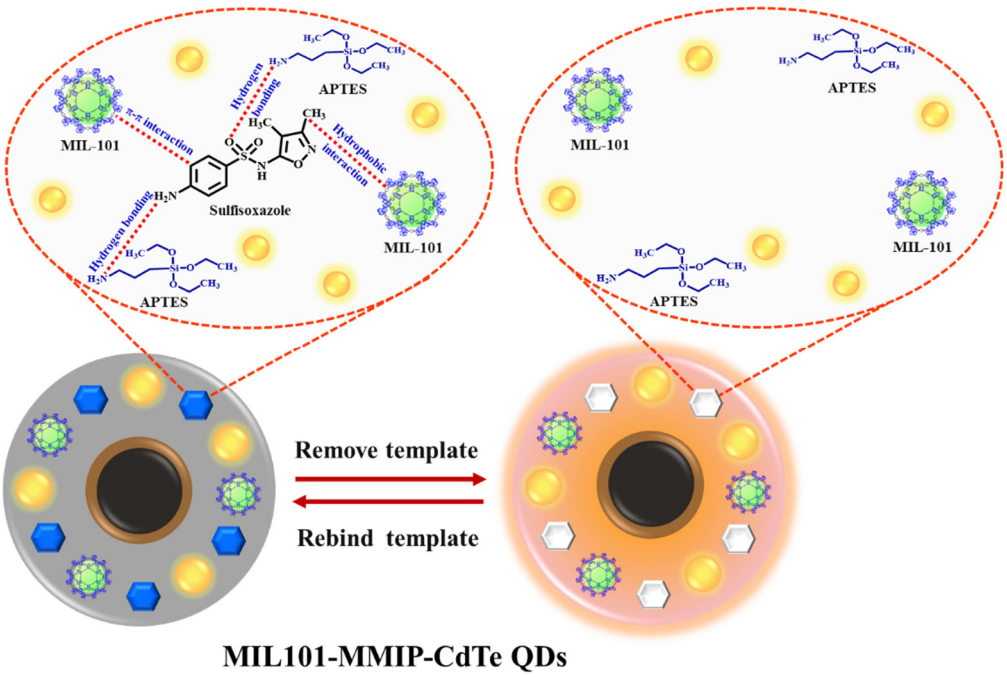

Figure 3 The interaction of the nanocomposite MIL101-MMIP-CdTe QDs toward sulfisoxazole (Orachorn *et al*., 2021)

For the determination of multiple target analytes, an HPLC is extensively utilized because it can simultaneously separate and determine multiple target compounds using a separation column and provide high sensitivity and good precision (Borahan *et al*., 2019; Magiera *et al*., 2013). However, concentrations of organic compounds that remain in real samples are quite low and coexisted with several matrix interferences (Shishov *et al*., 2019; Wu *et al*., 2021). Consequently, the sample preparation procedure before analysis by HPLC is usually required to enrich the target analytes and reduce matrix components (Liang *et al*., 2020; Wu *et al*., 2021). Various sample preparation methods have been developed and used for the extraction and enrichment of organic compounds such as liquid-liquid microextraction (LLME) (Hassan *et al*., 2019; Wang *et al*., 2020), stir bar sorptive extraction (SBSE) (Wang *et al*., 2021; Zang *et al*., 2021), solid-phase microextraction (SPME) (Wang *et al*., 2019; Wang *et al*., 2020), solid-phase extraction (SPE) (Amiri *et al*., 2021; Milanetti *et al*., 2019) and dispersive magnetic solid-phase extraction (D-MSPE) (Baile *et al*., 2019; Ferrone *et al*., 2018; Tong *et al*., 2019). Among these methods, D-MSPE has received great attention due to its uncomplicated operation, less time to isolate the adsorbent

from the sample solution and less amount of organic solvents (Tong *et al*., 2019). Furthermore, composite adsorbents employed in D-MSPE is not only easily prepared but also can be reused after washing with a suitable solvent (Klongklaew *et al*., 2020). The most significant part of D-MSPE is an adsorbent component, which can enhance the adsorption ability (Li *et al*., 2015). To create various shapes of composite adsorbents, alginate is a good choice to be used as a supporting material that can easily entrap other materials. It has several beneficial features including high stability, non-toxicity, simple preparation, good biocompatibility and biodegradability (Bezbaruah *et al*., 2009; Pinsrithong *et al*., 2018). The fabrication of composite alginate adsorbent with a high extraction efficiency of target analytes can be performed by incorporating other materials such as Fe_3O_4-SiO_2, GOx and MIL-101 into alginate hydrogel. Accordingly, a magnetic composite alginate hydrogel fiber was designed and fabricated by combining Fe_3O_4-SiO_2, GOx and MIL-101 (GOx/MIL-101/Fe_3O_4-SiO_2) within alginate hydrogel fiber employed in the D-MSPE technique to extract and enrich PAEs **(Paper III)**. The interactions between fabricated composite hydrogel fiber and PAEs are hydrogen bonding, hydrophobic and π-π interactions as depicted in **Figure 4**.

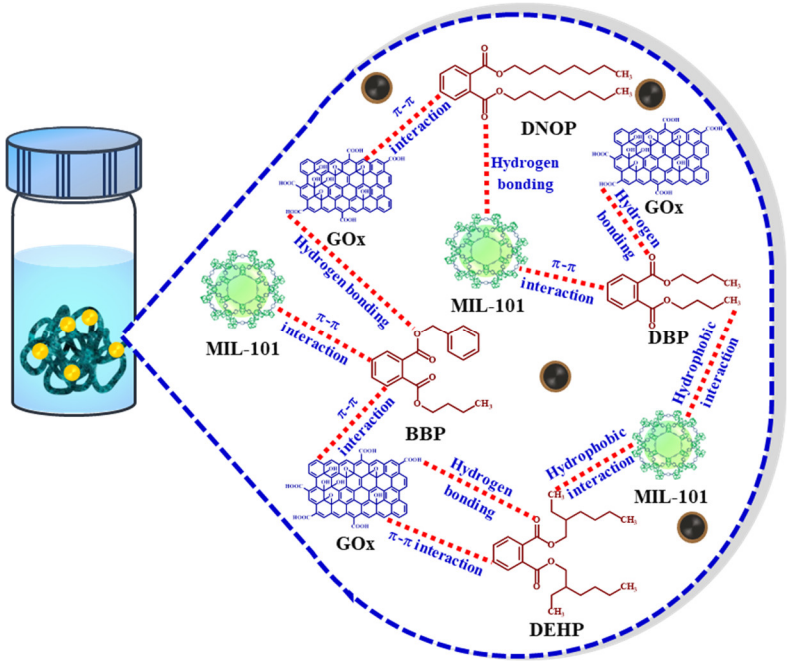

Figure 4 The interaction between the magnetic composite GOx/MIL-101/Fe_3O_4-SiO_2 alginate hydrogel fiber and phthalate esters (Orachorn *et al*., 2021)

The selectivity of D-MSPE adsorbent can be increased with MIP and the fabrication of adsorbent can be performed by embedding magnetic material into MIP to create MMIP that contains numerous specific recognition cavities on the polymer layer for the target analytes (Dinc *et al*., 2019). The binding ability of adsorbent toward target analytes can be enhanced by combining high affinity materials with MMIP. GQDs are an interesting carbon-based material with π-conjugated rings and various functional groups of hydroxyl and carboxyl, which can adsorb NSAIDs via π-π interaction and hydrogen bonding (Mahmoudi-Moghaddam *et al*., 2019). Another carbon-based material called mesoporous carbon (MPC) is also intriguing material to enhance the adsorption of target compounds because of its hydrophobic feature, leading to MPC can adsorb target analytes through hydrophobic interaction (Jeong *et al*., 2020). In addition, MPC has several advantages including huge surface area, high pore volume, low cost, and excellent chemical and thermal stability (Liu *et al*., 2022; Rechotnek *et al*., 2022). Consequently, a magnetic composite adsorbent of Fe_3O_4-SiO_2, GQDs and MPC embedded into a MIP (GQDs/Fe_3O_4-SiO_2/MPC/MIP) was created and used in the D-MSPE technique for the extraction of NSAIDs **(Paper IV)**. The composite MMIP adsorbent strongly adsorbs NSAIDs through hydrogen bonding and π-π interaction reinforced by hydrophobic interaction as shown in **Figure 5**.

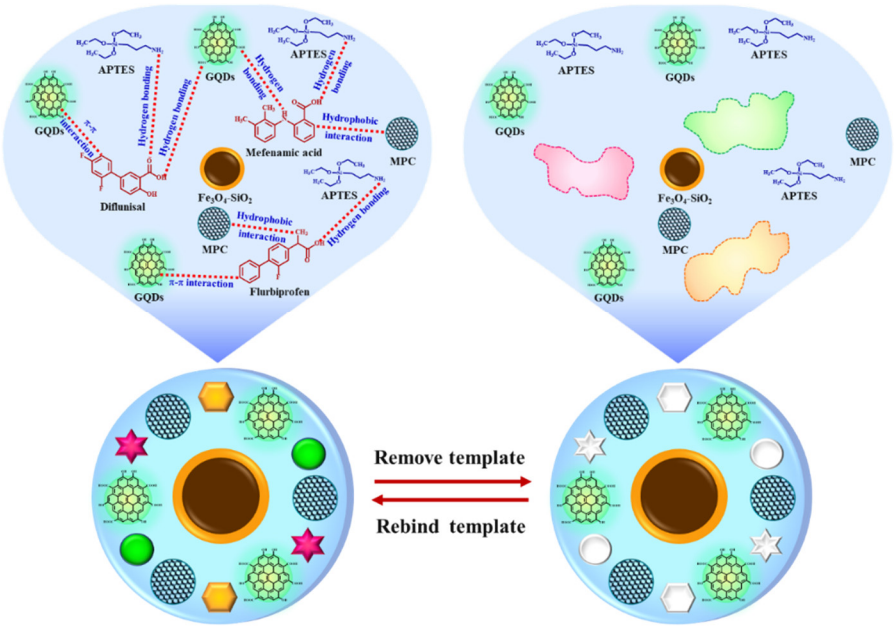

Figure 5 The interaction between the composite GQDs/Fe_3O_4-SiO_2/MPC/MIP adsorbent and nonsteroidal anti-inflammatory drugs (Orachorn *et al*., 2022)

1.2 Objective

The purposes of this thesis are to develop optosensor based on nanocomposite sensing probes using molecularly imprinted polymer composited with quantum dot nanoparticles for the determination of trace organic compounds in food and beverage samples and to develop composite adsorbents using suitable sample preparation techniques for the extraction and enrichment of trace organic compounds in beverage samples. This thesis including optosensor and sample preparation method consists of four sub-projects as follows:

Sub-project I: A nanocomposite fluorescent probe of polyaniline, graphene oxide and cadmium telluride quantum dots incorporated into molecularly imprinted polymer (PANI-GOx-MIP-CdTe QDs) for the determination of lomefloxacin in milk, chicken meat and egg.

Sub-project II: Dual nanohybrid magnetic fluorescent probes containing metal organic framework, graphene quantum dots and cadmium telluride quantum dots incorporated into magnetic molecularly imprinted polymer (MIL101-MMIP-GQDs and MIL101-MMIP-CdTe QDs) for the enrichment and simultaneous detection of mafenide and sulfisoxazole in milk samples.

Sub-project III: A magnetic composite adsorbent of graphene oxide, metal organic framework and silica-modified magnetite (GOx/MIL-101/Fe_3O_4-SiO_2) incorporated into alginate hydrogel fiber as dispersive magnetic solid-phase extraction (D-MSPE) adsorbent for the extraction and enrichment of the phthalate esters in water, juice and tea samples.

Sub-project IV: A highly selective magnetic adsorbent of graphene quantum dots, silica-modified magnetite and mesoporous carbon composited with molecularly imprinted polymer (GQDs/Fe_3O_4-SiO_2/MPC/MIP) for the extraction and determination of nonsteroidal anti-inflammatory drugs in milk samples.

2. Optosensor

Optosensor is a kind of chemical sensor that applies electromagnetic radiation to produce the analytical signal in a transducer (Jerónimo *et al*., 2007). The changing of optical response is caused by the interaction between the particular receptor and target analytes, which is associated with the concentration of target analytes in the sample (Aleksandra *et al*., 2012). Optosensor can be categorized based on the optical properties that have been measured such as fluorescence, chemiluminescence, phosphorescence, reflectance, absorbance and resonance (Piccirilli *et al*., 2009). In addition, it can measure numerous characteristics such as lifetime, light intensity and polarization (Jerónimo *et al*., 2007). The instrument commonly utilized in optosensor are UV-Visible spectrophotometer (Elik *et al*., 2022; Soylak *et al*., 2020), infrared spectrophotometer (Sakira *et al*., 2021) and fluorescence spectrometer (Li *et al*., 2018; Nurerk *et al*., 2016; Wang *et al*., 2019).

Fluorescence-based optosensor has gained much attention due to its rapid analysis time, high sensitivity, simple measurement and cost-effectiveness (Feng *et al*., 2019; Xia *et al*., 2012). The quantitative analysis of target analytes using the fluorescence sensor is generally performed by measuring the changing of the quenching or enhancement of the fluorescence emission **(Figure 6)** (Chullasat *et al*., 2018; Yang *et al*., 2017). Fluorescence sensors based on the measurement of fluorescence quenching have been reported for the determination of various organic compounds such as amoxicillin (Chullasat *et al*., 2018), propanil (Liu *et al*., 2020), ciprofloxacin (Yuphintharakun *et al*., 2018), tetracycline (Khawla *et al*., 2022), saxitoxin (Sun *et al*., 2018), leucomalachite green (Yang *et al*., 2017), lomefloxacin **(Paper I)**, mafenide and sulfisoxazole **(Paper II)**.

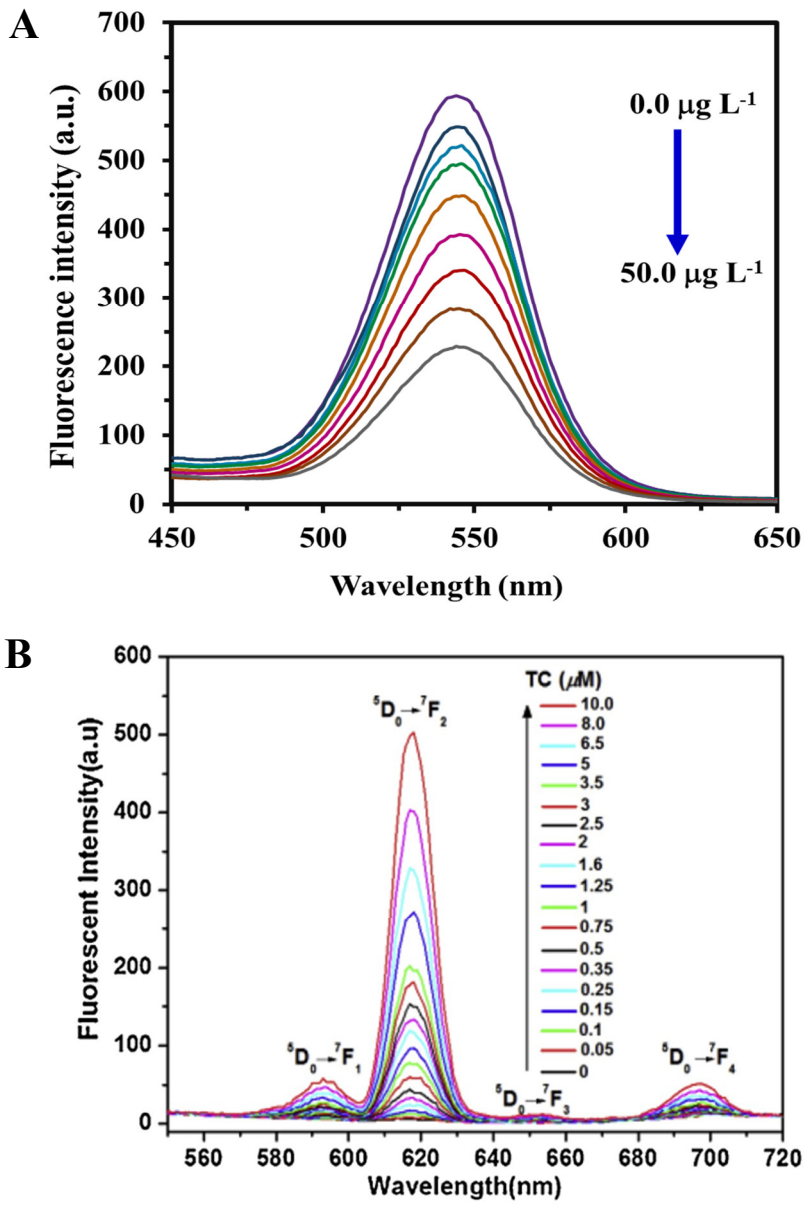

Figure 6 The fluorescence emission spectra based on the fluorescence quenching of PANI-GOx-MIP-CdTe QDs nanoprobe for lomefloxacin determination (A) (Reprinted from Orachorn and coworker, 2019; copyright with permission from Elsevier) (Orachorn *et al*., 2019) and the fluorescence enhancement of Ag@HNTs-Cit-Eu nanoprobe for tetracycline determination (B) (Reprinted from Xu and coworker, 2020; copyright with permission from Elsevier) (Xu *et al*., 2020)

3. Sample preparation technique

Sample preparation is a crucial step before analysis by an analytical instrument, which is used for the removal of matrix interferences in real sample and preconcentration of target analytes to increase sensitivity (Wang *et al*., 2021; Wojnowski *et al*., 2022). Currently, sample preparation has been developed and popularly applied in the fields of food analysis (Casado *et al*., 2020; Hewavitharana *et al*., 2020), environmental analysis (Cerutti *et al*., 2019; Yahaya *et al*., 2022), biological analysis (Alampanos *et al*., 2021; Li *et al*., 2021) and forensic analysis (Kabir *et al*., 2013; Manousi *et al*., 2021). According to recent trends, sample preparation techniques have evolved to offer superior advantages such as ease of operation, time saving, solvent-minimized extraction and environmental friendliness (Hussain *et al*., 2020; Kabir *et al*., 2013). Several sample preparation methods have been reported and utilized for the extraction and determination of organic compounds such as liquid-liquid microextraction (LLME) (Hassan *et al*., 2019; Wang *et al*., 2020), stir bar sorptive extraction (SBSE) (Wang *et al*., 2021; Zang *et al*., 2021), solid-phase microextraction (SPME) (Wang *et al*., 2019; Wang *et al*., 2020), solid-phase extraction (SPE) (Amiri *et al*., 2021; Huang *et al*., 2022; Milanetti *et al*., 2019) and dispersive magnetic solid-phase extraction (D-MSPE) (Baile *et al*., 2019; Ferrone *et al*., 2018; Tong *et al*., 2019). Among these methods, D-MSPE is a favored approach for analyte extraction because of its simple operation, rapid isolation of the adsorbent from sample solution and small volume of solvent usage (Tong *et al*., 2019; Kaewsuwan *et al*., 2017).

3.1 Dispersive magnetic solid-phase extraction

Dispersive magnetic solid-phase extraction (D-MSPE) is a sample preparation method modified from SPE mode, which is performed by directly dispersion of a magnetic adsorbent into sample solution (Fernández *et al*., 2020). The dispersibility of adsorbent can improve the contact surface between target compounds and magnetic adsorbent, leading to increasing extraction efficiency (Jing *et al*., 2019; Li *et al*., 2018). Additionally, the magnetic feature of adsorbent enables easy and fast isolation of adsorbent from solution through an attractive force of an external magnetic field, which can minimize the overall time of the extraction process (Jing *et al*., 2019;

Manousi *et al*., 2020). Compared with a traditional SPE mode, D-MSPE can simplify operations and avoid problems of cartridge clogging (Li *et al*., 2018; Maya *et al*., 2017).

The basic procedure of D-MSPE is illustrated in **Figure 7**. Initially, the magnetic composite adsorbents are dispersed into sample solution under a suitable stirring rate with adequate adsorption time to facilitate mass transfer of target compounds from sample solution to the magnetic composite adsorbents (Jiang *et al*., 2019). An external magnet is subsequently applied to isolate the magnetic composite adsorbents with adsorbed target compounds from solution. After discarding supernatant solution, the target analytes adsorbed on the magnetic composite adsorbents are desorbed by adding proper organic solvent for a sufficient period. Next, the fast isolation of the magnetic composite adsorbents from solution is performed by a magnet, and eluent with desorbed compounds is evaporated by a rotary evaporator. After solvent dryness, the residue is redissolved with mobile phase solution and filtered before analysis by an analytical instrument (Li *et al*., 2018; Vasconcelos *et al*., 2017). In addition, the used magnetic composite adsorbents can be reused to extract target compounds for the next cycle after being washed with appropriate solvent to assure that target compounds have not remained on the used adsorbents (Wierucka *et al*., 2014).

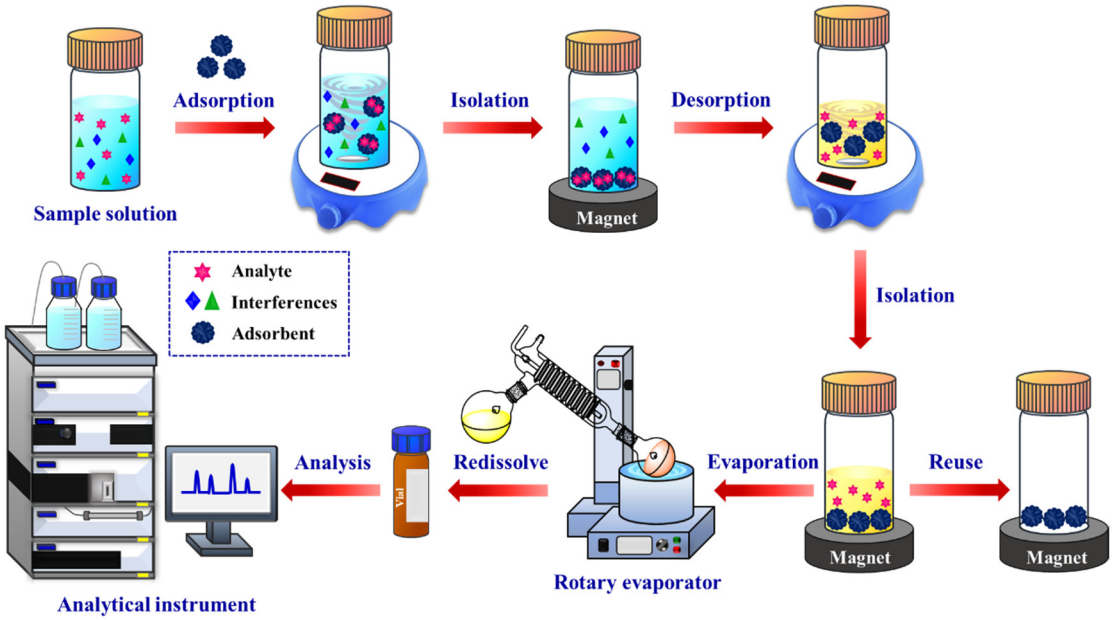

Figure 7 The procedure of dispersive magnetic solid-phase extraction (Orachorn *et al*., 2022)

4. Materials

4.1 Quantum dots

Quantum dots (QDs) also known as colloidal semiconductor nanocrystals are fluorescent nanomaterials that have dimensions smaller than the bulk-exciton Bohr radius (Frigerio *et al*., 2012; Wu *et al*., 2014). QDs have excellent optical properties including size-dependent emission, narrow and symmetric spectra in shape, good photostability, high fluorescence intensity and good dispersibility in aqueous solution (Wei *et al*., 2016; Wu *et al*., 2018). The distinctive optical characteristics of QDs are based on quantum confinement influences, caused by electron and hole restriction in all three dimensions (Hezinger *et al*., 2008). Generally, the diameter of QDs is in the range of 1 to 10 nm (10 to 50 atoms), resulting in a high ratio of surface to volume (Pouya *et al*., 2005; Vasudevan *et al*., 2015). Due to their small size, the energy levels of QDs can be separated to the valence band (lower energy level) and conduction band (higher energy level) (Frigerio *et al*., 2012). The band gap energy values of QDs between the valence band and conduction band directly depend on the size of QDs (Hezinger *et al*., 2008). The smaller size of QDs has larger band gap energy, which provides a shorter emission wavelength (blue shift). In contrast, the band gap energy is reduced when the size of QDs increases, leading to a longer emission wavelength (red shift) as illustrated in **Figure 8** (Drbohlavova *et al*., 2009; Frigerio *et al*., 2012).

Several types of QDs have been applied as fluorescent probes, which are usually composed of elements in groups II-VI, III-V or IV-VI such as cadmium telluride (CdTe) (Chullasat *et al*., 2018; Nurerk *et al*., 2016; Wu *et al*., 2018), cadmium sulfide (CdS) (Eskandari *et al*., 2017; Tayebi *et al*., 2016), cadmium selenide (CdSe) (Brahim *et al*., 2015; Zhang *et al*., 2018), zinc sulfide (ZnS) (Ren *et al*., 2015; Wang *et al*., 2018), zinc selenide (ZnSe) (Wu *et al*., 2014; Zhou *et al*., 2018), indium phosphide (InP) (Lee *et al*., 2013), lead selenide (PbSe) (Yu *et al*., 2012) and lead sulfide (PbS) (Pendyala *et al*., 2009). The emission wavelengths of QDs are ranged from visible to near-infrared and can be adjusted by varying their physicochemical properties such as size, core-shell component and shape (Cardoso Dos Santos *et al*., 2020; Hezinger *et al*., 2008).

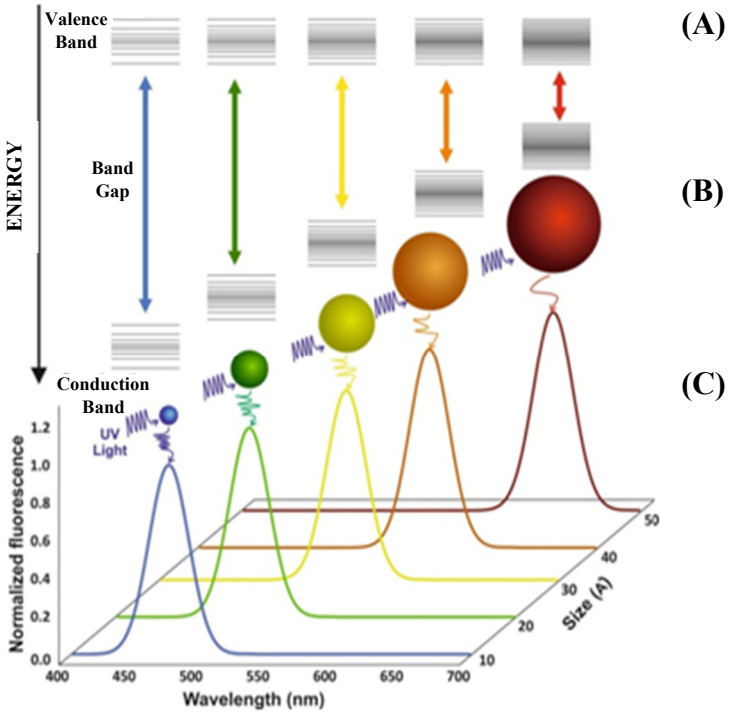

Figure 8 The band gap energy of QDs (A), various relative particle sizes of QDs (B) and size-dependent fluorescence emission spectra of QDs (C) (Reprinted from Samimi and coworker, 2017; copyright with permission from Medcrave) (Samimi *et al*., 2017)

Among various synthesis strategies of QDs, the colloidal method has attracted much attention for QDs preparation which provides excellent fluorescence efficiency and narrow range of size distribution (Frigerio *et al*., 2012). In addition, the surface of QDs should be stabilized by modifying with suitable stabilizing agents to enhance the dispersibility of QDs in aqueous solution and prevent aggregation of QDs (Vasudevan *et al*., 2015). A variety of stabilizers have been utilized as capping agents for the surface modification of QDs such as thioglycolic acid (TGA) (Chullasat *et al*., 2018; Wei *et al*., 2015), mercaptopropionic acid (MPA) (Bunkoed *et al*., 2015; Wang *et al*., 2019), glutathione (GSH) (Ensafi *et al*., 2015; Peng *et al*., 2018), mercaptosuccinic acid (MSA) (Thepmanee *et al*., 2020; Wei *et al*., 2014) and cysteamine (CA) (Ding *et al*., 2015; Ensafi *et al*., 2016). In recent years, the stabilizer with a short-chain thiol and other functional groups (carboxyl, hydroxyl and amino groups) has been popularly used as a capping agent because it provides high brightness

of QDs with a flexible surface and good stability (Frigerio *et al*., 2012; Nurerk *et al*., 2016). QDs have been applied as fluorescent probes for the detection of numerous analytes such as cyphenothrin (Ren *et al*., 2015), tetracycline (Han *et al*., 2020), paranitrophenol (Zhou *et al*., 2014), iron(III) ion (Fe^{3+}) (Tam *et al*., 2014), lead(II) ion (Pb^{2+}) (Qian *et al*., 2015), ciprofloxacin (Yuphintharakun *et al*., 2018), amoxicillin (Chullasat *et al*., 2018), salicylic acid (Bunkoed *et al*., 2015), lomefloxacin **(Paper I)**, mafenide and sulfisoxazole **(Paper II)**.

4.1.1 Cadmium telluride quantum dots

Cadmium telluride quantum dots (CdTe QDs) are semiconductor nanocrystals in group II-IV with a band gap energy of approximately 1.5 eV (Akbari *et al*., 2020). The emission wavelengths of CdTe QDs are ranged from 500 to 750 nm, which are depended on size of QDs (Smith *et al*., 2006). In addition, CdTe QDs have superior advantages over other inorganic QDs such as simple preparation under mild conditions and high fluorescence efficiency (Choudhary *et al*., 2019; Tall *et al*., 2021). In recent years, TGA-capped CdTe QDs have been extensively utilized as fluorescent probes for optosensor applications and reported for the determination of a variety of analytes such as salbutamol (Zhang *et al*., 2021), dopamine (Pourghobadi *et al*., 2018), chloramphenicol (Amjadi *et al*., 2016), amoxicillin (Chullasat *et al*., 2018), sarafloxacin (Chaowana *et al*., 2019), kaempferol (Tan *et al*., 2014), lomefloxacin **(Paper I)** and sulfisoxazole **(Paper II)**. The structure of TGA-capped CdTe QDs is represented in **Figure 9**.

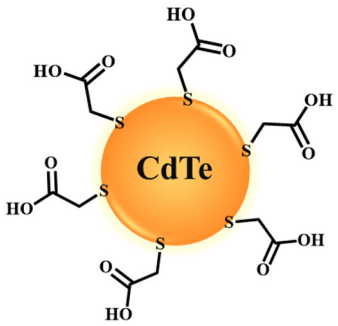

Figure 9 The structure of TGA-capped CdTe QDs

4.1.2 Graphene quantum dots

Graphene quantum dots (GQDs) are carbon-based fluorescent nanomaterials with zero-dimension, which consist of a single or few layers of graphene (Henna *et al*., 2020; Lin *et al*., 2014). The emission wavelengths of GQDs mainly occur in the range of 400 to 500 nm (Rocha *et al*., 2022). Recently, GQDs have been significantly interested owing to their low environmental toxicity, excellent photostability, high fluorescence response, chemical inertness and easy preparation (Bunkoed *et al*., 2020; Mehrzad-Samarin *et al*., 2017). These unique optical properties of GQDs are caused by quantum confinement and edge effect (Zhou *et al*., 2015). GQDs have π-conjugated structures with numerous functional groups of carboxyl and hydroxyl as illustrated in **Figure 10**, resulting in good dispersibility in aqueous solution. In addition, GQDs can be used as adsorption material for target compounds because they can produce strong π-π interaction with aromatic compounds and form hydrogen bonding of hydroxyl or carboxyl groups with various organic compounds (Mahmoudi-Moghaddam *et al*., 2019).

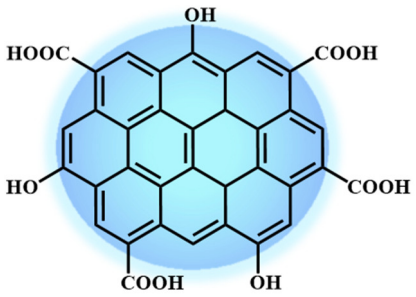

Figure 10 The structure of GQDs

For optosensor application, GQDs have been employed as fluorescent probes for the detection of several compounds such as paranitrophenol (Zhou *et al*., 2014), methamphetamine (Masteri-Farahani *et al*., 2020), norfloxacin (Bunkoed *et al*., 2020), dopamine (Zhou *et al*., 2015), sulfamethoxazole (Le *et al*., 2020), ascorbic acid (Liu *et al*., 2017), cephalexin (Chullasat *et al*., 2019), ceftazidime (Bunkoed *et al*., 2020) and mafenide **(Paper II)**.

4.2 Molecularly imprinted polymer

A molecularly imprinted polymer (MIP) is a highly cross-linked polymer that can form specific imprinted cavities for target compounds (Shi *et al*., 2019). The construction of MIP is performed through a copolymerization process by employing three major components of a template molecule (target compound), a functional monomer and a cross-linker (Basak *et al*., 2022). Before polymerization, there are two types of interactions for the binding between a template and a functional monomer including non-covalent and covalent interactions (Hasanah *et al*., 2021). One of the most popular processes in the pre-polymerization step is self-assembly due to its simple preparation, easy template removal and high-affinity binding (Bakhtiar *et al*., 2019; Song *et al*., 2022). In this approach, non-covalent interactions such as Van der Waals forces, hydrogen bonding, ionic and hydrophobic interactions are formed between a monomer and a template (Hasanah *et al*., 2021). Generally, the preparation procedure of MIP is carried out following three main steps **(Figure 11)**. Firstly, functional monomers are bound with templates via self-assembly in the pre-polymerization procedure. Secondly, cross-linkers are utilized to fix the template-monomer complexes and create strong three-dimensional polymers. Finally, templates are removed from polymer matrix using a suitable desorption solvent to generate numerous specific imprinted cavities, which are matched in size, functional group and shape to target compounds (Suwanwong *et al*., 2021; Vasapollo *et al*., 2011). MIP has several beneficial features including simple fabrication, high stability, low cost and easy surface modification with other materials (Fang *et al*., 2021).

MIP has been utilized in various fields such as solid-phase extraction (Madikizela *et al*., 2018), dispersive magnetic solid-phase extraction (Chang *et al*., 2017; Jalilian *et al*., 2021), solid-phase microextraction (Shahhoseini *et al*., 2022), optosensor (Fang *et al*., 2021), electrochemical sensor (Rebelo *et al*., 2021) and biosensor (Nawaz *et al*., 2021). For optosensor application, MIP composited with QDs has been employed as a fluorescent probe and reported for the determination of several organic compounds such as amoxicillin (Chullasat *et al*., 2018), norfloxacin (Chen *et al*., 2021), sulfadiazine (Shi *et al*., 2019), leucomalachite green (Yang *et al*., 2017), tetracycline (Zhang *et al*., 2016), thioridazine hydrochloride (Ensafi *et al*., 2019),

lomefloxacin **(Paper I)**, mafenide and sulfisoxazole **(Paper II)**. For the application of dispersive magnetic solid-phase extraction, MIP has been utilized as an adsorbent in the D-MSPE process and reported for the extraction and determination of various organic compounds such as phenolphthalein (Jalilian *et al*., 2021), polycyclic aromatic hydrocarbons (Azizi *et al*., 2020), glucocorticoids (Hang *et al*., 2022), bisphenol A (Chang *et al*., 2017), acrylamide (Baile *et al*., 2019) and nonsteroidal anti-inflammatory drugs **(Paper III)**.

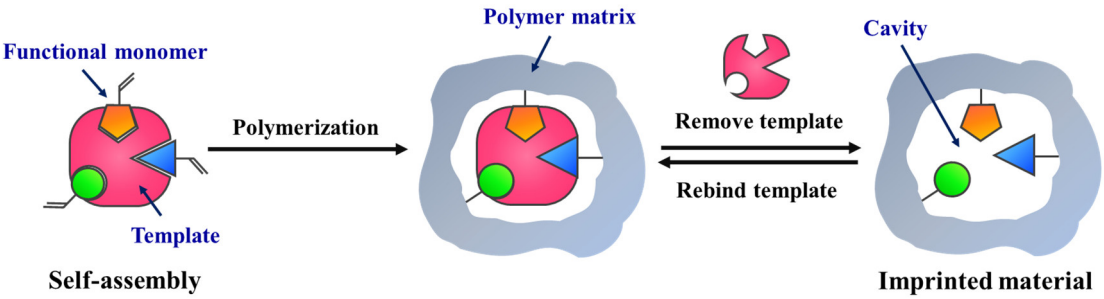

Figure 11 The preparation process of molecularly imprinted polymer

4.3 Alginate hydrogel

Alginate is a water-soluble biopolymer generated from brown algae or seaweed, which has extraordinary properties including non-toxicity, high stability and good biodegradability (Hu *et al*., 2021; Zare *et al*., 2016). Alginate is composed of linear polysaccharides of β-D-mannuronic acid (M) and α-L-guluronic acid (G), connected through (1→4) glycosidic linkages (Cao *et al*., 2020; Pasparakis *et al*., 2006). Furthermore, alginate can selectively bond with divalent cations such as calcium(II) ion (Ca^{2+}), copper(II) ion (Cu^{2+}) and barium(II) ion (Ba^{2+}) (Zare *et al*., 2016). This property enables a basic sol-gel transition into a three-dimensional network (3D-N) through cross-linking reaction to form a hydrogel, similar to an egg box model **(Figure 12)** (Kashima *et al*., 2012; Zare *et al*., 2016). Alginate hydrogel has gained much attention for the fabrication of adsorbents because it can be designed and created in numerous shapes, and has distinctive properties such as simple preparation, good stability, cost-effectiveness, good biocompatibility and biodegradability (Bezbaruah *et al*., 2009; Pinsrithong *et al*., 2018). In addition, alginate hydrogel has a hydrophilic feature that

can enhance the dispersibility of the adsorbents in aqueous solution, leading to decreasing extraction time (Pinsrithong *et al*., 2018).

The extraction of target compounds by alginate hydrogel in the D-MSPE process can be improved by incorporating magnetic materials and other adsorption materials within the hydrogel. Several adsorption materials have been reported including polypyrrole (Bunkoed *et al*., 2016; Pinsrithong *et al*., 2018), polyaniline (Klongklaew *et al*., 2020), reduced graphene oxide (Pinsrithong *et al*., 2018), multiwalled carbon nanotubes (Bunkoed *et al*., 2015), chitosan (Facchi *et al*., 2018), metal organic framework (Nurerk *et al*., 2020; Tan *et al*., 2019; **Paper III**) and graphene oxide (Klongklaew *et al*., 2020; Tasmia *et al*., 2020; **Paper III**).

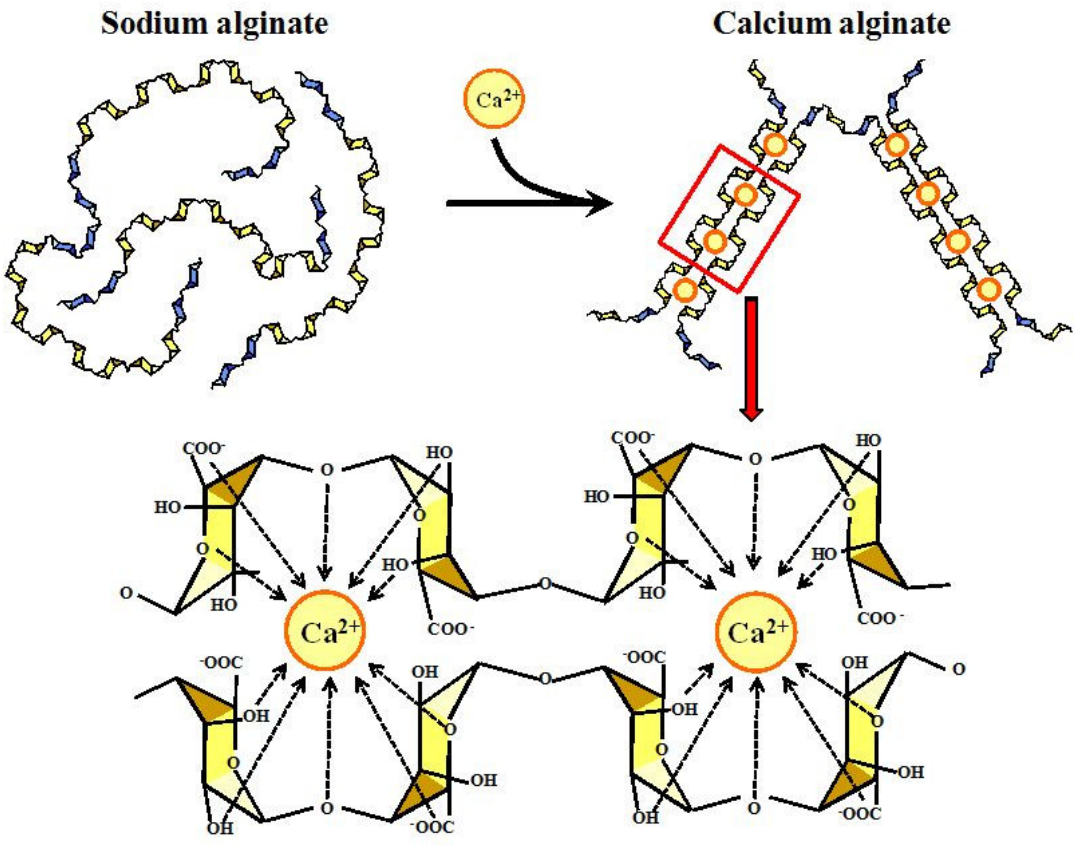

Figure 12 Gelation of homopolymeric blocks of α-L-guluronic acid junction with calcium ions (Egg-box model) (Reprinted from Kashima and coworker, 2012; copyright with permission from IntechOpen) (Kashima *et al*., 2012)

4.4 Adsorption materials

Adsorption materials are an important component of both the fluorescent probe and adsorbent because they can improve the binding ability of target compounds. The suitable materials are selected by considering their structure and unique properties to interact with target analytes. When the fluorescent probe or adsorbent is composited with adsorption materials, it should have superior features to the original components. In this thesis, polyaniline, graphene oxide, metal organic framework, graphene quantum dots and mesoporous carbon were utilized as adsorption materials for the fabrication of either composite fluorescent probes or composite adsorbents.

4.4.1 Polyaniline

Polyaniline (PANI) is one of the most popular conductive polymers to be used as an adsorption material due to its distinctive advantages such as uncomplicated synthesis, large surface area, excellent stability and environmental friendliness (Sadeghi *et al*., 2018; Zhang *et al*., 2018). Generally, the preparation of PANI can be performed through an oxidation reaction of aniline or any anilinium salt with an appropriate oxidizing agent such as ammonium persulfate under acidic conditions (Stejskal *et al*., 2010). The chemical structure of PANI is composed of benzene rings and amino groups **(Figure 13)**, which can not only produce strong π-π interaction with aromatic compounds but also possibly generate hydrogen bonding of amino groups with multiple organic compounds (Razavi *et al*., 2018; Sadeghi *et al*., 2018).

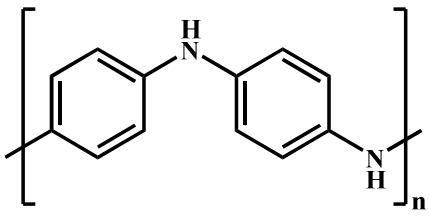

Figure 13 The chemical structure of polyaniline

PANI has been employed as an adsorption material in many applications such as optosensor (Ahmed *et al*., 2021; Wang *et al*., 2015), gas sensor (Liu *et al*., 2021; Wang *et al*., 2020), electrochemical sensor (Durai *et al*., 2020; Ponnaiah *et al*., 2018),

solid-phase extraction (Jian *et al*., 2019; Rattanakunsong *et al*., 2020), magnetic solid-phase extraction (Florez *et al*., 2019; He *et al*., 2020), solid-phase microextraction (Sereshti *et al*., 2021; Sun *et al*., 2021) and stir bar sorptive extraction (Lei *et al*., 2016). According to the advantages of PANI, it has been applied for the fabrication of composite fluorescent probes to adsorb various organic compounds such as picric acid (Ahmed *et al*., 2021), nucleic acid (Liu *et al*., 2011), Malathion (Berhanu *et al*., 2022) and lomefloxacin **(Paper I)**.

4.4.2 Graphene oxide

Graphene oxide (GOx) is a carbon-based material with a two-dimensional structure, which is an oxidized form of graphene (Pena-Pereira *et al*., 2021; Tong *et al*., 2022). GOx contains a single layer of sp^2 hybridized carbon atom and a variety of remarkable functional groups including hydroxyl, carboxyl and epoxy **(Figure 14)** (Morales-Benítez *et al*., 2022). According to its structure, GOx can strongly interact with various organic compounds through hydrogen bonding, π-π and hydrophobic interactions (Naing *et al*., 2016). Furthermore, GOx has many extraordinary advantages such as huge surface area, high chemical and thermal stability and good dispersibility in aqueous solution or organic solvents (Naing *et al*., 2016; Nebol'sin *et al*., 2020).

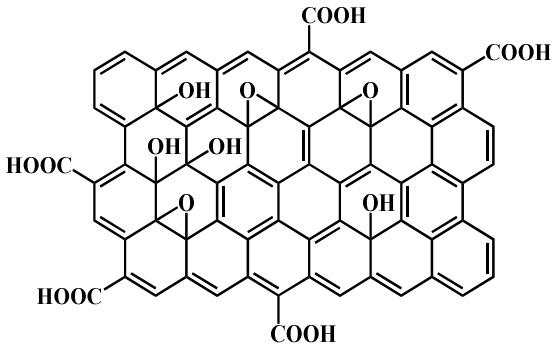

Figure 14 The structure of graphene oxide

In recent years, GOx has gained considerable attention as an adsorption material in numerous applications such as optosensor (Eskandari *et al*., 2017; Han *et al*., 2015; Li *et al*., 2017), electrochemical sensor (Afzali *et al*., 2020; Garcia *et al*., 2021), gas sensor (Biranje *et al*., 2022), solid-phase microextraction (Gao *et al*., 2021),

solid-phase extraction (Chullasat *et al*., 2017; Shi *et al*., 2015; Yu *et al*., 2018), matrix solid-phase dispersion (Chatzimitakos *et al*., 2019), and dispersive magnetic solid-phase extraction (Li *et al*., 2022; Majd *et al*., 2021; Manousi *et al*., 2020). For optosensor application, GOx has been utilized as a composite material in the fluorescent probes for the determination of various compounds such as virginiamycin (Li *et al*., 2017), 2,4,6-trichlorophenol (Han *et al*., 2015), cyanoguanidine (Liu *et al*., 2017), cefixime (Eskandari *et al*., 2017), zearalenone (Li *et al*., 2021) and lomefloxacin **(Paper I)**. The fabricated adsorbents using GOx in the D-MSPE process have been reported for the extraction and determination of multiple compounds such as polycyclic aromatic hydrocarbons (Majd *et al*., 2021; Zhang *et al*., 2017), triazine herbicides (Li *et al*., 2022), sulfonamides (Han *et al*., 2022), fluoroquinolones (Klongklaew *et al*., 2020) and phthalate esters **(Paper III)**.

4.4.3 Metal organic framework

Metal organic framework (MOF) is a hybrid crystalline porous material formed by coordinating inorganic metal ions with organic ligands (Li *et al*., 2022; Zheng *et al*., 2022). Among a variety of MOFs, Materials of Institute Lavoisier-101 (MIL-101) is an attractive type because it has many outstanding advantages including huge surface area, adjustable pore size and excellent stability in aqueous solution (Hou *et al*., 2020; Jia *et al*., 2020; Mertsoy *et al*., 2021). MIL-101(Cr) is generally formed by chromium and terephthalic acid ligands through coordinate covalent bonds **(Figure 15)**, which can effectively adsorb multiple organic compounds via hydrophobic and π-π interactions (Huo *et al*., 2012).

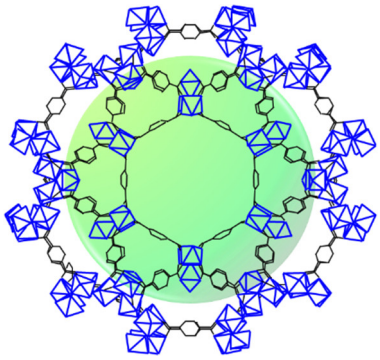

Figure 15 The crystal structure of MIL-101

Currently, MIL-101 has gained increasing attention as an adsorption material in several applications such as optosensor (Ding *et al*., 2022; Liu *et al*., 2018), electrochemical sensor (Cheng *et al*., 2020; Zhang *et al*., 2017), dispersive magnetic solid-phase extraction (Huo *et al*., 2012; Jia *et al*., 2020; Liang *et al*., 2018), dispersive micro-solid phase extraction (Jia *et al*., 2017; Li *et al*., 2015) and solid-phase microextraction (Xie *et al*., 2015). The fabricated fluorescent probes composited with MIL-101 for optosensor have been reported for the determination of multiple compounds such as enrofloxacin (Ding *et al*., 2022), pyrraline (Liu *et al*., 2018), 2,4-dinitrophenol (Yang *et al*., 2021), mafenide and sulfisoxazole **(Paper II)**. For the application of the D-MSPE, MIL-101 has been popularly utilized as an adsorption material for the fabrication of composite adsorbent to effectively extract and determine various compounds such as polycyclic aromatic hydrocarbons (Huo *et al*., 2012), phenytoin sodium (Jia *et al*., 2020), triazine herbicides (Liang *et al*., 2018), nonsteroidal anti-inflammatory drugs (Wang *et al*., 2017) and phthalate esters **(Paper III)**.

4.4.4 Mesoporous carbon

Mesoporous carbon (MPC) is a carbon-based material with pore diameters in the range of 2 to 50 nm, leading to a tremendously high surface area **(Figure 16)** (Holban *et al*., 2016; Rahman *et al*., 2021). According to its hydrophobic property, MPC can strongly adsorb the target compounds via hydrophobic interaction (Jeong *et al*., 2020). Furthermore, MPC has remarkable features including high pore volume, cost-effectiveness, and good chemical and thermal stability (Jeong *et al*., 2020; Liu *et al*., 2022). The arrangement of MPC has uniform worm-like particles with a pore structure as displayed in **Figure 17**.

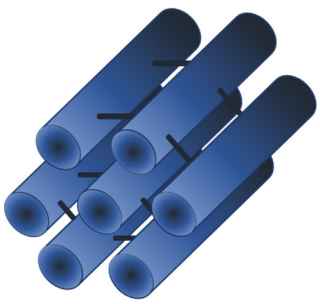

Figure 16 The structure of mesoporous carbon (CMK-3)

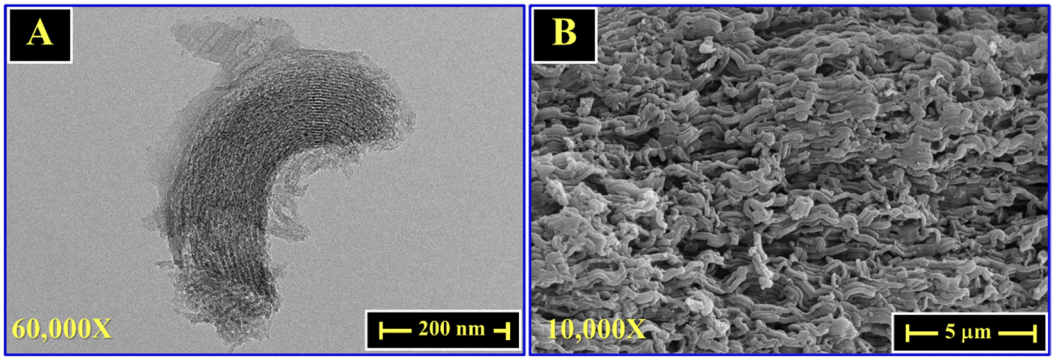

Figure 17 TEM image of MPC at 60000X (A) and SEM image of MPC at 10000X (B) (Reprinted from Orachorn and coworker, 2022; copyright with permission from Springer Nature) (Orachorn *et al*., 2022)

According to its distinctive properties, MPC has been widely employed as an adsorption material in numerous sample preparation methods such as dispersive magnetic solid-phase extraction (Yang *et al*., 2016; Zhang *et al*., 2021), solid-phase microextraction (Anbia *et al*., 2018; Saraji *et al*., 2016) and micro-solid-phase extraction (Lashgari *et al*., 2017). The magnetic adsorbents composited with MPC have been reported for the adsorption of multiple organic compounds such as phthalate esters (Yang *et al*., 2016), parabens (Zhang *et al*., 2021), dibenzothiophene (Farzin Nejad *et al*., 2013) and nonsteroidal anti-inflammatory drugs **(Paper IV)**.

5. Fluorescence measurement

5.1 Fluorescence measurement of the nanocomposite fluorescent probe

The intensity of fluorescence emission is measured and performed by a spectrofluorometer using the fabricated composite fluorescent probe as illustrated in **Figure 18**. Initially, the nanocomposite fluorescent probe is dispersed in the buffer solution at an appropriate pH value and thoroughly mixed with standard or sample solution. The mixture solution is subsequently incubated for an adequate period to achieve complete binding between the fluorescent probe and target compound. Then, the resulting solution is put into a quartz cell before being measured by an instrument. The detection of the target compound is performed by setting a suitable excitation wavelength for the fabricated fluorescent probe and recording a wide range of emission wavelengths to obtain the fluorescence emission intensity of the fabricated fluorescent

probe. The excitation wavelength of the fabricated PANI-GOx-MIP-CdTe QDs for lomefloxacin detection **(Paper I)** was fixed at 355 nm, and emission wavelengths were recorded ranging from 400 to 700 nm.

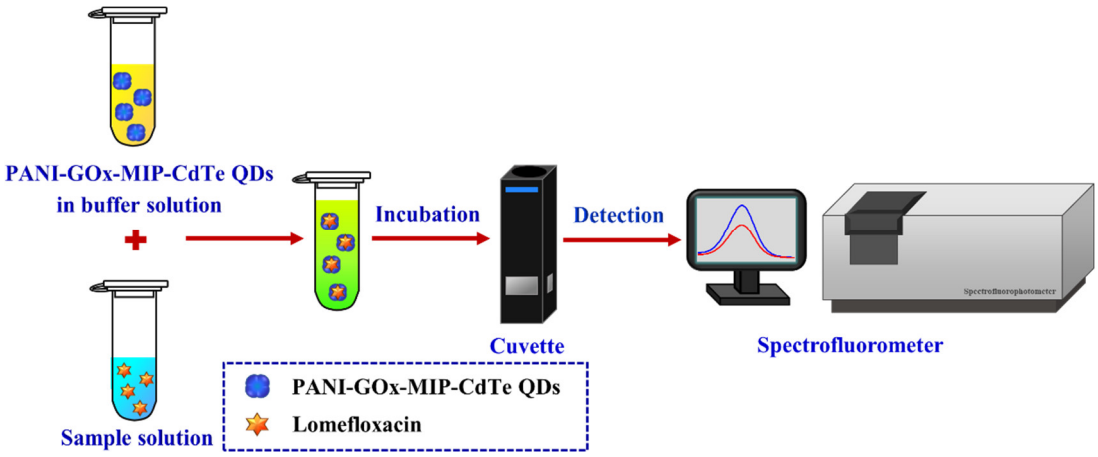

Figure 18 Detection procedure of target compounds using the nanocomposite fluorescent probes (Orachorn *et al*., 2019)

5.2 Fluorescence measurement of the dual magnetic composite fluorescent probes

The dual magnetic composite fluorescent probes are employed to enrich and simultaneously detect two target compounds. The procedure of fluorescence measurement using the developed dual optosensing probes is performed as demonstrated in **Figure 19**. Firstly, buffer solution with a suitable pH value is used to disperse dual fluorescent probes before being mixed with standard or sample solution. To accomplish full adsorption between target compounds and dual nanoprobes, the above mixture solution is incubated under stirring for a proper time. Then, the fluorescent probes adsorbed with target compounds are isolated by an external magnet, and residual solution is removed. Deionized water is subsequently put into the nanoprobes, and the obtained mixture is transferred to a quartz cuvette prior to instrumental measurement. The fluorescence emission intensities of dual probes are investigated and carried out by fixing a proper excitation wavelength for the fabricated nanoprobes and measuring emission wavelengths in a wide range. For the detection of mafenide and sulfisoxazole by the developed dual magnetic probes of MIL101-MMIP-GQDs and MIL101-MMIP-CdTe QDs **(Paper II)**, the excitation wavelength was set at 355 nm, and the emission wavelengths were recorded in the range of 400 to 700 nm.

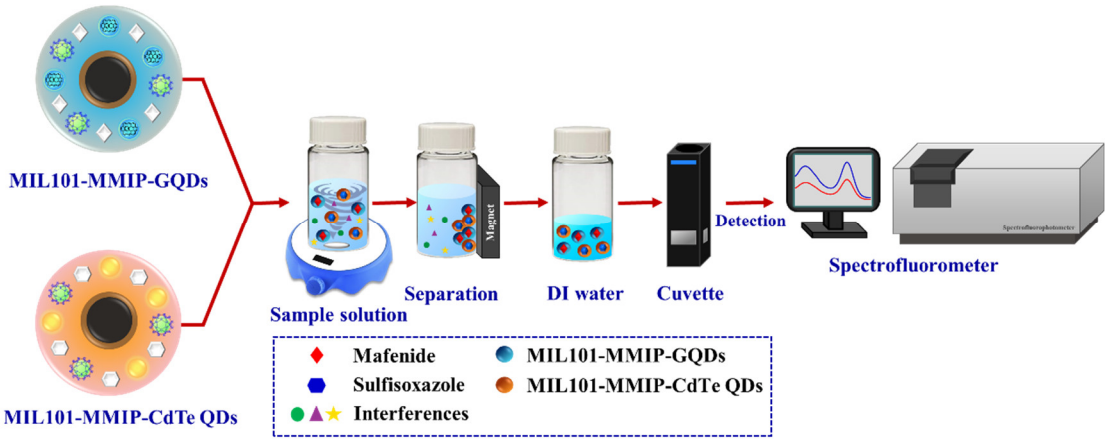

Figure 19 The fluorescence measurement of the dual magnetic composite fluorescent probes for the detection of mafenide and sulfisoxazole (Orachorn *et al*., 2021)

6. Fluorescence quenching mechanism

The fluorescence quenching of the composite fluorescent probes by target compounds is driven by hydrogen bonding between target compounds and amino groups (-NH_2) of the functional monomer (APTES) on the surface of the fluorescent probes. This leads to electron transfer from the conduction band of QDs to the lowest unoccupied molecular orbitals of target compounds, resulting in fluorescence quenching **(Figure 20)** (The Huy *et al*., 2014).

The mechanism of fluorescence quenching can be further confirmed by considering the UV-Vis absorption spectra of target compounds and the fluorescence emission spectra of the fabricated fluorescent probes. As demonstrated in **Figure 21**, the absorption spectrum of lomefloxacin did not overlap with the emission spectrum of the PANI-GOx-MIP-CdTe QDs probe **(Paper I)**. This result implied that the fluorescence quenching of the PANI-GOx-MIP-CdTe QDs nanoprobe by lomefloxacin was not caused by energy transfer but was based on electron transfer (Lu *et al*., 2017; Zhang *et al*., 2016).

The fluorescence quenching efficiency of the composite fluorescent probes by target compounds can be quantified according to the Stern-Volmer equation as follows (Kim *et al*., 2016):

$$\frac{F0}{F} = 1 + K_{SV}[C]$$

Where F0 and F are the fluorescence emission intensity of the nanoprobes in the absence and presence of target compounds, respectively. K_{SV} is the Stern-Volmer constant and [C] is the concentration of target compounds.

The sensitivity of the nanoprobes for the detection of target compounds can be described in terms of K_{SV}. In addition, the imprinting factor (IF) can be utilized to evaluate the specificity of the fabricated fluorescent probes and calculated by comparing the K_{SV} of molecularly imprinted polymer (MIP) and non-imprinted polymer (NIP) as following equation (Ding *et al*., 2017):

$$IF = \frac{K_{SV(MIP)}}{K_{SV(NIP)}}$$

In this thesis, the IF of the PANI-GOx-MIP-CdTe QDs probe **(Paper I)**, MIL101-MMIP-GQDs and MIL101-MMIP-CdTe QDs probes **(Paper II)** were 16.7, 5.1 and 4.4, respectively. These results indicated that the fabricated fluorescent probes were highly specific toward the target compounds.

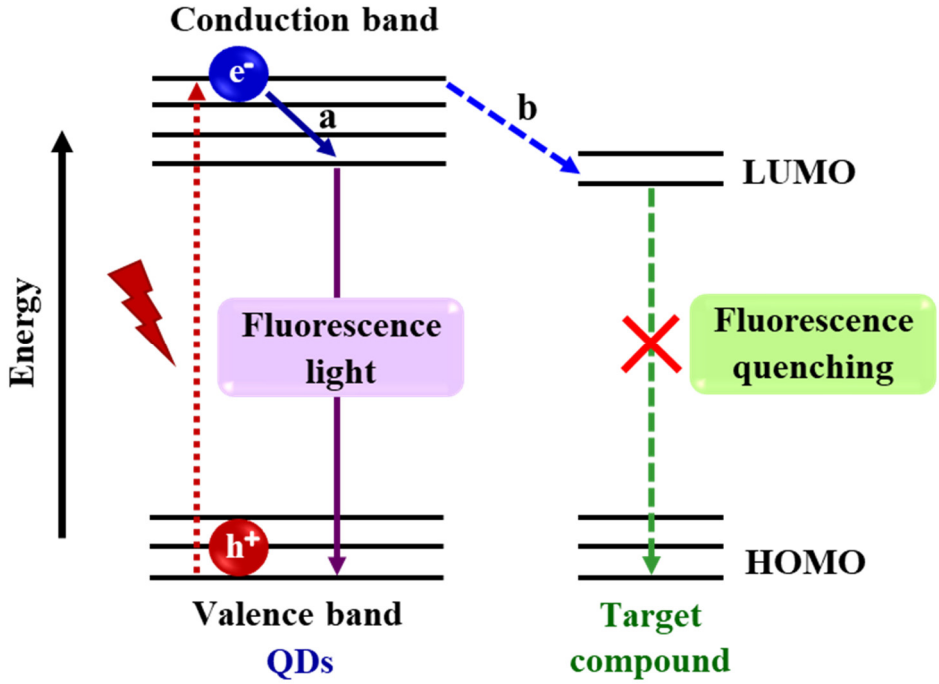

Figure 20 The fluorescence quenching mechanism of the fluorescent probe in the absence (a) and presence (b) of target compound

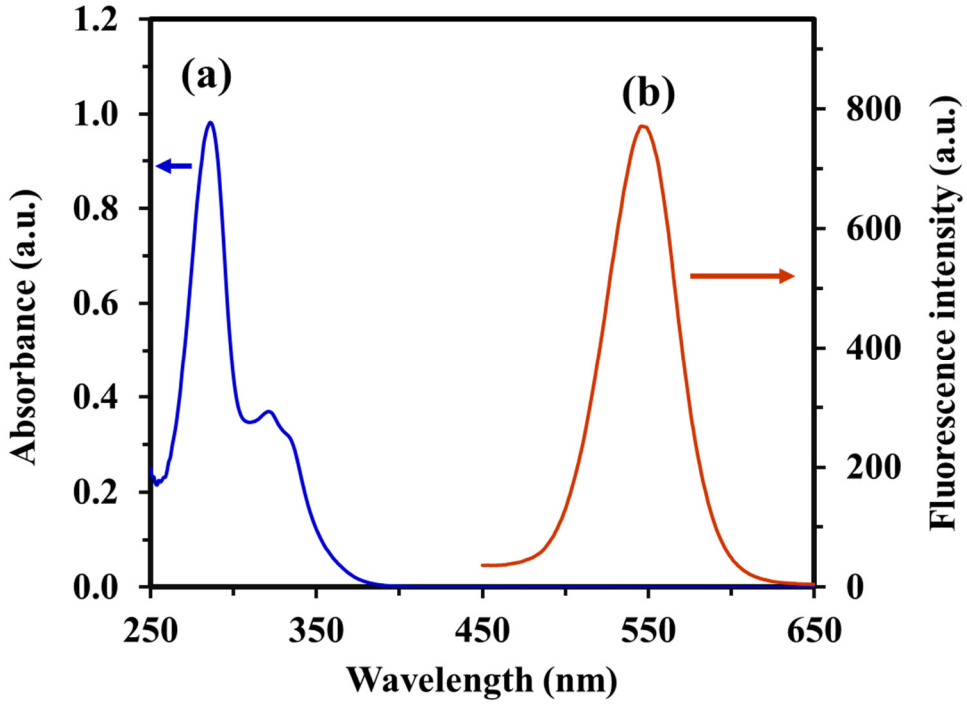

Figure 21 The UV-Vis absorption spectrum of lomefloxacin (a) and the fluorescence emission spectrum of the PANI- GOx-MIP-CdTe QDs nanoprobe (b) (Reprinted from Orachorn and coworker, 2019; copyright with permission from Elsevier) (Orachorn *et al*., 2019)

7. Optimization of the developed methods

7.1 Optimization of the fabricated fluorescent probes and determination condition

The fluorescence quenching capability of the composite fluorescent probes for the determination of target organic compounds depends on a variety of factors including incubation time, pH of dispersing solution and mole ratio of template to monomer to cross-linker. These factors are examined by considering the most excellent sensitivity (quenching efficiency) with the fastest measurement time to be optimal values for the determination condition.

7.1.1 Incubation time

The incubation time is the time required for the binding between specific imprinted cavities of the fluorescent probes and target compounds prior to measuring fluorescence to ensure complete adsorption at the fastest time. This factor was tested and performed by measurement of quenching efficiency (F0/F), and the shortest adsorption time that offered the best quenching efficiency was chosen as the most appropriate period. The optimal incubation time of the fabricated PANI-GOx-MIP-CdTe QDs probe and dual nanohybrid magnetic fluorescent probes (MIL101-MMIP-GQDs and MIL101-MMIP-CdTe QDs) was 20 min **(Paper I)** and 15 min **(Paper II)** for the detection of lomefloxacin and sulfonamides, respectively.

7.1.2 pH of dispersing solution

Before being bound with the target compound, the composite fluorescent probe must be prepared in the dispersing solution at a suitable pH due to the surrounding environment can affect the sensitivity and stability of the fluorescent probe for the detection of the target compound. To acquire the best binding efficiency between nanoprobe and target compound, the effect of pH is examined by dispersing the fabricated fluorescent probe in buffer solution at various pH and considering the sensitivity of the nanoprobe for the target compound detection. The reduced sensitivity of the fluorescent probe can occur in both extreme acidity and basicity of dispersing solution. The reason for lower sensitivity at low pH is the protonation of amino groups of both the target compound and specific imprinted cavities on the polymer layer of the nanoprobe by hydrogen ions, leading to reducing the possible interaction of hydrogen

bonding and causing the electrostatic repulsion between the nanoprobe and target compound. In a highly alkaline solution, sensitivity is also reduced because this condition can damage the silica structure of the polymer layer, resulting in less stability of the sensing probe. Considering the highest sensitivity, phosphate buffer was used as the most suitable dispersing solution at pH 8.0 for the PANI-GOx-MIP-CdTe QDs probe **(Paper I)** and pH 6.0 for the dual magnetic fluorescent probes of MIL101-MMIP-GQDs and MIL101-MMIP-CdTe QDs **(Paper II)** to detect lomefloxacin and sulfonamides (mafenide and sulfisoxazole), respectively.

7.1.3 Mole ratio of template to monomer to cross-linker

The effective fabrication of imprinted cavities of the composite fluorescent probes relies on the appropriate quantity of the MIP composition. The main component of the MIP probes includes a template molecule, a functional monomer and a cross-linker. Therefore, it is crucial to examine and optimize the mole ratio of template to monomer to cross-linker based on considering the best sensitivity of nanoprobes for the detection of target compounds. The functional monomer is a vital role used for binding interactions around template molecules prior to polymerization, leading to the subsequent formation of specific imprinted cavities for the templates. In this thesis, 3-aminopropyltriethoxysilane (APTES) was employed as a functional monomer in the MIP process because its structure has an amino group that can strongly interact with templates (lomefloxacin, mafenide and sulfisoxazole) via hydrogen bonding. The use of a low quantity of monomer leads to reduced sensitivity of the composite MIP probes because a number of generated imprinted cavities are not enough for the target compounds. The excessive amount of monomer also enables low sensitivity of nanoprobes since non-imprinted cavities are generated that can hinder the binding ability between specific imprinted sites and target compounds. The cross-linker is also an important factor to create a strong three-dimensional structure of a highly cross-linked polymer with numerous specific imprinted cavities. In this thesis, the MIP nanoprobes were fabricated using tetraethyl orthosilicate (TEOS) as a cross-linker. The decreasing sensitivity of the composite probe affected by a low quantity of cross-linker occurs due to the instability of the polymer layer. In contrast, the use of an excessive amount of cross-linker produced an extremely thick polymer structure, resulting in the

blockage of specific imprinted cavities and subsequent reducing sensitivity of the sensing probe. The optimum mole ratio of template to monomer to cross-linker for the fabrication of composite probes was 1:8:20 for the PANI-GOx-MIP-CdTe QDs probe **(Paper I)**, 1:30:15 for the MIL101-MMIP-GQDs probe and 1:8:25 for the MIL101-MMIP-CdTe QDs probe **(Paper II)**.

7.2 Optimization of the fabricated adsorbents and extraction condition

Several factors affect the extraction efficiency of the composite adsorbents for the extraction of target compounds including dosage of adsorbent, extraction time, desorption condition, sample volume, stirring rate and sample pH. These factors are tested and optimized by considering the best recovery coupled with the fastest operation time and the lowest solvent consumption.

7.2.1 Dosage of adsorbent

The use of different quantities of adsorbents can impact the adsorption capacity for the extraction of target compounds. The dosages of composite adsorbents utilized in D-MSPE were examined and optimized to achieve the best extraction recoveries with the least amount of adsorbents **(Table 1)**. The most proper quantities of adsorbents were 0.30 g for the GOx/MIL-101/Fe_3O_4-SiO_2 alginate hydrogel fiber adsorbent **(Paper III)** and 0.10 g for the GQDs/Fe_3O_4-SiO_2/MPC/MIP adsorbent **(Paper IV)**.

Table 1 Effect of adsorbent dosage of the fabricated composite adsorbents on the extraction recoveries of PAEs and NSAIDs

Composite adsorbent	Target analytes	Study range of adsorbent dosage (g)	Optimal adsorbent dosage (g)	Recovery (%)	RSD (%)	References
GOx/MIL-101/ Fe_3O_4-SiO_2 alginate hydrogel fiber	PAEs	0.10-1.0	0.30	85.2-91.4	<4.0	**Paper III**
GQDs/Fe_3O_4-SiO_2/MPC/MIP	NSAIDs	0.050-0.50	0.10	80.0-92.9	<4.0	**Paper IV**

7.2.2 Extraction time

In the adsorption step, the extraction time is an important factor influencing the binding ability between target compounds and the magnetic composite adsorbent. To acquire the best extraction efficiency with the fastest equilibrium time, the extraction recoveries of the developed D-MSPE methods using the developed composite adsorbents were evaluated at different times. The suitable extraction time with the highest recovery of PAEs and NSAIDs were 20 min **(Paper III)** and 30 min **(Paper IV)**, respectively. The extraction time on the extraction recoveries of target compounds extracted by the developed method was verified and optimized as illustrated in **Table 2**.

Table 2 Effect of extraction time on the extraction recoveries of PAEs and NSAIDs extracted by D-MSPE with the fabricated composite adsorbents

Composite adsorbent	Target analytes	Extraction time range (min)	Optimal extraction time (min)	Recovery (%)	RSD (%)	References
GOx/MIL-101/ Fe_3O_4-SiO_2 alginate hydrogel fiber	PAEs	5-30	20	83.5-94.3	<6.0	**Paper III**
GQDs/Fe_3O_4-SiO_2/MPC/MIP	NSAIDs	10-50	30	85.1-93.5	<3.0	**Paper IV**

7.2.3 Desorption condition

In the desorption step of D-MSPE, the elution efficiency of target compounds from the composite adsorbents depends on several important factors, consisting of type of desorption solvent, desorption volume and desorption time. Different kinds of solvents with various polarities are considered and examined as suitable desorption solvent according to the theory of like dissolves like with target compounds **(Table 3)** (Ning *et al*., 2022). Acetonitrile offered the best extraction recoveries of all target PAEs **(Paper III)**, while methanol provided the highest values

of three target NSAIDs **(Paper IV)**. These desorption solvents can greatly break the possible interactions occurring between the developed composite adsorbents and target compounds. Considering the excessive solvent consumption, the varied volume of elution solvent was optimized **(Table 4)**. The optimal volume of acetonitrile for the GOx/MIL-101/Fe_3O_4-SiO_2 alginate hydrogel fiber adsorbent **(Paper III)** and methanol for the GQDs/Fe_3O_4-SiO_2/MPC/MIP adsorbent **(Paper IV)** were 2.0 and 4.0 mL, respectively. To acquire the best elution efficiency with the shortest elution period, different times during the desorption process were also investigated and optimized **(Table 5)**. The most appropriate times were 15 and 20 min to completely desorb PAEs **(Paper III)** and NSAIDs **(Paper IV)** from the fabricated composite adsorbents, respectively.

Table 3 Effect of various desorption solvents on the extraction recoveries of PAEs and NSAIDs extracted by the developed D-MSPE

Composite adsorbent	Target analytes	Type of desorption solvent	Suitable desorption solvent	Recovery (%)	RSD (%)	References
GOx/MIL-101/Fe_3O_4-SiO_2 alginate hydrogel fiber	PAEs	Toluene Dichloromethane Ethyl acetate Methanol Acetone Acetonitrile	Acetonitrile	81.6-91.1	<7.0	**Paper III**
GQDs/Fe_3O_4-SiO_2/MPC/ MIP	NSAIDs	Methanol Ethanol Acetonitrile Acetone Ethyl acetate	Methanol	80.5-89.3	<5.0	**Paper IV**

Table 4 Effect of volume of the elution solvent on the extraction recoveries of PAEs and NSAIDs

Composite adsorbent	Target analytes	Study range (mL)	Optimum (mL)	Recovery (%)	RSD (%)	References
GOx/MIL-101/Fe_3O_4-SiO_2 alginate hydrogel fiber	PAEs	0.5-5.0	2.0	85.0-95.0	<4.0	**Paper III**
GQDs/Fe_3O_4-SiO_2/MPC/MIP	NSAIDs	1.0-6.0	4.0	85.1-94.6	<3.0	**Paper IV**

Table 5 Effect of desorption times on the extraction recoveries of PAEs and NSAIDs during the elution process

Composite adsorbent	Target analytes	Study range of desorption time (min)	Suitable desorption time (min)	Recovery (%)	RSD (%)	References
GOx/MIL-101/Fe_3O_4-SiO_2 alginate hydrogel fiber	PAEs	5-25	15	85.9-93.5	<6.0	**Paper III**
GQDs/Fe_3O_4-SiO_2/MPC/MIP	NSAIDs	10-50	20	86.5-94.6	<4.0	**Paper IV**

7.2.4 Sample volume

Sample volume is an essential parameter affecting both the extraction efficiency and the enrichment factor. The improvement of the enrichment of target compounds can be performed by the increasing volume of sample. However, the excessive volume of sample solution can cause decreasing recoveries due to the adsorption capacity of the composite adsorbent is not enough to adsorb all target compounds. Therefore, the effect of sample volume was optimized as demonstrated in **Table 6**. According to the highest sample volume providing the best extraction recoveries, 10.0 mL was selected as the most appropriate volume of sample solution for the extraction of PAEs **(Paper III)** and NSAIDs **(Paper IV)**.

Table 6 Effect of sample volume on the extraction recoveries of PAEs and NSAIDs extracted by D-MSPE using the fabricated composite adsorbents

Composite adsorbent	Target analytes	Study range (mL)	Optimum (mL)	Recovery (%)	RSD (%)	References
GOx/MIL-101/Fe_3O_4-SiO_2 alginate hydrogel fiber	PAEs	5.0-20.0	10.0	86.1-92.6	<5.0	**Paper III**
GQDs/Fe_3O_4 -SiO_2/MPC/ MIP	NSAIDs	5.0-20.0	10.0	80.1-84.0	<4.0	**Paper IV**

7.2.5 Stirring rate

In the adsorption procedure of D-MSPE, one of the necessary factor is the stirring rate affecting the dispersing ability of the magnetic composite adsorbents in the sample solution to adsorb target analytes. The suitable stirring rate leads to improving the mass transfer of the target compounds from solution to the composite adsorbents. In the case of low stirring rate, the extraction recoveries are low because the composite adsorbents cannot sufficiently disperse throughout the sample solution.

This impacts the low mass transfer of target compounds to the composite adsorbents. Furthermore, the low recoveries are also obtained at too high stirring speed because there is strong and excessive contact between the composite adsorbents and the container wall, which can not only damage the adsorbents but also decrease their reusability. The stirring rate at 1000 rpm offered the best extraction efficiency for both the GOx/MIL-101/Fe_3O_4-SiO_2 alginate hydrogel fiber adsorbent **(Paper III)** and the GQDs/Fe_3O_4-SiO_2/MPC/MIP adsorbent **(Paper IV)**. Thus, 1000 rpm was selected as the optimal value in the adsorption process **(Table 7)**.

Table 7 Effect of stirring rate on the extraction recoveries of PAEs and NSAIDs during the adsorption step in the D-MSPE

Composite adsorbent	Target analytes	Study range (rpm)	Optimum (rpm)	Recovery (%)	RSD (%)	References
GOx/MIL-101/Fe_3O_4-SiO_2 alginate hydrogel fiber	PAEs	500-1500	1000	80.0-86.2	<3.0	**Paper III**
GQDs/Fe_3O_4-SiO_2/MPC/MIP	NSAIDs	500-1500	1000	80.0-82.3	<4.0	**Paper IV**

7.2.6 Sample pH

The different pH of sample solution can impact both the stability of the composite adsorbent and the binding efficiency of the target compounds on the composite adsorbent. For the adsorption of PAEs, the GOx/MIL-101/Fe_3O_4-SiO_2 alginate hydrogel fiber adsorbent **(Paper III)** was employed and examined in sample solution at pH ranged from 3.0 to 11.0. The extraction recoveries of PAEs did not reduce in the pH range of 3.0 to 9.0, whereas the decreasing extraction efficiency occurred at pH 11.0 because PAEs were deprotonated to anionic form leading to reducing the possible interactions between the composite hydrogel fiber adsorbent and

PAEs. In case of the GQDs/Fe_3O_4-SiO_2/MPC/MIP adsorbent for the adsorption of NSAIDs **(Paper IV)**, the effect of pH varied from 3.0 to 11.0 was investigated, and the extraction efficiency was not significantly changed in the range of 5.0 to 9.0. Both extreme acidity and basicity of solution led to the reducing recoveries due to the change of chemical forms of the surface of the composite MMIP adsorbent and NSAIDs. Target NSAIDs were protonated to cationic form at pH 3.0, while the deprotonation of target NSAIDs occurred and the silica layer of composite MMIP adsorbent was ionized at pH 11.0. These changing chemical structures can impact the adsorption ability of target NSAIDs on the composite MMIP adsorbent. However, the pH of real samples (mineral water, vitamin water, juice, tea and milk) are not either lower pH 5.0 or higher pH 9.0. Therefore, the pH of sample was not necessary to be adjusted for both **Paper III** and **Paper IV** before extracting target compounds by composite adsorbents **(Table 8)**.

Table 8 Effect of sample pH on the recoveries of PAEs and NSAIDs using the developed composite adsorbents

Composite adsorbent	Target analytes	Study range	Optimum	Recovery (%)	RSD (%)	References
GOx/MIL-101/Fe_3O_4-SiO_2 alginate hydrogel fiber	PAEs	3.0-11.0	3.0-9.0	83.3-90.6	<7.0	**Paper III**
GQDs/Fe_3O_4-SiO_2/MPC/MIP	NSAIDs	3.0-11.0	5.0-9.0	86.9-95.8	<5.0	**Paper IV**

8. Analytical performance

The performance of both the developed optosensor using the fabricated fluorescent probes and the developed D-MSPE using the composite adsorbents were verified under optimal conditions. Linearity, limit of detection (LOD), limit of quantification (LOQ), sensitivity, accuracy, precision, reproducibility, reusability and selectivity were evaluated.

8.1 Linearity

The linearity is the capability range of an analytical approach to produce acceptable test results, which are directly proportional to target compound concentration in real samples (APVMA, 2004). The linearity is generally examined by plotting an ability range between average values of the analytical response (y-axis) and the concentration of target compounds (x-axis). The evaluation of linearity is carried out by measuring a minimum of five different concentrations of target compounds (ICH, 2005). The acceptable linear regression is obtained by considering a coefficient of determination (R^2) greater than 0.99 (AOAC, 2013). For optosensor, linearity is plotted between the quenching efficiency (F0/F) and the concentration of lomefloxacin (μg L^{-1}) **(Paper I)**, mafenide and sulfisoxazole (μg L^{-1}) **(Paper II)**. For chromatographic method, linearity is plotted between the peak area and the concentration of phthalate esters (μg L^{-1}) **(Paper III)** and nonsteroidal anti-inflammatory drugs (μg L^{-1}) **(Paper IV)**. The linearity of all sub-projects provided acceptable coefficient of determination (R^2) which were higher than 0.99, indicating that both the developed optosensor and chromatographic method exhibited good linearity for the determination of target compounds **(Table 9)**.

Table 9 Linearity and coefficient of determination (R^2) of the developed methods

Analytical method	Samples	Analytes	Linear range ($\mu g\ L^{-1}$)	R^2	Reference
PANI-GOx-MIP-CdTe QDs (Optosensor)	Milk, chicken meat and egg	Lomefloxacin	0.10-50.0	0.9999	**Paper I**
MIL101-MMIP-GQDs and MIL101-MMIP-CdTe QDs (Optosensor)	Milk	Mafenide and sulfisoxazole	0.10-25.0	0.9980-0.9994	**Paper II**
GOx/MIL-101/Fe_3O_4-SiO_2 alginate hydrogel fiber (HPLC-DAD)	Juice, tea, vitamin water and mineral water	PAEs	3.0-250.0	0.9980-0.9990	**Paper III**
GQDs/Fe_3O_4-SiO_2/MPC/MIP (HPLC-DAD)	Milk	NSAIDs	0.5-100.0	0.9973-0.9996	**Paper IV**

8.2 Limit of detection and limit of quantification

The limit of detection (LOD) is assigned as the minimum concentration of the target compound, which can be measured by a reliable analytical method under the optimal condition (Taverniers *et al*., 2004). The limit of quantification (LOQ) is specified as the minimum concentration of the target compound, which can be quantitatively evaluated under the optimal condition with acceptable accuracy and precision (Devreese *et al*., 2012). The estimation of LOD and LOQ can be performed with numerous methods depended on the used analytical techniques. In this thesis, LODs and LOQs were evaluated using two approaches according to the International Conference of Harmonization (ICH) guideline (ICH, 2005).

For optosensor using the fabricated composite fluorescent probe to determine lomefloxacin **(Paper I)**, mafenide and sulfisoxazole **(Paper II)**, LOD and LOQ were calculated based on the standard deviation of the signal response and the slope of the linearity as the following equation:

$$LOD = \frac{3S_b}{m}$$

$$LOQ = \frac{10S_b}{m}$$

Where S_b is the standard deviation of the signal response of blank (n = 20) and m is the slope of the linearity (sensitivity).

For the dispersive magnetic solid-phase extraction to determine phthalate esters **(Paper III)** and nonsteroidal anti-inflammatory drugs **(Paper IV)**, LOD and LOQ were evaluated based on the signal to noise ratio (S/N) of 3 (S/N≥3) and 10 (S/N≥10), respectively. The developed methods produced low LODs and LOQs, indicating that these methods can be applied to determine target compounds in real samples at ultra-trace levels **(Table 10)**.

Table 10 LODs and LOQs of the developed methods

Analytical method	Analytes	LOD ($\mu g\ L^{-1}$)	LOQ ($\mu g\ L^{-1}$)	Reference
PANI-GOx-MIP-CdTe QDs (Optosensor)	Lomefloxacin	0.07	0.22	**Paper I**
MIL101-MMIP-GQDs and MIL101-MMIP-CdTe QDs (Optosensor)	Mafenide	0.10	0.34	**Paper II**
	Sulfisoxazole	0.10	0.34	
GOx/MIL-101/Fe_3O_4-SiO_2 alginate hydrogel fiber (HPLC-DAD)	BBP	3.0	10.0	**Paper III**
	DBP	3.0	10.0	
	DEHP	5.0	15.0	
	DNOP	5.0	15.0	
GQDs/Fe_3O_4-SiO_2/MPC/MIP (HPLC-DAD)	Flurbiprofen	1.0	3.0	**Paper IV**
	Diflunisal	0.5	2.0	
	Mefenamic acid	0.5	2.0	

8.3 Sensitivity

The sensitivity of an analytical method is the change in the analytical response, which directly corresponds with the variation in the concentration of target compounds (Taverniers *et al*., 2004). In this thesis, the sensitivity of the developed methods was determined from the slope of linearity.

8.4 Accuracy

The accuracy of an analytical technique is assigned as the degree to which the defined value of the target compound in the sample is closely correlated with its actual value (APVMA, 2004). Recovery can be referred to the accuracy of the developed methods, which was carried out by comparing the acquired signal responses from the spiked sample and the standard solution at least three different concentrations and a minimum of three replications. The relative recovery was evaluated according to the following equation (AOAC, 2016):

$$\text{Relative recovery (\%)} = \frac{C_s - C_n}{C_a} \times 100$$

Where C_s is the concentration of the target compound in spiked sample, C_n is the concentration of the target compound in non-spiked sample and C_a is the concentration of the target compound added to the sample.

The acceptable recovery generally depends on both the concentration level of the target compound added to the sample and the used analytical techniques. According to the Association of Official Analytical Chemists (AOAC) guideline for ppb level, the recommended recovery values are in the range of 80 to 110% (AOAC, 2016). In this thesis, satisfactory recoveries of target analytes in real samples were acquired in the range of 80.4 to 99.6%, which were in the acceptable range **(Table 11)**.

Table 11 Recoveries of the developed methods

Analytical method	Samples	Analytes	Added ($\mu g\ L^{-1}$ or $\mu g\ kg^{-1}$)	Recovery (%)	Reference
PANI-GOx-MIP-CdTe QDs (Optosensor)	Milk, chicken meat and egg	Lomefloxacin	0.5 1.0 10.0 50.0	81.5-99.6	**Paper I**
MIL101-MMIP-GQDs and MIL101-MMIP-CdTe QDs (Optosensor)	Milk	Mafenide and sulfisoxazole	1.0 5.0 10.0 25.0	80.4-97.9	**Paper II**
GOx/MIL-101/ Fe_3O_4-SiO_2 alginate hydrogel fiber (HPLC-DAD)	Juice, tea, vitamin water and mineral water	PAEs	25.0 50.0 75.0 100.0	80.7-89.9	**Paper III**
GQDs/Fe_3O_4-SiO_2/MPC/MIP (HPLC-DAD)	Milk	NSAIDs	10.0 25.0 50.0	81.4-93.7	**Paper IV**

8.5 Precision

The precision of an analytical technique is specified as the degree of agreement to which the repeatability is measured under the optimal condition (Francotte *et al*., 1996). The percentage of relative standard deviation (RSD) can be referred to the precision of the developed methods, and it can be estimated using the equation as follows (AOAC, 2016):

$$\text{RSD (\%)} = \frac{\text{SD}}{\bar{X}} \times 100$$

Where SD is the standard deviation, $\bar{X}$ is the mean of *n* measurements and *n* is the total number of measurements. According to the AOAC guideline, the acceptable precision in terms of RSD is lower than 11% for ppb level (AOAC, 2016).

In this thesis, the precision of the developed optosensors for the determination of lomefloxacin **(Paper I)**, mafenide and sulfisoxazole **(Paper II)** was carried out by the measurement of three replications using the fabricated composite fluorescent probes. The precision of the developed optosensors was acquired with RSDs lower than 7%. The repeatability of the developed dispersive magnetic solid-phase extraction for the determination of phthalate esters **(Paper III)** and nonsteroidal anti-inflammatory drugs **(Paper IV)** was evaluated in terms of the inter-day and intra-day precision. The inter-day precision was performed by evaluating RSDs of spiked samples on different days (*n*=6), and the acquired RSDs of the developed methods were less than 5%. The intra-day precision was examined by evaluating RSDs of spiked samples within the same day (*n*=6), and the obtained RSDs of the developed methods were less than 4%. The precision of all sub-projects exhibited acceptable RSDs which were lower than 7%, indicating that the developed methods can be utilized for the determination of target compounds with good precision.

8.6 Reproducibility

The reproducibility of an analytical approach is assigned as the degree of agreement among the acquired results of identical materials when they are synthesized using the same procedure under different conditions (Francotte *et al*., 1996). The reproducibility is normally represented as relative standard deviation. In this thesis, the reproducibility of the developed methods was investigated by the preparation of six different times of the composite fluorescent probes or adsorbents on six different days under the same experimental conditions. The RSDs for the fabrication of composite fluorescent probes **(Paper I-II)** and composite adsorbents **(Paper III-IV)** were lower than 3 and 5%, respectively **(Table 12)**. These RSD values were acceptable according to AOAC guideline (lower than 16% for ppb level) (AOAC, 2016), which confirmed that the fabrication procedures of the developed fluorescent probes and adsorbents have good reproducibility.

Table 12 Reproducibility of the developed fluorescent probes and adsorbents

Developed methods	Analytes	Number of batches	RSD (%)	Reference
PANI-GOx-MIP-CdTe QDs fluorescent probe	Lomefloxacin	6	<2	**Paper I**
MIL101-MMIP-GQDs fluorescent probe	Mafenide	6	<3	**Paper II**
MIL101-MMIP-CdTe QDs fluorescent probe	Sulfisoxazole	6	<3	
GOx/MIL-101/Fe_3O_4-SiO_2 alginate hydrogel fiber adsorbent	PAEs	6	<1	**Paper III**
GQDs/Fe_3O_4-SiO_2/MPC/MIP adsorbent	NSAIDs	6	<5	**Paper IV**

8.7 Reusability

The reusability of an adsorbent is an important factor to examine the stability of the adsorbent. If the adsorbents can be reused, the fabrication time and analysis cost can be reduced. In this thesis, the reusability of the developed adsorbents was investigated by repeating the D-MSPE process. After the adsorption and desorption of target compounds from the first cycle, the used adsorbents were thoroughly washed with suitable desorption solvent and water before use for the next extraction cycles to prevent any carry-over effect from target compounds. Considering the recoveries better than 80%, the composite GOx/MIL-101/Fe_3O_4-SiO_2 alginate hydrogel fiber **(Paper III)** and the composite GQDs/Fe_3O_4-SiO_2/MPC/MIP adsorbent **(Paper IV)** can be reused up to 16 and 6 times, respectively. These results implied that the developed adsorbents have good stability during the extraction process.

8.8 Selectivity

The selectivity of an analytical method is specified as the extent to which the developed method can be utilized to determine specific analytes in the complex mixture without matrix interferences from other constituents (APVMA, 2004). The selectivity of optosensor is examined with other compounds that have similar structures of target analytes (Taverniers *et al*., 2004). In this thesis, the selectivity of the developed optosensors was tested by comparing the sensitivity of the fabricated composite fluorescent probes after interaction with target analytes and other analog structures. The PANI-GOx-MIP-CdTe QDs probe **(Paper I)** and the dual magnetic probes of MIL101-MMIP-GQDs and MIL101-MMIP-CdTe QDs **(Paper II)** exhibited much higher sensitivity toward target analytes than their analog structures. These results indicated that the generated imprinted cavities in the polymer layer of the fabricated probes are high specificity for target analytes.

9. Concluding remarks

The optosensor and sample preparation methods were successfully developed in this thesis. The nanocomposite fluorescent probes based optosensor were effectively created and used for the determination of trace lomefloxacin, mafenide and sulfisoxazole in food and beverage samples. The composite magnetic adsorbents based dispersive magnetic solid-phase extraction were successfully fabricated and employed for the extraction and enrichment and coupled with high performance liquid chromatography for the separation, identification and determination of multiple organic compounds including phthalate esters and nonsteroidal anti-inflammatory drugs in beverage samples.

In the first part, the quantitative analysis of target compounds using optosensor was based on the fluorescence quenching of molecularly imprinted polymer composited with quantum dots when the target analytes bind to the specific imprinted cavities of composite fluorescent probes. The first sub-project was a highly selective and sensitive nanocomposite fluorescent probe of cadmium telluride quantum dots, polyaniline and graphene oxide incorporated into a molecularly imprinted polymer (PANI-GOx-MIP-CdTe QDs) for the lomefloxacin determination. This developed nanoprobe was effectively utilized to detect trace lomefloxacin in milk, chicken meat

and egg samples. It provided satisfactory recoveries in the range of 81.5 to 99.6%, RSDs lower than 7% and a very low detection limit of 0.07 μg L^{-1} for lomefloxacin **(Paper I)**. The second sub-project was dual nanohybrid magnetic composite probes of metal organic framework, graphene quantum dots and cadmium telluride quantum dots incorporated into a magnetic molecularly imprinted polymer (MIL101-MMIP-GQDs and MIL101-MMIP-CdTe QDs). These nanoprobes were utilized in an optosensing system for the simultaneous detection of mafenide and sulfisoxazole at ultra-trace levels. The integration of MIP, Fe_3O_4-SiO_2, GQDs, CdTe QDs and MIL-101 exhibited excellent selectivity, high sensitivity and good adsorption ability. The dual magnetic composite probes provided superior benefits over conventional fluorescent probes, including improved enrichment, easy separation of probes from the solution and ability of two target analytes to be detected simultaneously. The satisfactory recoveries of dual nanoprobes for the detection of ultra-trace mafenide and sulfisoxazole in milk samples were achieved from 80.4 to 97.9% with RSDs lower than 5%. The detection limits were 0.10 μg L^{-1} for mafenide and sulfisoxazole **(Paper II)**. The analytical results acquired from these developed optosensors not only agreed well with the analytical results obtained from conventional high performance liquid chromatography but also offered greater sensitivity. The unique properties of these developed optosensors are easy preparation, rapid and convenient detection, excellent selectivity, high sensitivity and cost-effectiveness.

In another part, the fabricated composite adsorbents were employed as dispersive magnetic solid-phase extraction adsorbents to pre-concentrate the target analytes and reduce other interferences prior to high performance liquid chromatography analysis. The third sub-project was a composite adsorbent of graphene oxide, metal organic framework and silica-modified magnetite (GOx/MIL-101/Fe_3O_4-SiO_2) embedded into alginate hydrogel fiber for the extraction and enrichment of phthalate esters. The combination of graphene oxide and metal organic framework improved the adsorption efficiency of phthalate esters via hydrogen bonding, hydrophobic and π-π interactions. The magnetic property of the composite hydrogel fiber encouraged rapid and convenient isolation of adsorbent from solution. The GOx/MIL-101/Fe_3O_4-SiO_2 alginate hydrogel fiber was applied to determine phthalate esters in tea, water and juice samples with recoveries higher than 80%, RSDs below 8%

and low limit of detections (3.0 to 5.0 μg L^{-1}). The developed composite hydrogel adsorbent can be used to extract phthalate esters up to 16 cycles **(Paper III)**. The fourth sub-project was graphene quantum dots, silica-modified magnetite and mesoporous carbon embedded into a molecularly imprinted polymer (GQDs/Fe_3O_4-SiO_2/MPC/MIP) for the extraction and pre-concentration of nonsteroidal anti-inflammatory drugs (NSAIDs). The fabricated adsorbent exhibited a highly specific binding toward diflunisal, flurbiprofen and mefenamic acid. The combination of graphene quantum dots and mesoporous carbon with a magnetic molecularly imprinted polymer enhanced the extraction efficiency of NSAIDs through hydrophobic interaction, π-π stacking and hydrogen bonding. This applied composite GQDs/Fe_3O_4-SiO_2/MPC/MIP adsorbent for the extraction of NSAIDs in milk samples not only provided high extraction efficiency with recoveries higher than 81%, good precision with RSDs below 7% and low detection limits (0.5 to 1.0 μg L^{-1}) but also can be reused up to 6 times **(Paper IV)**. These developed methods have numerous outstanding properties including high extraction efficiency, low detection limits, good accuracy and precision. Furthermore, the benefits of these composite magnetic adsorbents are simple fabrication, convenience to use, low solvent consumption, good stability and reproducibility.

These developed strategies of optosensor and sample preparation techniques were successfully developed and employed for the determination of trace organic compounds in food and beverage samples, including chicken meat, egg, milk, vitamin water, mineral water, juice and tea, with good analytical performances. Moreover, they can be modified for the future determination of other trace organic compounds in various matrix samples.

10. References

Adenuga, A.A., Ayinuola, O., Adejuyigbe, E.A., Ogunfowokan, A.O., Biomonitoring of phthalate esters in breast-milk and urine samples as biomarkers for neonates' exposure, using modified quechers method with agricultural biochar as dispersive solid-phase extraction absorbent. *Microchemical Journal* 152 (2020), 104277.

Afzali, M., Mostafavi, A., Shamspur, T., A novel electrochemical sensor based on magnetic core@shell molecularly imprinted nanocomposite (Fe_3O_4@graphene oxide@MIP) for sensitive and selective determination of anticancer drug capecitabine. *Arabian Journal of Chemistry* 13(8) (2020), 6626-6638.

Ahmed, H.M., Ghali, M., Zahra, W., Ayad, M.M., Preparation of carbon quantum dots/polyaniline nanocomposite: Towards highly sensitive detection of picric acid. *Spectrochimica Acta Part A: Molecular and Biomolecular Spectroscopy* 260 (2021), 119967.

Akbari, M., Rahimi-Nasrabadi, M., pourmasud, S., Eghbali-Arani, M., Banafshe, H.R., Ahmadi, F., Ganjali, M.R., Sobhani nasab, A., CdTe quantum dots prepared using herbal species and microorganisms and their anti-cancer, drug delivery and antibacterial applications; a review. *Ceramics International* 46(8) (2020), 9979-9989.

Alampanos, V., Samanidou, V., An overview of sample preparation approaches prior to liquid chromatography methods for the determination of parabens in biological matrices. *Microchemical Journal* 164 (2021), 105995.

Aleksandra, L., Matejka, T., Špela Korent, U., 2012. Optical chemical sensors: Design and applications. In: Wen, W. (Ed.), Advances in Chemical Sensors, p. Ch. 1. *IntechOpen*.

Amiri, A., Ghaemi, F., Solid-phase extraction of non-steroidal anti-inflammatory drugs in human plasma and water samples using sol-gel-based metal-organic framework coating. *Journal of Chromatography A* 1648 (2021), 462168.

Amjadi, M., Jalili, R., Manzoori, J.L., A sensitive fluorescent nanosensor for chloramphenicol based on molecularly imprinted polymer-capped CdTe quantum dots. *Luminescence* 31(3) (2016), 633-639.

Anbia, M., kakoli khataei, N., Salehi, S., Ordered nanoporous carbon (CMK-3) coated fiber for solid-phase microextraction of benzene and chlorobenzenes in water samples. *Advances in Environmental Technology* 4(1) (2018), 13-22.

Annamalai, J., Vasudevan, N., Detection of phthalate esters in PET bottled drinks and lake water using esterase/PANI/CNT/CuNP based electrochemical biosensor. *Analytica Chimica Acta* 1135 (2020), 175-186.

AOAC, Guidelines for dietary supplements and botanicals. *AOAC Official Methods of Analysis* (2013), 1-32.

AOAC, Guidelines for standard method performance requirements. *AOAC Official Methods of Analysis* (2016), 1-18.

APVMA, Guidelines for the validation of analytical methods for active constituent, agricultural and veterinary chemical products. *Australian Pesticides & Veterinary Medicines Authority* (2004), 1-9.

Arabi, M., Ostovan, A., Bagheri, A.R., Guo, X., Wang, L., Li, J., Wang, X., Li, B., Chen, L., Strategies of molecular imprinting-based solid-phase extraction prior to chromatographic analysis. *TrAC Trends in Analytical Chemistry* 128 (2020), 115923.

Azizi, A., Shahhoseini, F., Bottaro, C.S., Magnetic molecularly imprinted polymers prepared by reversible addition fragmentation chain transfer polymerization for dispersive solid phase extraction of polycyclic aromatic hydrocarbons in water. *Journal of Chromatography A* 1610 (2020), 460534.

Bagheri, A.R., Arabi, M., Ghaedi, M., Ostovan, A., Wang, X., Li, J., Chen, L., Dummy molecularly imprinted polymers based on a green synthesis strategy for magnetic solid-phase extraction of acrylamide in food samples. *Talanta* 195 (2019), 390-400.

Baile, P., Vidal, L., Canals, A., A modified zeolite/iron oxide composite as a sorbent for magnetic dispersive solid-phase extraction for the preconcentration of nonsteroidal anti-inflammatory drugs in water and urine samples. *Journal of Chromatography A* 1603 (2019), 33-43.

Bakhtiar, S., Bhawani, S.A., Shafqat, S.R., Synthesis and characterization of molecular imprinting polymer for the removal of 2-phenylphenol from spiked blood serum

and river water. *Chemical and Biological Technologies in Agriculture* 6(1) (2019), 15.

Banan, K., Ghorbani-Bidkorbeh, F., Afsharara, H., Hatamabadi, D., Landi, B., Keçili, R., Sellergren, B., Nano-sized magnetic core-shell and bulk molecularly imprinted polymers for selective extraction of amiodarone from human plasma. *Analytica Chimica Acta* 1198 (2022), 339548.

Basak, S., Venkatram, R., Singhal, R.S., Recent advances in the application of molecularly imprinted polymers (MIPs) in food analysis. *Food Control* 139 (2022), 109074.

Berhanu, S., Habtamu, F., Tadesse, Y., Gonfa, F., Tadesse, T., Fluorescence sensor based on polyaniline supported Ag-ZnO nanocomposite for malathion detection. *Journal of Sensors* 2022 (2022), 9881935.

Bezbaruah, A.N., Krajangpan, S., Chisholm, B.J., Khan, E., Elorza Bermudez, J.J., Entrapment of iron nanoparticles in calcium alginate beads for groundwater remediation applications. *Journal of Hazardous Materials* 166(2) (2009), 1339-1343.

Biranje, P.M., Prakash, J., Alexander, R., Kaushal, A., Patwardhan, A.W., Joshi, J.B., Dasgupta, K., Ultra-fast detection and monitoring of cancerous volatile organic compounds in environment using graphene oxide modified CNT aerogel hybrid gas sensor. *Talanta Open* 6 (2022), 100148.

Borahan, T., Unutkan, T., Şahin, A., Bakırdere, S., A rapid and sensitive reversed phase-HPLC method for simultaneous determination of ibuprofen and paracetamol in drug samples and their behaviors in simulated gastric conditions. *Journal of Separation Science* 42(3) (2019), 678-683.

Bourais, I., Maliki, S., Mohammadi, H., Amine, A., Investigation of sulfonamides inhibition of carbonic anhydrase enzyme using multiphotometric and electrochemical techniques. *Enzyme and Microbial Technology* 96 (2017), 23-29.

Brahim, N.B., Mohamed, N.B.H., Echabaane, M., Haouari, M., Chaâbane, R.B., Negrerie, M., Ouada, H.B., Thioglycerol-functionalized CdSe quantum dots detecting cadmium ions. *Sensors and Actuators B: Chemical* 220 (2015), 1346-1353.

Bunkoed, O., Donkhampa, P., Nurerk, P., A nanocomposite optosensor of hydroxyapatite and graphene quantum dots embedded within highly specific polymer for norfloxacin detection. *Microchemical Journal* 158 (2020), 105127.

Bunkoed, O., Kanatharana, P., Mercaptopropionic acid-capped CdTe quantum dots as fluorescence probe for the determination of salicylic acid in pharmaceutical products. *Luminescence* 30(7) (2015), 1083-1089.

Bunkoed, O., Kanatharana, P., Extraction of polycyclic aromatic hydrocarbons with a magnetic sorbent composed of alginate, magnetite nanoparticles and multiwalled carbon nanotubes. *Microchimica Acta* 182(7) (2015), 1519-1526.

Bunkoed, O., Nurerk, P., Wannapob, R., Kanatharana, P., Polypyrrole-coated alginate/magnetite nanoparticles composite sorbent for the extraction of endocrine-disrupting compounds. *Journal of Separation Science* 39(18) (2016), 3602-3609.

Bunkoed, O., Raksawong, P., Chaowana, R., Nurerk, P., A nanocomposite probe of graphene quantum dots and magnetite nanoparticles embedded in a selective polymer for the enrichment and detection of ceftazidime. *Talanta* 218 (2020), 121168.

Cao, L., Lu, W., Mata, A., Nishinari, K., Fang, Y., Egg-box model-based gelation of alginate and pectin: A review. *Carbohydrate Polymers* 242 (2020), 116389.

Cardoso Dos Santos, M., Algar, W.R., Medintz, I.L., Hildebrandt, N., Quantum dots for Förster resonance energy transfer (FRET). *TrAC Trends in Analytical Chemistry* 125 (2020), 115819.

Casado, N., Morante-Zarcero, S., Pérez-Quintanilla, D., Câmara, J.S., Sierra, I., Two novel strategies in food sample preparation for the analysis of dietary polyphenols: Micro-extraction techniques and new silica-based sorbent materials. *Trends in Food Science & Technology* 98 (2020), 167-180.

Cerutti, S., Pacheco, P.H., Gil, R., Martinez, L.D., Green sample preparation strategies for organic/inorganic compounds in environmental samples. *Current Opinion in Green and Sustainable Chemistry* 19 (2019), 76-86.

Chang, T., Yan, X., Liu, S., Liu, Y., Magnetic dummy template silica sol-gel molecularly imprinted polymer nanospheres as magnetic solid-phase extraction

material for the selective and sensitive determination of bisphenol A in plastic bottled beverages. *Food Analytical Methods* 10(12) (2017), 3980-3990.

Chaowana, R., Bunkoed, O., A nanocomposite probe of polydopamine/molecularly imprinted polymer/quantum dots for trace sarafloxacin detection in chicken meat. *Analytical and Bioanalytical Chemistry* 411(23) (2019), 6081-6090.

Chatzimitakos, T.G., Karali, K.K., Stalikas, C.D., Magnetic graphene oxide as a convenient nanosorbent to streamline matrix solid-phase dispersion towards the extraction of pesticides from vegetables and their determination by GC-MS. *Microchemical Journal* 151 (2019), 104247.

Chen, S., Su, X., Yuan, C., Jia, C.Q., Qiao, Y., Li, Y., He, L., Zou, L., Ao, X., Liu, A., Liu, S., Yang, Y., A magnetic phosphorescence molecularly imprinted polymers probe based on manganese-doped ZnS quantum dots for rapid detection of trace norfloxacin residual in food. *Spectrochimica Acta Part A: Molecular and Biomolecular Spectroscopy* 253 (2021), 119577.

Cheng, J., Li, Y., Zhong, J., Lu, Z., Wang, G., Sun, M., Jiang, Y., Zou, P., Wang, X., Zhao, Q., Wang, Y., Rao, H., Molecularly imprinted electrochemical sensor based on biomass carbon decorated with MOF-derived Cr_2O_3 and silver nanoparticles for selective and sensitive detection of nitrofurazone. *Chemical Engineering Journal* 398 (2020), 125664.

Choudhary, Y.S., Nageswaran, G., Branched mercapto acid capped CdTe quantum dots as fluorescence probes for Hg^{2+} detection. *Sensing and Bio-Sensing Research* 23 (2019), 100278.

Chullasat, K., Kanatharana, P., Bunkoed, O., Nanocomposite optosensor of dual quantum dot fluorescence probes for simultaneous detection of cephalexin and ceftriaxone. *Sensors and Actuators B: Chemical* 281 (2019), 689-697.

Chullasat, K., Nurerk, P., Kanatharana, P., Davis, F., Bunkoed, O., A facile optosensing protocol based on molecularly imprinted polymer coated on CdTe quantum dots for highly sensitive and selective amoxicillin detection. *Sensors and Actuators B: Chemical* 254 (2018), 255-263.

Chullasat, K., Nurerk, P., Kanatharana, P., Kueseng, P., Sukchuay, T., Bunkoed, O., Hybrid monolith sorbent of polypyrrole-coated graphene oxide incorporated

into a polyvinyl alcohol cryogel for extraction and enrichment of sulfonamides from water samples. *Analytica Chimica Acta* 961 (2017), 59-66.

Devreese, M., De Baere, S., De Backer, P., Croubels, S., Quantitative determination of several toxicological important mycotoxins in pig plasma using multi-mycotoxin and analyte-specific high performance liquid chromatography-tandem mass spectrometric methods. *Journal of Chromatography A* 1257 (2012), 74-80.

Dinc, M., Esen, C., Mizaikoff, B., Recent advances on core-shell magnetic molecularly imprinted polymers for biomacromolecules. *TrAC Trends in Analytical Chemistry* 114 (2019), 202-217.

Ding, H., Jiao, H.-F., Shi, X.-Z., Sun, A.-L., Guo, X.-Q., Li, D.-X., Chen, J., Molecularly imprinted optosensing sensor for highly selective and sensitive recognition of sulfadiazine in seawater and shrimp samples. *Sensors and Actuators B: Chemical* 246 (2017), 510-517.

Ding, X., Ahmad, W., Zareef, M., Rong, Y., Zhang, Y., Wu, J., Ouyang, Q., Chen, Q., MIL-101(Cr)-induced nano-optical sensor for ultra-sensitive detection of enrofloxacin in aquatic products using a fluorescence turn-on mechanism via upconversion nanoparticles. *Sensors and Actuators B: Chemical* 365 (2022), 131915.

Ding, X., Qu, L., Yang, R., Zhou, Y., Li, J., A highly selective and simple fluorescent sensor for mercury (II) ion detection based on cysteamine-capped CdTe quantum dots synthesized by the reflux method. *Luminescence* 30(4) (2015), 465-471.

Drbohlavova, J., Adam, V., Kizek, R., Hubalek, J., Quantum dots-characterization, preparation and usage in biological Systems. *International Journal of Molecular Sciences* 10(2) (2009), 656-673.

Durai, L., Gopalakrishnan, A., Vishnu, N., Badhulika, S., Polyaniline sheathed black phosphorous: A novel, advanced platform for electrochemical sensing applications. *Electroanalysis* 32(2) (2020), 238-247.

El-Hamshary, M.S., Fouad, M.A., Hanafi, R.S., Al-Easa, H.S., El-Moghazy, S.M., Screening and optimization of samarium-assisted complexation for the determination of norfloxacin, levofloxacin and lomefloxacin in their

corresponding dosage forms employing spectrofluorimetry. *Spectrochimica Acta Part A: Molecular and Biomolecular Spectroscopy* 206 (2019), 578-587.

Elik, A., Sarac, H., Durukan, H., Demirbas, A., Altunay, N., Vortex assisted magnetic ionic liquid based dispersive liquid-liquid microextraction approach for determination of metribuzin in some plant samples with UV-Vis spectrophotometer. *Microchemical Journal* 181 (2022), 107809.

El-Sheikh, A.H., Qawariq, R.F., Abdelghani, J.I., Adsorption and magnetic solid-phase extraction of NSAIDs from pharmaceutical wastewater using magnetic carbon nanotubes: Effect of sorbent dimensions, magnetite loading and competitive adsorption study. *Environmental Technology & Innovation* 16 (2019), 100496.

Ensafi, A.A., Kazemifard, N., Rezaei, B., A simple and rapid label-free fluorimetric biosensor for protamine detection based on glutathione-capped CdTe quantum dots aggregation. *Biosensors and Bioelectronics* 71 (2015), 243-248.

Ensafi, A.A., Kazemifard, N., Rezaei, B., A simple and sensitive fluorimetric aptasensor for the ultrasensitive detection of arsenic(III) based on cysteamine stabilized CdTe/ZnS quantum dots aggregation. *Biosensors and Bioelectronics* 77 (2016), 499-504.

Ensafi, A.A., Zakery, M., Rezaei, B., An optical sensor with specific binding sites for the detection of thioridazine hydrochloride based on ZnO-QDs coated with molecularly imprinted polymer. *Spectrochimica Acta Part A: Molecular and Biomolecular Spectroscopy* 206 (2019), 460-465.

Environmental Protection Agency, National primary drinking water regulations; announcement of the results of EPA's review of existing drinking water standards and request for public comment and/or information on related issues. *Federal Register* 82(7) (2017), 3518-3552.

Eskandari, H., Amirzehni, M., Asadollahzadeh, H., Alizadeh Eslami, P., Molecularly imprinted polymers on CdS quantum dots for sensitive determination of cefixime after its preconcentration by magnetic graphene oxide. *New Journal of Chemistry* 41(15) (2017), 7186-7194.

European Commission, Commission Regulation (EU) No 37/2010 of 22 December 2009 on pharmacologically active substances and their classification regarding

maximum residue limits in foodstuffs of animal origin. *Official Journal of the European Union* L15 (2010), 1-72.

Facchi, D.P., Cazetta, A.L., Canesin, E.A., Almeida, V.C., Bonafé, E.G., Kipper, M.J., Martins, A.F., New magnetic chitosan/alginate/Fe_3O_4@SiO_2 hydrogel composites applied for removal of Pb(II) ions from aqueous systems. *Chemical Engineering Journal* 337 (2018), 595-608.

Fan, J.-P., Xu, X.-K., Xu, R., Zhang, X.-H., Zhu, J.-H., Preparation and characterization of molecular imprinted polymer functionalized with core/shell magnetic particles (Fe_3O_4@SiO_2@MIP) for the simultaneous recognition and enrichment of four taxoids in Taxus×media. *Chemical Engineering Journal* 279 (2015), 567-577.

Fang, L., Jia, M., Zhao, H., Kang, L., Shi, L., Zhou, L., Kong, W., Molecularly imprinted polymer-based optical sensors for pesticides in foods: Recent advances and future trends. *Trends in Food Science & Technology* 116 (2021), 387-404.

Farzin Nejad, N., Shams, E., Amini, M.K., Bennett, J.C., Synthesis of magnetic mesoporous carbon and its application for adsorption of dibenzothiophene. *Fuel Processing Technology* 106 (2013), 376-384.

Feng, J., Tao, Y., Shen, X., Jin, H., Zhou, T., Zhou, Y., Hu, L., Luo, D., Mei, S., Lee, Y.-I., Highly sensitive and selective fluorescent sensor for tetrabromobisphenol-A in electronic waste samples using molecularly imprinted polymer coated quantum dots. *Microchemical Journal* 144 (2019), 93-101.

Fernández, E., Vidal, L., Silvestre-Albero, J., Canals, A., Magnetic dispersive solid-phase extraction using a zeolite-based composite for direct electrochemical determination of lead(II) in urine using screen-printed electrodes. *Microchimica Acta* 187(1) (2020), 87.

Ferrone, V., Carlucci, M., Ettorre, V., Cotellese, R., Palumbo, P., Fontana, A., Siani, G., Carlucci, G., Dispersive magnetic solid phase extraction exploiting magnetic graphene nanocomposite coupled with UHPLC-PDA for simultaneous determination of NSAIDs in human plasma and urine. *Journal of Pharmaceutical and Biomedical Analysis* 161 (2018), 280-288.

Florez, D.H.A., Dutra, F.V.A., Borges, K.B., Magnetic solid phase extraction employing a novel restricted access material based on mesoporous polyaniline coated with hydrophilic monomers and casein for determination of antibiotics in milk samples. *Microchemical Journal* 150 (2019), 104145.

Francotte, E., Davatz, A., Richert, P., Development and validation of chiral high-performance liquid chromatographic methods for the quantitation of valsartan and of the tosylate of valinebenzyl ester. *Journal of Chromatography B: Biomedical Sciences and Applications* 686(1) (1996), 77-83.

Frigerio, C., Ribeiro, D.S.M., Rodrigues, S.S.M., Abreu, V.L.R.G., Barbosa, J.A.C., Prior, J.A.V., Marques, K.L., Santos, J.L.M., Application of quantum dots as analytical tools in automated chemical analysis: A review. *Analytica Chimica Acta* 735 (2012), 9-22.

Fu, L., Chen, Q., Chen, J., Ren, L., Tang, L., Shan, W., Magnetic carbon nanotubes-molecularly imprinted polymer coupled with HPLC for selective enrichment and determination of ferulic acid in traditional chinese medicine and biological samples. *Journal of Chromatography B* 1180 (2021), 122870.

Gao, W., Cheng, J., Yuan, X., Tian, Y., Covalent organic framework-graphene oxide composite: A superior adsorption material for solid phase microextraction of bisphenol A. *Talanta* 222 (2021), 121501.

Garcia, S.M., Wong, A., Khan, S., Sotomayor, M.D.P.T., A simple, sensitive and efficient electrochemical platform based on carbon paste electrode modified with Fe_3O_4@MIP and graphene oxide for folic acid determination in different matrices. *Talanta* 229 (2021), 122258.

Golzari Aqda, T., Behkami, S., Bagheri, H., Porous eco-friendly fibers for on-line micro solid-phase extraction of nonsteroidal anti-inflammatory drugs from urine and plasma samples. *Journal of Chromatography A* 1574 (2018), 18-26.

Gui, R., Jin, H., Recent advances in synthetic methods and applications of photo-luminescent molecularly imprinted polymers. *Journal of Photochemistry and Photobiology C: Photochemistry Reviews* 41 (2019), 100315.

Han, S., Li, X., Wang, Y., Chen, S., Graphene oxide-based fluorescence molecularly imprinted composite for recognition and separation of 2,4,6-trichlorophenol. *RSC Advances* 5(3) (2015), 2129-2136.

Han, S., Yang, L., Wen, Z., Chu, S., Wang, M., Wang, Z., Jiang, C., A dual-response ratiometric fluorescent sensor by europium-doped CdTe quantum dots for visual and colorimetric detection of tetracycline. *Journal of Hazardous Materials* 398 (2020), 122894.

Han, X., Zhang, X., Zhong, L., Yu, X., Zhai, H., Preparation of sulfamethoxazole molecularly imprinted polymers based on magnetic metal-organic frameworks/graphene oxide composites for the selective extraction of sulfonamides in food samples. *Microchemical Journal* 177 (2022), 107259.

Hang, Q., Yin, H., Yuan, Y., Jiang, X., Zhao, L., Xiong, Z., Magnetic molecularly imprinted polymers based on eco-friendly deep eutectic solvent for recognition and extraction of three glucocorticoids in lotion. *Microchemical Journal* 183 (2022), 107975.

Hasanah, A.N., Safitri, N., Zulfa, A., Neli, N., Rahayu, D., Factors affecting preparation of molecularly imprinted polymer and methods on finding template-monomer interaction as the key of selective properties of the materials. *Molecules* 26(18) (2021), 5612.

Hassan, M., Alshana, U., Switchable-hydrophilicity solvent liquid-liquid microextraction of non-steroidal anti-inflammatory drugs from biological fluids prior to HPLC-DAD determination. *Journal of Pharmaceutical and Biomedical Analysis* 174 (2019), 509-517.

He, M., Su, S., Chen, B., Hu, B., Simultaneous speciation of inorganic selenium and tellurium in environmental water samples by polyaniline functionalized magnetic solid phase extraction coupled with ICP-MS detection. *Talanta* 207 (2020), 120314.

Henna, T.K., Pramod, K., Graphene quantum dots redefine nanobiomedicine. *Materials Science and Engineering: C* 110 (2020), 110651.

Hewavitharana, G.G., Perera, D.N., Navaratne, S.B., Wickramasinghe, I., Extraction methods of fat from food samples and preparation of fatty acid methyl esters for gas chromatography: A review. *Arabian Journal of Chemistry* 13(8) (2020), 6865-6875.

Hezinger, A.F.E., Teßmar, J., Göpferich, A., Polymer coating of quantum dots-A powerful tool toward diagnostics and sensorics. *European Journal of Pharmaceutics and Biopharmaceutics* 68(1) (2008), 138-152.

Holban, A.M., Grumezescu, A.M., Andronescu, E., 2016. Chapter 10 - Inorganic nanoarchitectonics designed for drug delivery and anti-infective surfaces. In: Grumezescu, A.M. (Ed.), Surface Chemistry of Nanobiomaterials, pp. 301-327. *William Andrew Publishing*.

Hong, R.Y., Feng, B., Chen, L.L., Liu, G.H., Li, H.Z., Zheng, Y., Wei, D.G., Synthesis, characterization and MRI application of dextran-coated Fe_3O_4 magnetic nanoparticles. *Biochemical Engineering Journal* 42(3) (2008), 290-300.

Hou, X., Shi, J., Wang, N., Wen, Z., Sun, M., Qu, J., Hu, Q., Removal of antibiotic tetracycline by metal-organic framework MIL-101(Cr) loaded nano zero-valent iron. *Journal of Molecular Liquids* 313 (2020), 113512.

Hu, C., Lu, W., Mata, A., Nishinari, K., Fang, Y., Ions-induced gelation of alginate: Mechanisms and applications. *International Journal of Biological Macromolecules* 177 (2021), 578-588.

Huang, C., Yang, J., Ma, J., Tan, W., Wu, L., Shan, B., Wang, S., Chen, J., Li, Y., An efficient mixed-mode strong anion-exchange adsorbent based on functionalized polyethyleneimine for simultaneous solid phase extraction and purification of bisphenol analogues and monoalkyl phthalate esters in human urine. *Microchemical Journal* 180 (2022), 107536.

Huo, S.-H., Yan, X.-P., Facile magnetization of metal-organic framework MIL-101 for magnetic solid-phase extraction of polycyclic aromatic hydrocarbons in environmental water samples. *Analyst* 137(15) (2012), 3445-3451.

Hussain, D., Raza Naqvi, S.T., Ashiq, M.N., Najam-ul-Haq, M., Analytical sample preparation by electrospun solid phase microextraction sorbents. *Talanta* 208 (2020), 120413.

ICH, Validation of analytical procedures: Text and methodology. *ICH Harmonised Tripartite Guideline* (2005), 1-17.

Jalilian, N., Ebrahimzadeh, H., Asgharinezhad, A.A., Khodayari, P., Magnetic molecularly imprinted polymer for the selective dispersive micro solid phase

extraction of phenolphthalein in urine samples and herbal slimming capsules prior to HPLC-PDA analysis. *Microchemical Journal* 160 (2021), 105712.

Jeong, S., Valdez, J.E., Miękus, N., Kwon, J.Y., Kwon, W., Bączek, T., Chung, D.S., Facile and highly efficient three-phase single drop microextraction in-line coupled with capillary electrophoresis. *Journal of Chromatography A* 1655 (2021), 462520.

Jeong, Y., Cui, M., Choi, J., Lee, Y., Kim, J., Son, Y., Khim, J., Development of modified mesoporous carbon (CMK-3) for improved adsorption of bisphenol-A. *Chemosphere* 238 (2020), 124559.

Jerónimo, P.C.A., Araújo, A.N., Conceição B.S.M. Montenegro, M., Optical sensors and biosensors based on sol-gel films. *Talanta* 72(1) (2007), 13-27.

Jia, M., Zhu, Y., Guo, D., Bi, X., Hou, X., Surface molecularly imprinted polymer based on core-shell Fe_3O_4@MIL-101(Cr) for selective extraction of phenytoin sodium in plasma. *Analytica Chimica Acta* 1128 (2020), 211-220.

Jia, X., Zhao, P., Ye, X., Zhang, L., Wang, T., Chen, Q., Hou, X., A novel metal-organic framework composite MIL-101(Cr)@GO as an efficient sorbent in dispersive micro-solid phase extraction coupling with UHPLC-MS/MS for the determination of sulfonamides in milk samples. *Talanta* 169 (2017), 227-238.

Jian, N., Qian, L., Wang, C., Li, R., Xu, Q., Li, J., Novel nanofibers mat as an efficient, fast and reusable adsorbent for solid phase extraction of non-steroidal anti-inflammatory drugs in environmental water. *Journal of Hazardous Materials* 363 (2019), 81-89.

Jiang, H.-L., Li, N., Cui, L., Wang, X., Zhao, R.-S., Recent application of magnetic solid phase extraction for food safety analysis. *TrAC Trends in Analytical Chemistry* 120 (2019), 115632.

Jing, W., Zhou, Y., Wang, J., Ni, M., Bi, W., Chen, D.D.Y., Dispersive magnetic solid-phase extraction coupled to direct analysis in real time mass spectrometry for high-throughput analysis of trace environmental contaminants. *Analytical Chemistry* 91(17) (2019), 11240-11246.

Kabir, A., Holness, H., Furton, K.G., Almirall, J.R., Recent advances in micro-sample preparation with forensic applications. *TrAC Trends in Analytical Chemistry* 45 (2013), 264-279.

Kaewsuwan, W., Kanatharana, P., Bunkoed, O., Dispersive magnetic solid phase extraction using octadecyl coated silica magnetite nanoparticles for the extraction of tetracyclines in water samples. *Journal of Analytical Chemistry* 72(9) (2017), 957-965.

Kashima, K., Imai, M., 2012. Advanced membrane material from marine biological polymer and sensitive molecular-size recognition for promising separation technology. In: Robert, Y.N. (Ed.), Advancing Desalination, p. Ch. 1. *IntechOpen*.

Khawla, M., Zouhour, H., Yves, C., Souhaira, H., Rym, M., ZnS quantum dots as fluorescence sensor for quantitative detection of tetracycline. *Optical Materials* 125 (2022), 112103.

Kim, Y., Chang, J.Y., Fabrication of a fluorescent sensor by organogelation: CdSe/ZnS quantum dots embedded molecularly imprinted organogel nanofibers. *Sensors and Actuators B: Chemical* 234 (2016), 122-129.

Klimberg, I.W., Cox, C.E., Fowler, C.L., King, W., Kim, S.S., Callery-D'Amico, S., A Controlled trial of levofloxacin and lomefloxacin in the treatment of complicated urinary tract infection. *Urology* 51(4) (1998), 610-615.

Klongklaew, P., Kanatharana, P., Bunkoed, O., Development of doubly porous composite adsorbent for the extraction of fluoroquinolones from food samples. *Food Chemistry* 309 (2020), 125685.

Lashgari, M., Yamini, Y., Basheer, C., Lee, H.K., Ordered mesoporous carbon as sorbent for the extraction of N-nitrosamines in wastewater and swimming pool water. *Journal of Chromatography A* 1513 (2017), 35-41.

Le, T.H., Lee, H.J., Kim, J.H., Park, S.J., Highly selective fluorescence sensor based on graphene quantum dots for sulfamethoxazole determination. *Materials* 13(11) (2020), 2521.

Lee, J.C., Jang, E.-P., Jang, D.S., Choi, Y., Choi, M., Yang, H., Solvothermal preparation and fluorescent properties of color-tunable InP/ZnS quantum dots. *Journal of Luminescence* 134 (2013), 798-805.

Lei, Y., He, M., Chen, B., Hu, B., Polyaniline/cyclodextrin composite coated stir bar sorptive extraction combined with high performance liquid chromatography-

ultraviolet detection for the analysis of trace polychlorinated biphenyls in environmental waters. *Talanta* 150 (2016), 310-318.

Li, N., Jiang, H.-L., Wang, X., Wang, X., Xu, G., Zhang, B., Wang, L., Zhao, R.-S., Lin, J.-M., Recent advances in graphene-based magnetic composites for magnetic solid-phase extraction. *TrAC Trends in Analytical Chemistry* 102 (2018), 60-74.

Li, N., Zhang, L., Nian, L., Cao, B., Wang, Z., Lei, L., Yang, X., Sui, J., Zhang, H., Yu, A., Dispersive micro-solid-phase extraction of herbicides in vegetable oil with metal-organic framework MIL-101. *Journal of Agricultural and Food Chemistry* 63(8) (2015), 2154-2161.

Li, N., Zhang, T., Chen, G., Xu, J., Ouyang, G., Zhu, F., Recent advances in sample preparation techniques for quantitative detection of pharmaceuticals in biological samples. *TrAC Trends in Analytical Chemistry* 142 (2021), 116318.

Li, S., Li, J., Luo, J., Zhang, Q., Zhang, L., A fluorescence switch sensor for detection of virginiamycin based on graphene oxide-supported carbon quantum dots and molecularly imprinted polymer. *RSC Advances* 7(89) (2017), 56359-56364.

Li, T., Song, Y., Li, J., Zhang, M., Shi, Y., Fan, J., New low viscous hydrophobic deep eutectic solvents in vortex-assisted liquid-liquid microextraction for the determination of phthalate esters from food-contacted plastics. *Food Chemistry* 309 (2020), 125752.

Li, X., Dong, Q., Tian, Q., Sial, A., Wang, H., Wen, H., Pan, B., Zhang, K., Qin, J., Wang, C., Recent advance in metal- and covalent-organic framework-based photocatalysis for hydrogen evolution. *Materials Today Chemistry* 26 (2022), 101037.

Li, X., Jiao, H.-F., Shi, X.-Z., Sun, A., Wang, X., Chai, J., Li, D.-X., Chen, J., Development and application of a novel fluorescent nanosensor based on FeSe quantum dots embedded silica molecularly imprinted polymer for the rapid optosensing of cyfluthrin. *Biosensors and Bioelectronics* 99 (2018), 268-273.

Li, Y., Li, Y., Zhang, D., Tan, W., Shi, J., Li, Z., Liu, H., Yu, Y., Yang, L., Wang, X., Gong, Y., Zou, X., A fluorescence resonance energy transfer probe based on functionalized graphene oxide and upconversion nanoparticles for sensitive and rapid detection of zearalenone. *LWT* 147 (2021), 111541.

Li, Y., Wu, X., Li, Z., Zhong, S., Wang, W., Wang, A., Chen, J., Fabrication of $CoFe_2O_4$-graphene nanocomposite and its application in the magnetic solid phase extraction of sulfonamides from milk samples. *Talanta* 144 (2015), 1279-1286.

Li, Y., Xu, X., Guo, H., Bian, Y., Li, J., Zhang, F., Magnetic graphene oxide-based covalent organic frameworks as novel adsorbent for extraction and separation of triazine herbicides from fruit and vegetable samples. *Analytica Chimica Acta* 1219 (2022), 339984.

Liang, L., Wang, X., Sun, Y., Ma, P., Li, X., Piao, H., Jiang, Y., Song, D., Magnetic solid-phase extraction of triazine herbicides from rice using metal-organic framework MIL-101(Cr) functionalized magnetic particles. *Talanta* 179 (2018), 512-519.

Liang, S., Jian, N., Cao, J., Zhang, H., Li, J., Xu, Q., Wang, C., Rapid, simple and green solid phase extraction based on polyaniline nanofibers-mat for detecting non-steroidal anti-inflammatory drug residues in animal-origin food. *Food Chemistry* 328 (2020), 127097.

Lietman, P.S., Fluoroquinolone Toxicities. *Drugs* 49(2) (1995), 159-163.

Lin, L., Rong, M., Luo, F., Chen, D., Wang, Y., Chen, X., Luminescent graphene quantum dots as new fluorescent materials for environmental and biological applications. *TrAC Trends in Analytical Chemistry* 54 (2014), 83-102.

Lin, Z.-z., Zhang, H.-y., Peng, A.-h., Lin, Y.-d., Li, L., Huang, Z.-y., Determination of malachite green in aquatic products based on magnetic molecularly imprinted polymers. *Food Chemistry* 200 (2016), 32-37.

Liu, A., Lv, S., Jiang, L., Liu, F., Zhao, L., Wang, J., Hu, X., Yang, Z., He, J., Wang, C., Yan, X., Sun, P., Shimanoe, K., Lu, G., The gas sensor utilizing polyaniline/ MoS_2 nanosheets/ SnO_2 nanotubes for the room temperature detection of ammonia. *Sensors and Actuators B: Chemical* 332 (2021), 129444.

Liu, C.-X., Zhao, J., Zhang, R.-R., Zhang, Z.-M., Xu, J.-J., Sun, A.-L., Chen, J., Shi, X.-Z., Development and application of fluorescence sensor and test strip based on molecularly imprinted quantum dots for the selective and sensitive detection of propanil in fish and seawater samples. *Journal of Hazardous Materials* 389 (2020), 121884.

Liu, H., Na, W., Liu, Z., Chen, X., Su, X., A novel turn-on fluorescent strategy for sensing ascorbic acid using graphene quantum dots as fluorescent probe. *Biosensors and Bioelectronics* 92 (2017), 229-233.

Liu, H., Ni, T., Mu, L., Zhang, D., Wang, J., Wang, S., Sun, B., Sensitive detection of pyrraline with a molecularly imprinted sensor based on metal-organic frameworks and quantum dots. *Sensors and Actuators B: Chemical* 256 (2018), 1038-1044.

Liu, H., Zhou, K., Chen, X., Wang, J., Wang, S., Sun, B., Graphene oxide-sensitized molecularly imprinted opto-polymers for charge-transfer fluorescent sensing of cyanoguanidine. *Food Chemistry* 235 (2017), 14-20.

Liu, S., Wang, L., Luo, Y., Tian, J., Li, H., Sun, X., Polyaniline nanofibres for fluorescent nucleic acid detection. *Nanoscale* 3(3) (2011), 967-969.

Liu, X., Tong, Y., Zhang, L., Tailorable yolk-shell Fe_3O_4@graphitic carbon submicroboxes as efficient extraction materials for highly sensitive determination of trace sulfonamides in food samples. *Food Chemistry* 303 (2020), 125369.

Liu, Y., Xiao, M., Liu, S., Zhao, X., Tian, Y., Wang, X., A novel oil-water microemulsion strategy for controllable synthesis of large mesoporous carbon nanoparticles. *Carbon* 200 (2022), 361-374.

Lu, J.-Q., Jin, F., Sun, T.-Q., Zhou, X.-W., Multi-spectroscopic study on interaction of bovine serum albumin with lomefloxacin-copper(II) complex. International *Journal of Biological Macromolecules* 40(4) (2007), 299-304.

Lu, X., Wei, F., Xu, G., Wu, Y., Yang, J., Hu, Q., Surface molecular imprinting on silica-coated CdTe quantum dots for selective and sensitive fluorescence detection of p-aminophenol in water. *Journal of Fluorescence* 27(1) (2017), 181-189.

Madikizela, L.M., Tavengwa, N.T., Chimuka, L., Applications of molecularly imprinted polymers for solid-phase extraction of non-steroidal anti-inflammatory drugs and analgesics from environmental waters and biological samples. *Journal of Pharmaceutical and Biomedical Analysis* 147 (2018), 624-633.

Magiera, S., Gülmez, Ş., Michalik, A., Baranowska, I., Application of statistical experimental design to the optimisation of microextraction by packed sorbent for the analysis of nonsteroidal anti-inflammatory drugs in human urine by ultra-high pressure liquid chromatography. *Journal of Chromatography A* 1304 (2013), 1-9.

Mahmoudi-Moghaddam, H., Tajik, S., Beitollahi, H., A new electrochemical DNA biosensor based on modified carbon paste electrode using graphene quantum dots and ionic liquid for determination of topotecan. *Microchemical Journal* 150 (2019), 104085.

Majd, M., Nojavan, S., Determination of polycyclic aromatic hydrocarbons in soil, tree leaves, and water samples by magnetic dispersive solid-phase extraction based on β-cyclodextrin functionalized graphene oxide followed by GC-FID. *Microchemical Journal* 171 (2021), 106852.

Manousi, N., Rosenberg, E., Deliyanni, E., Zachariadis, G.A., Samanidou, V., Magnetic solid-phase extraction of organic compounds based on graphene oxide nanocomposites. *Molecules* 25(5) (2020), 1148.

Manousi, N., Samanidou, V., Green sample preparation of alternative biosamples in forensic toxicology. *Sustainable Chemistry and Pharmacy* 20 (2021), 100388.

Masteri-Farahani, M., Mashhadi-Ramezani, S., Mosleh, N., Molecularly imprinted polymer containing fluorescent graphene quantum dots as a new fluorescent nanosensor for detection of methamphetamine. *Spectrochimica Acta Part A: Molecular and Biomolecular Spectroscopy* 229 (2020), 118021.

Maya, F., Palomino Cabello, C., Frizzarin, R.M., Estela, J.M., Turnes Palomino, G., Cerdà, V., Magnetic solid-phase extraction using metal-organic frameworks (MOFs) and their derived carbons. *TrAC Trends in Analytical Chemistry* 90 (2017), 142-152.

Mehrzad-Samarin, M., Faridbod, F., Dezfuli, A.S., Ganjali, M.R., A novel metronidazole fluorescent nanosensor based on graphene quantum dots embedded silica molecularly imprinted polymer. *Biosensors and Bioelectronics* 92 (2017), 618-623.

Mertsoy, E.Y., Sert, E., Atalay, S., Atalay, F.S., Fabrication of chromium based metal organic framework (MIL-101)/activated carbon composites for acetylation of

glycerol. *Journal of the Taiwan Institute of Chemical Engineers* 120 (2021), 93-105.

Milanetti, E., Carlucci, G., Olimpieri, P.P., Palumbo, P., Carlucci, M., Ferrone, V., Correlation analysis based on the hydropathy properties of non-steroidal anti-inflammatory drugs in solid-phase extraction (SPE) and reversed-phase high performance liquid chromatography (HPLC) with photodiode array detection and their applications to biological samples. *Journal of Chromatography A* 1605 (2019), 360351.

Morales-Benítez, I., Montoro-Leal, P., García-Mesa, J.C., Verdeja-Galán, J., Alonso, E.I.V., Magnetic graphene oxide as a valuable material for the speciation of trace elements. *TrAC Trends in Analytical Chemistry* 157 (2022), 116777.

Mukhopadhyay, A., Joshi, N., Chattopadhyay, K., De, G., A facile synthesis of PEG-coated magnetite (Fe_3O_4) nanoparticles and their prevention of the reduction of cytochrome c. *ACS Applied Materials & Interfaces* 4(1) (2012), 142-149.

Naing, N.N., Li, S.F.Y., Lee, H.K., Evaluation of graphene-based sorbent in the determination of polar environmental contaminants in water by micro-solid phase extraction-high performance liquid chromatography. *Journal of Chromatography A* 1427 (2016), 29-36.

Nawaz, N., Abu Bakar, N.K., Muhammad Ekramul Mahmud, H.N., Jamaludin, N.S., Molecularly imprinted polymers-based DNA biosensors. *Analytical Biochemistry* 630 (2021), 114328.

Nebol'sin, V.A., Galstyan, V., Silina, Y.E., Graphene oxide and its chemical nature: Multi-stage interactions between the oxygen and graphene. *Surfaces and Interfaces* 21 (2020), 100763.

Ning, Y., Ye, Y., Liao, W., Xu, Y., Wang, W., Wang, A.-j., Triazine-based porous organic polymer as pipette tip solid-phase extraction adsorbent coupled with HPLC for the determination of sulfonamide residues in food samples. *Food Chemistry* 397 (2022), 133831.

Nurerk, P., Chaowana, R., Limbut, W., Bunkoed, O., A hierarchical composite adsorbent of cotton fibers modified with a hydrogel incorporating a metal organic framework and cetyl trimethyl ammonium bromide for the extraction and enrichment of phthalate esters. *Microchemical Journal* 158 (2020), 105220.

Nurerk, P., Kanatharana, P., Bunkoed, O., A selective determination of copper ions in water samples based on the fluorescence quenching of thiol-capped CdTe quantum dots. *Luminescence* 31(2) (2016), 515-522.

Orachorn, N., Bunkoed, O., A nanocomposite fluorescent probe of polyaniline, graphene oxide and quantum dots incorporated into highly selective polymer for lomefloxacin detection. *Talanta* 203 (2019), 261-268.

Orachorn, N., Bunkoed, O., Nanohybrid magnetic composite optosensing probes for the enrichment and ultra-trace detection of mafenide and sulfisoxazole. *Talanta* 228 (2021), 122237.

Orachorn, N., Bunkoed, O., A composite adsorbent of graphene quantum dots, mesoporous carbon, and molecularly imprinted polymer to extract nonsteroidal anti-inflammatory drugs in milk. *Microchimica Acta* 189(12) (2022), 446.

Orachorn, N., Klongklaew, P., Bunkoed, O., A composite of magnetic GOx@MOF incorporated in alginate hydrogel fiber adsorbent for the extraction of phthalate esters. *Microchemical Journal* 171 (2021), 106827.

Pasparakis, G., Bouropoulos, N., Swelling studies and in vitro release of verapamil from calcium alginate and calcium alginate-chitosan beads. *International Journal of Pharmaceutics* 323(1) (2006), 34-42.

Pena-Pereira, F., Romero, V., de la Calle, I., Lavilla, I., Bendicho, C., Graphene-based nanocomposites in analytical extraction processes. *TrAC Trends in Analytical Chemistry* 142 (2021), 116303.

Pendyala, N.B., Koteswara Rao, K.S.R., Efficient Hg and Ag ion detection with luminescent PbS quantum dots grown in poly vinyl alcohol and capped with mercaptoethanol. *Colloids and Surfaces A: Physicochemical and Engineering Aspects* 339(1) (2009), 43-47.

Peng, C.-F., Zhang, Y.-Y., Qian, Z.-J., Xie, Z.-J., Fluorescence sensor based on glutathione capped CdTe QDs for detection of Cr^{3+} ions in vitamins. *Food Science and Human Wellness* 7(1) (2018), 71-76.

Piccirilli, G.N., Escandar, G.M., Flow injection analysis with on-line nylon powder extraction for room-temperature phosphorescence determination of thiabendazole. *Analytica Chimica Acta* 646(1) (2009), 90-96.

Pinsrithong, S., Bunkoed, O., Hierarchical porous nanostructured polypyrrole-coated hydrogel beads containing reduced graphene oxide and magnetite nanoparticles for extraction of phthalates in bottled drinks. *Journal of Chromatography A* 1570 (2018), 19-27.

Ponnaiah, S.K., Periakaruppan, P., Vellaichamy, B., New electrochemical sensor based on a silver-doped iron oxide nanocomposite coupled with polyaniline and its sensing application for picomolar-level detection of uric acid in human blood and urine samples. *The Journal of Physical Chemistry B* 122(12) (2018), 3037-3046.

Pourghobadi, Z., Mirahmadpour, P., Zare, H., Fluorescent biosensor for the selective determination of dopamine by TGA-capped CdTe quantum dots in human plasma samples. *Optical Materials* 84 (2018), 757-762.

Pouya, S., Koochesfahani, M., Snee, P., Bawendi, M., Nocera, D., Single quantum dot (QD) imaging of fluid flow near surfaces. *Experiments in Fluids* 39(4) (2005), 784-786.

Qian, Z.S., Shan, X.Y., Chai, L.J., Chen, J.R., Feng, H., A fluorescent nanosensor based on graphene quantum dots–aptamer probe and graphene oxide platform for detection of lead (II) ion. *Biosensors and Bioelectronics* 68 (2015), 225-231.

Rahman, M.M., Ara, M.G., Alim, M.A., Uddin, M.S., Najda, A., Albadrani, G.M., Sayed, A.A., Mousa, S.A., Abdel-Daim, M.M., Mesoporous carbon: A versatile material for scientific applications. *International Journal of Molecular Sciences* 22(9) (2021), 4498.

Rattanakunsong, N., Bunkoed, O., A porous composite monolith sorbent of polyaniline, multiwall carbon nanotubes and chitosan cryogel for aromatic compounds extraction. *Microchemical Journal* 154 (2020), 104562.

Razavi, N., Es'haghi, Z., Employ of magnetic polyaniline coated chitosan nanocomposite for extraction and determination of phthalate esters in diapers and wipes using gas chromatography. *Microchemical Journal* 142 (2018), 359-366.

Rebelo, P., Costa-Rama, E., Seguro, I., Pacheco, J.G., Nouws, H.P.A., Cordeiro, M.N.D.S., Delerue-Matos, C., Molecularly imprinted polymer-based

electrochemical sensors for environmental analysis. *Biosensors and Bioelectronics* 172 (2021), 112719.

Rechotnek, F., Fragal, E.H., Galdioli Pellá, M.C., Fragal, V.H., Silva, R., Enhancement of selectivity towards the synthesis of hydrogen peroxide by dimensional effect in mesoporous carbon. *Microporous and Mesoporous Materials* 333 (2022), 111741.

Ren, X., Chen, L., Quantum dots coated with molecularly imprinted polymer as fluorescence probe for detection of cyphenothrin. *Biosensors and Bioelectronics* 64 (2015), 182-188.

Ren, X., Liu, H., Chen, L., Fluorescent detection of chlorpyrifos using Mn(II)-doped ZnS quantum dots coated with a molecularly imprinted polymer. *Microchimica Acta* 182(1) (2015), 193-200.

Rocha, A.P.d.M., Alayo, M.I., da Silva, D.M., Synthesis of nitrogen-doped graphene quantum dots from sucrose carbonization. *Applied Sciences* 12(17) (2022), 8686.

Sadeghi, M.M., Rad, A.S., Ardjmand, M., Mirabi, A., Preparation of magnetic nanocomposite based on polyaniline/Fe_3O_4 towards removal of lead (II) ions from real samples. *Synthetic Metals* 245 (2018), 1-9.

Saenz-Aguirre, C., Amaya-Tapia, G., Andrade-Villanueva, J., Perez-Gomez, R., Morfin-Otero, R., Rodriguez-Noriega, E., Comparison of the safety and efficacy of lomefloxacin and amoxicillin in the treatment of acute exacerbations of chronic bronchitis: Results from a Latin American multicenter study. *International Journal of Antimicrobial Agents* 2(1) (1992), 49-54.

Saghatforoush, L.A., Sanati, S., Mehdizadeh, R., Hasanzadeh, M., Solvothermal synthesis of $Cd(OH)_2$ and CdO nanocrystals and application as a new electrochemical sensor for simultaneous determination of norfloxacin and lomefloxacin. *Superlattices and Microstructures* 52(4) (2012), 885-893.

Sakaguchi, M., Makino, M., Ohura, T., Yamamoto, K., Enomoto, Y., Takase, H., Surface modification of Fe_3O_4 nanoparticles with dextran via a coupling reaction between naked Fe_3O_4 mechano-cation and naked dextran mechano-anion: A new mechanism of covalent bond formation. *Advanced Powder Technology* 30(4) (2019), 795-806.

Sakira, A.K., Mees, C., Braekeleer, K.D., Delporte, C., Yameogo, J., Yabre, M., Some, T.I., Antwerpen, P.V., Mertens, D., Kauffmann, J.M., Determination of the quality of metronidazole formulations by near-infrared spectrophotometric analysis. *Talanta Open* 3 (2021), 100027.

Samimi, E., Karami, P., Ahar, M.J., A review on aptamer-conjugated quantum dot nanosystems for cancer imaging and theranostic. *Journal of Nanomedicine Research* 5 (2017), 1-8.

Saraji, M., Mehrafza, N., Mesoporous carbon–zirconium oxide nanocomposite derived from carbonized metal organic framework: A coating for solid-phase microextraction. *Journal of Chromatography A* 1460 (2016), 33-39.

Sereshti, H., Karami, F., Nouri, N., Farahani, A., Electrochemically controlled solid phase microextraction based on a conductive polyaniline-graphene oxide nanocomposite for extraction of tetracyclines in milk and water. *Journal of the Science of Food and Agriculture* 101(6) (2021), 2304-2311.

Shahhoseini, F., Azizi, A., Bottaro, C.S., A critical evaluation of molecularly imprinted polymer (MIP) coatings in solid phase microextraction devices. *TrAC Trends in Analytical Chemistry* 156 (2022), 116695.

Shi, R., Yan, L., Xu, T., Liu, D., Zhu, Y., Zhou, J., Graphene oxide bound silica for solid-phase extraction of 14 polycyclic aromatic hydrocarbons in mainstream cigarette smoke. *Journal of Chromatography A* 1375 (2015), 1-7.

Shi, T., Tan, L., Fu, H., Wang, J., Application of molecular imprinting polymer anchored on CdTe quantum dots for the detection of sulfadiazine in seawater. *Marine Pollution Bulletin* 146 (2019), 591-597.

Shishov, A., Nechaeva, D., Bulatov, A., HPLC-MS/MS determination of non-steroidal anti-inflammatory drugs in bovine milk based on simultaneous deep eutectic solvents formation and its solidification. *Microchemical Journal* 150 (2019), 104080.

Silpcharu, K., Sam-ang, P., Chansaenpak, K., Sukwattanasinitt, M., Rashatasakhon, P., Selective fluorescent sensors for gold(III) ion from N-picolyl sulfonamide spirobifluorene derivatives. *Journal of Photochemistry and Photobiology A: Chemistry* 402 (2020), 112823.

Smith, A.M., Ruan, G., Rhyner, M.N., Nie, S., Engineering luminescent quantum dots for in vivo molecular and cellular imaging. *Annals of Biomedical Engineering* 34(1) (2006), 3-14.

Socas-Rodríguez, B., Hernández-Borges, J., Salazar, P., Martín, M., Rodríguez-Delgado, M.Á., Core-shell polydopamine magnetic nanoparticles as sorbent in micro-dispersive solid-phase extraction for the determination of estrogenic compounds in water samples prior to high-performance liquid chromatography-mass spectrometry analysis. *Journal of Chromatography A* 1397 (2015), 1-10.

Song, Z., Li, J., Lu, W., Li, B., Yang, G., Bi, Y., Arabi, M., Wang, X., Ma, J., Chen, L., Molecularly imprinted polymers based materials and their applications in chromatographic and electrophoretic separations. *TrAC Trends in Analytical Chemistry* 146 (2022), 116504.

Soylak, M., Ozdemir, B., Yilmaz, E., An environmentally friendly and novel amine-based liquid phase microextraction of quercetin in food samples prior to its determination by UV-vis spectrophotometry. *Spectrochimica Acta Part A: Molecular and Biomolecular Spectroscopy* 243 (2020), 118806.

Stejskal, J., Sapurina, I., Trchová, M., Polyaniline nanostructures and the role of aniline oligomers in their formation. *Progress in Polymer Science* 35(12) (2010), 1420-1481.

Sun, A., Chai, J., Xiao, T., Shi, X., Li, X., Zhao, Q., Li, D., Chen, J., Development of a selective fluorescence nanosensor based on molecularly imprinted-quantum dot optosensing materials for saxitoxin detection in shellfish samples. *Sensors and Actuators B: Chemical* 258 (2018), 408-414.

Sun, M., Feng, J., Ji, X., Li, C., Han, S., Sun, M., Feng, Y., Feng, J., Sun, H., Polyaniline/titanium dioxide nanorods functionalized carbon fibers for in-tube solid-phase microextraction of phthalate esters prior to high performance liquid chromatography-diode array detection. *Journal of Chromatography A* 1642 (2021), 462003.

Suwanwong, Y., Boonpangrak, S., Molecularly imprinted polymers for the extraction and determination of water-soluble vitamins: A review from 2001 to 2020. *European Polymer Journal* 161 (2021), 110835.

Tall, A., da Costa, K.R., de Oliveira, M.J., Tapsoba, I., Rocha, U., Sales, T.O., Goulart, M.O.F., Santos, J.C.C., Photoluminescent nanoprobes based on thiols capped CdTe quantum dots for direct determination of thimerosal in vaccines. *Talanta* 221 (2021), 121545.

Tam, T.V., Trung, N.B., Kim, H.R., Chung, J.S., Choi, W.M., One-pot synthesis of N-doped graphene quantum dots as a fluorescent sensing platform for Fe^{3+} ions detection. *Sensors and Actuators B: Chemical* 202 (2014), 568-573.

Tan, S.C., Lee, H.K., A hydrogel composite prepared from alginate, an amino-functionalized metal-organic framework of type MIL-101(Cr), and magnetite nanoparticles for magnetic solid-phase extraction and UHPLC-MS/MS analysis of polar chlorophenoxy acid herbicides. *Microchimica Acta* 186(8) (2019), 545.

Tan, X., Liu, S., Shen, Y., He, Y., Yang, J., Quantum dots (QDs) based fluorescence probe for the sensitive determination of kaempferol. *Spectrochimica Acta Part A: Molecular and Biomolecular Spectroscopy* 133 (2014), 66-72.

Tanwar, S., Di Carro, M., Magi, E., Innovative sampling and extraction methods for the determination of nonsteroidal anti-inflammatory drugs in water. *Journal of Pharmaceutical and Biomedical Analysis* 106 (2015), 100-106.

Tasmia, Shah, J., Jan, M.R., Eco-friendly alginate encapsulated magnetic graphene oxide beads for solid phase microextraction of endocrine disrupting compounds from water samples. *Ecotoxicology and Environmental Safety* 190 (2020), 110099.

Taverniers, I., De Loose, M., Van Bockstaele, E., Trends in quality in the analytical laboratory. II. Analytical method validation and quality assurance. *TrAC Trends in Analytical Chemistry* 23(8) (2004), 535-552.

Tayebi, M., Tavakkoli Yaraki, M., Mogharei, A., Ahmadieh, M., Tahriri, M., Vashaee, D., Tayebi, L., Thioglycolic acid-capped CdS quantum dots conjugated to α-amylase as a fluorescence probe for determination of starch at Low concentration. *Journal of Fluorescence* 26(5) (2016), 1787-1794.

The Huy, B., Seo, M.-H., Zhang, X., Lee, Y.-I., Selective optosensing of clenbuterol and melamine using molecularly imprinted polymer-capped CdTe quantum dots. *Biosensors and Bioelectronics* 57 (2014), 310-316.

Thepmanee, O., Prapainop, K., Noppha, O., Rattanawimanwong, N., Siangproh, W., Chailapakul, O., Songsrirote, K., A simple paper-based approach for arsenic determination in water using hydride generation coupled with mercaptosuccinic-acid capped CdTe quantum dots. *Analytical Methods* 12(21) (2020), 2718-2726.

Tong, Y., Li, S., Wu, Y., Guo, J., Zhou, B., Zhou, Q., Jiang, L., Niu, J., Zhang, Y., Liu, H., Yuan, S., Huang, S., Zhan, Y., Graphene oxide modified magnetic polyamidoamide dendrimers based magnetic solid phase extraction for sensitive measurement of polycyclic aromatic hydrocarbons. *Chemosphere* 296 (2022), 134009.

Tong, Y., Liu, X., Zhang, L., Green construction of Fe_3O_4@GC submicrocubes for highly sensitive magnetic dispersive solid-phase extraction of five phthalate esters in beverages and plastic bottles. *Food Chemistry* 277 (2019), 579-585.

Urraca, J.L., Castellari, M., Barrios, C.A., Moreno-Bondi, M.C., Multiresidue analysis of fluoroquinolone antimicrobials in chicken meat by molecularly imprinted solid-phase extraction and high performance liquid chromatography. *Journal of Chromatography A* 1343 (2014), 1-9.

Vasapollo, G., Sole, R.D., Mergola, L., Lazzoi, M.R., Scardino, A., Scorrano, S., Mele, G., Molecularly imprinted polymers: present and future prospective. *International Journal of Molecular Sciences* 12(9) (2011), 5908-5945.

Vasconcelos, I., Fernandes, C., Magnetic solid phase extraction for determination of drugs in biological matrices. *TrAC Trends in Analytical Chemistry* 89 (2017), 41-52.

Vasudevan, D., Gaddam, R.R., Trinchi, A., Cole, I., Core-shell quantum dots: Properties and applications. *Journal of Alloys and Compounds* 636 (2015), 395-404.

Wang, T., Liu, S., Gao, G., Zhao, P., Lu, N., Lun, X., Hou, X., Magnetic solid phase extraction of non-steroidal anti-inflammatory drugs from water samples using a metal organic framework of type Fe_3O_4/MIL-101(Cr), and their quantitation by UPLC-MS/MS. *Microchimica Acta* 184(8) (2017), 2981-2990.

Wang, W., Li, Z., Zhang, S., Yang, X., Zang, X., Wang, C., Wang, Z., Triazine-based porous organic framework as adsorbent for solid-phase microextraction of some organochlorine pesticides. *Journal of Chromatography A* 1602 (2019), 83-90.

Wang, X., Ding, H., Yu, X., Shi, X., Sun, A., Li, D., Zhao, J., Characterization and application of molecularly imprinted polymer-coated quantum dots for sensitive fluorescent determination of diethylstilbestrol in water samples. *Talanta* 197 (2019), 98-104.

Wang, X., Gong, L., Zhang, D., Fan, X., Jin, Y., Guo, L., Room temperature ammonia gas sensor based on polyaniline/copper ferrite binary nanocomposites. *Sensors and Actuators B: Chemical* 322 (2020), 128615.

Wang, X., Lu, Y., Shi, L., Yang, D., Yang, Y., Novel low viscous hydrophobic deep eutectic solvents liquid-liquid microextraction combined with acid base induction for the determination of phthalate esters in the packed milk samples. *Microchemical Journal* 159 (2020), 105332.

Wang, X., Wang, J., Du, T., Kou, H., Du, X., Lu, X., Zn (II)-imidazole derived metal azolate framework as an effective adsorbent for double coated solid-phase microextraction of sixteen polycyclic aromatic hydrocarbons. *Talanta* 214 (2020), 120866.

Wang, X., Zhang, J., Zou, W., Wang, R., Facile synthesis of polyaniline/carbon dot nanocomposites and their application as a fluorescent probe to detect mercury. *RSC Advances* 5(52) (2015), 41914-41919.

Wang, Y., Chen, J., Ihara, H., Guan, M., Qiu, H., Preparation of porous carbon nanomaterials and their application in sample preparation: A review. *TrAC Trends in Analytical Chemistry* 143 (2021), 116421.

Wang, Y., Yang, M., Ren, Y., Fan, J., Ratiometric determination of hydrogen peroxide based on the size-dependent green and red fluorescence of CdTe quantum dots capped with 3-mercaptopropionic acid. *Microchimica Acta* 186(5) (2019), 277.

Wang, Z., He, M., Chen, B., Hu, B., Triazine covalent organic polymer coated stir bar sorptive extraction coupled with high performance liquid chromatography for the analysis of trace phthalate esters in mineral water and liquor samples. *Journal of Chromatography A* 1660 (2021), 462665.

Wang, Z., Zhang, Y., Zhang, B., Lu, X., Mn^{2+} doped ZnS QDs modified fluorescence sensor based on molecularly imprinted polymer/sol-gel chemistry for detection of serotonin. *Talanta* 190 (2018), 1-8.

Wei, X., Hao, T., Xu, Y., Lu, K., Li, H., Yan, Y., Zhou, Z., Facile polymerizable surfactant inspired synthesis of fluorescent molecularly imprinted composite sensor via aqueous CdTe quantum dots for highly selective detection of λ-cyhalothrin. *Sensors and Actuators B: Chemical* 224 (2016), 315-324.

Wei, X., Meng, M., Song, Z., Gao, L., Li, H., Dai, J., Zhou, Z., Li, C., Pan, J., Yu, P., Yan, Y., Synthesis of molecularly imprinted silica nanospheres embedded mercaptosuccinic acid-coated CdTe quantum dots for selective recognition of λ-cyhalothrin. *Journal of Luminescence* 153 (2014), 326-332.

Wei, X., Zhou, Z., Hao, T., Li, H., Dai, J., Gao, L., Zheng, X., Wang, J., Yan, Y., Simple synthesis of thioglycolic acid-coated CdTe quantum dots as probes for norfloxacin lactate detection. *Journal of Luminescence* 161 (2015), 47-53.

Wierucka, M., Biziuk, M., Application of magnetic nanoparticles for magnetic solid-phase extraction in preparing biological, environmental and food samples. *TrAC Trends in Analytical Chemistry* 59 (2014), 50-58.

Wise, R., Honeybourne, D., Pharmacokinetics and pharmacodynamics of fluoroquinolones in the respiratory tract. *European Respiratory Journal* 14(1) (1999), 221.

Wojnowski, W., Tobiszewski, M., Pena-Pereira, F., Psillakis, E., AGREEprep - Analytical greenness metric for sample preparation. *TrAC Trends in Analytical Chemistry* 149 (2022), 116553.

Wu, C., Sun, Y., Wang, Y., Duan, W., Hu, J., Zhou, L., Pu, Q., 7-(Diethylamino)coumarin-3-carboxylic acid as derivatization reagent for 405 nm laser-induced fluorescence detection: A case study for the analysis of sulfonamides by capillary electrophoresis. *Talanta* 201 (2019), 16-22.

Wu, D., Chen, Z., Huang, G., Liu, X., ZnSe quantum dots based fluorescence sensors for Cu^{2+} ions. *Sensors and Actuators A: Physical* 205 (2014), 72-78.

Wu, J., Xiao, D., Zhao, H., He, H., Peng, J., Wang, C., Zhang, C., He, J., A nanocomposite consisting of graphene oxide and Fe_3O_4 magnetic nanoparticles

for the extraction of flavonoids from tea, wine and urine samples. *Microchimica Acta* 182(13) (2015), 2299-2306.

Wu, L., Lin, Z.-Z., Zeng, J., Zhong, H.-P., Chen, X.-M., Huang, Z.-Y., Detection of malachite green in fish based on magnetic fluorescent probe of CdTe QDs/nano-Fe_3O_4@MIPs. *Spectrochimica Acta Part A: Molecular and Biomolecular Spectroscopy* 196 (2018), 117-122.

Wu, P., Hou, X., Xu, J.-J., Chen, H.-Y., Electrochemically generated versus photoexcited luminescence from semiconductor nanomaterials: Bridging the valley between two worlds. *Chemical Reviews* 114(21) (2014), 11027-11059.

Wu, Q., Song, Y., Wang, Q., Liu, W., Hao, L., Wang, Z., Wang, C., Combination of magnetic solid-phase extraction and HPLC-UV for simultaneous determination of four phthalate esters in plastic bottled juice. *Food Chemistry* 339 (2021), 127855.

Wu, Y., Zhou, Q., Yuan, Y., Wang, H., Tong, Y., Zhan, Y., Sheng, X., Sun, Y., Zhou, X., Enrichment and sensitive determination of phthalate esters in environmental water samples: A novel approach of MSPE-HPLC based on PAMAM dendrimers-functionalized magnetic-nanoparticles. *Talanta* 206 (2020), 120213.

Xia, Q., Yang, Y., Liu, M., Aluminium sensitized spectrofluorimetric determination of fluoroquinolones in milk samples coupled with salting-out assisted liquid-liquid ultrasonic extraction. *Spectrochimica Acta Part A: Molecular and Biomolecular Spectroscopy* 96 (2012), 358-364.

Xie, L., Liu, S., Han, Z., Jiang, R., Liu, H., Zhu, F., Zeng, F., Su, C., Ouyang, G., Preparation and characterization of metal-organic framework MIL-101(Cr)-coated solid-phase microextraction fiber. *Analytica Chimica Acta* 853 (2015), 303-310.

Xu, J., Zhang, B., Jia, L., Bi, N., Zhao, T., Metal-enhanced fluorescence detection and degradation of tetracycline by silver nanoparticle-encapsulated halloysite nano-lumen. *Journal of Hazardous Materials* 386 (2020) 121630.

Yahaya, N., Ishak, S.M., Mohamed, A.H., Kamaruzaman, S., Mohamad Zain, N.N., Waras, M.N., Hassan, Y., Aziz, N.A., Miskam, M., Wan Abdullah, W.N., Recent applications of electrospun nanofibres in microextraction based-sample

preparation techniques for determination of environmental pollutants. *Current Opinion in Environmental Science & Health* 26 (2022), 100323.

Yang, J., Lin, Z.-Z., Zhong, H.-P., Chen, X.-M., Huang, Z.-Y., Determination of leucomalachite green in fish using a novel MIP-coated QDs probe based on synchronous fluorescence quenching effect. *Sensors and Actuators B: Chemical* 252 (2017), 561-567.

Yang, J.-M., Kou, Y.-K., Sulfo-modified MIL-101 with immobilized carbon quantum dots as a fluorescence sensing platform for highly sensitive detection of DNP. *Inorganica Chimica Acta* 519 (2021), 120276.

Yang, R., Liu, Y., Yan, X., Liu, S., Simultaneous extraction and determination of phthalate esters in aqueous solution by yolk-shell magnetic mesoporous carbon-molecularly imprinted composites based on solid-phase extraction coupled with gas chromatography-mass spectrometry. *Talanta* 161 (2016), 114-121.

Yang, S., Sun, X., Chen, Y., A novel fluorescence enhancement probe based on L-Cystine modified copper nanoclusters for the detection of 2,4,6-trinitrotoluene. *Materials Letters* 194 (2017), 5-8.

Yi, Y.-N., Li, G.-R., Wang, Y.-S., Zhou, Y.-Z., Zhu, H.-M., Simultaneous determination of norfloxacin and lomefloxacin in milk by first derivative synchronous fluorescence spectrometry using Al (III) as an enhancer. *Analytica Chimica Acta* 707(1) (2011), 128-134.

Yu, L., Ma, F., Ding, X., Wang, H., Li, P., Silica/graphene oxide nanocomposites: Potential adsorbents for solid phase extraction of trace aflatoxins in cereal crops coupled with high performance liquid chromatography. *Food Chemistry* 245 (2018), 1018-1024.

Yu, Y., Zhang, K., Li, Z., Sun, S., Synthesis and luminescence characteristics of DHLA-capped PbSe quantum dots with biocompatibility. *Optical Materials* 34(5) (2012), 793-798.

Yuphintharakun, N., Nurerk, P., Chullasat, K., Kanatharana, P., Davis, F., Sooksawat, D., Bunkoed, O., A nanocomposite optosensor containing carboxylic functionalized multiwall carbon nanotubes and quantum dots incorporated into a molecularly imprinted polymer for highly selective and sensitive detection of

ciprofloxacin. *Spectrochimica Acta Part A: Molecular and Biomolecular Spectroscopy* 201 (2018), 382-391.

Zang, L., He, M., Wu, Z., Chen, B., Hu, B., Imine-linked covalent organic frameworks coated stir bar sorptive extraction of non-steroidal anti-inflammatory drugs from environmental water followed by high performance liquid chromatography-ultraviolet detection. *Journal of Chromatography A* 1659 (2021), 462647.

Zare, M., Ramezani, Z., Rahbar, N., Development of zirconia nanoparticles-decorated calcium alginate hydrogel fibers for extraction of organophosphorous pesticides from water and juice samples: Facile synthesis and application with elimination of matrix effects. *Journal of Chromatography A* 1473 (2016), 28-37.

Zhang, G., Tan, L., Cheng, H., Li, F., Liu, X., Lu, J., Different interesting enhanced influence from polyaniline and poly(o-toluidine) on electrocatalytic activities of Pt on them toward electrooxidation of methanol. *International Journal of Hydrogen Energy* 43(33) (2018), 16049-16060.

Zhang, J., Wei, Y., Qiu, S., Xiong, Y., A highly selective and simple fluorescent probe for salbutamol detection based on thioglycolic acid-capped CdTe quantum dots. *Spectrochimica Acta Part A: Molecular and Biomolecular Spectroscopy* 247 (2021), 119107.

Zhang, L., Chen, L., Fluorescence probe based on hybrid mesoporous silica/quantum dot/molecularly imprinted polymer for detection of tetracycline. *ACS Applied Materials & Interfaces* 8(25) (2016), 16248-16256.

Zhang, Q., Zhi, Y., Bao, L., Zheng, Y., Wang, X., Jiang, L., Wu, Y., Determination of six parabens in biological samples by magnetic solid-phase extraction with magnetic mesoporous carbon adsorbent and UHPLC-MS/MS. *Journal of Chromatography B* 1179 (2021), 122817.

Zhang, W., Zhang, Z., Li, Y., Chen, J., Li, X., Zhang, Y., Zhang, Y., Novel nanostructured MIL-101(Cr)/XC-72 modified electrode sensor: A highly sensitive and selective determination of chloramphenicol. *Sensors and Actuators B: Chemical* 247 (2017), 756-764.

Zhang, Y., Zhou, H., Zhang, Z.-H., Wu, X.-L., Chen, W.-G., Zhu, Y., Fang, C.-F., Zhao, Y.-G., Three-dimensional ionic liquid functionalized magnetic graphene

oxide nanocomposite for the magnetic dispersive solid phase extraction of 16 polycyclic aromatic hydrocarbons in vegetable oils. *Journal of Chromatography A* 1489 (2017), 29-38.

Zhang, Z., Chen, J., Yang, Q., Lan, K., Yan, Z., Chen, J., Eco-friendly intracellular microalgae synthesis of fluorescent CdSe QDs as a sensitive nanoprobe for determination of imatinib. *Sensors and Actuators B: Chemical* 263 (2018), 625-633.

Zheng, L., Wang, F., Jiang, C., Ye, S., Tong, J., Dramou, P., He, H., Recent progress in the construction and applications of metal-organic frameworks and covalent-organic frameworks-based nanozymes. *Coordination Chemistry Reviews* 471 (2022), 214760.

Zhou, X., Wang, A., Yu, C., Wu, S., Shen, J., Facile synthesis of molecularly imprinted graphene quantum dots for the determination of dopamine with affinity-adjustable. *ACS Applied Materials & Interfaces* 7(22) (2015), 11741-11747.

Zhou, Y., Qu, Z.-b., Zeng, Y., Zhou, T., Shi, G., A novel composite of graphene quantum dots and molecularly imprinted polymer for fluorescent detection of paranitrophenol. *Biosensors and Bioelectronics* 52 (2014), 317-323.

Zhou, Z., Li, T., Xu, W., Huang, W., Wang, N., Yang, W., Synthesis and characterization of fluorescence molecularly imprinted polymers as sensor for highly sensitive detection of dibutyl phthalate from tap water samples. *Sensors and Actuators B: Chemical* 240 (2017), 1114-1122.

Zhou, Z.-Q., Yan, R., Zhao, J., Yang, L.-Y., Chen, J.-L., Hu, Y.-J., Jiang, F.-L., Liu, Y., Highly selective and sensitive detection of Hg^{2+} based on fluorescence enhancement of Mn-doped ZnSe QDs by Hg^{2+}-Mn^{2+} replacement. *Sensors and Actuators B: Chemical* 254 (2018), 8-15.

Appendices

Paper I

Orachorn, N., Bunkoed, O., A nanocomposite fluorescent probe of polyaniline, graphene oxide and quantum dots incorporated into highly selective polymer for lomefloxacin detection. ***Talanta*** 203 (2019), 261-268.

(Reprinted with permission of Elsevier)

Talanta 203 (2019) 261–268

Contents lists available at ScienceDirect

Talanta

journal homepage: www.elsevier.com/locate/talanta

A nanocomposite fluorescent probe of polyaniline, graphene oxide and quantum dots incorporated into highly selective polymer for lomefloxacin detection

Naphatsakorn Orachorn, Opas Bunkoed*

Center of Excellence for Innovation in Chemistry, Department of Chemistry, Faculty of Science, Prince of Songkla University, Hat Yai, Songkhla, 90112, Thailand

ARTICLE INFO

Keywords:
Quantum dots
Lomefloxacin
Polyaniline
Graphene oxide
Molecularly imprinted polymer

ABSTRACT

A nanocomposite fluorescent probe based on fluorescence quenching was fabricated and utilized for the detection of lomefloxacin. The fabricated probe integrated the high sensitivity of quantum dots, the excellent selectivity of molecularly imprinted polymer and the high adsorption affinity of graphene oxide and polyaniline. The probe exhibited good sensitivity, high specificity, and rapidity for lomefloxacin monitoring. Fluorescence emission was reduced linearly by lomefloxacin from 0.10 to 50.0 μg L^{-1} and the probe exhibited a low limit of detection of 0.07 μg L^{-1}. The nanooptosensor successfully detected lomefloxacin in milk, chicken meat and egg samples. Recoveries were obtained in the range of 81.5–99.6% and the RSDs were below 7%. The results of this method agreed well with results of HPLC but provided higher sensitivity. This easily fabricated nanocomposite probe could be developed into a highly sensitive and selective optosensor to detect other organic compounds in various complex samples.

1. Introduction

Lomefloxacin is a fluoroquinolone (FQs) antibiotic drug extensively used in human and animal patients to treat respiratory tract diseases, skin and urinary tract infections, and bronchitis [1,2]. If misused it can leave residues in animal products and can cause side effects such as nausea, diarrhea and headache in humans [3]. Accumulated in the human body after long-term consumption of animal products with residual contamination, lomefloxacin may lead to carcinogenesis, mutagenesis and drug tolerance [4]. The development of a reliable method of detecting lomefloxacin in food samples is, therefore, necessary. Several methods have been applied for the determination of lomefloxacin. These methods have included high performance liquid chromatography [5,6], capillary electrophoresis [7] and voltammetry [8,9]. Although these methods are highly sensitive, selective and precise, most of them have limitations. They can be time-consuming, and require complicated pretreatment and expensive equipment. Spectrofluorimetry is an interesting alternative method that avoids these drawbacks due to its simple measurement procedure, short analysis time and cost-effectiveness [10–12]. The sensitivity and selectivity of spectrofluorimetry can be improved using nanocomposite fluorescent probes. To further improve sensitivity, the fluorescent probe can be composited with quantum dot (QD) nanoparticles. QDs have good optical properties, such as symmetric and narrow emission spectra [13] and good photostability [14]. To enhance the selectivity of composite fluorescent probes, molecularly imprinted polymer (MIP) is an interesting material which provides high specificity for target analytes. MIPs are normally prepared by a sol-gel process in the presence of template molecules (target analytes), a functional monomer and a cross-linker [15]. After complete polymerization, the template is removed from the polymer layer to leave specific recognition cavities complementary in shape, size and functional groups to the template [16]. In addition to their low cost and good stability, MIPs can be easily prepared. Moreover, the affinity binding between lomefloxacin and the fluorescent probe can be improved by compositing QDs and MIP with graphene oxide (GOx), which has a large surface area. GOx contains π structures, hydroxyl groups, epoxide groups and carboxyl groups. GOx can adsorb target analytes via π-π interactions and hydrogen bonding with a strong affinity [17,18]. Furthermore, the adsorption of lomefloxacin can also be improved with polyaniline (PANI). PANI is a conductive polymer that contains π structures and amine groups to contribute strong π-π interactions and hydrogen bonding with target analytes [19]. In addition, PANI is easy to prepare, has a large surface area and good chemical stability [20].

In this work, nanprobes containing GOx, PANI and CdTe QDs incorporated into MIP were synthesized and used for lomefloxacin

* Corresponding author.
E-mail addresses: opas.b@psu.ac.th, opas1bunkoed@hotmail.com (O. Bunkoed).

https://doi.org/10.1016/j.talanta.2019.05.082
Received 19 April 2019; Received in revised form 18 May 2019; Accepted 18 May 2019
Available online 22 May 2019
0039-9140/

detection. The quantitative analysis of lomefloxacin was based on the quenching of fluorescence intensity due to rebinding of lomefloxacin with specific recognition sites on the surface of the nanocomposite fluorescent probe. The developed fluorescent probe was applied for detection of lomefloxacin in milk, chicken meat and egg samples. The accuracy of the nanooptosensor was evaluated by analysis of lomefloxacin in spiked samples and also by comparing the experimental results with results from a HPLC method.

2. Experimental

2.1. Chemicals and reagents

Lomefloxacin hydrochloride (> 98.0), Tellurium (99.8), 3-aminopropyltriethoxysilane (APTES, ≥98%), thioglycolic acid (TGA), sodium borohydride ($NaBH_4$), tetraethyl orthosilicate (TEOS, ≥99%) and graphene oxide were from Sigma-Aldrich (MO, USA). Cadmium chloride ($CdCl_2{\cdot}5H_2O$), sodium dihydrogen orthophosphate ($NaH_2PO_4{\cdot}2H_2O$) and di-sodium hydrogen orthophosphate dodecahydrate ($Na_2HPO_4{\cdot}12H_2O$) were from Univar. Sodium hydroxide, ammonia solution (25% $NH_3{\cdot}H_2O$) and ethanol were from RCI Labscan (Bangkok, Thailand).

2.2. Instrumental

Fluorescence measurement was carried out with an RF5301PC spectrofluorophotometer (Shimadzu, Tokyo, Japan). UV–Vis absorption spectra were recorded with an AvaSpec-2048 spectrometer (Apeldoorn, the Netherlands). Fourier transform infrared (FTIR) spectra were recorded using a BX FTIR spectroscope (PerkinElmer, Ma, USA). Scanning electron microscope (SEM) images of nanocomposite PANI-GOx-MIP-QDs were acquired using a JSM-5200 scanning electron microscope (JEOL, Tokyo, Japan). Transmission electron microscope (TEM) images were obtained on a Philips TECNAI 20 (Eindhoven, the Netherlands).

2.3. Synthesis of TGA-capped CdTe QDs

The synthesis method of CdTe QDs was modified from a previous work [21]. Briefly, 45.0 mg of $CdCl_2$ was dissolved in deionized water (100 mL), 30 µL of TGA was added to the solution and pH was adjusted to 11.5 with NaOH (1.0 M). The solution was purged with N_2 gas for 15 min. After purging, 0.50 mL of NaHTe solution, prepared by reacting 51 mg of Te with 45 mg of $NaBH_4$ in 2.0 mL of deionized water, was injected into the solution with stirring. The solution was heated at 90 °C for 10 min. Synthesized CdTe QD nanoparticles were precipitated from the solution with ethanol and centrifuged at 5000 rpm for 15 min. The synthesized CdTe QD nanoparticles were stored in a desiccator before use.

2.4. Synthesis of polyaniline

Polyaniline was synthesized by the oxidation reaction of aniline and ammonium persulfate [22]. First, 150 µL of aniline monomer was dissolved in 5.0 mL of 1.0 M HCl in darkness and 93 mg of ammonium persulfate was dissolved in 5.0 mL of 1.0 M HCl. Both solutions were then mixed in darkness for 1 h. The color of the solution mixture changed to dark green.

2.5. Synthesis of PANI-GOx-MIP-QDs nanocomposite probe

The PANI-GOx-MIP-QDs nanocomposite probe was synthesized by a sol-gel process (Fig. 1). First, 0.5 mg of graphene oxide was dispersed in deionized water (5.0 mL) and 9.7 mg of lomefloxacin hydrochloride and 47.8 µL of APTES were added to the solution and stirred for 1 h. Next, 5.0 mL of CdTe QDs were added and stirred for 1 h. Then, 112.8 µL of TEOS (cross-linker), 150.0 µL of 25% ammonia solution and 40.0 µL of polyaniline solution were added and the mixture was stirred for 6 h. The template molecules were removed from the nanocomposite probe by washing three times with 30 mL of ethanol. The PANI-GOx-MIP-QDs nanocomposite probe was collected by centrifugation at 5000 rpm for 10 min and dried at 60 °C. The non-imprinted polymer probe (PANI-GOx-NIP-QDs) was prepared by the same method without the addition of lomefloxacin.

2.6. Fluorescence measurement

The PANI-GOx-MIP-QDs or PANI-GOx-NIP-QDs nanoprobe were dispersed in 10 mM phosphate buffer (pH 8.0) and 30 µL was mixed with 100 µL of lomefloxacin standard or sample solution. The mixture solution was incubated for 20 min at 25 °C and transferred into a quartz cell for measurement. Detection was performed by fixing the excitation wavelength at 355 nm and recording the fluorescence emission at 400–700 nm.

2.7. Pretreatment of food samples

Milk, chicken meat and egg samples were obtained from supermarkets in Hat Yai, Thailand. The extraction method of lomefloxacin from milk samples was modified from a previous report [23]. A 10.0 g sample of milk was centrifuged at 5000 rpm for 20 min to remove fat. To precipitate proteins, 15.0 mL of acetonitrile was added into the defatted milk, vortexed for 1 min and then centrifuged at 5000 rpm for 10 min. The supernatant was collected and evaporated at 50 °C and re-dissolved with deionized water (10.0 mL) before analysis with the nanoprobes.

The lomefloxacin was extracted from chicken meat samples according to a previous report [24] in which 1.0 g of chicken meat was extracted with 2.0 mL of ethanol by sonication for 10 min and then centrifuged at 5000 rpm for 10 min. The supernatant was collected and defatted with 2.0 mL of hexane by centrifugation at 5000 rpm for 5 min. The ethanol phase was evaporated at 50 °C and re-dissolved with deionized water (10.0 mL) before analysis.

The extraction procedure of lomefloxacin in egg samples was adapted from a previous report [25]. Briefly, 5.0 g of homogenized whole egg samples was extracted with 10.0 mL of acetonitrile using sonication for 15 min and then centrifuged at 5000 rpm for 10 min. The supernatant was collected in a 50 mL polypropylene tube and defatted by vortexing for 1 min with 2 mL of hexane followed by centrifugation at 5000 rpm for 10 min. The supernatant was separated and evaporated at 50 °C and re-dissolved with deionized water (10.0 mL) before analysis.

2.8. Analysis of lomefloxacin by HPLC method

HPLC analysis was performed using the Hewlett-Packard 1100 series HPLC system (Agilent Technologies, Germany). The data were acquired and evaluated using ChemStation software. The column was a Fortis C_{18} (5 µm, 4.6 mm × 15 cm). The mobile phase consisted of 25 mM of phosphoric acid (80%) and acetonitrile (20%) at a flow rate of 0.9 mL min^{-1}. Lomefloxacin was detected with a fluorescence detector (FLD) at excitation and emission wavelengths of 280 and 450 nm, respectively.

3. Results and discussions

3.1. Characterization of nanocomposite fluorescence probe

The TGA-capped CdTe QDs showed maximum absorption at about 500 nm and maximum fluorescence emission at about 545 nm (Fig. S1). The synthesized TGA-capped CdTe QDs exhibited fluorescence emission of high intensity in a symmetric spectrum indicative of a highly sensitive optosensor. The particle size of CdTe QDs was estimated from the

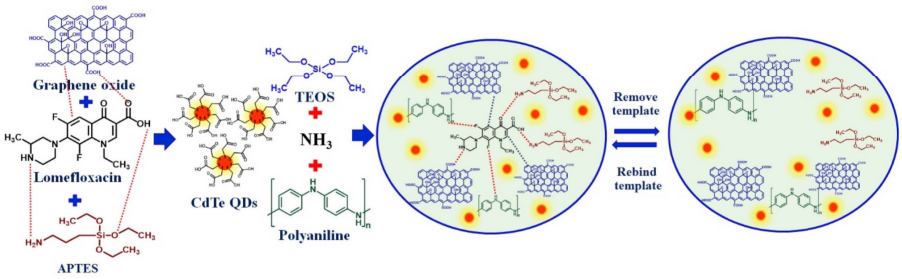

Fig. 1. The fabrication procedure of PANI-GOx-MIP-QDs nanoprobe for lomefloxacin detection.

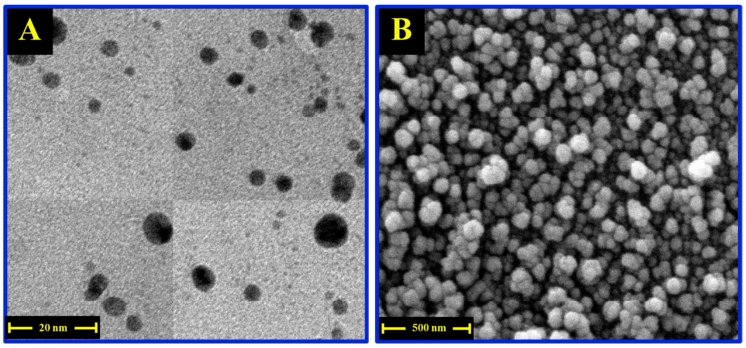

Fig. 2. TEM image of TGA-CdTe QDs (A) and SEM image of PANI-GOx-MIP-QDs fluorescent nanoprobe (B).

maximum absorption to be 2.34 nm [21]. The estimated particle size was agreed well with the TEM image as showed in Fig. 2A and the particle size distribution histogram is shown in Fig. S2. The morphology of the nanocomposite probe was investigated by SEM (Fig. 2B). The surface of the PANI-GOx-MIP-QDs nanocomposite fluorescent probe was rough and the average particle size was around 100 nm. The morphology indicates the presence of specific recognition cavities on the surface of the composite probe.

In the FT-IR spectrum of the synthesized TGA-capped CdTe QDs (Fig. S3a), the peaks at 1388 and 1600 cm^{-1} correspond to symmetric and asymmetric stretching of the carboxylate group. The characteristic peaks at 3450 and 1230 cm^{-1} correspond to O–H and C–O stretching of carboxylic groups. In the FT-IR spectrum of the PANI-GOx-MIP-QDs nanocomposite probe (Fig. S3b), the absorption peaks at 1062 and 765 cm^{-1} are due to Si–O–Si asymmetric stretching and Si–O vibration of the silica layer. The absorption peak at 1475 cm^{-1} is assigned to C═C stretching of the benzenoid ring of PANI. The absorption peak at approximately 1725 cm^{-1} is attributed to the C═O stretching of the carbonyl group of GOx. These results confirmed that GOx and PANI were successfully composited with the MIP. The quantum yield (QY) of CdTe QDs, MIP-QDs and PANI-GO-MIP-QDs were 0.91, 0.64 and 0.53, respectively, using Rhodamine 6G as the fluorescence standard.

The nanocomposite PANI-GOx-MIP-QDs probe in the presence of the template (lomefloxacin) exhibited a low fluorescence emission (Fig. 3). After the template was removed, the emission signal was restored almost to the same level as the emission signal of the non-imprinted polymer probe. This result implied that the template had been successfully removed from the nanocomposite probe and that the probe could rebind with template molecules.

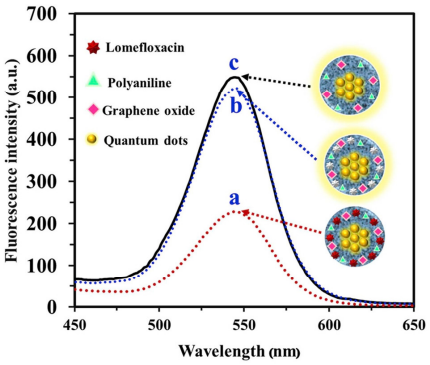

Fig. 3. Fluorescence spectra of PANI-GOx-MIP-QDs before (a) and after template removal (b) and PANI-GOx-NIP-QDs nanoprobe (c).

3.2. Sensitivity of different nanoprobes

Different nanoprobes were evaluated for their sensitivity of detection of lomefloxacin. These nanoprobes comprised NIP-QDs, MIP-QDs,

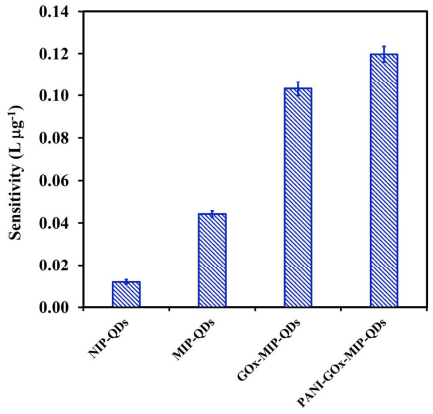

Fig. 4. The sensitivity of different nanoprobes for the detection of lomefloxacin.

GOx-MIP-QDs and PANI-GOx-MIP-QDs. PANI-GOx-MIP-QDs exhibited the highest sensitivity for the detection of lomefloxacin (Fig. 4). The high level of sensitivity of this nanoprobe was due to the presence of recognition cavities in the MIP and the presence of the functional groups of graphene oxide and polyaniline which interacted with lomefloxacin through hydrogen bonding and π-π interaction.

3.3. Optimization of experimental condition

3.3.1. Incubation time

To obtain the highest quenching efficiency at the shortest analysis time, we investigated the adsorption equilibrium time between the recognition cavities of the nanocomposite probe and lomefloxacin. Quenching efficiency increased with increasing incubation time up to 20 min and then it remained constant (Fig. 5A). Thus, the incubation time of 20 min was selected as the optimum value for lomefloxacin detection.

3.3.2. Ratio of template to monomer and cross-linker

The properties of the recognition sites of nanocomposite probes depend on the composition of the MIP. Factors that affect the properties include the amounts of template, functional monomer and cross-linker used to fabricate the MIP. Therefore, the influence of the ratio of template to monomer to cross-linker was investigated. The ratio of template to monomer of 1:6 gave the highest sensitivity (Fig. 5B). Low sensitivity was obtained at low amounts of monomer due to the smaller number of functional groups (-NH_2) present on the surface of the nanocomposite probe. Sensitivity was also low when too large a proportion of monomer was used in fabricating the probe. In this case, the thickness of the MIP layer inhibited binding between lomefloxacin and the specific recognition cavities. The ratio of template to cross-linker of 1:20 produced the highest sensitivity (Fig. 5C). Sensitivity decreased at low amounts of cross-linker due to the weak structure of the obtained MIP layer. On the other hand, at too high an amount of cross-linker, the MIP structure was too dense which impaired the formation of recognition sites. Therefore, for further investigation, the MIP was fabricated using the ratio of 1:6:20 of lomefloxacin to APTES to TEOS.

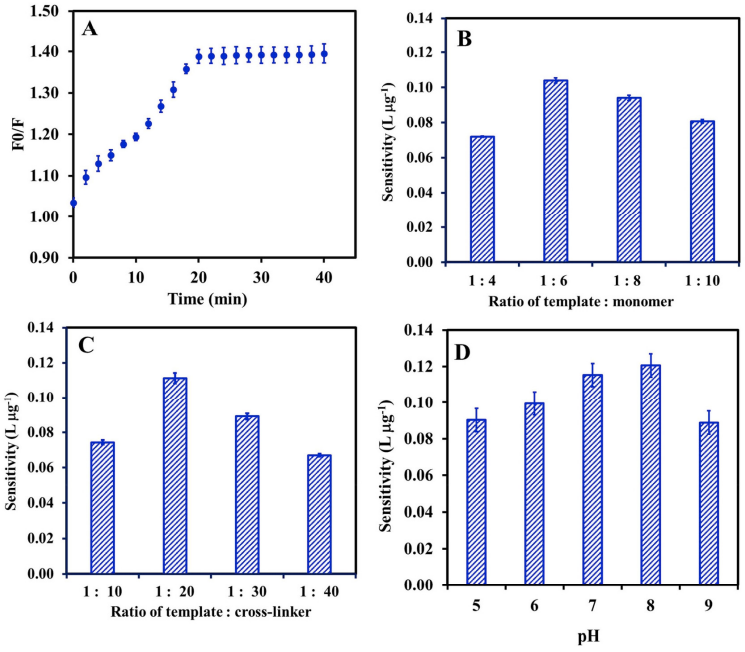

Fig. 5. The effect of incubation time (A), ratio of template to monomer (B), ratio of template to cross-linker (C) and pH of fluorescent probe solution (D).

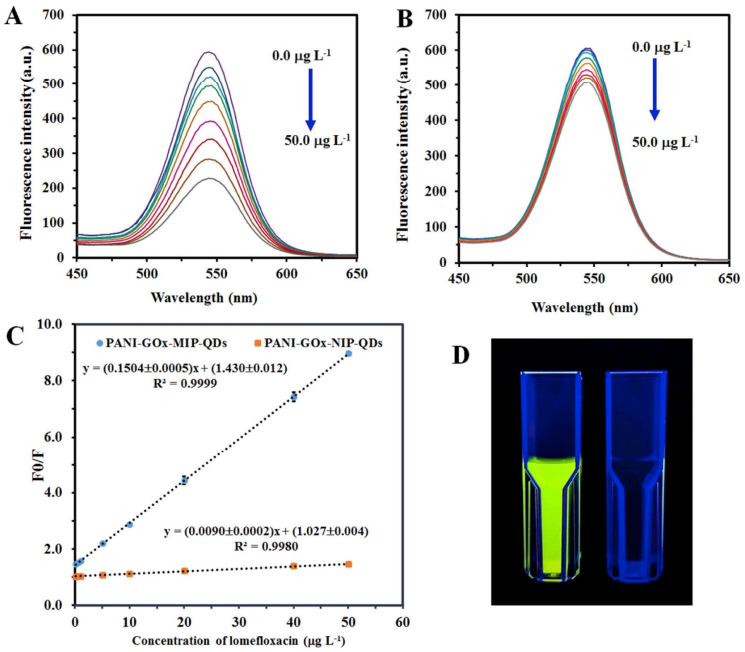

Fig. 6. The fluorescence spectra of PANI-GOx-MIP-QDs nanocomposite probe (A), PANI-GOx-NIP-QDs nanoprobe (B), linear calibration curve (C) and photograph of PANI-GOx-MIP-QDs with (right) and without (left) lomefloxacin (D).

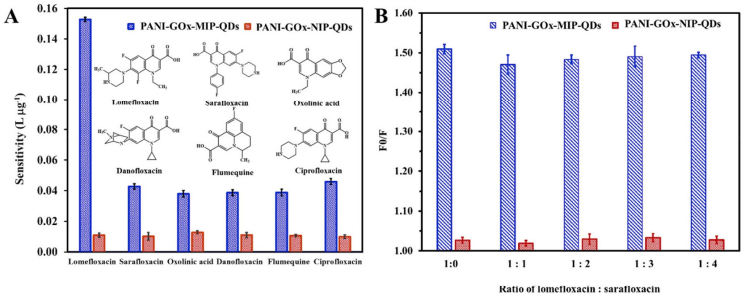

Fig. 7. The selectivity of PANI-GOx-MIP-QDs nanoprobe (A) and competitive study (B).

3.3.3. *Effect of pH*

The PANI-GOx-MIP-QDs nanoprobes were dispersed in phosphate buffer at pH 5, 6, 7, 8 and 9 before being mixed with lomefloxacin. The nanocomposite probe exhibited the highest sensitivity at pH 8 (Fig. 5D). At pH below 8, sensitivity was low due to reduced hydrogen bonding between lomefloxacin and binding sites. The reduction in hydrogen bonding was caused by the lack of hydrogen ions under the acidic condition [26]. Sensitivity was also reduced at pH above 8 because the silica structure of the MIP layer was not stable under the alkaline condition. Therefore, for the detection of lomefloxacin, the nanocomposite PANI-GOx-MIP-QDs nanoprobes were dispersed in phosphate buffer at pH 8.0.

3.4. *Analytical performance for the analysis of lomefloxacin and fluorescence quenching mechanism*

To evaluate the potential of the nanocomposite fluorescent probe in real samples, analytical performance was investigated under the optimized condition. The fluorescence intensity of the PANI-GOx-MIP-QDs probe decreased linearly with increasing lomefloxacin concentration (Fig. 6A) and the emission intensity of PANI-GOx-NIP-QDs decreased only slightly (Fig. 6B). The PANI-GOx-MIP-QDs fluorescence probe

Table 1
The determination of lomefloxacin in milk, chicken meat and egg samples.

Sample	Concentration of lomefloxacin (μg kg^{-1})		Recovery (%)	RSD (%)
	Added	Found		
Milk 1	0.00	n.d.	–	–
	0.5	0.48	96.0	1.3
	1.0	0.96	96.0	0.8
	10.0	8.78	87.8	1.1
	50.0	48.91	97.8	0.5
Milk 2	0.00	n.d.	–	–
	0.5	0.47	94.0	0.6
	1.0	0.95	95.0	2.2
	10.0	9.35	93.5	0.6
	50.0	49.79	99.6	0.3
Milk 3	0.00	n.d.	–	–
	0.5	0.44	88.9	1.9
	1.0	0.86	85.8	2.9
	10.0	8.78	87.8	1.2
	50.0	47.76	95.5	0.4
Milk 4	0.00	n.d.	–	–
	0.5	0.44	88.7	1.7
	1.0	0.85	84.9	2.7
	10.0	8.49	84.9	1.0
	50.0	48.19	96.4	0.4
Chicken meat I	0.00	n.d	–	–
	0.5	0.43	85.9	3.9
	1.0	0.89	88.8	6.5
	10.0	8.92	89.2	3.7
	50.0	48.90	97.8	0.3
Chicken meat II	0.00	0.83	–	–
	0.5	1.26	86.2	5.5
	1.0	1.69	85.8	5.4
	10.0	9.17	83.5	3.0
	50.0	48.58	95.5	1.8
Chicken meat III	0.00	n.d.	–	–
	0.5	0.43	86.5	3.3
	1.0	0.86	85.9	6.5
	10.0	8.15	81.5	1.4
	50.0	47.39	94.8	1.9
Egg I	0.00	1.24	–	–
	0.5	1.69	89.2	5.6
	1.0	2.13	88.3	4.8
	10.0	9.55	83.1	1.1
	50.0	49.15	95.8	2.6
Egg II	0.00	1.39	–	–
	0.5	1.83	88.1	3.6
	1.0	2.22	83.2	2.6
	10.0	10.59	92.0	1.0
	50.0	48.38	94.0	3.7
Egg III	0.00	n.d.	–	–
	0.5	0.45	90.9	4.6
	1.0	0.94	94.0	2.6
	10.0	9.10	91.0	3.8
	50.0	47.37	94.7	1.6

exhibited a good linearity in the range of 0.1–50.0 μg L^{-1}, y = (0.1504 ± 0.0005)x + (1.430 ± 0.012), with a determination coefficient (R^2) of 0.9999 (Fig. 6C). A photograph of PANI-GOx-MIP-QDs in solution with and without lomefloxacin is shown in Fig. 6D. Calculated based on the 3SD/slope and 10SD/slope, the developed optosensor provided a limit of detection (LOD) of 0.07 μg L^{-1} and a limit of quantification (LOQ), of 0.22 μg L^{-1}. The very low LOD and LOQ implied that the nanocomposite probe has a high sensitivity which can detect lomefloxacin even at very low concentrations.

The quenching mechanism of the PANI-GOx-MIP-QDs by lomefloxacin was described according to the Stern-Volmer equation as follows:

$$F0/F = 1 + KSV[C],$$

where F0 and F are the fluorescence emission of the PANI-GOx-MIP-QDs nanoprobe in the absence and presence of lomefloxacin, respectively, K_{SV} is the Stern-Volmer constant, and [C] is the lomefloxacin concentration. From the ratio of the K_{SV} of MIP and NIP (IF = $K_{SV(MIP)}/K_{SV(NIP)}$), the imprinting factor (IF) of the nanocomposite probe was calculated to be 16.7. This imprinting factor indicated that the fabricated nanocomposite probe produced large specific recognition sites for binding with lomefloxacin. Consequently, this highly specific fluorescent probe can detect lomefloxacin in complex samples.

The emission spectrum of the PANI-GOx-MIP-QDs nanoprobe was in the range of 475–625 nm, which does not overlap with the absorption spectrum of lomefloxacin (Fig. S4). This result implied that the quenching mechanism of the PANI-GOx-MIP-QDs nanoprobe by lomefloxacin is not due to energy resonance transfer but is based on photo-induced electron transfer.

3.5. The selectivity of nanocomposite fluorescence probe

The selectivity of the PANI-GOx-MIP-QDs nanoprobe for the determination of lomefloxacin was investigated by comparing the sensitivity of the probe towards other analog structures. These analogs were sarafloxacin, danofloxacin, ciprofloxacin, flumequine and oxolinic acid. The PANI-GOx-MIP-QDs nanoprobe exhibited much higher sensitivity towards lomeflocxacin than towards the other analog structures (Fig. 7A). The PANI-GOx-NIP-QDs nanoprobe, on the other hand, showed no significant difference in sensitivity towards lomefloxacin and the other analog structure molecules. Competitive binding was studied by measuring the fluorescence change in the nanocomposite PANI-GOx-MIP-QDs probe in the presence of different ratios of lomefloxacin to sarafloxacin. As shown in Fig. 7B, fluorescence quenching was not significantly different at higher sarafloxacin concentrations. This result confirmed that the generated recognition cavities are highly specific for lomefloxacin.

3.6. The stability and reproducibility of PANI-GOx-MIP-QDs nanoprobe

The stability of the fabricated PANI-GOx-MIP-QDs nanoprobe was evaluated by measuring fluorescence intensity every 30 min. Fluorescence intensity did not significantly change over 5 h (> 95%) (Fig. S5). This result implied that the MIP layer helped enhance the photostability of the QDs, which increased the stability of the fluorescent probe.

The synthesis reproducibility of the nanoprobe was also investigated based on lot-to-lot preparation. Six different lots of the nanoprobe were synthesized under the same experimental condition. The RSD of sensitivity was 2% (Fig. S6) which indicated that the fabrication procedure has a good reproducibility.

3.7. Analysis of lomefloxacin in real samples

The nanooptosensor was utilized for the determination of lomefloxacin in milk, chicken meat and egg samples. Before analysis by the developed nanooptosensor, all samples were pretreated as described in section 2.7. Low concentrations of lomefloxacin were found in some milk, chicken and egg samples. However, the found concentrations were much lower than the MRL value. The accuracy of the nanooptosensor was also evaluated by measuring lomefloxacin concentration in milk, chicken meat and egg samples spiked at different concentrations (0.5, 1.0, 10.0, 50.0 μg kg^{-1}). Recoveries were obtained in the range of 81.5–99.6% with an RSD lower than 7% (Table 1). These results implied that the developed nanooptosensor has a good accuracy and can therefore provide a reliable method of detecting lomefloxacin in real samples containing various matrix interferences.

3.8. Comparison between the nanooptosensor and HPLC technique

The results obtained with the nanooptosensor were compared with results from detection by HPLC. Spiked milk samples were analyzed

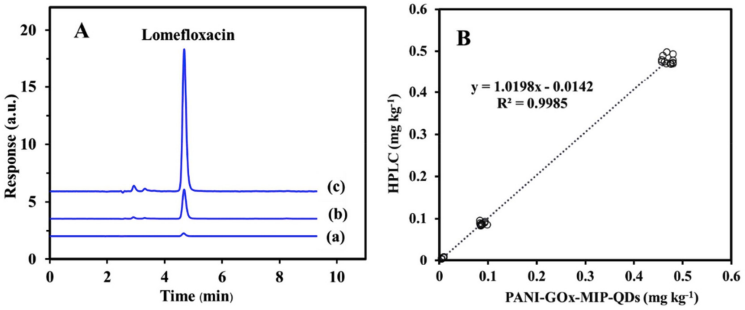

Fig. 8. The HPLC chromatogram of lomefloxacin at different concentration; a = 0.01, b = 0.1, c = 0.5 mg kg^{-1} (A) and the correlation curve between the nanooptosensor and HPLC method (B).

Table 2
Comparison of the nanooptosensor using PANI-GOx-MIP-QDs nanoprobes and other methods for lomefloxacin detection.

Analytical method	Samples	Linear range (μg L^{-1} or μg kg^{-1})	LOD (μg L^{-1} or μg kg^{-1})	Recovery (%)	RSD (%)	References
SPE-enhanced Spectrofluorimetry	Plasma and Urine	50–450	15	93.0–99.0	< 3.1	[10]
UA-DLLME- HPLC-UV	Pharmaceutical wastewater	10–2000	0.37	90.9–104.8	2.5–4.1	[6]
Colorimetric	Urine	70–1760	35	102.1–103.9	1–3	[27]
HPLC-UV	Pharmaceutical tablet	400–24000	520	96.9–103.6	< 1.0	[28]
Differential pulse adsorptive stripping voltammetry	Urine and Serum	1.0–10.0	0.3	95.7–103.0	0.8–3.8	[8]
Differential pulse stripping voltammetry	Milk, Honey and Egg	10–80	1.60	63.0–99.0	–	[9]
CE-electrochemists- luminescence	Urine	200–80000	60	94.5–96.5	4.3–4.9	[7]
Spectrofluorimetry	Pure powder and Pharmaceutical tablets	77–1552	23	99.3–101.3	0.7–0.9	[11]
Spectrofluorimetry	Pharmaceutical formulations	10–3000	8.0	99.1–103.0	0.4–2.1	[29]
HPLC-FLD	Chicken	10–500	12.2	68.0–76.0	3.0–8.0	[5]
PANI-GOx-MIP-QDs Spectrofluorimetry	Milk, chicken meat and egg	0.1–50.0	0.07	81.5–99.6	< 7.0	This work

using both methods. The HPLC chromatogram of lomefloxacin in spiked milk samples at different concentrations are shown in Fig. 8A. As can be seen in Fig. 8B, the results produced by the nanooptosensor agreed well with the results from HPLC with a correlation coefficient of 0.9985. This result implied that the nanooptosensor can be an effective and reliable alternative method for lomefloxacin detection in food samples. Moreover, comparison with other previous works showed that the developed nanooptosensor provided a wider linear range and much lower detection limit than other methods (Table 2). Meanwhile, accuracy in terms of recovery and precision is comparable with previous works. The comparison can confirm that the developed optosensor using PANI-GOx-MIP-QDs probe is highly sensitive for lomefloxacin detection. Moreover, this method is shorter analysis time, simpler to operate and had a cheaper analysis cost than chromatographic methods which require expensive instrument and use large amounts of organic solvents as mobile phase. In addition, the selectivity of this optosensor was improved with the use of MIPs, without requiring complicated separation procedures crucial for other methods.

4. Conclusion

A highly sensitive and selective nanocomposite fluorescent probe was successfully fabricated with good affinity for lomefloxacin detection. The quantitative analysis was based on the quenching of emission intensity when the target compounds bound to the specific recognition cavities of the nanocomposite probe. This nanooptosensor was used to analyze trace lomefloxacin in milk, chicken meat and egg samples. It showed a good recovery (81.5–99.6%) and provided a very low limit of detection. The nanoprobe fabrication procedure can be modified for the determination of other compounds. The results of this method agreed well with results of a conventional HPLC method but the fabricated probe had a higher sensitivity which detected target analytes at very low concentration. The others advantages of this nanosensor include rapid and convenient detection, accuracy and cost-effectiveness.

Acknowledgements

The authors thank Prince of Songkla University (grant No. SCI6202115N-0) and the Thailand Research Fund (TRF), Office of the Higher Education Commission and Center of Excellence for Innovation in Chemistry (PERCH-CIC) for financial support. The authors thank Mr. Thomas Duncan Coyne for English proofreading.

Appendix A. Supplementary data

Supplementary data to this article can be found online at https://doi.org/10.1016/j.talanta.2019.05.082.

References

[1] M.H. Gotfried, W. Travis Ellison, Safety and efficacy of lomefloxacin versus cefaclor in the treatment of acute exacerbations of chronic bronchitis, Am. J. Med. 92 (1992) S108–S113 https://doi.org/10.1016/0002-9343(92)90320-B.
[2] R. Wise, D. Honeybourne, Pharmacokinetics and pharmacodynamics of fluoroquinolones in the respiratory tract, Eur. Respir. J. 14 (1999) 221–229 https://doi.org/10.1034/j.1399-3003.1999.14a38.x.
[3] P.S. Lietman, Fluoroquinolone toxicities: an update, Drugs 49 (1995) 159–163 https://doi.org/10.2165/00003495-199500492-00026.
[4] Y.N. Yi, G.R. Li, Y.S. Wang, Y.Z. Zhou, H.M. Zhu, Simultaneous determination of norfloxacin and lomefloxacin in milk by first derivative synchronous fluorescence

spectrometry using Al (III) as an enhancer, Anal. Chim. Acta 707 (2011) 128–134 https://doi.org/10.1016/j.aca.2011.09.029.
[5] J.L. Urraca, M. Castellari, C.A. Barrios, M.C. Moreno-Bondi, Multiresidue analysis of fluoroquinolone antimicrobials in chicken meat by molecularly imprinted solid-phase extraction and high performance liquid chromatography, J. Chromatogr. A. 1343 (2014) 1–9 https://doi.org/10.1016/j.chroma.2014.03.045.
[6] H. Yan, H. Wang, X. Qin, B. Liu, J. Du, Ultrasound-assisted dispersive liquid-liquid microextraction for determination of fluoroquinolones in pharmaceutical wastewater, J. Pharm. Biomed. Anal. 54 (2011) 53–57 https://doi.org/10.1016/j.jpba.2010.08.007.
[7] H. Sun, L. Li, M. Su, Simultaneous determination of lidocaine, proline and lomefloxacin in human urine by CE with electrochemiluminescence detection, Chromatographia 67 (2008) 399–405 https://doi.org/10.1365/s10337-008-0518-5.
[8] J.L. Vílchez, L. Araujo, A. Prieto, A. Navalón, Differential-pulse adsorptive stripping voltammetric determination of the antibacterial lomefloxacin, J. Pharm. Biomed. Anal. 26 (2001) 23–29 https://doi.org/10.1016/S0731-7085(01)00391-0.
[9] Y.S. Zhong, Y.N. Ni, S. Kokot, Application of differential pulse stripping voltammetry and chemometrics for the determination of three antibiotic drugs in food samples, Chin. Chem. Lett. 23 (2012) 339–342 https://doi.org/10.1016/j.cclet.2012.01.007.
[10] M. Amoli-Diva, K. Pourghazi, S. Hajjaran, Dispersive micro-solid phase extraction using magnetic nanoparticle modified multi-walled carbon nanotubes coupled with surfactant-enhanced spectrofluorimetry for sensitive determination of lomefloxacin and ofloxacin from biological samples, Mater. Sci. Eng. C 60 (2016) 30–36 https://doi.org/10.1016/j.msec.2015.11.013.
[11] M.S. El-Hamshary, M.A. Fouad, R.S. Hanafi, H.S. Al-Easa, S.M. El-Moghazy, Screening and optimization of samarium-assisted complexation for the determination of norfloxacin, levofloxacin and lomefloxacin in their corresponding dosage forms employing spectrofluorimetry, Spectrochim. Acta Mol. Biomol. Spectrosc. 206 (2019) 578–587 https://doi.org/10.1016/j.saa.2018.08.053.
[12] J. Feng, Y. Tao, X. Shen, H. Jin, T. Zhou, Y. Zhou, L. Hu, D. Luo, S. Mei, Y.I. Lee, Highly sensitive and selective fluorescent sensor for tetrabromobisphenol-A in electronic waste samples using molecularly imprinted polymer coated quantum dots, Microchem. J. 144 (2019) 93–101 https://doi.org/10.1016/j.microc.2018.08.041.
[13] L. Wu, Z.Z. Lin, J. Zeng, H.P. Zhong, X.M. Chen, Z.Y. Huang, Detection of malachite green in fish based on magnetic fluorescent probe of CdTe QDs/nano-Fe3O4@MIPs, Spectrochim. Acta Mol. Biomol. Spectrosc. 196 (2018) 117–122 https://doi.org/10.1016/j.saa.2018.02.016.
[14] L. Wu, Z.Z. Lin, H.P. Zhong, A.H. Peng, X.M. Chen, Z.Y. Huang, Rapid detection of malachite green in fish based on CdTe quantum dots coated with molecularly imprinted silica, Food Chem. 229 (2017) 847–853 https://doi.org/10.1016/j.foodchem.2017.02.144.
[15] E. Turiel, A. Martín-Esteban, Molecularly imprinted polymers for sample preparation: a review, Anal. Chim. Acta 668 (2010) 87–99 https://doi.org/10.1016/j.aca.2010.04.019.
[16] M.R. Chao, C.W. Hu, J.L. Chen, Glass substrates crosslinked with tetracycline-imprinted polymeric silicate and CdTe quantum dots as fluorescent sensors, Anal. Chim. Acta 925 (2016) 61–69 https://doi.org/10.1016/j.aca.2016.04.037.
[17] N.N. Naing, S.F.Y. Li, H.K. Lee, Evaluation of graphene-based sorbent in the determination of polar environmental contaminants in water by micro-solid phase extraction-high performance liquid chromatography, J. Chromatogr. A. 1427 (2016) 29–36 https://doi.org/10.1016/j.chroma.2015.12.012.
[18] J. Wu, D. Xiao, H. Zhao, H. He, J. Peng, C. Wang, C. Zhang, J. He, A nanocomposite consisting of graphene oxide and Fe3O4magnetic nanoparticles for the extraction of flavonoids from tea, wine and urine samples, Microchim. Acta. 182 (2015) 2299–2306 https://doi.org/10.1007/s00604-015-1575-8.
[19] H. Kebiche, D. Debarnot, A. Merzouki, F. Poncin-Epaillard, N. Haddaoui, Relationship between ammonia sensing properties of polyaniline nanostructures and their deposition and synthesis methods, Anal. Chim. Acta 737 (2012) 64–71 https://doi.org/10.1016/j.aca.2012.06.003.
[20] H. Bagheri, M. Saraji, Conductive polymers as new media for solid-phase extraction: isolation of chlorophenols from water sample, J. Chromatogr. A. 986 (2003) 111–119 https://doi.org/10.1016/S0021-9673(02)01972-6.
[21] O. Bunkoed, P. Kanatharana, Mercaptopropionic acid-capped CdTe quantum dots as fluorescence probe for the determination of salicylic acid in pharmaceutical products, Luminescence 30 (2015) 1083–1089 https://doi.org/10.1002/bio.2862.
[22] T. Chaiphet, O. Bunkoed, C. Thammakhet, P. Thavarungkul, P. Kanatharana, A novel microextractor stick (polyaniline/zinc film/stainless steel) for polycyclic aromatic hydrocarbons in water, J. Environ. Sci. Health A Tox. Hazard. Subst. Environ. Eng. 49 (2014) 882–891 https://doi.org/10.1080/10934529.2014.893791.
[23] M. Camara, A. Gallego-Pico, R.M. Garcinuno, P. Fernandez-Hernando, J.S. Durand-Alegria, P.J. Sanchez, An HPLC-DAD method for the simultaneous determination of nine beta-lactam antibiotics in Ewe milk, Food Chem. 141 (2013) 829–834 https://doi.org/10.1016/j.foodchem.2013.02.131.
[24] B. Liu, H. Yan, F. Qiao, Y. Geng, Determination of clenbuterol in porcine tissues using solid-phase extraction combined with ultrasound-assisted dispersive liquid-liquid microextraction and HPLC-UV detection, J. Chromatogr. B. 879 (2011) 90–94 https://doi.org/10.1016/j.jchromb.2010.11.017.
[25] L. Sun, L. Jia, X. Xie, K. Xie, J. Wang, J. Liu, L. Cui, G. Zhang, G. Dai, J. Wang, Quantitative analysis of amoxicillin, its major metabolites and ampicillin in eggs by liquid chromatography combined with electrospray ionization tandem mass spectrometry, Food Chem. 192 (2016) 313–318 https://doi.org/10.1016/j.foodchem.2015.07.028.
[26] X. Ren, L. Chen, Preparation of molecularly imprinted polymer coated quantum dots to detect nicosulfuron in water samples, Anal. Bioanal. Chem. 407 (2015) 8087–8095 https://doi.org/10.1007/s00216-015-8982-x.
[27] M. Gao, L. Li, S. Lu, Q. Liu, H. He, Silver nanoparticles for the visual detection of lomefloxacin in the presence of cystine, Spectrochim. Acta Mol. Biomol. Spectrosc. 205 (2018) 72–78 https://doi.org/10.1016/j.saa.2018.05.072.
[28] M.I. Santoro, N.M. Kassab, A.K. Singh, E.R. Kedor-Hackmam, Quantitative determination of gatifloxacin, levofloxacin, lomefloxacin and pefloxacin fluoroquinolonic antibiotics in pharmaceutical preparations by high-performance liquid chromatography, J. Pharm. Biomed. Anal. 40 (2006) 179–184 https://doi.org/10.1016/j.jpba.2005.06.018.
[29] Y. Zhou, Q. Lu, C. Liu, S. She, L. Wang, A novel spectrofluorimetric method for determination of lomefloxacin based on supramolecular inclusion complex between it and p-sulfonated calyx[4]arene, Anal. Chim. Acta 552 (2005) 152–159 https://doi.org/10.1016/j.aca.2005.07.038.

Supporting information

A nanocomposite fluorescent probe of polyaniline, graphene oxide and quantum dots incorporated into highly selective polymer for lomefloxacin detection

Naphatsakorn Orachorn, Opas Bunkoed*

Center of Excellence for Innovation in Chemistry, Department of Chemistry, Faculty of Science, Prince of Songkla University, Hat Yai, Songkhla 90112, Thailand

Corresponding author: Tel: +66 74288453; Fax: +66 74558841

Email address: opas.b@psu.ac.th, opas1bunkoed@hotmail.com

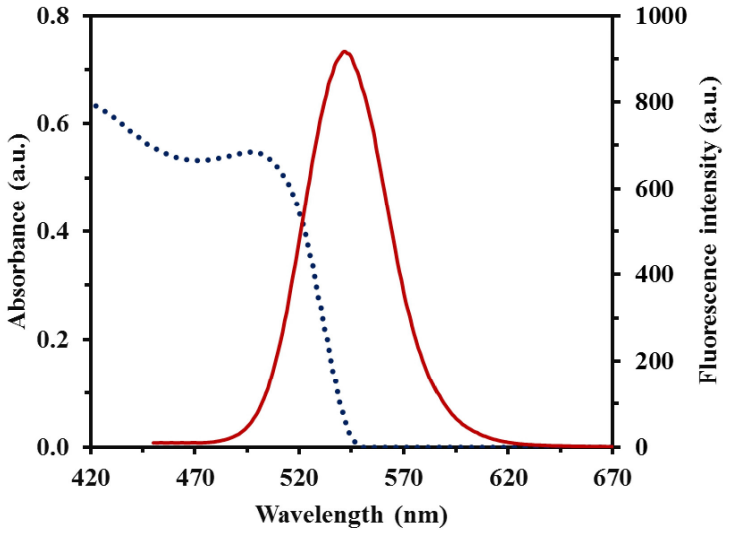

Fig. S1 UV-Vis Spectrum (dotted line) and fluorescence spectrum (solid line) of TGA-capped CdTe QDs

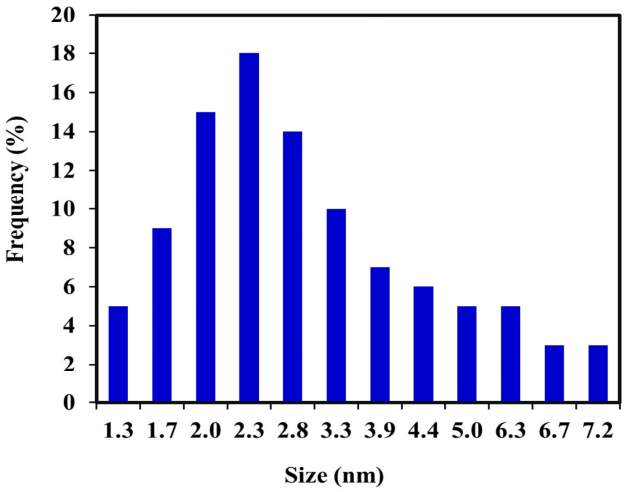

Fig. S2 The particle size distribution histogram of CdTe QDs

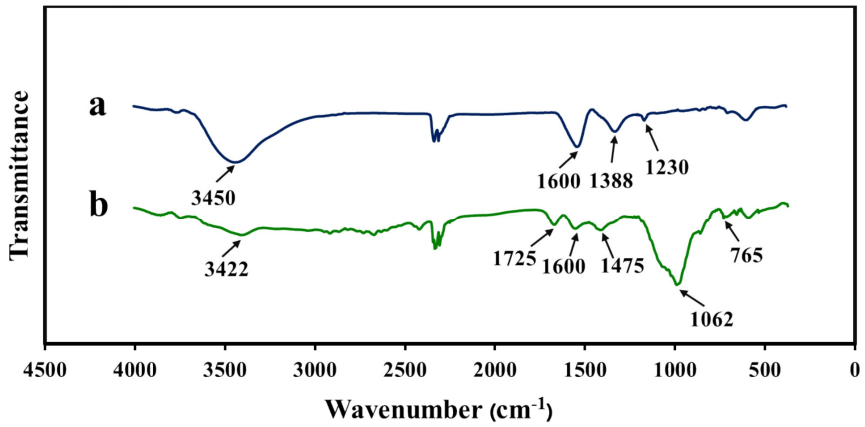

Fig. S3 FT-IR spectra of TGA-capped CdTe QDs (a) and PANI-GOx-MIP-QDs composite nanoprobe

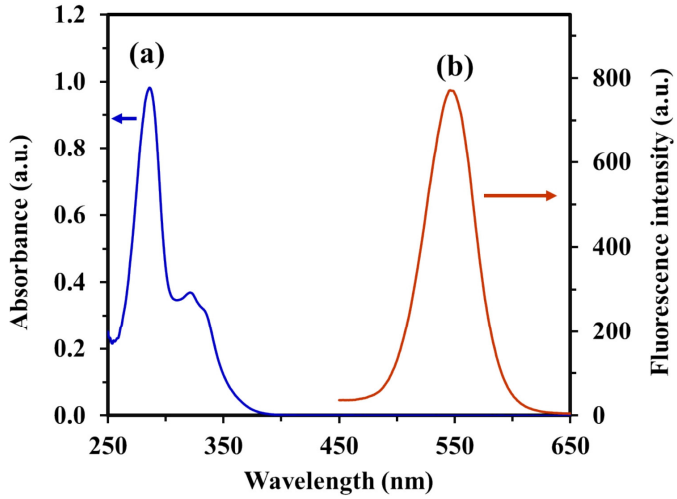

Fig. S4 Absorption spectrum of lomefloxacin (a) and fluorescence emission spectrum of PANI- GOx-MIP-QDs nanocomposite probe (b).

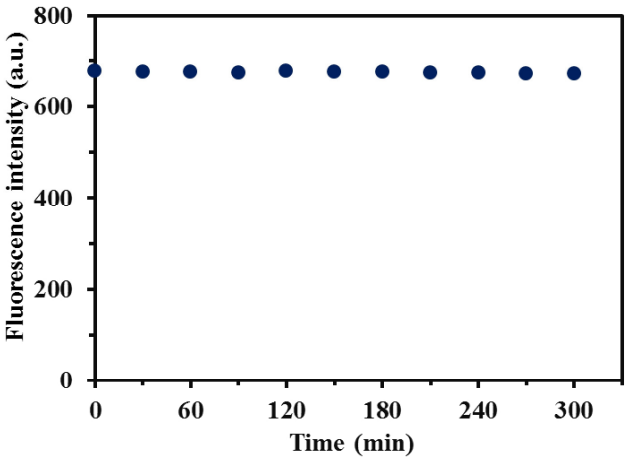

Fig. S5 The stability of PANI-GOx-MIP-QDs nanoprobe in 10 mM phosphate buffer solution (pH 8.0).

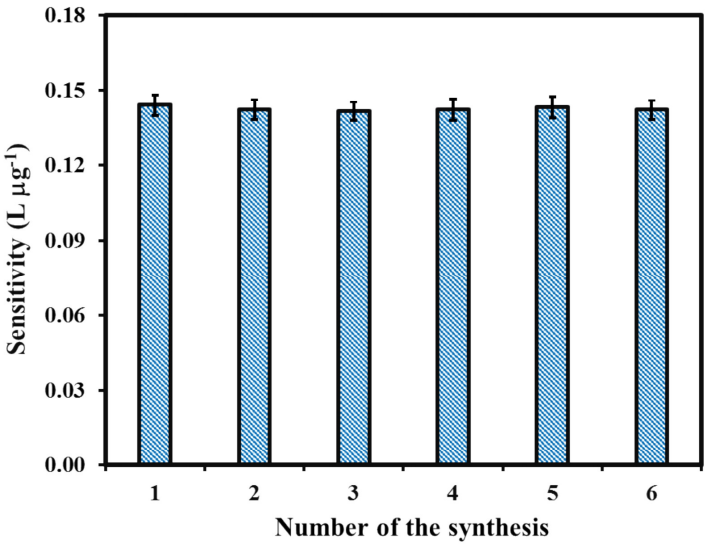

Fig. S6 The fabrication reproducibility of PANI-GOx-MIP-QDs nanoprobe

Paper II

Orachorn, N., Bunkoed, O., Nanohybrid magnetic composite optosensing probes for the enrichment and ultra-trace detection of mafenide and sulfisoxazole. ***Talanta*** 228 (2021), 122237.

Talanta 228 (2021) 122237

Contents lists available at ScienceDirect

Talanta

journal homepage: www.elsevier.com/locate/talanta

Nanohybrid magnetic composite optosensing probes for the enrichment and ultra-trace detection of mafenide and sulfisoxazole

Naphatsakorn Orachorn, Opas Bunkoed *

Center of Excellence for Innovation in Chemistry, Division of Physical Science, Faculty of Science, Prince of Songkla University, Hat Yai, Songkhla, 90112, Thailand

ARTICLE INFO

Keywords:
Quantum dots
Magnetic molecularly imprinted polymer
Mafenide
Sulfisoxazole
MIL-101
Fluorescence

ABSTRACT

Nanohybrid magnetic optosensing probes were designed and fabricated to enrich and detect ultra-trace levels of mafenide and sulfisoxazole simultaneously. The probes combined the high affinity of MIL-101 and the sensitivity of graphene quantum dots (GQDs) and cadmium telluride quantum dots (CdTe QDs) with the selectivity and rapid separation provided by a magnetic molecularly imprinted polymer (MMIP). Since the MIL101-MMIP-GQD and MIL101-MMIP-CdTe QD probes produced high fluorescence emission intensities at 435 and 572 nm, respectively, mafenide and sulfisoxazole could be simultaneously detected. Quantitative analysis was based on fluorescence quenching produced by binding between target molecules and imprinted recognition cavities. In the optimal experimental condition, emission intensity was quenched linearly with increasing analyte concentration from 0.10 to 25.0 μg L^{-1}. Limit of detection was 0.10 μg L^{-1} for mafenide and sulfisoxazole. The developed optosensor was applied to detect ultra-trace amounts of mafenide and sulfisoxazole in bovine milk. Recoveries of mafenide and sulfisoxazole in spiked bovine milk ranged from 80.4 to 97.9% with RSDs <5% and the analysis results agreed well with HPLC analysis. The proposed probes provided excellent sensitivity, selectivity, ease and convenience of use.

1. Introduction

Mafenide and sulfisoxazole are sulfonamide antibiotics, used in veterinary medicine almost everywhere to heal bacterial infections and promote growth in livestock. However, the overuse of mafenide and sulfisoxazole can leave residual traces of the drugs in animal products. Transmitted to humans through the food chain, these residuals are potentially carcinogenic in nature and can induce health problems such as hypersensitive allergic reaction, drug resistance, and endocrine disorders [1]. To protect public health, the EU has established MRL of 100 μg kg^{-1} for sulfonamides in animal tissue and milk. Therefore, the development of a reliable and accurate method for the simultaneous detection of mafenide and sulfisoxazole is essential.

Several analytical methods have been reported for the measurement of mafenide and sulfisoxazole such as high performance liquid chromatography (HPLC) [2], capillary electrophoresis (CE) [3], electrochemical detection [4] and fluorescence spectroscopy [5]. HPLC is the most extensively used method for the determination of mafenide and sulfisoxazole. Although the technique provides good separation and precision [6], it requires expensive equipment, complicated sample pretreatment and large volumes of solvent as the mobile phase. It is also time-consuming. Fluorescence spectroscopy is an attractive alternative method that avoids these limitations [7]. Measurement is simple and analysis is quick and cost-effective [8]. However, for ultra-trace level analysis of complex sample matrices, the sensitivity and selectivity of the method need to be improved.

Improvements to the sensitivity of the analytical method can be realized with quantum dots (QDs), which are an interesting sensing material. They present good optical properties such as size-dependent fluorescence emission, symmetrical and narrow emission spectra, high fluorescence intensity and excellent photo-stability [9]. Cadmium telluride quantum dots (CdTe QDs) are widely used as a sensing material because of their high fluorescence intensity [10]. They are also easily synthesized under mild conditions. Graphene quantum dots (GQDs) are also a good choice due to their low toxicity and robust chemical inertness [11,12]. To enhance the selectivity of the analytical method, QD nanoparticles can be composited with molecularly imprinted polymer (MIP) [13].

MIP has attracted much attention because of its high specificity for target analytes [14]. MIP has usually been prepared using a functional

* Corresponding author.
E-mail address: opas.b@psu.ac.th (O. Bunkoed).

https://doi.org/10.1016/j.talanta.2021.122237
Received 7 December 2020; Received in revised form 15 February 2021; Accepted 16 February 2021
Available online 22 February 2021

monomer and a cross-linker in the presence of template molecules of the target analyte [15]. After removal of the template from the polymer layer, specific recognition cavities are obtained that are complementary in size, shape and functional group to the template [16,17]. To further improve sensitivity for ultra-trace analysis, an enrichment function can be included by incorporating magnetite nanoparticles (Fe_3O_4) into the MIP layer to create a magnetic molecularly imprinted polymer (MMIP). Generally, the surface of Fe_3O_4 has been modified with silica (SiO_2) to prevent aggregation and improve chemical stability [18]. Binding affinity between target analytes and a magnetic composite fluorescent probe can also be improved by including high affinity materials in the composite probe. MIL-101 is a type of metal organic framework (MOF) which has been used as an affinity material due to its large surface area, tunable pore size and good stability [19,20]. MIL-101 is constructed by coordinating chromium with terephthalic acid ligands, which can adsorb mafenide and sulfisoxazole through strong π-π interaction and hydrogen bonding.

In this work, nanohybrid magnetic composite fluorescent probes were fabricated consisting of MIL-101 with GQDs or CdTe QDs composited with MMIP. The MIL101-MMIP-GQD and MIL101-MMIP-CdTe QD fluorescent probes were designed for the detection of mafenide and sulfisoxazole. A nanocomposite magnetic fluorescence probes can enrich or preconcentrate the target analytes which can be detected at ultra-trace level. The probes exhibited a strong emission intensity at different wavelengths, which enabled simultaneous detection of the target molecules. The nanohybrid magnetic composite fluorescent probes were applied to determine ultra-trace levels of mafenide and sulfisoxazole in bovine milk samples. The accuracy of the probes was evaluated by comparing their performance with an HPLC method.

2. Experimental

2.1. Chemicals and instrumentals

Details of the used chemicals and instruments are given in the Supplementary Information.

2.2. Synthesis of MIL101

MIL101 was synthesized via a hydrothermal method [21]. The detail

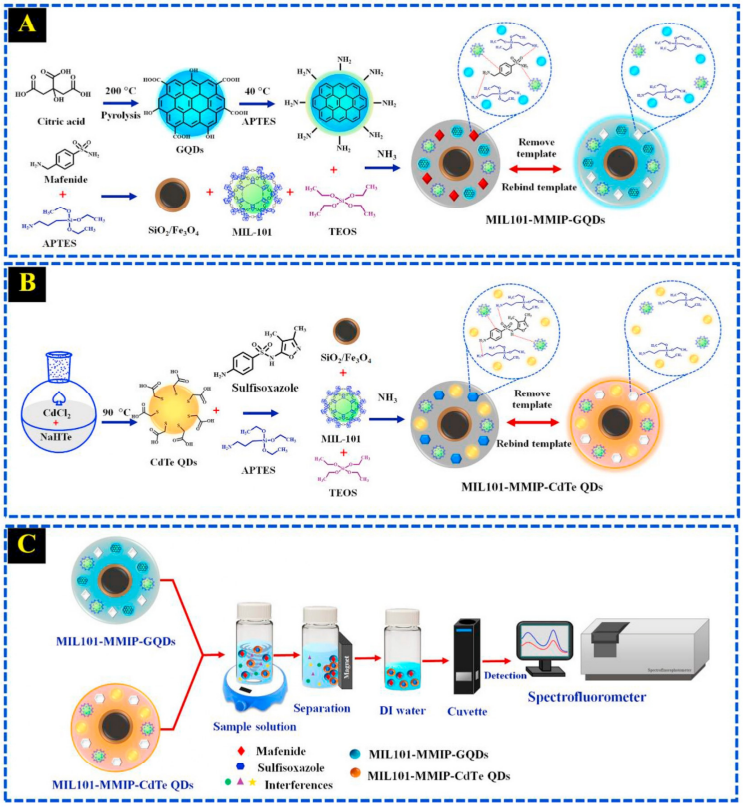

Fig. 1. The illustration shows the fabrication procedures of nanohybrid magnetic composite MIL101-MMIP-GQD (A) and MIL101-MMIP-CdTe QD probes (B) for mafenide and sulfisoxazole detection and the detection procedure using the nanohybrid optosensing probes (C).

for the synthesis of MIL101 is provided in the Supplementary Information.

2.3. Synthesis of silica modified magnetite nanoparticles (SiO_2/Fe_3O_4)

Fe_3O_4 nanoparticles were synthesized via co-precipitation [22]. The protocols for the synthesis of silica modified magnetite nanoparticles can be found in the Supplementary Information.

2.4. Synthesis of GQDs and nanohybrid magnetic MIL101-MMIP-GQD optosensing probe

GQDs were prepared by pyrolysis of citric acid [23]. First, 2.0 g of citric acid were heated to 200 °C, when they became a pale yellow liquid. Then, the liquid citric acid was added into 100 mL of 0.25 M NaOH and the mixture was stirred for 30 min. The acquired solution was dialyzed for 24 h using a dialysis membrane and then stored at 4 °C.

The nanohybrid magnetic composite MIL101-MMIP-GQD probes were synthesized by a sol-gel copolymerization process as illustrated in Fig. 1A. First, a 20 mL solution of GQDs was heated to 40 °C and 1.5 mL of APTES was then added under vigorous stirring for 30 min to produce APTES-coated GQDs. To imprint the template molecules, 5.0 mL of 45 mM mafenide was mixed with 1.6 mL of APTES and stirred for 30 min. Then, 10 mg of SiO_2/Fe_3O_4, 10 mg of MIL101, 0.8 mL of TEOS, 5.0 mL of the APTES-coated GQDs and 5.0 mL of a 25% w/v NH_3 were added and the whole was stirred for 30 min to allow polymerization. After polymerization, the template molecules of mafenide were removed from the polymer layer by washing with 20 mL of ethanol (three times). Lastly, the nanohybrid magnetic composite MIL101-MMIP-GQD probes were collected and dried at 50 °C. Nanohybrid magnetic composite non-imprinted polymer GQD (MIL101-MNIP-GQD) probes were also prepared using the identical procedure without the addition of template molecules.

2.5. Synthesis of TGA-capped CdTe QDs

The TGA-capped CdTe QDs were synthesized following a reported method [24]. The details for the synthesis can be found in the Supplementary Information.

2.6. Synthesis of nanohybrid magnetic composite MIL101-MMIP-CdTe QD optosensing probe

Nanohybrid magnetic composite MIL101-MMIP-CdTe QD probes were prepared via a sol-gel method as illustrated in Fig. 1B. First, 6.7 mg of sulfisoxazole (template molecule) were dissolved in 5.0 mL of DI water and mixed with 48 μL of APTES. After stirring for 1 h, 5.0 mL of the synthesized TGA-capped CdTe QDs were added and stirred for 1 h. After stirring, 10 mg of SiO_2/Fe_3O_4, 10 mg of MIL101, 145 μL of TEOS and 150 μL of 25% w/v NH_3 were added and the mixture was stirred for 4 h. Synthesized nanohybrid probes were then collected and washed with 20 mL of ethanol (three times) to remove template (sulfisoxazole). Finally, the nanohybrid magnetic composite cadmium telluride quantum dot (MIL101-MMIP-CdTe QD) probes were dried at 50 °C. Nanohybrid magnetic non-imprinted polymer cadmium telluride quantum dot (MIL101-MNIP-CdTe QD) probes were also fabricated using the same method without adding template molecules of sulfisoxazole.

2.7. Fluorescence measurement

The fluorescence measurement procedure was illustrated in Fig. 1C. The MIL101-MMIP-GQD and MIL101-MMIP-CdTe QD probes (1.0 mg mL^{-1}) were dispersed in 10 mM of phosphate buffer at pH 6.0. Then, 1.0 mL of nanoprobes in buffer was mixed with 2.0 mL of either sulfisoxazole or mafenide standard or sample and stirred for 15 min to enable binding. The nanoprobes, now bound with the target analyte, were separated using a magnet and the remaining solution was discarded. The separated nanoprobes were dispersed in 200 μL of DI water and the mixture was transferred into a quartz cell to measure the intensity of the fluorescence emission. Fluorescence was induced at an excitation wavelength of 355 nm and emissions were measured from 400 to 700 nm.

2.8. Sample pretreatment of bovine milk samples

The extraction procedure of mafenide and sulfisoxazole from bovine milk was adapted from a previous work [25]. Briefly, a 10.0 mL aliquot of bovine milk was transferred into a 50 mL polypropylene tube and defatted using centrifugation at 5000 rpm for 20 min. The defatted milk was then mixed with 15.0 mL of acetonitrile to precipitate proteins. The mixture solution was then vortexed for 1 min and centrifuged at 5000 rpm for 10 min to separate the phases. The acetonitrile phase was separated and evaporated at 50 °C. Finally, the dry extract was re-dissolved with DI water and analyzed by the developed optosensor.

2.9. Determination of mafenide and sulfisoxazole by HPLC

HPLC analysis of mafenide and sulfisoxazole was carried out using the Hewlett-Packard 1100 series (Agilent Technologies, Waldbronn, Germany). The analytical column was a Fortis C18 (4.6 mm × 15 cm, 5 μm). The mobile phase was a mixture of 0.2% acetic acid and acetonitrile (50:50, v/v) flowing at a constant 1.0 mL min^{-1}. Mafenide and sulfisoxazole were detected with a diode array detector (DAD) at 270 nm.

3. Results and discussion

3.1. Characterization of nanohybrid magnetic composite optosensing probes

The synthesized components of the composite probes and the fabricated composite probes were characterized using FT-IR spectroscopy. The spectrum of synthesized MIL-101 (Fig. S1Aa and S1Bg) showed characteristic peaks at 1625, 1408 and 593 cm^{-1} due to the C = O stretching, O–C–O symmetric stretching and COO- bending of the dicarboxylate linker, respectively. The peak at 1510 cm^{-1} was due to the C═C stretching of benzene. The peaks at 1018 and 749 cm^{-1} were attributed to the deformation vibration of C–H in benzene. In the spectrum of SiO_2/Fe_3O_4 (Fig. S1Ab and Bh), the peaks at 1083 and 586 cm^{-1} corresponded to the Si–O–Si stretching of silica and Fe–O–Fe stretching of magnetite, respectively. The spectrum of GQDs (Fig. S1Ac) showed a broad band around 3416 cm^{-1} due to O–H stretching. The peaks at 2913 and 1388 cm^{-1} were attributed to C–H stretching. The band at 1588 cm^{-1} was due to the C═C stretching of the aromatic ring. In the spectrum of mafenide (Fig. S1Ad), the peak at 3206 cm^{-1} indicated N–H stretching. The absorption peak at about 1503 cm^{-1} was due to C═C stretching in the aromatic ring. The peaks at 1339 and 1210 cm^{-1} were attributed to asymmetric and symmetric stretching of the S═O group, respectively. The bands at 1157 and 583 cm^{-1} indicated C–N and C–S stretching, respectively. In the spectrum of MIL101-MMIP-GQDs before the removal of mafenide (Fig. S1Ae), peaks at 1076 and 779 cm^{-1} corresponded to the Si–O–Si asymmetric stretching vibration and the Si–O vibration band of the silica layer. The other characteristic peaks appeared at the same wavenumbers they appeared at in the spectrum of mafenide. After removal of the mafenide template, the peaks of mafenide were no longer present (Fig. S1Af). The peaks at 461 and 780 cm^{-1} were due to Si–O vibration, while the peak at 588 cm^{-1} indicated the Fe–O–Fe stretching of magnetite.

The spectrum of TGA-capped CdTe QDs (Fig. S1Bi) showed peaks at 3442 and 1230 cm^{-1} that were attributed to O–H and C–O stretching of the carboxylic group, respectively. The peaks at 1594 and 1386 cm^{-1} indicated asymmetric and symmetric stretching of the carboxylate

group. The spectrum of sulfisoxazole (Fig. S1Bj) exhibited strong absorption peaks at 3486 and 3382 cm^{-1} which corresponded to N–H stretching. The peaks at around 1597 and 1345 cm^{-1} were respectively attributed to C═N stretching and S═O asymmetric stretching. The peaks at 1163, 1092 and 575 cm^{-1} indicated C–N, C–O and C–S stretching, respectively. The spectrum of MIL101-MMIP-CdTe QDs before removal of the sulfisoxazole (Fig. S1Bk) presented a peak at 1630 cm^{-1} that was due to C═O stretching. The bands at 1062 and 748 cm^{-1} corresponded to Si–O–Si asymmetric vibration and Si–O vibration. The other peaks were present at the same wavenumbers they were present at in the spectrum of sulfisoxazole. After the removal of sulfisoxazole from MIL101-MMIP-CdTe QDs, the peaks related to sulfisoxazole were no longer present (Fig. S1Bl). The bands at 457 and 749 cm^{-1} were due to Si–O vibration and the peak at 592 cm^{-1} indicated Fe–O–Fe stretching of magnetite. These results confirmed that the magnetic nanocomposite MIL101-MMIP-GQDs and MIL101-MMIP-CdTe QDs were successfully synthesized and contained specific cavities for binding to mafenide and sulfisoxazole. No significant difference was observed between the FT-IR spectra of MMIP after removal of template and MNIP due to their similar compositions. FT-IR spectra of MIL101-MNIP-GQDs and MIL101-MNIP-CdTe QDs are shown in Fig. S2A and B.

In the UV–Vis absorption spectra of synthesized GQDs and CdTe QDs, the maximum absorption wavelengths were approximately 359 and 528 nm, respectively (Fig. S3 A and B). The average particle size of GQDs was estimated from a TEM image (Fig. 2A) to be approximately 2.50 nm. The particle size of the CdTe QDs was calculated using the absorption peak of CdTe QDs substituted in an equation previously reported [24]. The estimated particle size of CdTe QDs was around 2.95 nm, which was in agreement with the TEM image (Fig. 2B). The surface morphologies of SiO_2/Fe_3O_4, MIL101, MIL101-MMIP-GQDs and MIL101-MMIP-CdTe QDs were characterized using SEM. The SEM images of SiO_2/Fe_3O_4 and MIL101 are shown in Fig S4A and B and their particles size were about 100 and 200 nm, respectively (Fig. S4C and D). The SEM images of both MIL101-MMIP-GQDs (Fig. 2C) and MIL101-MMIP-CdTe QDs (Fig. 2D) revealed uniformly spherical particles with slightly rough surfaces. The TEM images of MIL101-MMIP-GQDs and MIL101-MMIP-CdTe QDs nanocomposite probes exhibited spherical nanoparticles (Fig. S5A and B). Estimated from the TEM images, the average diameters of MIL101-MMIP-GQDs and MIL101-MMIP-CdTe QDs were 401 ± 20 and 421 ± 35 nm, respectively.

The fluorescence emission spectrum of MIL101-MMIP-GQDs before the removal of mafenide template molecules indicated fluorescence emission of relatively low intensity (Fig. 3A(a)). Emission intensity was 48.0% that of the non-imprinted MIL101-MNIP-GQDs. Meanwhile, before sulfisoxazole template removal, the intensity of MIL101-MMIP-CdTe QDs was 50.5% that of the non-imprinted MIL101-MNIP-CdTe QDs. After the removal of the templates, the intensity of fluorescence emission from both MIL101-MMIP-QD probes (Fig. 3A(b)) increased almost to the same level as MIL101-MNIP-QD probes (Fig. 3A(c)). This result implied that template molecules of both mafenide and sulfisoxazole were successfully removed from the MMIP layer. Therefore, the nanohybrid magnetic composite probes could be used to detect mafenide and sulfisoxazole at the same time. The MIL101-MMIP-GQD (Fig. 3B) and MIL101-MMIP-CdTe QD (Fig. 3C) probes in DI water were photographed under UV light before (right) and after (left) the removal of template molecules.

3.2. Detection of mafenide and sulfisoxazole by different types of nanoprobes

Different types of magnetic nanocomposite fluorescent probes were evaluated by comparing their sensitivity for the detection of mafenide and sulfisoxazole. MNIP-GQDs, MMIP-GQDs and MIL101-MMIP-GQDs were used to determine mafenide (Fig. 4A) and MNIP-CdTe QDs,

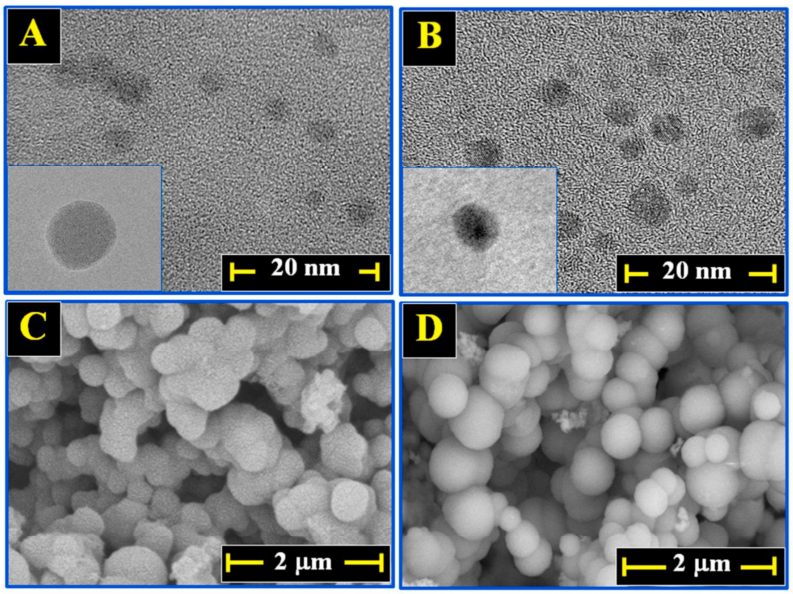

Fig. 2. TEM images are of GQD nanoparticles (A) and CdTe QD nanoparticles (B). SEM images are of MIL101-MMIP-GQDs (C) and MIL101-MMIP-CdTe QDs (D).

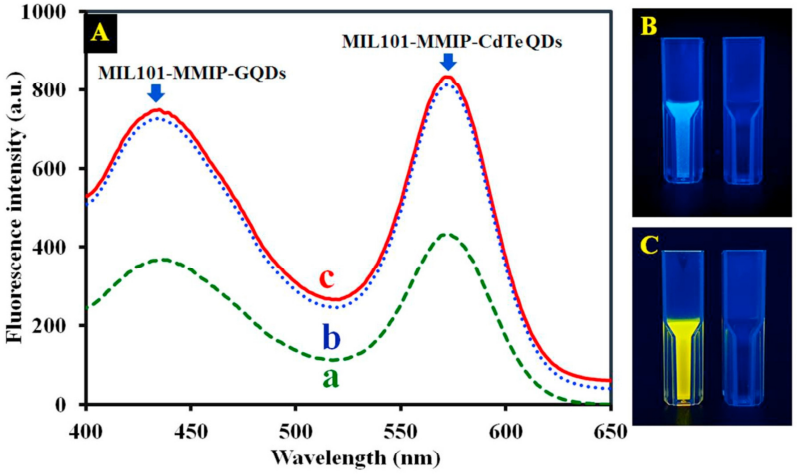

Fig. 3. (A) The fluorescence spectra were produced by nanohybrid magnetic composite MMIP fluorescent probes before (a), and after (b) the removal of template molecules and by a nanohybrid magnetic composite MNIP probe (c). The photographs show DI water containing MIL101-MMIP-GQDs (B) before (right) and after (left) template molecule removal and MIL101-MMIP-CdTe QDs (C) before (right) and after (left) template removal.

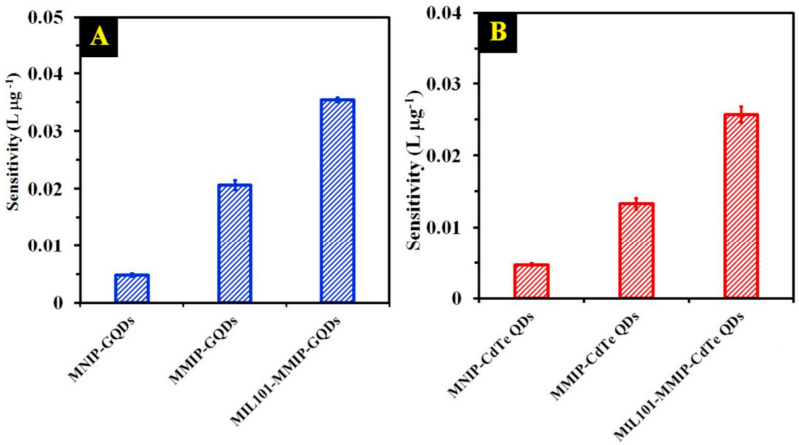

Fig. 4. The sensitivity of different nanoprobes for the detection of mafenide (A) and sulfisoxazole (B).

MMIP-CdTe QDs and MIL101-MMIP-CdTe QDs were used to detect sulfisoxazole (Fig. 4B). The MIL101-MMIP-GQDs and MIL101-MMIP-CdTe QDs exhibited the highest sensitivity toward mafenide and sulfisoxazole, respectively. The high sensitivity of these probes was due to the high adsorption affinity of MIL-101 with the target analytes and the imprinted recognition cavities for mafenide and sulfisoxazole. MIL-101 increased quenching efficiency since it can adsorb analytes via π-π interaction and hydrogen bonding. The MNIP-GQDs and MNIP-CdTe QDs demonstrated the lowest sensitivity toward mafenide and sulfisoxazole detection, respectively. The low sensitivity of these magnetic non-imprinted polymer probes was due to the absence of imprinted recognition cavities for binding the analytes. These results confirmed that incorporating MIL-101 into the nanohybrid magnetic probes improved their sensitivity toward their target molecules.

3.3. Optimization

The incubation time, the pH of the dispersion solution and the mole ratio of template to monomer to cross-linker are important parameters that affected the detection of mafenide and sulfisoxazole. These

parameters were investigated to determine the optimum values that provided the highest quenching efficiency and the shortest analysis time.

3.3.1. Effect of incubation time

Before measuring fluorescence, enough time must elapse for binding to be completed between the target analytes and the specific recognition cavities of the probe. In this study, the incubation time for binding between the nanohybrid magnetic composite probes and target analytes was varied from 0 to 40 min. Complete binding had occurred after 15 min (Fig. 5A). This was the first time point that produced the highest quenching efficiency (F0/F), and was therefore selected as the most suitable incubation time.

3.3.2. pH of dispersion solution

The solution condition affected quenching of the nanohybrid magnetic composite probes by the target analytes. To investigate the effect of pH value on the sensitivity of the nanohybrid probes, MIL101-MMIP-GQDs and MIL101-MMIP-CdTe QDs were dispersed in citrate-phosphate or phosphate buffer solutions in pH ranges from 4.0 to 8.0 and applied to determine mafenide and sulfisoxazole. The sensitivity was achieved from the target analytes in the concentration range of 0.10–25.0 μg L^{-1}. The sensitivity of both probes was highest in a dispersion solution at pH 6 (Fig. 5B). At pH lower than 6, both MIL101-MMIP-GQDs and MIL101-MMIP-CdTe QDs exhibited decreased sensitivity because the amino groups of the functional monomers on the surface of the nanoprobes were protonated. As a result, binding between the probes and their respective targets, mafenide and sulfisoxazole, was reduced. Sensitivity was also low above pH 6 because of the deprotonation of target analytes, and the ionization of the silica layer, which made the magnetic polymer less stable. Thus, phosphate buffers at pH 6 were considered the optimum pH condition of dispersion solutions for the determination of mafenide and sulfisoxazole by the respective probes.

3.3.3. Mole ratio of template to monomer to cross-linker

The formation of imprinted polymers depends upon the quantity of polymerization precursor. These include the template molecule (TM), monomer (MN) and cross-linker (CL). In this study, the mole ratio of TM: MN: CL was investigated to optimize the fabrication of the MIL101-MMIP-GQDs and MIL101-MMIP-CdTe QDs. The most appropriate mole proportion (TM: MN: CL) for the synthesis of MIL101-MMIP-GQDs was 1:30:15 (Fig. 5C) and for the fabrication of MIL101-MMIP-CdTe QDs, the most suitable mole ratio was 1:8:25 (Fig. 5D). When the quantity of MN used was low, the sensitivity of the nanohybrid magnetic probes decreased because not enough imprinted recognition cavities were formed to bind with the available target analytes. Sensitivity was also low when higher quantities of MN were used because non-imprinted sites were formed that could block the formation of binding sites during polymerization. The quantity of CL used was also a major factor in the synthesis of the nanohybrid magnetic composite probes. The use of low amounts of CL led to low sensitivity due to the physical instability of the probes. High quantities of CL also produced probes of low sensitivity because the generated polymer layer was too thick. The resultant inhibition of binding between template molecules and APTES monomer impaired the production of imprinted recognition cavities.

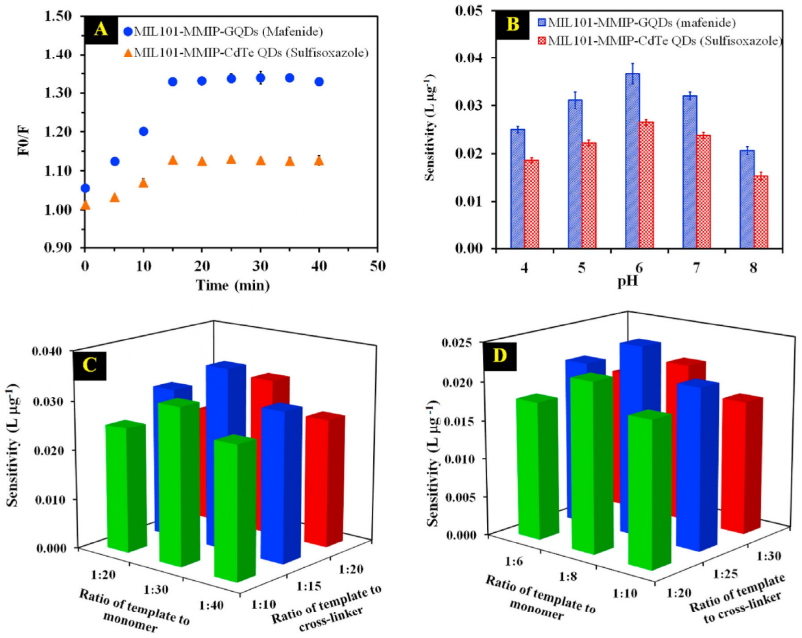

Fig. 5. Effect of incubation time (A) on fluorescence quenching of nanocomposite probes (concentration of target analytes of 5.0 μg L^{-1}), pH of dispersion solution on sensitivity (B), mole ratio of template to monomer to cross-linker on the sensitivity of nanohybrid magnetic MIL101-MMIP-GQDs (C) and MIL101-MMIP-CdTe QDs probes (D).

3.4. Analytical performance

The analytical performances of the MIL101-MMIP-GQD and MIL101-MMIP-CdTe QD probes were validated in the optimal condition. Linearity, and limits of detection (LOD) and quantification (LOQ) were determined. The intensity of fluorescence emissions of both probes was significantly quenched by increasing concentrations of mafenide and sulfisoxazole (Fig. 6A). While, the emission intensities of the MIL101-MNIP-GQD and MIL101-MNIP-CdTe QD probes were only slightly quenched (Fig. 6B). The linear ranges of the MIL101-MMIP-GQD and MIL101-MMIP-CdTe QD probes were from 0.10 to 25.0 μg L^{-1} with coefficients of determination (R^2) of 0.9980 and 0.9994, respectively (Fig. 6C and D). LOD, based on the $3SD_{blank}$/slope of mafenide and sulfisoxazole, was 0.10 μg L^{-1}. The LOQ, based on $10SD_{blank}$/slope of mafenide and sulfisoxazole was 0.34 μg L^{-1}. These results implied that the nanohybrid magnetic composite probes can be used to simultaneously detect mafenide and sulfisoxazole at ultra-trace levels. As demonstrated in Fig. S6A and B, additional different concentration of mafenide into dual nanocomposite probe solution, the fluorescence intensity of MIL101-MMIP-GQDs decreased while the emission intensity of MIL101-MMIP-CdTe QDs is not affected. Whereas, the fluorescence intensity of MIL101-MMIP-CdTe QDs decreased in the present of sulfisoxazole and the fluorescence intensity of MIL101-MMIP-GQDs is not effected.

3.5. Quenching mechanism

Fluorescence quenching was driven by hydrogen bonding between mafenide and sulfisoxazole and amino groups (-NH_2) of the functional monomer (APTES) on the surface of the nanohybrid magnetic probes. Electron transfer occurred from the high energy band of orbitals in the conduction band of QDs to the lowest unoccupied molecular orbitals of the target analytes (mafenide and sulfisoxazole) [26]. In addition, binding between the analytes and nanohybrid probes improved due to the affinity between the analytes and MIL-101. The quenching mechanism was confirmed by the UV–Vis absorption spectra of target analytes (mafenide and sulfisoxazole) and fluorescence emission spectra of nanoprobes. In these spectra, there were no overlap between the absorption spectra of analytes and emission spectra of the nanoprobes. These results indicated that fluorescence quenching did not occur from energy transfer (Fig. S7) [27,28].

The fluorescence quenching efficiency of mafenide and sulfisoxazole could be quantified according to the Stern-Volmer equation,

$$F0 / F = 1 + K_{SV}[C],$$

where F0 and F are the fluorescence emission intensity of the nanohybrid magnetic probes in the absence and presence of the quenching target analytes. K_{SV} is the Stern-Volmer constant and [C] is the concentration of quenching target analytes. The sensitivity of the

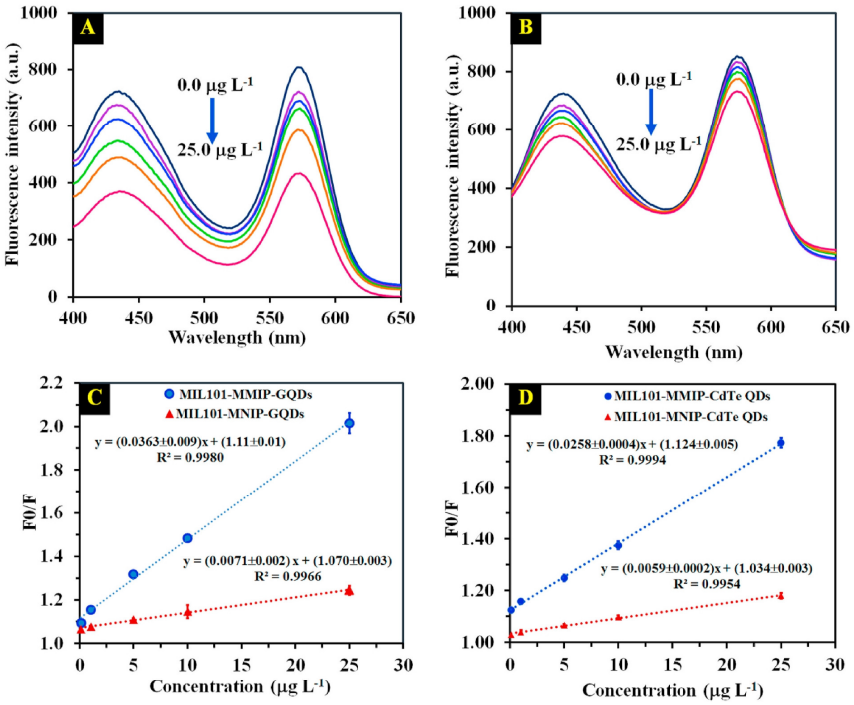

Fig. 6. The fluorescence spectra were produced by MIL101-MMIP-GQDs and MIL101-MMIP- CdTe QDs (A) and MIL101-MNIP-GQDs and MIL101-MNIP-CdTe QDs (B) in the presence of different concentrations of mafenide and sulfisoxazole. Calibration curves of MIL101-MMIP-GQDs and MIL101-MNIP-GQDs for mafenide (C) and calibration curves of MIL101-MMIP-CdTe QDs and MIL101-MNIP-CdTe QDs for sulfisoxazole (D).

nanocomposite probe for detection of mafenide and sulfisoxazole can be described by Ksv. A high value of Ksv indicates high sensitivity. The imprinting factor (IF) of the nanohybrid magnetic probes was calculated by comparing the K_{SV} of MMIP and MNIP. The IF values of MIL101-MMIP-GQDs and MIL101-MMIP-CdTe QDs for mafenide and sulfisoxazole detection were 5.11 and 4.37, respectively. The nanohybrid magnetic probes were, therefore, highly specific toward the target analytes.

3.6. Selectivity and competitive study

To evaluate the selectivity of the MIL101-MMIP-GQD and MIL101-MMIP-CdTe QD probes toward mafenide and sulfisoxazole, the sensitivity of the probes was compared after interaction with analog chemical structures of mafenide and sulfisoxazole. The analog structures used included sulfathiazole, sulfamerazine and sulfamonomethoxine. The probes demonstrated higher sensitivity toward mafenide and sulfisoxazole than their analog structures (Fig. 7). The non-imprinted MIL101-MNIP-GQD and MIL101-MNIP-CdTe QD probes exhibited low sensitivity toward mafenide, sulfisoxazole and the analog structures because they did not have recognition cavities in their polymer layers.

To ensure the selectivity of the nanohybrid magnetic composite probes, competitive binding was tested by measuring the quenching efficiency (F0/F) of an optosensor in the presence of various ratios of mafenide and sulfisoxazole to sulfathiazole. The quenching of the nanohybrid probes was not noticeably changed in the presence of high concentrations of sulfathiazole (Fig. S8). The generated recognition cavities in the imprinted polymer layer of the MIL101-MMIP-GQD and MIL101-MMIP-CdTe QD probes were highly specific for mafenide and sulfisoxazole in terms of size, shape and functionality.

3.7. Stability and reproducibility

The stability of the nanohybrid magnetic composite probes was investigated by measuring the fluorescence intensity of nanoprobes dispersed in phosphate buffer at pH 6.0. The fluorescence intensities of MIL101-MMIP-GQDs and MIL101-MMIP-CdTe QDs were measured every 30 min and no significant change was observed over 300 min (Fig. S9). In addition, the stability of MIL101-MMIP-GQDs and MIL101-MMIP-CdTe QDs in powder form was also investigated after storage in a desiccator over time. The intensity of the emissions produced by the nanohybrid probes was not significantly changed after 6 months of storage. These results indicated the good stability of the synthesized nanohybrid magnetic composite probes.

The reproducibility of the fabricated probes was determined by means of six different batches of nanohybrid probes prepared at different times. The RSDs of the six lots of MIL101-MMIP-GQDs and MIL101-MMIP-CdTe QDs were 2.5 and 2.7%, respectively (Fig. S10). This result indicated the good reproducibility of the synthesized nanohybrid magnetic probes.

3.8. Analysis of milk samples

To evaluate the viability of the nanohybrid magnetic composite probes in real-world application, the MIL101-MMIP-GQDs and MIL101-MMIP-CdTe QDs were applied to simultaneously detect mafenide and sulfisoxazole in bovine milk. The pretreatment procedure of milk samples for analysis with the nanooptosensor was described in section 2.8. As displayed in Table 1, low concentrations of mafenide (0.36–0.45 μg L^{-1}) were found in some milk samples. A recovery test was also carried out to evaluate the accuracy of the developed nano-optosensor by spiking standard solutions of mafenide and sulfisoxazole in milk at 1.0, 5.0, 10.0 and 25.0 μg L^{-1}. The obtained recoveries were in the range of 80.4–97.9% with RSDs <5%. Additionally, the results obtained with the developed optosensor from the detection of mafenide and sulfisoxazole in milk samples were compared with HPLC method. The HPLC chromatograms of mafenide and sulfisoxazole spiked in milk samples at various concentrations are shown in Fig. 8. The results obtained with the nanooptosensor were not only in good agreement with the HPLC results, with a R^2 better than 0.99, but also demonstrated the superior sensitivity of the developed sensor toward these analytes in real samples. The developed nanohybrid optosensor produced accurate and reliable

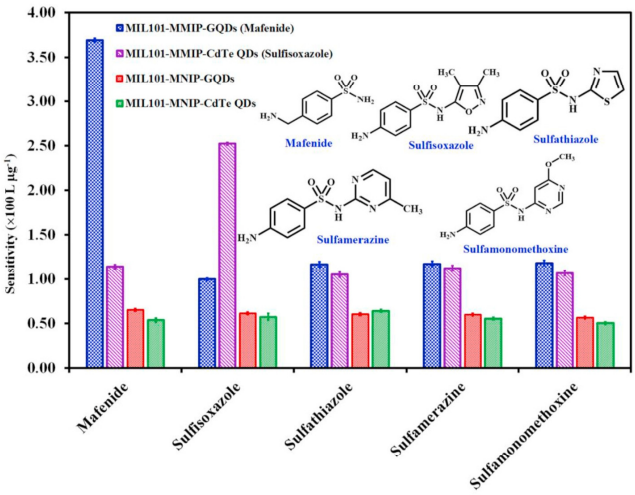

Fig. 7. The chart illustrates the selectivity of the nanohybrid magnetic composite MIL101-MMIP-GQD and MIL101-MMIP-CdTe QD probes toward mafenide and sulfisoxazole.

Table 1
The determination of mafenide and sulfisoxazole in milk using nanohybrid magnetic composite probes of MIL101-MMIP-GQDs and MIL101-MMIP-CdTe QDs and HPLC method.

Samples	Added (μg L^{-1})	Optosensor				HPLC			
		Mafenide		Sulfisoxazole		Mafenide		Sulfisoxazole	
		Found (μg L^{-1})	Recovery ± RSD (%)	Found (μg L^{-1})	Recovery ±RSD (%)	Found (μg L^{-1})	Recovery ± RSD (%)	Found (μg L^{-1})	Recovery ± RSD (%)
Milk 1	0.0	0.36	–	n.d.	–	0.35	–	n.d.	–
	1.0	1.17	80.9 ± 0.5	0.82	82.1 ± 1.1	1.15	84.0 ± 4.3	0.84	84.0 ± 3.2
	5.0	4.94	91.7 ± 0.4	4.70	94.0 ± 2.8	5.01	93.2 ± 2.9	4.81	96.2 ± 3.5
	10.0	9.70	93.4 ± 1.1	9.68	96.8 ± 3.3	9.87	95.2 ± 4.5	9.43	94.3 ± 3.1
	25.0	24.66	97.2 ± 0.3	23.98	95.9 ± 0.4	24.80	97.8 ± 1.5	24.1	96.4 ± 2.1
Milk 2	0.0	n.d.	–	n.d.	–	n.d.	–	n.d.	–
	1.0	0.92	92.0 ± 3.5	0.95	95.0 ± 2.6	0.89	89.0 ± 2.1	0.97	97.0 ± 3.6
	5.0	4.84	96.8 ± 2.1	4.81	96.2 ± 4.6	4.89	97.8 ± 3.6	4.80	96.0 ± 1.6
	10.0	9.46	94.6 ± 2.6	9.65	96.5 ± 1.6	9.23	92.3 ± 4.1	9.61	96.1 ± 1.8
	25.0	24.08	96.3 ± 1.5	24.06	96.2 ± 2.5	23.9	95.6 ± 2.8	24.1	96.4 ± 3.9
Milk 3	0.0	0.45	–	n.d.	–	0.42	–	n.d.	–
	1.0	1.26	80.4 ± 0.3	0.87	87.0 ± 3.8	1.30	88.0 ± 1.8	0.90	90.0 ± 2.9
	5.0	4.82	87.4 ± 1.6	4.36	87.3 ± 2.4	4.91	89.8 ± 4.8	4.40	88.0 ± 4.9
	10.0	9.57	91.2 ± 1.3	9.51	95.1 ± 2.0	9.98	95.6 ± 2.6	9.43	94.3 ± 2.1
	25.0	24.42	95.9 ± 0.4	22.10	88.4 ± 1.4	24.39	95.9 ± 2.8	23.9	95.6 ± 1.7
Milk 4	0.0	n.d.	–	n.d.	–	n.d.	–	n.d.	–
	1.0	0.98	97.9 ± 0.3	0.90	90.4 ± 2.7	0.94	94.0 ± 1.0	0.87	87.0 ± 2.8
	5.0	4.76	95.3 ± 1.0	4.81	96.2 ± 1.2	4.80	96.0 ± 1.6	4.82	96.4 ± 3.9
	10.0	9.34	93.4 ± 2.0	9.70	97.0 ± 2.0	9.35	93.5 ± 1.9	9.80	98.0 ± 4.0
	25.0	24.41	97.7 ± 1.4	24.36	97.4 ± 0.3	24.40	97.6 ± 3.0	24.30	97.2 ± 4.1

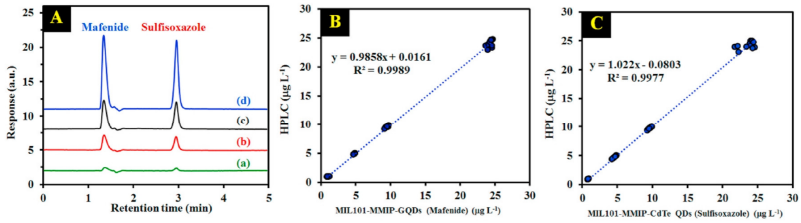

Fig. 8. HPLC chromatograms (A) were produced by mafenide and sulfisoxazole in spiked milk samples at 1.0 μg L^{-1} (a), 5.0 μg L^{-1} (b), 10.0 μg L^{-1} (c) and 25.0 μg L^{-1} (d). Plots show the correlation between results from the proposed sensor and HPLC for the detection of mafenide (B) and sulfisoxazole (C).

results that can enable the simultaneous detection of ultra-trace levels of mafenide and sulfisoxazole in milk samples. Other advantages of the developed optosensor included a rapid and simple procedure, require cost-effective instrument and environmentally friendly.

The performance of an optosensor was compared with performances of other methods from previous works (Table 2). LODs were much lower than other previous works and the obtained recoveries and RSDs of this method were comparable to those in previous reports. This comparison demonstrated that the nanohybrid magnetic composite probes using MIL101-MMIP-GQDs and MIL101-MMIP-CdTe QDs were highly sensitive devices for the simultaneous determination of ultra-trace levels of mafenide and sulfisoxazole in real samples. Meanwhile, the developed

Table 2
The analytical performances of the developed nanooptosensor using MIL101-MMIP-GQD and MIL101-MMIP-CdTe QD probes and other methods of detection of mafenide and sulfisoxazole.

Analytical method	Analyte	Sample	Linear range (μg L^{-1} or μg kg^{-1})	LOD (μg L^{-1} or μg kg^{-1})	Recovery (%)	RSD (%)	Reference
HPLC-DAD	Sulfisoxazole	Milk	30–800	10	81.9–115.0	<10	[29]
LC-MS/MS	Sulfisoxazole	Chicken meat	1–10	0.2	72.7–116.7	<10	[30]
CZE-UV	Sulfisoxazole	Chicken meat	50-1000	7.86	96.3–104	<13	[31]
Electrochemical	Sulfisoxazole	Milk, river and tap water	500-10,000	10	96.4–102.6	<6	[32]
HPLC-UV	Sulfisoxazole	Milk	50-2000	2.23	67.0–105.7	<9	[33]
UPLC-ECD	Sulfisoxazole	Shrimp	10-10,000	3.29	81.1–108.9	<5	[34]
HPLC-MS/MS	Sulfisoxazole	Milk, pork and fish meat	5-1000	0.55	80.1–107.1	<10	[35]
HPLC-UV	Mafenide	Pharmaceutical formulation	2000–100,000	490	94.8–101.8	<5	[36]
UPLC-MS/MS	Mafenide	Poultry feather	1–100	0.5	89–115	<20	[37]
Spectrofluorimetry MIL101-MMIP-GQDs	Mafenide	Milk	0.10–25.0	0.10	80.4–97.9	<4	This work
and MIL101-MMIP-CdTe QDs	Sulfisoxazole	Milk	0.10–25.0	0.10	82.1–97.4	<5	This work

dual optosensor achieved good selectivity using MMIP layers, without the requirement of an HPLC column or complicated separation process. The advantages of the proposed nanoprobes are shorter analysis time, ease of separation, improved enrichment, and rapid and convenient detection. The cost of equipment is lower than required by chromatographic techniques, which also use a large volume of organic solvents as the mobile phase. Therefore, the nanohybrid magnetic probes can be used as an efficient method with obvious advantages for the ultra-trace detection of mafenide and sulfisoxazole in complex samples.

4. Conclusion

Nanohybrid magnetic composite probes were successfully fabricated based on MIL-101, GQDs and CdTe QDs incorporated into MMIP. The probes were used in a nano-optosensing system for the simultaneous detection of ultra-trace levels of mafenide and sulfisoxazole. The combination of MIL-101, GQDs, CdTe QDs, SiO_2/Fe_3O_4 and molecularly imprinted polymer demonstrated its suitability for trace or ultra-trace analysis through good adsorption, high sensitivity and excellent selectivity. The quantitative analysis was based on the electron-transfer driven quenching of fluorescence emission intensity when mafenide and sulfisoxazole bound with recognition cavities imprinted in the surface polymer layer of the nanohybrid composite probes. The other benefits of the nanohybrid optosensor included simple measurement, ease of separation, improved enrichment, rapidity and inexpensive equipment. Accuracy, based on recoveries achieved, was in a satisfactory range from 80.4 to 97.9% with RSDs below 5%. The detection limits of mafenide and sulfisoxazole at their specific sensors were 0.10 μg L^{-1}. The results obtained from the dual optosensor were not only in good agreement with the results of detection by conventional high performance liquid chromatography but also exhibited the superior sensitivity of the developed optosensor toward the target analytes in real samples.

Declaration of competing interest

The authors declare that they have no known competing financial interests or personal relationships that could have appeared to influence the work reported in this paper.

Acknowledgements

This work was supported by National Research Council of Thailand (NRCT5-RSA63022-03). Center of Excellence for Innovation in Chemistry (PERCH-CIC), Ministry of Higher Education, Science, Research and Innovation. Naphatsakorn Orachorn was supported by Science Achievement Scholarship of Thailand (SAST). The authors thank Mr. Thomas Duncan Coyne for English proofreading.

Appendix A. Supplementary data

Supplementary data to this article can be found online at https://doi.org/10.1016/j.talanta.2021.122237.

Author statement

Naphatsakorn Orachorn: Methodology, Software, Validation, Writing – original draft, Conceptualization, Opas Bunkoed: Methodology, Conceptualization, Formal analysis, Investigation, Resources, Data curation, Writing – review & editing, Supervision, Project administration, Funding acquisition.

References

[1] X. Liu, Y. Tong, L. Zhang, Tailorable yolk-shell Fe_3O_4@graphitic carbon submicroboxes as efficient extraction materials for highly sensitive determination of trace sulfonamides in food samples, Food Chem. 303 (2020) 125369, https://doi.org/10.1016/j.foodchem.2019.125369.

[2] Y. Li, X. Wu, Z. Li, S. Zhong, W. Wang, A. Wang, J. Chen, Fabrication of CoFe2O4 graphene nanocomposite and its application in the magnetic solid phase extraction of sulfonamides from milk samples, Talanta 144 (2015) 1279–1286, https://doi.org/10.1016/j.talanta.2015.08.006.

[3] C. Wu, Y. Sun, Y. Wang, W. Duan, J. Hu, L. Zhou, Q. Pu, 7-(Diethylamino) coumarin-3-carboxylic acid as derivatization reagent for 405 nm laser-induced fluorescence detection: a case study for the analysis of sulfonamides by capillary electrophoresis, Talanta 201 (2019) 16–22, https://doi.org/10.1016/j.talanta.2019.03.093.

[4] I. Bourais, S. Maliki, H. Mohammadi, A. Amine, Investigation of sulfonamides inhibition of carbonic anhydrase enzyme using multiphotometric and electrochemical techniques, Enzym. Microb. Technol. 96 (2017) 23–29, https://doi.org/10.1016/j.enzmictec.2016.09.007.

[5] N. Rodríguez, M.C. Ortiz, L.A. Sarabia, A. Herrero, A multivariate multianalyte screening method for sulfonamides in milk based on front-face fluorescence spectroscopy, Anal. Chim. Acta 657 (2010) 136–146, https://doi.org/10.1016/j.aca.2009.10.048.

[6] K. Chullasat, P. Nurerk, P. Kanatharana, P. Kueseng, T. Sukchuay, O. Bunkoed, Hybrid monolith sorbent of polypyrrole-coated graphene oxide incorporated into a polyvinyl alcohol cryogel for extraction and enrichment of sulfonamides from water samples, Anal. Chim. Acta 961 (2017) 59–66, https://doi.org/10.1016/j.aca.2017.01.052.

[7] X. Wang, T. Hou, T. Lu, F. Li, Autonomous exonuclease III-assisted Isothermal cycling signal amplification: a facile and highly sensitive fluorescence DNA glycosylase activity assay, Anal. Chem. 86 (2014) 9626–9631, https://doi.org/10.1021/ac502125z.

[8] J. Feng, Y. Tao, X. Shen, H. Jin, T. Zhou, Y. Zhou, L. Hu, D. Luo, S. Mei, Y.I. Lee, Highly sensitive and selective fluorescent sensor for tetrabromobisphenol-A in electronic waste samples using molecularly imprinted polymer coated quantum dots, Microchem. J. 144 (2019) 93–101, https://doi.org/10.1016/j.microc.2018.08.041.

[9] X. Wei, T. Hao, Y. Xu, K. Lu, H. Li, Y. Yan, Z. Zhou, Facile polymerizable surfactant inspired synthesis of fluorescent molecularly imprinted composite sensor via aqueous CdTe quantum dots for highly selective detection of λ-cyhalothrin, Sensor. Actuator. B Chem. 224 (2016) 315–324, https://doi.org/10.1016/j.snb.2015.10.048.

[10] A. Tall, K.R. Costa, M.J. Oliveira, I. Tapsoba, U. Rocha, T.O. Sales, M.O.F. Goulart, J.C.C. Santos, Photoluminescent nanoprobes based on thiols capped CdTe quantum dots for direct determination of thimerosal in vaccines, Talanta 221 (2021) 121545, https://doi.org/10.1016/j.talanta.2020.121545.

[11] M. Mehrzad-Samarin, F. Faridbod, A.S. Dezfuli, M.R. Ganjali, A novel metronidazole fluorescent nanosensor based on graphene quantum dots embedded silica molecularly imprinted polymer, Biosens. Bioelectron. 92 (2017) 618–623, https://doi.org/10.1016/j.bios.2016.10.047.

[12] Q. Wang, L. Li, X. Wang, C. Dong, S. Shuang, Graphene quantum dots wrapped square-plate-like MnO_2 nanocomposite as a fluorescent turn-on sensor for glutathione, Talanta 219 (2020) 121180, https://doi.org/10.1016/j.talanta.2020.121180.

[13] S. Huang, L. Tan, L. Zhang, J. Wu, L. Zhang, Y. Tang, H. Wang, Y. Liang, Molecularly imprinted mesoporous silica embedded with perovskite $CsPbBr_3$ quantum dots for the fluorescence sensing of 2,2-dichlorovinyl dimethyl phosphate, Sens. Actuators B-Chem. 325 (2020) 128751, https://doi.org/10.1016/j.snb.2020.128751.

[14] M. Nurrokhimah, P. Nurerk, P. Kanatharana, O. Bunkoed, A nanosorbent consisting of a magnetic molecularly imprinted polymer and graphene oxide for multi-residue analysis of cephalosporins, Microchim. Acta 186 (2019), https://doi.org/10.1007/s00604-019-3985-5.

[15] E. Turiel, A. Martín-Esteban, Molecularly imprinted polymers for sample preparation: a review, Anal. Chim. Acta 668 (2010) 87–99, https://doi.org/10.1016/j.aca.2010.04.019.

[16] S. Ansari, S. Masoum, Recent advances and future trends on molecularly imprinted polymer-based fluorescence sensors with luminescent carbon dots, Talanta 223 (2021) 121411, https://doi.org/10.1016/j.talanta.2020.121411.

[17] Y. Cao, X. Hu, T. Zhao, Y. Mao, G. Fang, S. Wang, A core-shell molecularly imprinted optical sensor based on the upconversion nanoparticles decorated with Zinc-based metal-organic framework for selective and rapid detection of octopamine, Sens. Actuators B-Chem. 326 (2021) 128838, https://doi.org/10.1016/j.snb.2020.128838.

[18] W. Kaewsuwan, P. Kanatharana, O. Bunkoed, Dispersive magnetic solid phase extraction using octadecyl coated silica magnetite nanoparticles for the extraction of tetracyclines in water samples, J. Anal. Chem. 72 (2017) 957–965, https://doi.org/10.1134/S1061934817090143.

[19] L. Lian, X. Zhang, J. Hao, J. Lv, X. Wang, B. Zhu, D. Lou, Magnetic solid-phase extraction of fluoroquinolones from water samples using titanium-based metal-organic framework functionalized magnetic microspheres, J. Chromatogr. A 1579 (2018) 1–8, https://doi.org/10.1016/j.chroma.2018.10.019.

[20] C. Lin, Z. Zou, Z. Lei, L. Wang, Y. Song, Fluorescent metal-organic frameworks MIL-101(Al)-NH_2 for rapid and sensitive detection of ellagic acid, Spectrochim. Acta 242 (2020) 118739, https://doi.org/10.1016/j.saa.2020.118739.

[21] P. Nurerk, M. Llompart, P. Donkhampa, O. Bunkoed, T. Dagnac, Solid-phase extraction based on MIL-101 adsorbent followed by gas chromatography tandem mass spectrometry for the analysis of multiclass organic UV filters in water, J. Chromatogr. A 1610 (2020) 460564, https://doi.org/10.1016/j.chroma.2019.460564.

[22] P. Klongklaew, P. Kanatharana, O. Bunkoed, Development of doubly porous composite adsorbent for the extraction of fluoroquinolones from food samples,

Food Chem. 309 (2020) 125685, https://doi.org/10.1016/j.foodchem.2019.125685.

[23] K. Chullasat, P. Kanatharana, O. Bunkoed, Nanocomposite optosensor of dual quantum dot fluorescence probes for simultaneous detection of cephalexin and ceftriaxone, Sensor. Actuator. B Chem. 281 (2019) 689–697, https://doi.org/10.1016/j.snb.2018.11.003.

[24] O. Bunkoed, P. Kanatharana, Mercaptopropionic acid-capped CdTe quantum dots as fluorescence probe for the determination of salicylic acid in pharmaceutical products, Luminescence 30 (2015) 1083–1089, https://doi.org/10.1002/bio.2862.

[25] M. Roca, R.L. Althaus, M.P. Molina, Thermodynamic analysis of the thermal stability of sulphonamides in milk using liquid chromatography tandem mass spectrometry detection, Food Chem. 136 (2013) 376–383, https://doi.org/10.1016/j.foodchem.2012.08.055.

[26] B. The Huy, M.H. Seo, X. Zhang, Y.I. Lee, Selective optosensing of clenbuterol and melamine using molecularly imprinted polymer-capped CdTe quantum dots, Biosens. Bioelectron. 57 (2014) 310–316, https://doi.org/10.1016/j.bios.2014.02.041.

[27] L. Zhang, L. Chen, Fluorescence probe based on hybrid mesoporous silica/quantum dot/molecularly imprinted polymer for detection of tetracycline, ACS Appl. Mater. Interfaces 8 (2016) 16248–16256, https://doi.org/10.1021/acsami.6b04381.

[28] X. Lu, F. Wei, G. Xu, Y. Wu, J. Yang, Q. Hu, Surface molecular imprinting on silica-coated CdTe quantum dots for selective and sensitive fluorescence detection of p-aminophenol in water, J. Fluoresc. 27 (2017) 181–189. http://doi:10.1007/s10895-016-1944-7.

[29] I.S. Ibarra, J.M. Miranda, J.A. Rodriguez, C. Nebot, A. Cepeda, Magnetic solid phase extraction followed by high-performance liquid chromatography for the determination of sulphonamides in milk samples, Food Chem. 157 (2014) 511–517, https://doi.org/10.1016/j.foodchem.2014.02.069.

[30] X. Zhou, W.-Q. Chen, Y.-Q. Ding, B.-Q. Zhu, Z.-Y. Fan, J.-W. Luo, Rapid determination of sulfonamides in chicken using two-dimensional online cleanup mode with three columns coupled to liquid chromatography tandem mass spectrometry, J. Chromatogr. B 1114–1115 (2019) 110–118, https://doi.org/10.1016/j.jchromb.2019.03.015.

[31] T. Li, Z.-G. Shi, M.-M. Zheng, Y.-Q. Feng, Multiresidue determination of sulfonamides in chicken meat by polymer monolith microextraction and capillary zone electrophoresis with field-amplified sample stacking, J. Chromatogr. A 1205 (2008) 163–170, https://doi.org/10.1016/j.chroma.2008.08.017.

[32] A.M. Bueno, A.M. Contento, Á. Ríos, Validation of a screening method for the rapid control of sulfonamide residues based on electrochemical detection using multiwalled carbon nanotubes-glassy carbon electrodes, Anal. Methods 5 (2013) 6821–6829, https://doi.org/10.1039/C3AY41437J.

[33] W. Zhang, C. Duan, M. Wang, Analysis of seven sulphonamides in milk by cloud point extraction and high performance liquid chromatography, Food Chem. 126 (2011) 779–785, https://doi.org/10.1016/j.foodchem.2010.11.072.

[34] N. Thammasoontaree, P. Rattanarat, N. Ruecha, W. Siangproh, N. Rodthongkum, O. Chailapakul, Ultra-performance liquid chromatography coupled with graphene/polyaniline nanocomposite modified electrode for the determination of sulfonamide residues, Talanta 123 (2014) 115–121, https://doi.org/10.1016/j.talanta.2014.02.004.

[35] Y. Zhao, R. Wu, H. Yu, J. Li, L. Liu, S. Wang, X. Chen, T.W.D. Chan, Magnetic solid-phase extraction of sulfonamide antibiotics in water and animal-derived food samples using core-shell magnetite and molybdenum disulfide nanocomposite adsorbent, J. Chromatogr. A 1610 (2020) 460543, https://doi.org/10.1016/j.chroma.2019.460543.

[36] A.K. Dash, J.S. Harrison, Ion-pair chromatographic method for the analysis of mafenide acetate, J. Chromatogr. A 708 (1995) 83–88, https://doi.org/10.1016/0021-9673(95)00361-.

[37] D. Suo, P. Wang, Z. Xiao, S. Zhang, H. Zhuang, Y. Li, X. Su, Multiresidue determination of 27 sulfonamides in poultry feathers and its application to a sulfamethazine pharmacokinetics study on laying hen feathers and sulfonamide residue monitoring on poultry feathers, J. Agric. Food Chem. 67 (2019) 11236–11243, https://doi.org/10.1021/acs.jafc.9b02782.

Supplementary Information

Nanohybrid magnetic composite optosensing probes for the enrichment and ultra-trace detection of mafenide and sulfisoxazole

Naphatsakorn Orachorn, Opas Bunkoed*

Center of Excellence for Innovation in Chemistry, Division of Physical Science, Faculty of Science, Prince of Songkla University, Hat Yai, Songkhla 90112, Thailand

Corresponding author: Email address: opas.b@psu.ac.th

2.1. Chemicals and instrumentals

Sulfisoxazole, mafenide, thioglycolic acid (TGA), citric acid, terephthalic acid, sodium borohydride ($NaBH_4$), 3-aminopropyltriethoxysilane (APTES, ≥98%) and tetraethyl orthosilicate (TEOS, ≥97%) were purchased from Tokyo Chemical Industry Co. Ltd. (Tokyo, Japan). Tellurium powder (99.8%), sodium acetate, $Cl_2Fe{\cdot}4H_2O$ and $Cl_3Fe{\cdot}6H_2O$ were purchased from Sigma-Aldrich (MO, USA). Cadmium chloride ($CdCl_2{\cdot}2.5H_2O$), $NaH_2PO_4{\cdot}2H_2O$ and $Na_2HPO_4{\cdot}12H_2O$ were purchased from Univar. Chromium (III) nitrate nonahydrate ($CrN_3O_9{\cdot}9H_2O$) was from HiMedia Laboratories Pvt. Ltd (Mumbai, India). Sodium hydroxide (NaOH), ethanol and ammonia solution (25% $NH_3{\cdot}H_2O$) were from RCI Labscan (Bangkok, Thailand). Dialysis membrane was obtained from Spectrum Laboratories, Inc. (Rancho Dominguez, CA, USA).

Fluorescence was measured using a RF-5301 spectrofluorometer (Shimadzu, Tokyo, Japan). UV-Vis absorption was measured with an AvaSpec-2048 spectrometer (Apeldoorn, the Netherlands). Fourier transform infrared (FTIR) spectra were recorded using a BX FTIR spectroscope (PerkinElmer, Ma, USA). Scanning electron microscope (SEM) images were acquired using the JSM-5200 scanning electron microscope (JEOL, Tokyo, Japan). Transmission electron microscope (TEM) images were obtained using the Philips TECNAI 20 (Eindhoven, the Netherlands).

2.2 Synthesis of MIL-101

MIL-101 was synthesized via a hydrothermal method. First, 6.0 g of chromium nitrate nonahydrate, 2.5 g of terephthalic acid and 0.3 g of sodium acetate were added to 75 mL of DI water, mixed to homogeneity and transferred to a Teflon-lined stainless steel vessel. The vessel was then sealed and heated at 200 °C for 12 h. The resultant fine, green crystals of MIL-101 were washed with 100 mL DI water and 20 mL of dimethylformamide. The primary product of MIL-101 was then further purified in the Teflon-lined stainless steel vessel by heating for

10 h at 100 °C in 75 mL of ethanol. The obtained final product of MIL-101 was washed with 20 mL of ethanol and DI water, and dried in an oven at 80 °C for 24 h.

2.3 Synthesis of silica modified magnetite nanoparticles (SiO_2/Fe_3O_4)

First, Fe_3O_4 nanoparticles were synthesized via co-precipitation. Briefly, 9.0 g of $FeCl_3{\cdot}6H_2O$ and 3.0 g of $FeCl_2{\cdot}4H_2O$ were dissolved in 160 mL of DI water in a three-necked flask. The mixture solution was heated until the temperature was 80 °C and then 20 mL of ammonium hydroxide was rapidly added. The solution was continuously stirred for 1 h. Fe_3O_4 nanoparticles were separated from the solution using an external magnet, washed three times with 50 mL of DI water and dried at 80 °C for 6 h.

In a sol-gel process, SiO_2/Fe_3O_4 was prepared by adding 2.0 g of Fe_3O_4 into a solution containing 100 mL of ethanol, 50 mL of DI water and 2.0 mL of NH_4OH (30 %v/v). The solution mixture was stirred at 40 °C for 15 min and then 2.0 mL of TEOS was added to the solution and stirring was maintained for 12 h. The synthesized SiO_2/Fe_3O_4 nanoparticles were washed with 20 mL of ethanol and DI water and dried at 60 °C for 4 h.

2.5 Synthesis of TGA-capped CdTe QDs

Briefly, 50 mg of Te powder and 45 mg of sodium borohydride were dissolved in 2.0 mL of DI water and stirred for 10 min to obtain a purple solution of NaHTe. Meanwhile, 45 mg of $CdCl_2$ and 30 μL of TGA were dissolved in 100 mL of DI water and adjusted to pH 11.5 with 1.0 M sodium hydroxide. This second mixture solution was placed into a three-necked flask and purged with N_2 gas for 20 min. After purging, the solution was heated to 90 °C and 0.50 mL of the prepared NaHTe was rapidly injected into the solution. An orange solution of TGA-capped CdTe QDs was obtained, which was continuously heated for 1 h. The TGA-capped CdTe QDs were precipitated with ethanol to eliminate excess reagents and centrifuged at 4000 rpm for 10 min. The resulting TGA-capped CdTe QDs were kept in a desiccator until used.

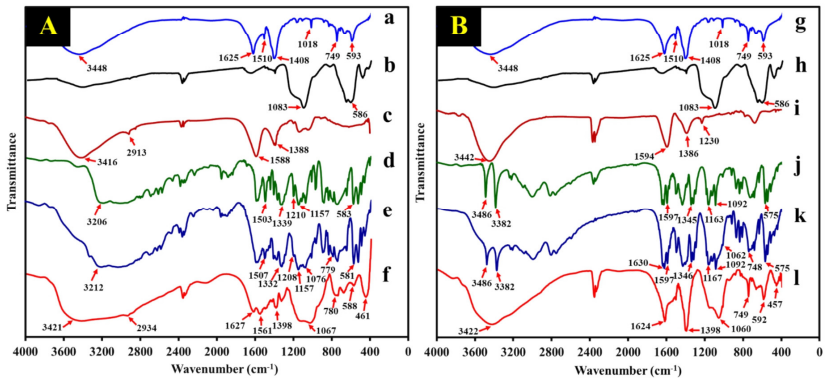

Fig. S1 FT-IR spectra are of the individual components and the fabricated composite probes of MIL101-MMIP-GQDs for the detection of mafenide (A) and MIL101-MMIP-CdTe QDs for sulfisoxazole detection (B). Spectra a and g are both of MIL-101, spectra b and h are both of SiO_2/Fe_3O_4, spectrum c is of GQDs, spectrum d is of mafenide, spectrum e is of the MIL101-MMIP-GQDs before the removal of mafenide, and spectrum f is of MIL101-MMIP-GQDs after the removal of mafenide. Spectrum i is of TGA-capped CdTe QDs, spectrum j is of sulfisoxazole, spectrum k is of MIL101-MMIP-CdTe QDs before the removal of sulfisoxazole and spectrum l is of MIL101-MMIP-CdTe QDs after the removal of sulfisoxazole.

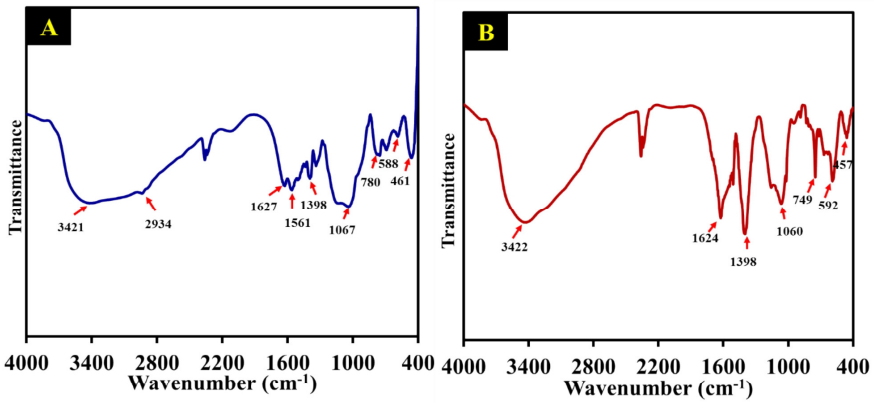

Fig. S2 FT-IR spectra of MIL101-MNIP-GQDs (A) and MIL101-MNIP-CdTe QDs (B)

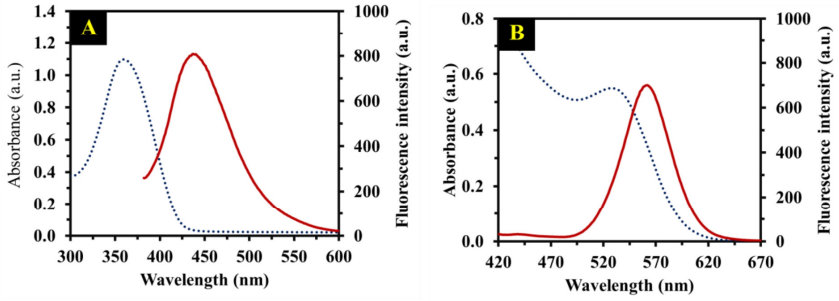

Fig. S3 The UV-Vis spectrum (dotted line) and fluorescence spectrum (solid line) (A) are of GQDs and the UV-Vis Spectrum (dotted line) and fluorescence spectrum (solid line) (B) are of TGA-capped CdTe QDs.

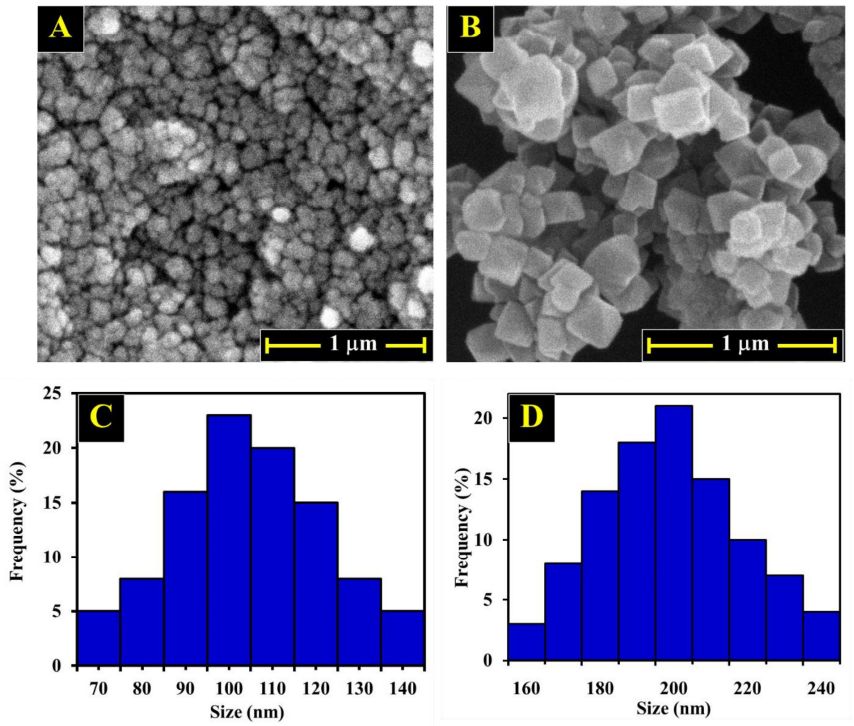

Fig. S4 SEM images of SiO_2/Fe_3O_4 (A), MIL101 (B) and size distribution histogram of SiO_2/Fe_3O_4 (C) and MIL101 (D).

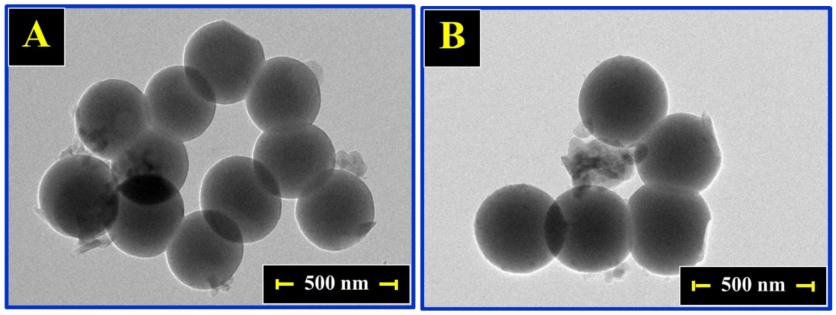

Fig. S5 TEM images of MIL101-MMIP-GQDs (A) and MIL101-MMIP-CdTe QDs nanocomposite probes (B)

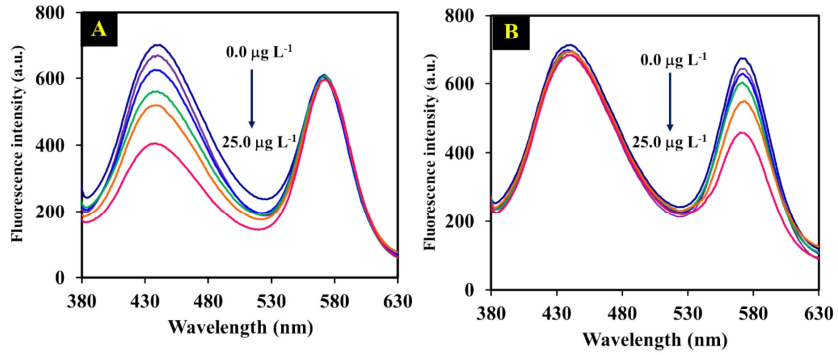

Fig. S6 Fluorescence intensity of dual nanocomposite probes in the present of mafenide (A) and sulfisoxazole (B)

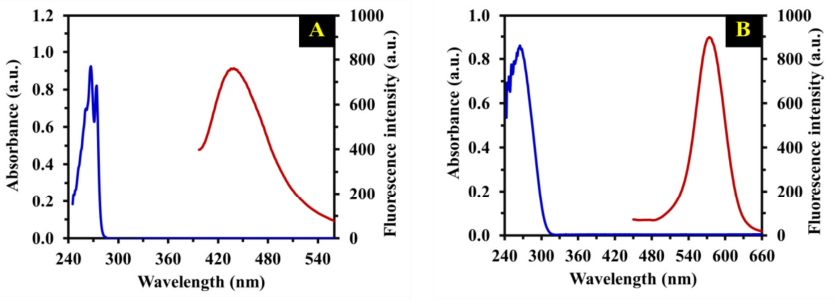

Fig. S7 (A) The UV-Vis absorption spectrum is of mafenide (blue line) and the fluorescence emission spectrum is of MIL101-MMIP-GQDs (red line) and (B) the UV-Vis absorption spectrum is of sulfisoxazole (blue line) and the fluorescence emission spectrum is of MIL101-MMIP-CdTe QDs (red line)

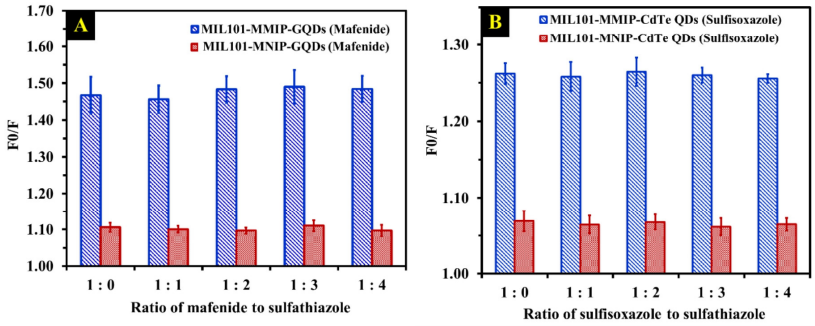

Fig. S8 Competitive study of nanohybrid magnetic composite MIL101-MMIP-GQDs (A) and MIL101-MMIP-CdTe QDs (B) probes for mafenide and sulfisoxazole detection.

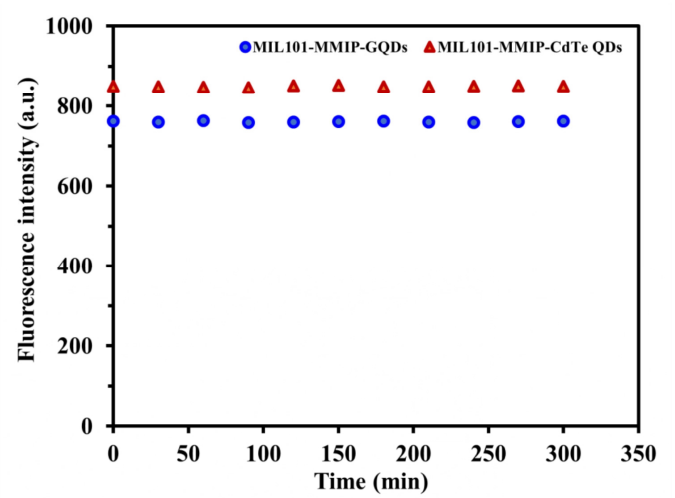

Fig. S9 The stability of nanohybrid magnetic composite MIL101-MMIP-GQD and MIL101-MMIP-CdTe QD probes

9

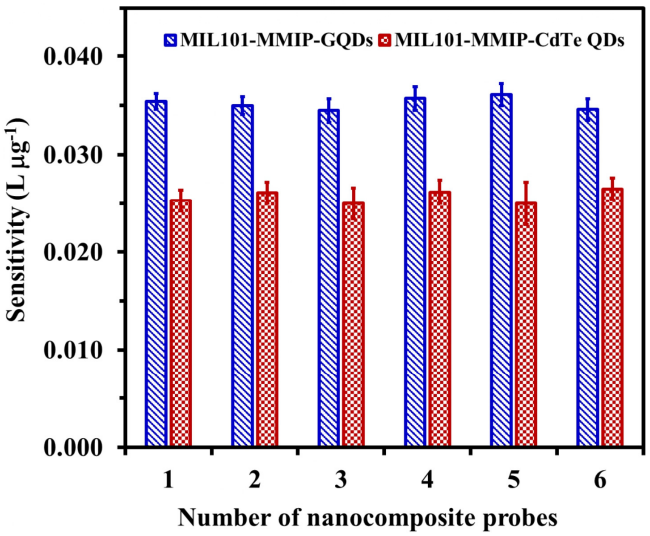

Fig. S10 The reproducibility of nanohybrid magnetic composite probes for the simultaneous detection of mafenide and sulfisoxazole

Paper III

Orachorn, N., Klongklaew, P., Bunkoed, O., A composite of magnetic GOx@MOF incorporated in alginate hydrogel fiber adsorbent for the extraction of phthalate esters. ***Microchemical Journal*** 171 (2021), 106827.

(Reprinted with permission of Elsevier)

Microchemical Journal 171 (2021) 106827

Contents lists available at ScienceDirect

Microchemical Journal

journal homepage: www.elsevier.com/locate/microc

A composite of magnetic GOx@MOF incorporated in alginate hydrogel fiber adsorbent for the extraction of phthalate esters

Naphatsakorn Orachorn, Pattamaporn Klongklaew, Opas Bunkoed *

Center of Excellence for Innovation in Chemistry, Division of Physical Science, Faculty of Science, Prince of Songkla University, Hat Yai, Songkhla 90110, Thailand

ARTICLE INFO

Keywords:
Phthalate esters
Composite hydrogel fiber
Graphene oxide
Metal organic framework
Dispersive magnetic solid phase extraction
Alginate

ABSTRACT

A composite alginate hydrogel magnetic fiber adsorbent was developed for the extraction and enrichment of phthalate esters. The adsorbent was fabricated by integrating graphene oxide (GOx), a metal organic framework (MOF) and magnetite nanoparticles (Fe_3O_4) into alginate hydrogel fiber. The developed composite hydrogel fiber adsorbent was characterized. The fabrication procedure and extraction condition included the amount of GOx and MOF in the composite fiber, the dosage of composite hydrogel fiber adsorbent, the extraction time, desorption condition, sample volume, stirring rate and sample pH were optimized. The composite hydrogel fiber adsorbent was used for the extraction and coupled with high performance liquid chromatography for the separation, identification and determination of phthalate esters in water, juice and tea. Applied composite adsorbent for the extraction of phthalate esters and quantitative analysis with HPLC technique provided good linearity in the ranges of 3.0–250.0 μg L^{-1} for benzyl butyl phthalate and dibutyl phthalate, and 5.0–250.0 μg L^{-1} for bis(2-ethylhexyl) phthalate and di-n-octyl phthalate. The coefficients of determination were >0.998. The limits of detection and limits of quantification were achieved in the range of 3.0–5.0 μg L^{-1} and 10.0–15.0 μg L^{-1}, respectively. The developed method was successfully applied to determine phthalate esters in water, juice and tea with satisfactory recoveries from 80.7 to 89.9 % with RSDs lower than 8 %. The developed composite alginate hydrogel fiber adsorbent showed good accuracy, precision, and reproducibility and could be reused 16 times. The extraction procedure was simple and convenient.

1. Introduction

Phthalate esters (PAEs) are versatile chemical reagents. They are extensively applied in the plastics industry as plasticizers or polymer additives and to enhance the softness, elasticity, durability and workability of consumer products [1]. However, the chemical interactions between PAEs and polymer chains are not stable and PAEs can physically bond to other compounds [2]. At elevated temperatures, PAEs can easily be released and migrate into food where their degradation products can present human health hazards such as reproductive toxicity, teratogenicity, mutagenicity and endocrine system disorders [3]. Some PAEs include benzyl butyl phthalate (BBP), bis (2-ethylhexyl) phthalate (DEHP), di-n-octyl phthalate (DNOP) and dibutyl phthalate (DBP) have been listed as priority environmental pollutants by the United States Environmental Protection Agency (US EPA). In addition, the maximum contaminant level (MCL) of DEHP in drinking water has been established at 6.0 μg L^{-1} [4]. In the interests of human health, therefore, it is important to develop an effective method of monitoring PAEs, which are typically determined by high performance liquid chromatography (HPLC). Although this method is reliable and can simultaneously determine several PAEs using a separation column [5], the concentration of PAEs in real samples is rather low and coexists with various matrix components. Consequently, sample preparation is required to pretreat and concentrate PAEs before analysis with the HPLC system and several methods have been reported to enrich analytes and remove interferences. These methods have included liquid-liquid micro-extraction (LLME) [6], solid phase extraction (SPE) [7], solid phase micro-extraction (SPME) [8], magnetic solid phase extraction (MSPE) [9] and stir-bar sorptive extraction (SBSE) [10].

Among these pretreatment methods, an MSPE technique based on hydrogel fiber has attracted attention because the fiber-type adsorbents are quickly prepared, easy to isolate from the sample solution and exhibit faster adsorption kinetics owing to the large surface area of the long, thin fibers. Alginate is an interesting material for hydrogel adsorbent fabrication because it can be designed and produced in various shapes, and has essential properties such as non-toxicity, good

* Corresponding author.
E-mail address: opas.b@psu.ac.th (O. Bunkoed).

https://doi.org/10.1016/j.microc.2021.106827
Received 24 May 2021; Received in revised form 6 September 2021; Accepted 8 September 2021
Available online 11 September 2021

stability, biodegradability and biocompatibility. Moreover, alginate can selectively bond with multivalent cations such as Ca^{2+}. This property enables a basic sol-gel transition into a three-dimensional network (3D-N) in a calcium chloride solution without the use of harsh organic chemicals [11]. A commonly used magnetic material for MPSE is magnetite nanoparticles (Fe_3O_4) [12,13]. Nevertheless, naked Fe_3O_4 nanoparticles have poor stability, and aggregate and oxidize easily. Silica coated magnetite nanoparticles (Fe_3O_4-SiO_2) are a better choice because they improve the dispersibility and stability of Fe_3O_4 nanoparticles and facilitate their modification with other materials.

The extraction of target PAEs by hydrogel fiber can be improved by incorporating other materials within the alginate hydrogel. Graphene oxide (GOx) is a carbon-based hydrophobic material with a large surface area and excellent adsorption ability [14]. The GOx structure comprises π-conjugated and numerous functional groups of carboxyl, hydroxyl and epoxy, which can efficiently adsorb organic compounds through π-π stacking and hydrogen bonding [15]. The fabricated adsorbents using Fe_3O_4 nanoparticles combined with GOx have been reported for the adsorption of various compounds such as phthalate esters [16], sulfonamides [17], pesticides [18], fluoroquinolones [19] and cephalosporins [20]. Additionally, metal organic framework (MOF) also offers large surface areas and highly porous structures of size-tunable pores [21]. They are prepared from metal ions and organic ligands. Among various type of MOF, Materials of Institute Lavoisier (MIL-101) is an attractive, cost-effective MOF structure because it is completely stable in the aqueous phase, has good chemical stability, large surface area and comprises abundant multifunctional groups. For the extraction of PAEs, which contain an aromatic ring and a hydrophobic part, they can adsorb MIL-101 via π-π and hydrophobic interactions.

In the present work, a magnetic composite of GOx, MIL-101 and silica coated Fe_3O_4 nanoparticles was incorporated in alginate hydrogel fiber (GOx/MIL-101/Fe_3O_4-SiO_2 alginate hydrogel fiber) to extract PAEs by MSPE. The fiber was used to adsorb PAEs via π-π interaction and hydrogen bonding reinforced by the hydrophobic effect. Four PAEs, including benzyl butyl phthalate (BBP), dibutyl phthalate (DBP), bis(2-ethylhexyl) phthalate (DEHP) and di-n-octyl phthalate (DNOP), were extracted using the proposed composite hydrogel fiber adsorbent and simultaneously separated using C18 column and detected with HPLC-DAD. In order to evaluate the extraction performance of the GOx/MIL-101/Fe_3O_4-SiO_2 alginate hydrogel fibers, the system was applied to extract target PAEs at low concentration levels in real samples of complex matrices that included water, juice and tea.

2. Experimental

2.1. Chemical and reagents

Iron (II) chloride tetrahydrate ($FeCl_2{\cdot}4H_2O$), calcium chloride powder, sodium acetate anhydrous and hydrochloric acid were from Merck KGaA, Darmstadt, Germany. Iron (III) chloride hexahydrate ($FeCl_3{\cdot}6H_2O$), graphene oxide powder and alginic acid sodium salt were from Sigma-Aldrich, Steinheim, Germany. Sodium hydroxide pellets and chromium (III) nitrate nonahydrate were from Loba Chemie and HiMedia Laboratories Pvt. Ltd., Mumbai, India. Acetonitrile, ethanol, methanol and dimethylformamide were from RCI Labscan Limited., Bangkok, Thailand. Ammonium hydroxide was from J.T.Baker Chemical Company, United States, USA. Terephthalic acid, tetraethyl orthosilicate (TEOS), benzyl butyl phthalate (BBP), bis (2-ethylhexyl) phthalate (DEHP), di-n-octyl phthalate (DNOP), dibutyl phthalate (DBP) were from Tokyo Chemical Industry, Japan.

2.2. Instrumental

The target PAEs were determined by HPLC coupled with a DAD detector (1100 series, Agilent Technologies Inc., USA) after separation in a C18 column (150 mm I.D. × 4.6 mm ×5 μm of particles size, Fortis Technologies Ltd., United Kingdom). To obtain good separation peaks and a short analysis time, the mobile phase was ultrapure water (line A) and acetonitrile (line B) pumped at 1.0 mL min^{-1} using the following gradient mode: 80 %B at 0–4 min, 90 %B at 4–8 min, 100 %B at 8–13 min and 80 %B at 13–15 min. The wavelength of detection was fixed at 226 nm for all PAEs. The functional groups of composite alginate fiber were investigated by FT-IR spectroscope (PerkinElmer Inc., USA). Brunauer-Emmett-Teller (BET) analysis (TriStar II 3020 series) was used to investigate the surface area of the composite alginate fiber and scanning electron microscopy (SEM-JSM 5200) was used to inspect the morphology of the adsorbent surface. X-ray diffraction (XRD) patterns were acquired using the Empyrean X-ray diffractometer (PANalytical, Netherlands). Thermal stability of the composite alginate fiber was examined through the thermal gravimetric analysis (TGA) using STA8000 (PerkinElmer Inc., USA).

2.3. Synthesis of MIL-101

A hydrothermal process was used to synthesize MIL-101 and the preparation procedure was adapted from previous work [22]. The mixture solution, containing chromium nitrate nonahydrate (8.0 %w/v), terephthalic acid (3.0 %w/v) and sodium acetate (0.4 %w/v), was loaded into a Teflon-lined hydrothermal autoclave, and the reaction proceeded at 200 °C for 12 h. Unreacted precursors were removed by washing the product five times with 30 mL of deionized (DI) water and then once with 20 mL of dimethylformamide. To further purify the synthesized MIL-101 particles, the washed particles were placed in a Teflon-lined hydrothermal autoclave with 75 mL of ethanol and heated at 100 °C for 10 h. The final product of MIL-101 was washed with 50 mL of DI water and dried at 90 °C for 12 h.

2.4. Synthesis of silica coated magnetite nanoparticles

Magnetite nanoparticles (Fe_3O_4) were synthesized by a co-precipitation method [12]. Firstly, 8.8 g of $FeCl_3{\cdot}6H_2O$ and 3.2 g of $FeCl_2{\cdot}4H_2O$ were put into a three-necked flask containing 150 mL of DI water, and the reaction temperature was raised to 80 °C. Then, 18 mL of 30 %v/v NH_4OH was added and continuously refluxed for 1 h. Then, the obtained Fe_3O_4 nanoparticles were isolated using a magnet, washed three times with 50 mL of DI water, and then dried at 85 °C for 6 h.

To coat the Fe_3O_4 nanoparticles with silica, 4.0 g of the synthesized Fe_3O_4 nanoparticles was placed in a mixture solution of 100 mL of DI water, 200 mL of ethanol and 4 mL of NH_4OH. The mixture solution was stirred at 40 °C for 20 min and 4.0 mL of tetraethyl orthosilicate was then injected into the solution. After stirring for 12 h, the obtained product was collected with a magnet and purified by washing three times with 50 mL of ethanol and DI water. Finally, the cleaned Fe_3O_4-SiO_2 nanoparticles were dried at 70 °C for 5 h.

2.5. Preparation of composite hydrogel fiber adsorbent

The preparation procedure of the composite GOx/MIL-101/Fe_3O_4-SiO_2 alginate hydrogel fibers is represented in Fig. 1A. First, 2.0 g of alginic acid powder were dissolved in 100 mL of DI water under stirring. Then, 0.10 g of GOx, 0.50 g of MIL-101 and 0.10 g of Fe_3O_4-SiO_2 were added together to the alginic acid solution. After the solution was thoroughly mixed, a glass syringe was filled with 5 mL of the solution, which then carefully injected into calcium chloride solution (5 %w/v) through a needle to form a single fiber of magnetic composite alginate hydrogel. The syringe was hanged above the $CaCl_2$ solution with the end of the needle over the surface of solution about 1.0 cm. The composite hydrogel fiber rapidly formed when the mixture solution came into contact with $CaCl_2$ solution and the composite fiber was further incubated in $CaCl_2$ solution for 2 h to complete Ca-alginate hydrogel formation. Finally, the fibers was separated from the solution by magnet and washed with DI water two times to remove free $CaCl_2$ from the

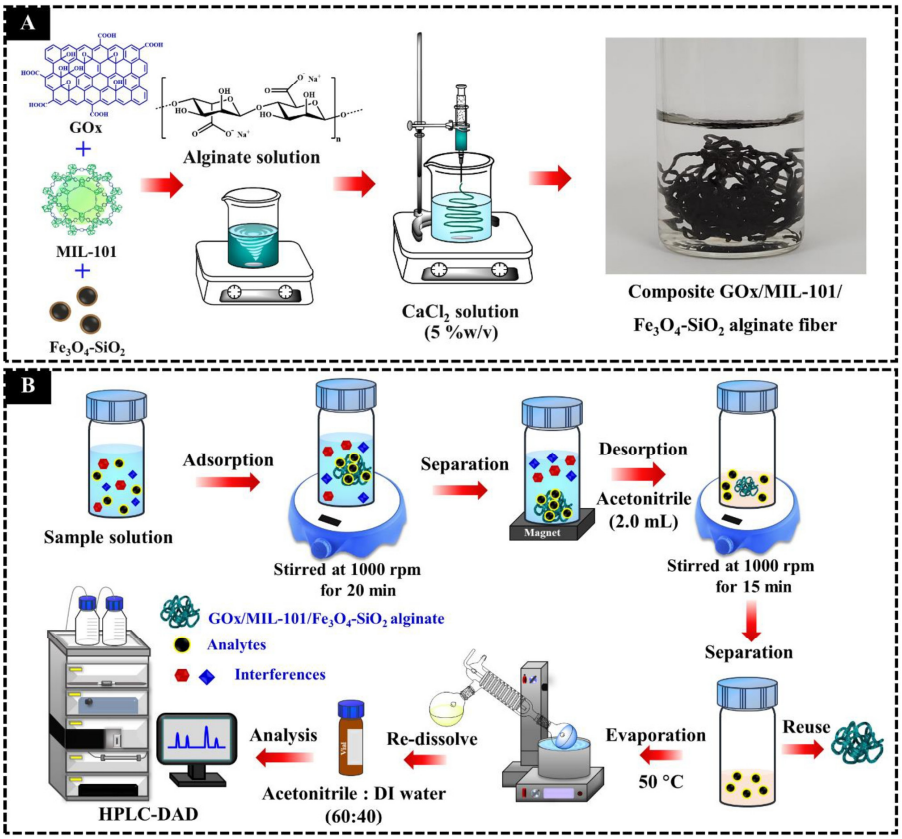

Fig. 1. The illustrations present the preparation procedure of magnetic composite GOx/MIL-101/Fe_3O_4-SiO_2 alginate hydrogel fibers (A) and the dispersive magnetic solid phase extraction procedure for the determination of PAEs using the developed hydrogel fiber sorbent (B).

hydrogel fiber surface.

2.6. Dispersive magnetic solid phase extraction procedure of phthalate esters

The fabricated composite GOx/MIL-101/Fe_3O_4-SiO_2 alginate hydrogel fibers were added and dispersed into DI water spiked with standard solution or real sample solution and stirred at 1000 rpm for 20 min to completely adsorb target PAEs. The composite magnetic alginate hydrogel fibers adsorbent with adsorbed PAEs were separated from the aqueous solution using a neodymium (NdFeB) permanent magnet. To desorb target PAEs from the composite magnetic alginate hydrogel fiber, 2.0 mL of acetonitrile were added into the extraction bottle and stirred for 15 min. After desorption, the composite magnetic hydrogel fiber adsorbents were isolated using external magnet and the elution solvent (acetonitrile) containing desorbed analytes was evaporated until dry at 50 °C. The residue was dissolved in 1.0 mL of acetonitrile: DI water at the ratio of 60:40 and filtered with a nylon syringe filter (13 mm, pore size 0.22 μm) before being transferred to a 2.0 mL amber vial for analysis by HPLC. The used GOx/MIL-101/Fe_3O_4-SiO_2 alginate hydrogel fibers were washed with 2.0 mL of acetonitrile to prevent any carry over effect from the analytes and soaked in DI water for 5 min before reuse. The dispersive magnetic solid phase extraction (d-MSPE) process using GOx/MIL-101/Fe_3O_4-SiO_2 alginate hydrogel fibers was illustrated in Fig. 1B.

2.7. Extraction procedure of commercial C18 SPE sorbent

The detail of extraction procedure using C18 sorbent for PAEs can be found in the Supporting Information.

2.8. Sample pretreatment of mineral water, vitamin water, juice and tea samples

The details of sample pretreatment of mineral water, vitamin water, juice and tea samples are given in the Supporting Information.

3. Results and discussion

3.1. Characterization of nanocomposite hydrogel fiber

The functional groups in the alginate, Fe_3O_4-SiO_2, GOx, MIL-101, composite GOx/MIL-101/Fe_3O_4-SiO_2 alginate hydrogel, composite GOx/Fe_3O_4-SiO_2 alginate hydrogel and composite MIL-101/Fe_3O_4-SiO_2 alginate hydrogel were investigated by FTIR spectroscopy. The peaks at 1626, 1406 and 1029 cm^{-1} in the alginate spectrum (Fig. S1a) were attributed to O═C—O asymmetric stretching, O═C—O symmetric stretching and C—O stretching, respectively. The Fe_3O_4-SiO_2 spectrum (Fig. S1b) exhibited adsorption peaks at 1086 and 586 cm^{-1} from the stretching of Si—O—Si and Fe—O—Fe, respectively. In the spectrum of GOx (Fig. S1c), the adsorption peaks at 3448, 1630 and 1410 cm^{-1} originated from O—H and C═O stretching and C—H bending in GOx. The synthesized MIL-101 spectrum (Fig. S1d) demonstrated characteristic bands at 1627, 1406 and 592 cm^{-1}, corresponding to C═O and O═C—O stretching and COO− bending, respectively. The band at 1548

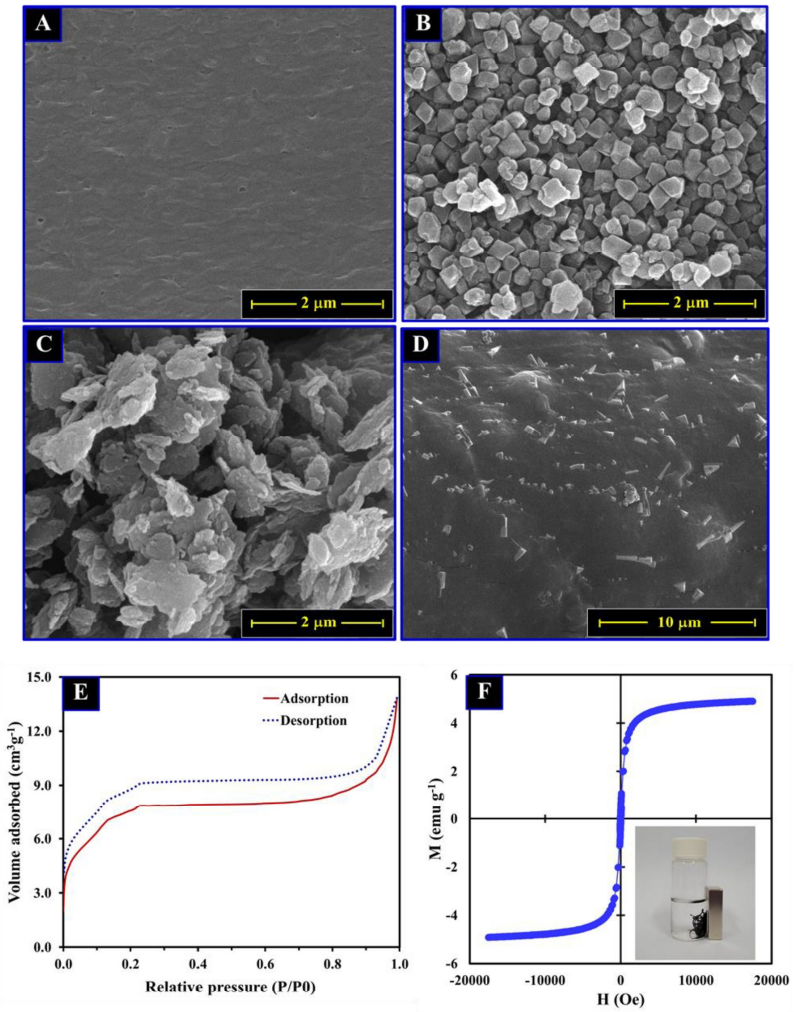

Fig. 2. SEM images are of alginate hydrogel (A), the MIL-101 (B), graphene oxide (C), and the composite GOx/MIL-101/Fe_3O_4-SiO_2 alginate hydrogel (D). The N_2 adsorption-desorption isotherm (E) and VSM curve (F) are of the composite GOx/MIL-101/Fe_3O_4-SiO_2 alginate hydrogel. The inset photograph shows the simple isolation of the composite magnetic hydrogel fiber adsorbent from solution using a magnet (F).

cm^{-1} was attributed to the C═C stretching of the benzene ring. The other peaks at 1018 and 749 cm^{-1} were due to the deformation vibration from C—H in the benzene ring. The spectrum of the composite GOx/MIL-101/Fe_3O_4-SiO_2 alginate hydrogel fiber (Fig. S1e) confirmed that Fe_3O_4-SiO_2, GOx and the MIL-101 were successfully composited in the hydrogel fiber. In the spectrum of GOx/Fe_3O_4-SiO_2 (Fig. S1f), the absorption peaks at 3448, 1630 and 1410 cm^{-1} appeared at the same wavenumbers in the GOx spectrum. The other peaks at 1086 and 586 cm^{-1} corresponded to peaks in the spectrum of Fe_3O_4-SiO_2. In the MIL-101/Fe_3O_4-SiO_2 spectrum (Fig. S1g), the characteristic peak at 1627, 1548, 1406, 1018, 749 and 592 cm^{-1} presented at the same wavenumbers in the MIL-101 spectrum and the absorption peak at 1086 cm^{-1} related to the Fe_3O_4-SiO_2 spectrum. These results insisted that the GOx/Fe_3O_4-SiO_2 and MIL-101/Fe_3O_4-SiO_2 alginate hydrogel sorbents were successfully prepared.

The crystalline structure of composite GOx/MIL-101/Fe_3O_4-SiO_2 alginate fiber adsorbent was further confirmed by X-ray diffraction analysis (XRD) (Fig. S2). The peak of composite sorbent at 2θ of 9.08° appeared at the same 2θ in the MIL-101 spectrum and the characteristic peak at 2θ of 26.49° attributed to the phase structure of GOx. The other specific peaks at 2θ of 30.27°, 35.60°, 53.82°, 57.22°, 62.93° and 75.30° corresponded to peaks in the Fe_3O_4-SiO_2 spectrum. These XRD patterns affirmed that MIL-101, GOx and Fe_3O_4-SiO_2 were successfully embedded in the hydrogel fibers.

TGA analysis was investigated in order to evaluate the thermal stability of composite GOx/MIL-101/Fe_3O_4-SiO_2 alginate hydrogel fiber adsorbent. TGA curve showed a small weight loss up to about 100 °C due to the removal of interstitial water from the adsorbent (Fig. S3). This result exhibited that the composite GOx/MIL-101/Fe_3O_4-SiO_2 alginate hydrogel fiber adsorbent has a good stability under the extraction condition of room temperature (25 to 30 °C).

In SEM images, the alginate hydrogel fiber exhibited a smooth surface (Fig. 2A), while, the MIL-101 presented octahedral particles (Fig. 2B). GOx presented a rough surface composed of flakes with large surface areas to facilitate adsorption (Fig. 2C). The SEM image of the composite GOx/MIL-101/Fe_3O_4-SiO_2 alginate hydrogel fiber (Fig. 2D) revealed a morphology that indicated the successful integration of the MIL-101 and GOx in the alginate hydrogel sorbent. Fig. 2E showed the N_2 adsorption-desorption isotherm of the developed composite hydrogel fiber adsorbent, which provided a BET surface area of 25.5425 $m^2\ g^{-1}$. The magnetic property of the composite GOx/MIL-101/Fe_3O_4-SiO_2 alginate hydrogel fiber was determined using a vibrating sample magnetometer (VSM). The VSM curve (Fig. 2F) revealed a maximum saturation of 4.912 emu g^{-1}. The composite magnetic fiber was easily isolated from the sample solution using a magnet (inset Fig. 2F).

3.2. Optimization of hydrogel fiber fabrication and extraction

The affecting parameters for the fabrication of the composite hydrogel fiber adsorbent and the extraction condition were optimized. These parameters included the amount of GOx and MIL-101 in the composite fiber, the dosage of composite hydrogel fiber adsorbent, the extraction time, desorption condition, sample volume, stirring rate and sample pH. The extraction performances were determined from absolute recovery (AR), which was calculated from the equation AR (%) = $(C_{Final}V_{Final}/C_{Initial}V_{Initial}) \times 100$, where C_{Final} is the concentration of PAEs in the reconstituted solution, $C_{Initial}$ is the concentration of PAEs spiked in water, and V_{Final} and $V_{Initial}$ are the volume of the reconstituted solution and sample volume, respectively.

The results are provide as the average ± standard deviation (SD) of three replicates.

3.2.1. Amount of GOx and MIL-101

The optimal amount of GOx and MIL-101 to be incorporated into the hydrogel fiber was determined by varying the weight ratio of GOx to MIL-101 in the synthesis reaction. The ratios were expressed as %w/v where volume was 100 mL of DI water. The effect of the different ratios was observed on recovery. The highest percent recovery was achieved with a sorbent fabricated using a GOx: MIL-101 ratio of 0.10:0.50 %w/v (Fig. S4) and this ratio was also the lowest amount that provided this extraction efficiency. Lower amounts of both GOx and MIL-101 produced lower extraction recoveries due to the lower number of adsorption sites available to target PAEs. Therefore, the composite GOx/MIL-101/Fe_3O_4-SiO_2 alginate hydrogel fiber was prepared using GOx and MIL-101 at 0.10:0.50 %w/v.

3.2.2. Dosage of composite hydrogel fiber

The amount of adsorbent used during extraction normally affects the recovery of target analytes. Increasing the adsorbent dosage can improve recovery. The effect of the sorbent dosage on the extraction of PAEs was investigated at 0.10, 0.30, 0.50, 0.80 and 1.00 g. Extraction recovery was higher at 0.30 g than at a dosage of 0.10 g but recovery remained constant up to 1.00 g (Fig. S5). Therefore, 0.30 g of composite GOx/MIL-101/Fe_3O_4-SiO_2 alginate hydrogel fiber was applied to extract PAEs.

3.2.3. Extraction time

The extraction time is the time required for the optimal adsorption between phthalate esters and composite GOx/MIL-101/Fe_3O_4-SiO_2 alginate hydrogel fiber. The adsorption time was investigated from 5 to 30 min. Extraction recoveries increased with increasing adsorption time from 5 to 20 min and then recoveries remained constant (Fig. S6). Thus, the extraction of PAEs using the composite GOx/MIL-101/Fe_3O_4-SiO_2 alginate hydrogel fiber was limited to 20 min.

3.2.4. Desorption condition

The desorption in terms of the type of desorption solvent used, its volume and desorption time was optimized to achieve the highest extraction recovery with low solvent consumption and short analysis time. A desorption solvent of acetonitrile provided the highest extraction efficiency (Fig. S7) and then the volume of acetonitrile of 0.5, 1.0, 2.0, 3.0, 4.0 and 5.0 mL were investigated. The desorption of PAEs from the composite hydrogel fiber could be completed in 2.0 mL of the solvent (Fig. S8). The desorption time was then evaluated from 5 to 25 min and the results indicated that 15 min was the optimum desorption time. Extraction recoveries increased to this time and then remained constant (Fig. S9). Therefore, the optimal desorption condition was considered to be 2.0 mL of acetonitrile for 15 min under stirring.

3.2.5. Sample volume

Sample volume influences extraction efficiency and increasing the sample volume can also enhance the enrichment of target analytes. A high enrichment factor can improve the limit of detection of the method. In this work, the effect of sample volume was investigated from 5.0 to 20.0 mL. Recoveries decreased when the volume of sample was >10.0 mL (Fig. S10). Recoveries decreased at larger sample volume may be due to the amount of adsorbent per volume decreased leading to the difficult transference of target PAEs to the surface of adsorbent in larger of sample volume [18]. Taking into consideration both extraction recovery and the enrichment factor, 10.0 mL was chosen as the optimal sample volume for the determination of PAEs extracted with the composite GOx/MIL-101/Fe_3O_4-SiO_2 alginate fiber.

3.2.6. Stirring rate

The stirring rate used during the adsorption of PAEs in the sample solution on the composite hydrogel fiber was investigated from 500 to 1500 rpm. Low extraction recoveries were obtained at stirring rates of 500 and 800 rpm due to the low mass transfer rate of PAEs from sample solution to the adsorbent. Recoveries were highest under stirring at 1000 rpm. At faster stirring rates, repeatability was poor, and relative standard deviations were high. In addition, at higher stirring rates, there was increased contact between the adsorbent and the wall of the

container, which reduced the reusability of the adsorbent. Based on the results of this study (Fig. S11), 1000 rpm was selected as the optimal stirring rate of the sample solution.

3.2.7. Sample pH

Sample pH is generally crucial for the adsorption of analytes on the surface of an adsorbent and also affects the stability of the adsorbent. Using the composite GOx/MIL-101/Fe_3O_4-SiO_2 alginate fiber to extract PAEs in aqueous samples, the effect of pH was investigated from 3.0 to 11.0 by adjusting with HCl or NaOH. Sample pH of 3.0, 5.0, 7.0 and 9.0 did not affect the extraction efficiency of PAEs but recovery decreased at pH 11.0 (Fig. S12), the recoveries decreased at pH 11.0 due to the deprotonation of PAEs led to anion forms in the strong alkaline condition, which could reduce the interaction (i.e., hydrogen bonding) between PAEs and the fabricated composite hydrogel fiber adsorbents [23]. Since, the pH of real samples does not normally exceed 9.0, adjustment of the sample pH would not be necessary.

3.2.8. Types of composite hydrogel fiber adsorbent

Magnetic alginate hydrogel fiber adsorbents of different compositions were evaluated for their ability to extract the four phthalate esters of interest. The adsorbent compositions included MIL-101/Fe_3O_4-SiO_2, GOx/Fe_3O_4-SiO_2 and GOx/MIL-101/Fe_3O_4-SiO_2 hydrogel fibers. The MIL-101/Fe_3O_4-SiO_2 and GOx/Fe_3O_4-SiO_2 hydrogel fibers were prepared under the same condition with GOx/MIL-101/Fe_3O_4-SiO_2 hydrogel fiber but without GOx and MIL-101, respectively. The fabrication of these composite hydrogel fiber adsorbent was confirmed by SEM images as demonstrated in Fig. S13. The composite GOx/MIL-101/Fe_3O_4-SiO_2 alginate hydrogel adsorbent achieved the highest extraction recovery (Fig. 3), which implied that integrating both the MIL-101 and GOx enhanced the adsorption of PAEs. The possible interaction between PAEs and the adsorbent is demonstrated in Fig. S14. The highly efficient adsorption of phthalate esters by the composite adsorbent was facilitated via hydrogen bonding and hydrophobic and π-π interactions. The results of this study confirmed the suitability of the composite GOx/MIL-101/Fe_3O_4-SiO_2 magnetic alginate hydrogel fiber to extract and determine PAEs in real samples.

3.3. Analytical performance

The analytical performance of the developed method using the fabricated composite GOx/MIL-101/Fe_3O_4-SiO_2 hydrogel fiber adsorbent to extract PAEs and analysis with HPLC were evaluated. The linearity, limit of detection (LOD), limit of quantification (LOQ) and repeatability of the method are given in Table S1. The good linearity ranged from 3.0 to 250.0 μg L^{-1} for BBP and DBP and from 5.0 to 250.0 μg L^{-1} for DEHP and DNOP. The LODs and LOQs were determined based on signal-to-noise ratios (S/N) of 3 and 10, respectively. The LOD and LOQ of BBP and DBP were 3.0 and 10.0 μg L^{-1}, respectively, while the LOD and LOQ of DEHP and DNOP were 5.0 and 15.0 μg L^{-1}, respectively. These results indicated that the developed method could be utilized to extract and determine trace PAEs in real samples. The repeatability of the developed method was evaluated in term of intra-day and inter-day precision. The relative standard deviation (RSD) values ranged from 2.0 % to 3.1 % for intra-day (n = 6) and the RSDs of inter-day (n = 6) ranged from 3.5 % to 4.8 % which were acceptable by the AOAC guidelines. A linear regression of the calibration curve was performed using Microsoft Excel software. The enrichment factors (EFs) were determined according to following equation; EFs = $C_{Final}/C_{Initial}$, Where C_{Final} is the final concentration of PAEs in extracted phase and $C_{Initial}$ is the concentration of PAEs in sample solution. C_{Final} is calculated from the calibration curves. EFs were determined under 10.0 mL of aqueous solution with spiked PAEs at concentration of 20.0 μg L^{-1}.

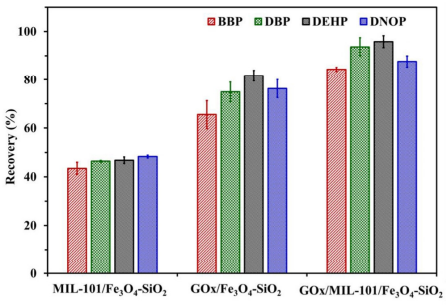

Fig. 3. The chart shows the extraction recoveries of phthalate esters achieved with variations of the composite hydrogel adsorbent.

3.4. Reproducibility and reusability

The fabrication reproducibility of the GOx/MIL-101/Fe_3O_4-SiO_2 alginate hydrogel fiber was evaluated in terms of batch-to-batch fabrications. Six different batches were prepared at different times in the same condition and used to extract PAEs at 50.0 μg L^{-1}. The RSDs of the average recoveries of six different batches <1.0 % which implied that the fabrication procedure of GOx/MIL-101/Fe_3O_4-SiO_2 alginate hydrogel fiber had a good reproducibility (Fig. S15).

The reusability of the composite GOx/MIL-101/Fe_3O_4-SiO_2 alginate hydrogel fiber was evaluated. After the extraction and desorption of PAEs, the used composite fiber was washed with 2.0 mL of acetonitrile and 2.0 mL of DI water. The composite fiber was then re-used to extract PAEs and the PAEs were again desorbed. The extraction recovery of target PAEs was better than 80 % for sixteen extraction and desorption cycles (Fig. S16). The reduced recovery after sixteen cycles may have been due to the loss of GOx and MIL-101 from the composite fiber during the extraction, desorption or washing steps. This result demonstrated the good stability of the composite GOx/MIL-101/Fe_3O_4-SiO_2 alginate fiber and that it could be reused sixteen times with acceptable recoveries.

3.5. Real sample analysis

The magnetic composite GOx/MIL-101/Fe_3O_4-SiO_2 alginate hydrogel fiber adsorbent coupled with HPLC was applied to determine PAEs in real samples including water, juice and tea in plastic bottles. The analysis results are summarized in Table S2. Low concentrations of DBP were found in some samples, while DEHP was detected below the limit of quantification. The accuracy of the method was also evaluated by spiking standard PAEs in real samples at four different levels (Table 1) and relative recovery (%) in real sample was calculated as follows:

$$Relative\ recovery\ (\%) = \left(C_{Found} - C_{Sample}/C_{Added}\right) \times 100$$

Where, C_{Found} is concentration of PAEs after adding a known amount of standard, C_{Sample} is concentration of PAEs in sample and C_{Added} is concentration of standard spiked in sample. Good recoveries were achieved from all samples from 80.7 to 89.9 % with RSDs lower than 8 %. HPLC chromatograms of a real sample without extraction, a real sample with extraction using magnetic composite GOx/MIL-101/Fe_3O_4-SiO_2 alginate hydrogel fiber, a spiked sample and standard PAEs are shown in Fig. 4. The results indicated the good accuracy of the developed method and that it could be utilized for the extraction of PAEs in different sample matrices.

In addition, the effect of the matrix interferences was also evaluated by comparing the slopes of the standard calibration curve and the spiked curve using two-way ANOVA, their slopes showed significant

Table 1
The determination and recoveries of phthalate esters in spiked samples.

Samples	Added (μg L^{-1})	Recovery (%)			
		BBP	DBP	DEHP	DNOP
Mineral water	25.0	84.2 ± 0.8	82.0 ± 2.0	88.8 ± 2.9	86.0 ± 1.5
	50.0	81.6 ± 1.1	83.2 ± 2.5	82.2 ± 1.3	83.5 ± 0.2
	75.0	82.7 ± 2.2	84.9 ± 2.2	81.4 ± 1.3	81.5 ± 1.9
	100.0	82.7 ± 2.0	87.5 ± 1.8	80.7 ± 0.8	81.9 ± 1.1
Vitamin water	25.0	83.7 ± 1.0	81.7 ± 1.6	84.2 ± 5.6	84.5 ± 4.0
	50.0	81.4 ± 1.0	82.6 ± 3.5	85.6 ± 2.6	82.9 ± 0.8
	75.0	82.3 ± 0.6	82.2 ± 1.3	84.1 ± 1.9	81.0 ± 0.9
	100.0	81.7 ± 1.4	81.2 ± 1.5	82.7 ± 0.1	81.8 ± 1.6
Juice	25.0	81.6 ± 2.1	82.7 ± 2.3	88.5 ± 4.6	89.9 ± 2.6
	50.0	82.1 ± 2.5	83.3 ± 2.9	86.1 ± 1.6	84.3 ± 1.4
	75.0	81.4 ± 1.4	82.7 ± 1.5	83.8 ± 1.5	81.9 ± 0.6
	100.0	82.0 ± 0.9	81.6 ± 0.8	83.8 ± 0.3	82.3 ± 3.1
Tea	25.0	83.4 ± 0.6	83.8 ± 2.6	81.7 ± 0.9	89.6 ± 7.3
	50.0	81.7 ± 0.5	85.2 ± 1.9	85.4 ± 2.2	84.6 ± 2.1
	75.0	83.2 ± 2.1	83.0 ± 1.7	83.5 ± 2.1	82.3 ± 1.6
	100.0	83.1 ± 1.6	81.9 ± 0.3	82.8 ± 3.1	83.0 ± 0.8

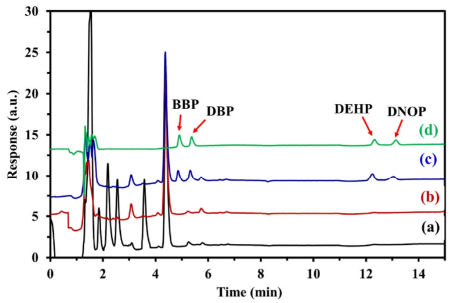

Fig. 4. HPLC chromatograms are of a real sample without extraction (a), a real sample with extraction using composite GOx/MIL-101/Fe_3O_4-SiO_2 alginate hydrogel fibers (b), a spiked sample (c) and standard phthalate esters (d).

differences which indicated that matrix effect was observed. Therefore, the matrix matched calibration is used to quantitative analysis of real samples.

3.6. Comparison with commercial sorbent and previous works

The analytical performance of the composite GOx/MIL-101/Fe_3O_4-SiO_2 alginate hydrogel fiber was compared with the performance of a C18 SPE sorbent. Both sorbents achieved recoveries >80 % (Fig. S17) which were within the acceptable range expected by the AOAC guidelines [24]. However, the extraction procedure of the composite magnetic alginate hydrogel fiber adsorbent is easier and faster. In addition, the composite fiber adsorbent can be reused which reduces cost and saves time spent preparing the adsorbent. The composite GOx/MIL-101/Fe_3O_4-SiO_2 alginate hydrogel fiber could be an alternative adsorbent to determine PAEs.

The analytical performance of the proposed method was compared with the performances of previously published methods (Table 2). The detection limit, recovery and RSD of the developed method were either better than or comparable to those achieved by other reported methods. The reusability (16 times) of the composite GOx/MIL-101/Fe_3O_4-SiO_2 alginate fiber sorbent was better than all the other sorbents. These results indicated that the composite GOx/MIL-101/Fe_3O_4-SiO_2 alginate hydrogel fiber could be an effective, accurate and efficient sorbent for the determination and extraction of PAEs in real samples.

MISPME = Molecularly imprinted solid-phase microextraction; $mSiO_2$@MWCNTs = mesoporous silica-coated multiwalled carbon nanotubes; MISPE = Molecularly imprinted solid-phase extraction; M−HAzo = Magnetic *o*-hydroxyazobenzene; MHSPE = Mixed hemimicelles solid-phase extraction; Fe_3O_4@GC = Fe_3O_4@graphitic carbon; 3D N-Co@C/HCF = Three-dimensional magnetic porous N-Co@carbon dodecahedron/hierarchical carbon framework; d-MSPE = Dispersion magnetic solid phase extraction; Fe_3O_4@C_{18}@Ba^{2+}-ALG = Barium alginate modified octadecyl functionalized Fe_3O_4 magnetic nanoparticles; ZIF-8 = Zeolitic imidazolate framework-8; g-MNDC = Magnetic N-doped mesoporous carbon; DCHP = Dicyclohexyl phthalate; DMP = Dimethyl phthalate; DAP = Diallyl phthalate; DPRP = Dipropyl phthalate; DEP = Diethyl phthalate; ACN = Acetonitrile; MeOH = Methanol

3.7. Adsorption kinetics

To describe the mechanism of adsorbent-adsorbate interaction between the composite GOx/MIL-101/Fe_3O_4-SiO_2 alginate hydrogel fiber and PAEs, intraparticle diffusion (IPD), and pseudo-first-order (PFO) and pseudo-second-order (PSO) kinetics models were investigated. The suitability of a kinetics model depends on the coefficient of determination (R^2) of fit index of each model (Table S3). The coefficient of determination (R^2) of the pseudo-second-order was closer to 1 than the R^2 of the other adsorption kinetic models (Figs. S18–S20). This result confirmed that the developed GOx/MIL-101/Fe_3O_4-SiO_2 alginate fibers adsorbed phthalate esters via a chemisorption mechanism [34]. The adsorption capacities of the developed composite hydrogel fibers at equilibrium were calculated using the following equation:

$Qe = \frac{(C_0 - C_e)V}{m}$ where Q_e is the adsorption capacity at equilibrium (μg g^{-1}), and C_e and C_0 (μg L^{-1}) are the equilibrium and initial concentrations of phthalate esters, respectively, V is the volume of sample (L) and m is the amount of composite hydrogel fibers.

4. Conclusion

A composite magnetic hydrogel fiber was designed and fabricated for use as a dispersive magnetic solid phase extraction adsorbent. The composite hydrogel fiber was composed of graphene oxide, a metal organic framework and silica-coated magnetite nanoparticles incorporated into alginate hydrogel fiber. The integration of graphene oxide and the metal organic framework enhanced the extraction of phthalate esters via hydrogen bonding, and π-π and hydrophobic interactions. The silica-coated magnetite nanoparticles facilitated the fast and convenient separation of the adsorbent from the sample solution and the desorption solvent. The composite alginate hydrogel fiber adsorbent exhibited a satisfactory extraction efficiency toward phthalate esters, recoveries > 80 %. The developed composite showed good accuracy, precision, and reproducibility and can be reused.

Table 2
The performances of the developed method using the GOx/MIL-101/Fe_3O_4-SiO_2 alginate fiber sorbent were compared with those of reported methods for the extraction and determination of phthalate esters.

Analytical methods	Sample preparation methods	Analytes	Sample matrix	Solvent type	Solvent volume (mL)	Total time	Sample volume (mL)	Reuse time	LOD (μg L^{-1})	Recovery (%)	RSD (%)	References
HPLC-UV	MISPME	DBP	Mineral water and soft drinks	ACN	4.0	>24 h	2	5	3.0	90.3–98.1	< 3	[25]
HPLC-DAD	Decanoic acid coated-Fe_3O_4	BBP, DBP, DCHP, DNOP	Liquor	MeOH	0.5	–	5	5	0.9–2.4	88.9–105.4	2.9–3.8	[26]
HPLC-UV	$mSiO_2$@MWCNTs (SPE)	DMP, DBP, DNOP	Water	ACN	4.0	–	25	6	0.3–0.5	89.8–96.3	3.8–7.7	[27]
HPLC-UV	M–HAzo (MSPE)	DAP, DPRP, BBP, DBP	Bottled juice	MeOH	0.3	21 min	50	15	0.08–0.50	78.0–115.0	2.9–7.8	[5]
HPLC-UV	Fe_3O_4/*meso*-SiO_2 NPs (MHSPE)	BBP, DBP, DEHP, DNOP	Environmental water	MeOH	6.0	25 min	250	3	0.012–0.032	80.6–102.4	2.3–5.4	[28]
HPLC-UV	Fe_3O_4@GC (d-MSPE)	DMP, DEP, BBP, DBP, DCHP	Beverages and plastic bottles	ACN	1.2	25 min	25	5	0.01–0.28	80.0–112.8	0.9–8.8	[29]
HPLC-UV	3D N-Co@C/HCF (d-MSPE)	DMP, DEP, BBP, DBP, DCHP	Green tea, water and beverages	ACN	6.0	30 min	10	7	0.023–0.113	87.1–107.2	<5	[30]
HPLC-UV	Fe_3O_4@C_{18}@Ba^{2+}-ALG (MSPE)	DPRP, DBP, DCHP, DNOP	Environmental water	ACN	8.0	>30 min	500	8	0.019–0.059	72.1–112.6	<9	[31]
HPLC-DAD	Fe_3O_4@ZIF-8 (MSPE)	DMP, DEP, DBP, BBP, DNOP	Environmental water	MeOH	1.0	16 min	20	10	0.08–0.24	85.6–103.6	2.1–5.8	[32]
HPLC-UV	g-MNDC (MSPE)	DEP, DAP, DBP	Soft drinks	MeOH	0.6	16 min	50	10	0.1–0.3	83.2–119.0	4.7–6.2	[33]
HPLC-DAD	GOx/MIL-101/Fe_3O_4-SiO_2 alginate fiber (MSPE)	BBP, DBP, DEHP, DNOP	Mineral water, vitamin water, juice and tea	ACN	2.0	35 min	10	16	3.0–5.0	80.7–89.9	0.1–7.3	This work

CRediT authorship contribution statement

Naphatsakorn Orachorn: Methodology, Formal analysis, Software, Validation, Writing – original draft. **Pattamaporn Klongklaew:** Methodology, Formal analysis, Writing – review & editing. **Opas Bunkoed:** Conceptualization, Formal analysis, Investigation, Resources, Data curation, Writing – review & editing, Supervision, Project administration, Funding acquisition.

Declaration of Competing Interest

The authors declare that they have no known competing financial interests or personal relationships that could have appeared to influence the work reported in this paper.

Acknowledgements

This work was supported by the National Research Council of Thailand (No. NRCT5-RSA63022-03) and The Center of Excellence for Innovation in Chemistry (PERCH-CIC), Ministry of Higher Education, Science, Research and Innovation. Naphatsakorn Orachorn was supported by Science Achievement Scholarship of Thailand (SAST). Pattamaporn Klongklaew was supported by the Royal Golden Jubilee PhD Program, the National Research Council of Thailand and the Thailand Research Fund (TRF). The authors thank Mr. Thomas Duncan Coyne for English proofreading.

Appendix A. Supplementary data

Supplementary data to this article can be found online at https://doi.org/10.1016/j.microc.2021.106827.

References

[1] A.A. Adenuga, O. Ayinuola, E.A. Adejuyigbe, A.O. Ogunfowokan, Biomonitoring of phthalate esters in breast-milk and urine samples as biomarkers for neonates' exposure, using modified quechers method with agricultural biochar as dispersive solid-phase extraction absorbent, Microchem. J. 152 (2020) 104277, https://doi.org/10.1016/j.microc.2019.104277.
[2] T. Li, Y. Song, J. Li, M. Zhang, Y. Shi, J. Fan, New low viscous hydrophobic deep eutectic solvents in vortex-assisted liquid-liquid microextraction for the determination of phthalate esters from food-contacted plastics, Food Chem. 309 (2020) 125752, https://doi.org/10.1016/j.foodchem.2019.125752.
[3] Y. Wu, Q. Zhou, Y. Yuan, H. Wang, Y. Tong, Y. Zhan, X. Sheng, Y.i. Sun, X. Zhou, Enrichment and sensitive determination of phthalate esters in environmental water samples: A novel approach of MSPE-HPLC based on PAMAM dendrimers-functionalized magnetic-nanoparticles, Talanta 206 (2020) 120213, https://doi.org/10.1016/j.talanta.2019.120213.
[4] Y.-H. Pang, Q.i. Yue, Y.-Y. Huang, C. Yang, X.-F. Shen, Facile magnetization of covalent organic framework for solid-phase extraction of 15 phthalate esters in beverage samples, Talanta 206 (2020) 120194, https://doi.org/10.1016/j.talanta.2019.120194.
[5] Q. Wu, Y. Song, Q. Wang, W. Liu, L. Hao, Z. Wang, C. Wang, Combination of magnetic solid-phase extraction and HPLC-UV for simultaneous determination of four phthalate esters in plastic bottled juice, Food Chem. 339 (2021) 127855, https://doi.org/10.1016/j.foodchem.2020.127855.
[6] XiuLi Wang, Y. Lu, L. Shi, D. Yang, Y. Yang, Novel low viscous hydrophobic deep eutectic solvents liquid-liquid microextraction combined with acid base induction for the determination of phthalate esters in the packed milk samples, Microchem. J. 159 (2020) 105332, https://doi.org/10.1016/j.microc.2020.105332.
[7] E.T. Özer, B. Osman, T. Yazıcı, Dummy molecularly imprinted microbeads as solid-phase extraction material for selective determination of phthalate esters in water,

J. Chromatogr. A 1500 (2017) 53–60, https://doi.org/10.1016/j.chroma.2017.04.013.

[8] D. Wu, F.u. Liu, T. Tian, J.-F. Wu, G.-C. Zhao, Copper ferrite nanoparticles as novel coating appropriated to solid-phase microextraction of phthalate esters from aqueous matrices, Microchem. J. 162 (2021) 105845, https://doi.org/10.1016/j.microc.2020.105845.

[9] Q. Wu, M. Liu, X. Ma, W. Wang, C. Wang, X. Zang, Z. Wang, Extraction of phthalate esters from water and beverages using a graphene-based magnetic nanocomposite prior to their determination by HPLC, Microchim. Acta 177 (1-2) (2012) 23–30, https://doi.org/10.1007/s00604-011-0752-7.

[10] C. Shen, T. Wu, X. Zang, Hollow fiber stir bar sorptive extraction combined with GC–MS for the determination of phthalate esters from children's food, Chromatographia 82 (3) (2019) 683–693, https://doi.org/10.1007/s10337-018-3679-x.

[11] M. Zare, Z. Ramezani, N. Rahbar, Development of zirconia nanoparticles-decorated calcium alginate hydrogel fibers for extraction of organophosphorous pesticides from water and juice samples: Facile synthesis and application with elimination of matrix effects, J. Chromatogr. A 1473 (2016) 28–37, https://doi.org/10.1016/j.chroma.2016.10.071.

[12] W. Kaewsuwan, P. Kanatharana, O. Bunkoed, Dispersive magnetic solid phase extraction using octadecyl coated silica magnetite nanoparticles for the extraction of tetracyclines in water samples, J. Anal. Chem. 72 (9) (2017) 957–965, https://doi.org/10.1134/S1061934817090143.

[13] O. Bunkoed, P. Nurerk, R. Wannapob, P. Kanatharana, Polypyrrole-coated alginate/magnetite nanoparticles composite sorbent for the extraction of endocrine-disrupting compounds, J. Sep. Sci. 39 (18) (2016) 3602–3609, https://doi.org/10.1002/jssc.v39.1810.1002/jssc.201600647.

[14] C. Lou, D. Guo, K. Zhang, C. Wu, P. Zhang, Y. Zhu, Simultaneous determination of 11 phthalate esters in bottled beverages by graphene oxide coated hollow fiber membrane extraction coupled with supercritical fluid chromatography, Anal. Chim. Acta 1007 (2018) 71–79, https://doi.org/10.1016/j.aca.2017.12.018.

[15] I.A. Senosy, H.-M. Guo, M.-N. Ouyang, Z.-H. Lu, Z.-H. Yang, J.-H. Li, Magnetic solid-phase extraction based on nano-zeolite imidazolate framework-8-functionalized magnetic graphene oxide for the quantification of residual fungicides in water, honey and fruit juices, Food Chem 325 (2020) 126944, https://doi.org/10.1016/j.foodchem.2020.126944.

[16] J.I. Abdelghani, R.S. Freihat, A.H. El-Sheikh, Magnetic solid phase extraction of phthalate products from bottled, injectable and tap waters using graphene oxide: Effect of oxidation method of graphene, J. Environ. Chem. Eng. 8 (2) (2020) 103527, https://doi.org/10.1016/j.jece.2019.103527.

[17] P.S. Gao, Y. Guo, X. Li, X. Wang, J. Wang, F. Qian, H. Gu, Z. Zhang, Magnetic solid phase extraction of sulfonamides based on carboxylated magnetic graphene oxide nanoparticles in environmental waters, J. Chromatogr. A 1575 (2018) 1–10, https://doi.org/10.1016/j.chroma.2018.09.015.

[18] S. Moradi Shahrebabak, M. Saber-Tehrani, M. Faraji, M. Shabanian, P. Aberoomand-Azar, Simultaneous magnetic solid phase extraction of acidic and basic pesticides using triazine-based polymeric network modified magnetic nanoparticles/graphene oxide nanocomposite in water and food samples, Microchem. J. 146 (2019) 630–639, https://doi.org/10.1016/j.microc.2019.01.047.

[19] R. Xiao, S. Wang, M.H. Ibrahim, H.I. Abdu, D. Shan, J. Chen, X. Lu, Three-dimensional hierarchical frameworks based on molybdenum disulfide-graphene oxide-supported magnetic nanoparticles for enrichment fluoroquinolone antibiotics in water, J. Chromatogr. A 1593 (2019) 1–8, https://doi.org/10.1016/j.chroma.2019.02.005.

[20] J. Wu, H. Zhao, D. Xiao, P.H. Chuong, J. He, H. He, Mixed hemimicelles solid-phase extraction of cephalosporins in biological samples with ionic liquid-coated magnetic graphene oxide nanoparticles coupled with high-performance liquid chromatographic analysis, J. Chromatogr. A 1454 (2016) 1–8, https://doi.org/10.1016/j.chroma.2016.05.071.

[21] J. González-Sálamo, M.Á. González-Curbelo, J. Hernández-Borges, M.Á. Rodríguez-Delgado, Use of Basolite® F300 metal-organic framework for the dispersive solid-phase extraction of phthalic acid esters from water samples prior to LC-MS determination, Talanta 195 (2019) 236–244, https://doi.org/10.1016/j.talanta.2018.11.049.

[22] Z. Huang, H.K. Lee, Micro-solid-phase extraction of organochlorine pesticides using porous metal-organic framework MIL-101 as sorbent, J. Chromatogr. A 1401 (2015) 9–16, https://doi.org/10.1016/j.chroma.2015.04.052.

[23] N. Jalilian, H. Ebrahimzadeh, A.A. Asgharinezhad, Preparation of magnetite/multiwalled carbon nanotubes/metal-organic framework composite for dispersive magnetic micro solid phase extraction of parabens and phthalate esters from water samples and various types of cream for their determination with liquid chromatography, J. Chromatogr. A 1608 (2019) 460426, https://doi.org/10.1016/j.chroma.2019.460426.

[24] AOAC International, Appendix F: Guidelines for standard method performance requirements AOAC Official Method of, Analysis 2016 (2016) 1–18.

[25] S. Soheilifar, M.-J. Rajabi-Moghaddam, G. Karimi, A. Mohammadinejad, V. S. Motamedshariaty, S.A. Mohajeri, Application of molecularly imprinted polymer in solid-phase microextraction coupled with HPLC-UV for analysis of dibutyl phthalate in bottled water and soft drink samples, J. Liq. Chromatogr. Relat. Technol. 41 (9) (2018) 552–560, https://doi.org/10.1080/10826076.2018.1488138.

[26] J. Wang, L. Zhang, D. Xin, Y. Yang, Dispersive micro-solid-phase extraction based on decanoic acid coated-Fe_3O_4 nanoparticles for HPLC analysis of phthalate esters in liquor samples, J. Food Sci. 80 (11) (2015) C2452–C2458, https://doi.org/10.1111/1750-3841.13101.

[27] X. Deng, X. Chen, X. Jiang, Solid-phase extraction of phthalate esters from aqueous samples using mesoporous silica-coated multiwalled carbon nanotubes and their determination by HPLC, Nano 09 (04) (2014) 1450054, https://doi.org/10.1142/S1793292014500544.

[28] P. L. Liu, Y. P. Xu, P. Zheng, H. W. Tong, Y. X. Liu, Z. G. Zha, Q. D. Su, S. M. Liu, Mesoporous silica-coated magnetic nanoparticles for mixed hemimicelles solid-phase extraction of phthalate esters in environmental water samples with liquid chromatographic analysis, J Chin Chem Soc 60 (1) (2013) 53–62, https://doi.org/10.1002/jccs.201200096.

[29] Y. Tong, X. Liu, L. Zhang, Green construction of Fe_3O_4@GC submicrocubes for highly sensitive magnetic dispersive solid-phase extraction of five phthalate esters in beverages and plastic bottles, Food Chem. 277 (2019) 579–585, https://doi.org/10.1016/j.foodchem.2018.11.021.

[30] Y. Wang, Y. Tong, X. Xu, L. Zhang, Developed magnetic multiporous 3D N-Co@C/HCF as efficient sorbent for the extraction of five trace phthalate esters, Anal. Chim. Acta 1054 (2019) 176–183, https://doi.org/10.1016/j.aca.2018.12.046.

[31] S. Zhang, H. Niu, Y. Cai, Y. Shi, Barium alginate caged Fe_3O_4@C18 magnetic nanoparticles for the pre-concentration of polycyclic aromatic hydrocarbons and phthalate esters from environmental water samples, Anal. Chim. Acta 665 (2) (2010) 167–175, https://doi.org/10.1016/j.aca.2010.03.026.

[32] X. Liu, Z. Sun, G. Chen, W. Zhang, Y. Cai, R. Kong, X. Wang, Y. Suo, J. You, Determination of phthalate esters in environmental water by magnetic zeolitic imidazolate framework-8 solid-phase extraction coupled with high-performance liquid chromatography, J. Chromatogr. A 1409 (2015) 46–52, https://doi.org/10.1016/j.chroma.2015.07.068.

[33] M. Li, C. Jiao, X. Yang, C. Wang, Q. Wu, Z. Wang, Magnetic N-doped mesoporous carbon as an adsorbent for the magnetic solid-phase extraction of phthalate esters from soft drinks, J. Sep. Sci. 40 (8) (2017) 1637–1643, https://doi.org/10.1002/jssc.v40.810.1002/jssc.201601262.

[34] J.P. Simonin, On the comparison of pseudo-first order and pseudo-second order rate laws in the modeling of adsorption kinetics, Chem. Eng. J. 300 (2016) 254–263, https://doi.org/10.1016/j.cej.2016.04.079.

Supporting information

A composite of magnetic GOx@MOF incorporated in alginate hydrogel fiber adsorbent for the extraction of phthalate esters

Naphatsakorn Orachorn, Pattamaporn Klongklaew and Opas Bunkoed*

Center of Excellence for Innovation in Chemistry, Division of Physical Science, Faculty of Science, Prince of Songkla University, Hat Yai, Songkhla 90110, Thailand

Corresponding author**:** Opas Bunkoed, Ph.D.

Email address**:** opas.b@psu.ac.th

2.7 Extraction procedure using commercial C18 SPE sorbent

The Oasis HLB cartridges were connected to an SPE manifold, which was linked to a vacuum pump. The SPE cartridges were firstly conditioned by rinsing with 2.0 mL of acetonitrile and then with 2.0 mL of DI water. Then, 10.0 mL of spiked standard solution was passed through SPE cartridges and the PAEs were adsorbed on the adsorbent in this step. The adsorbed PAEs were eluted with 2.0 mL of acetonitrile and then the eluent containing desorbed PAEs was evaporated to dryness at 50 °C. The residue was redissolved with 1.0 mL of the mixture of acetonitrile and DI water (ratio of 60:40) and filtered with a nylon syringe filter (13 mm, pore size 0.22 μm) and analyzed by HPLC.

2.8 Sample pretreatment of mineral water, vitamin water, juice and tea samples

Mineral and vitamin water samples were directly extracted using a developed composite hydrogel fiber adsorbent without further sample pretreatment process. Meanwhile, the sample preparation of juice and tea samples were carried out by 10 times dilution with DI water before being extracted using a fabricated GOx/MIL-101/Fe_3O_4-SiO_2 hydrogel fiber and analyzed by an HPLC.

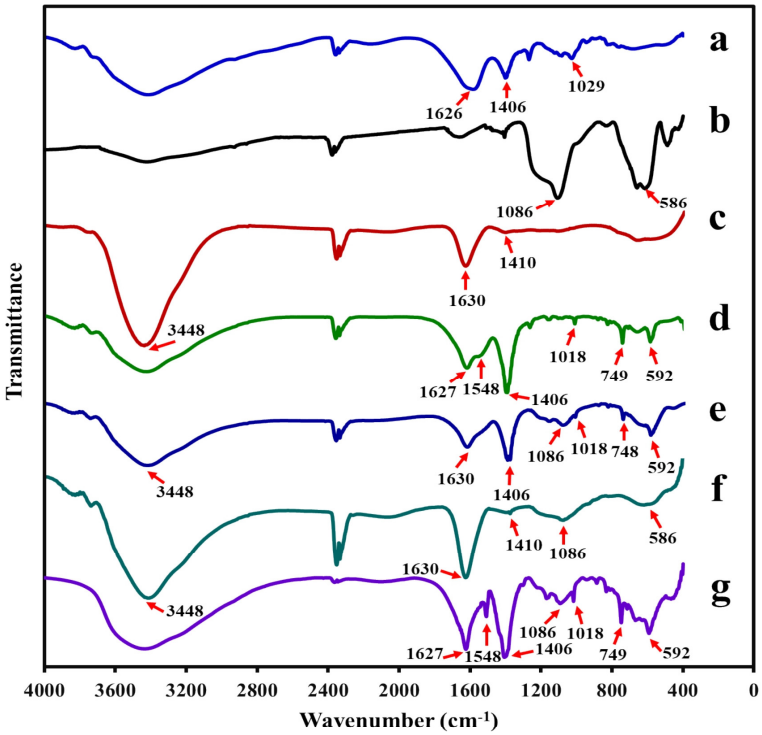

Fig. S1 FTIR spectra are of alginate hydrogel (a), Fe_3O_4-SiO_2 (b), GOx (c), MIL-101 (d), composite GOx/MIL-101/Fe_3O_4-SiO_2 alginate hydrogel (e), composite GOx/Fe_3O_4-SiO_2 alginate hydrogel (f) and composite MIL-101/Fe_3O_4-SiO_2 alginate hydrogel (g).

4

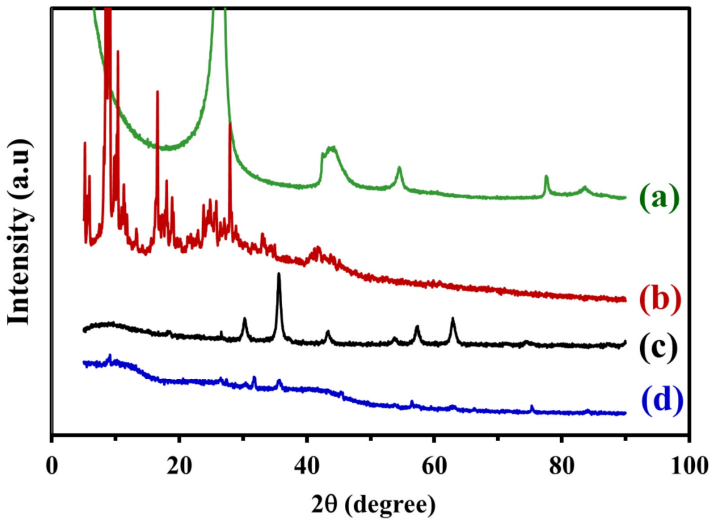

Fig. S2 The XRD patterns of GOx (a), MIL-101 (b), Fe_3O_4-SiO_2 (c) and composite GOx/MIL-101/Fe_3O_4-SiO_2 alginate hydrogel fiber (d)

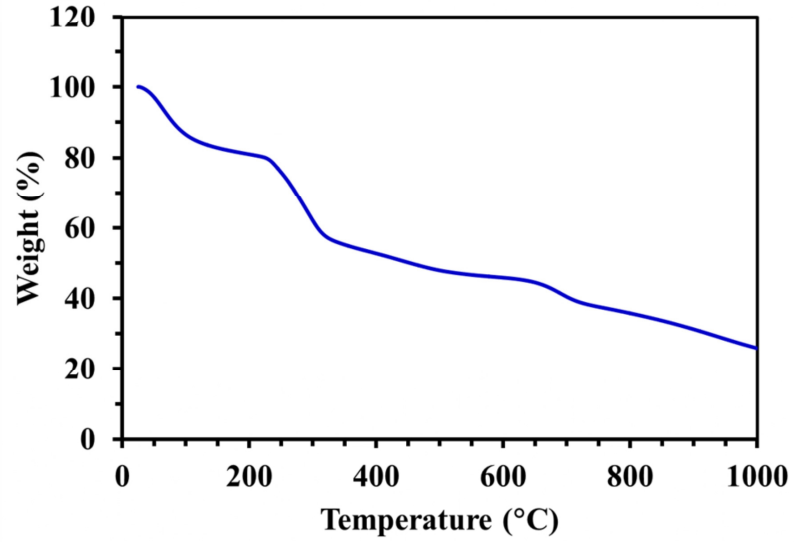

Fig. S3 TGA curve of composite GOx/MIL-101/Fe_3O_4-SiO_2 alginate hydrogel fiber

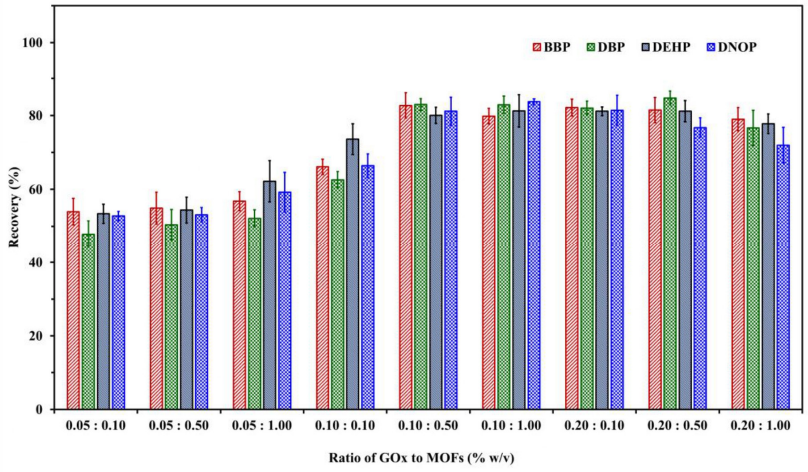

Fig. S4 The effect on recovery of various amounts of GOx and MIL-101 incorporated in the GOx/MIL-101/Fe_3O_4-SiO_2 alginate hydrogel fiber for the extraction of phthalate esters.

6

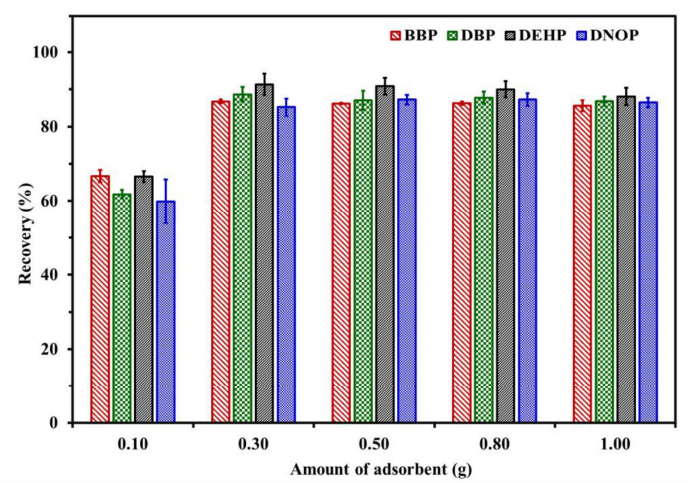

Fig. S5 The chart shows the effect of different doses of composite GOx/MIL-101/Fe_3O_4-SiO_2 alginate hydrogel fiber on recovery of phthalate esters.

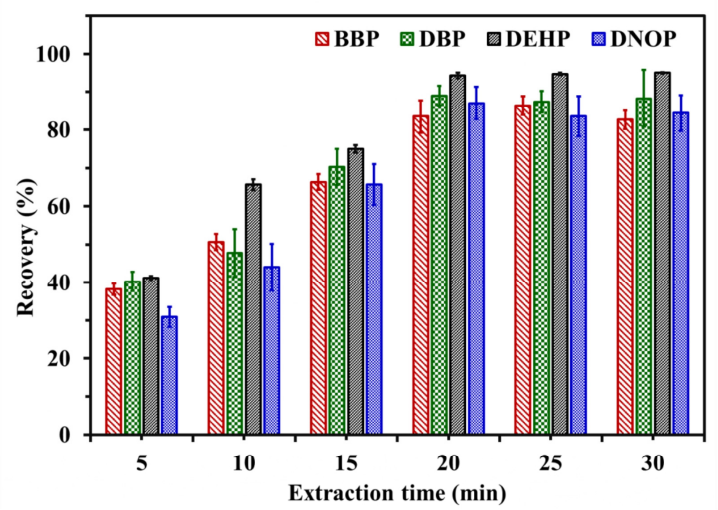

Fig. S6 The chart shows the effect of extraction time on the recovery of phthalate esters using the composite GOx/MIL-101/Fe_3O_4-SiO_2 alginate hydrogel fiber.

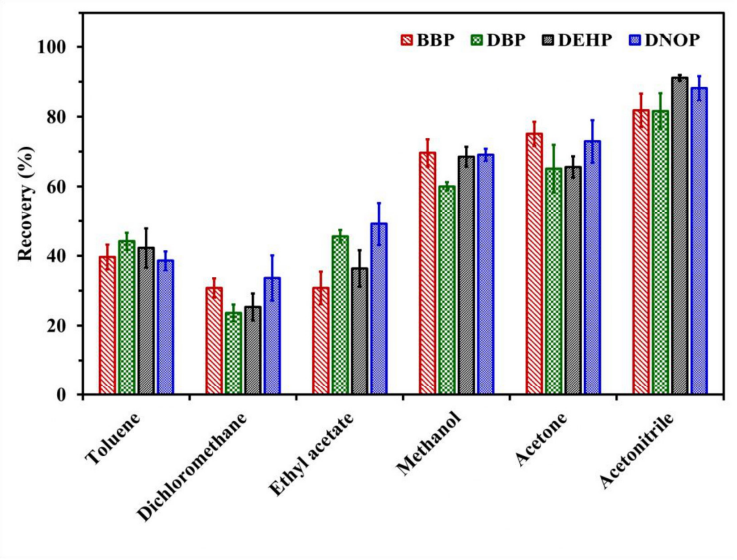

Fig. S7 The chart shows the effect of different desorption solvents on the recovery of phthalate esters from the composite GOx/MIL-101/Fe_3O_4-SiO_2 alginate fiber.

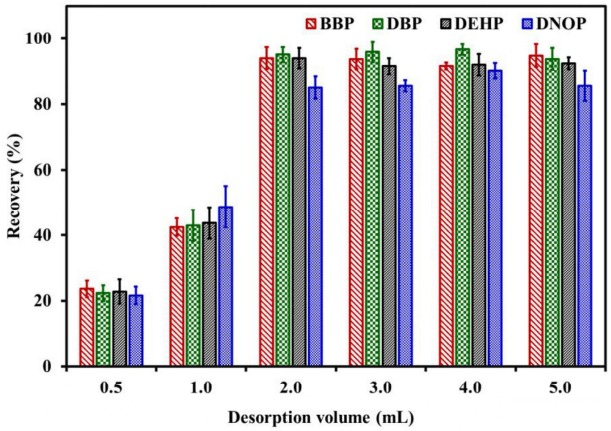

Fig. S8 The desorption volume of acetonitrile was varied to determine the effect on the elution of phthalate esters from the composite GOx/MIL-101/Fe_3O_4-SiO_2 alginate fiber.

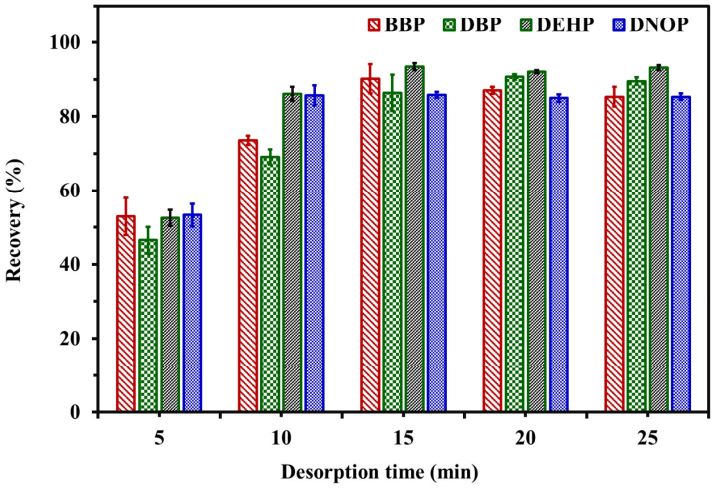

Fig. S9 Desorption time was varied to optimize the elution of phthalate esters from the composite GOx/MIL-101/Fe_3O_4-SiO_2 alginate fiber using 2.0 mL of acetonitrile.

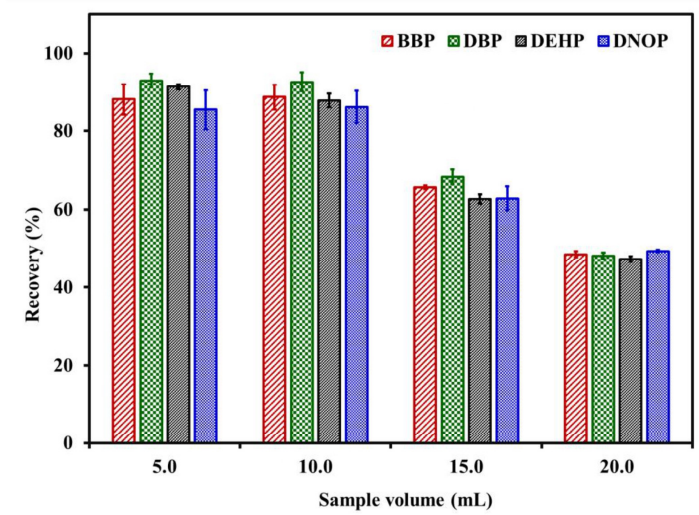

Fig. S10 The chart shows the effect of sample volume on the recovery of phthalate esters extracted using the composite GOx/MIL-101/Fe_3O_4-SiO_2 alginate fiber.

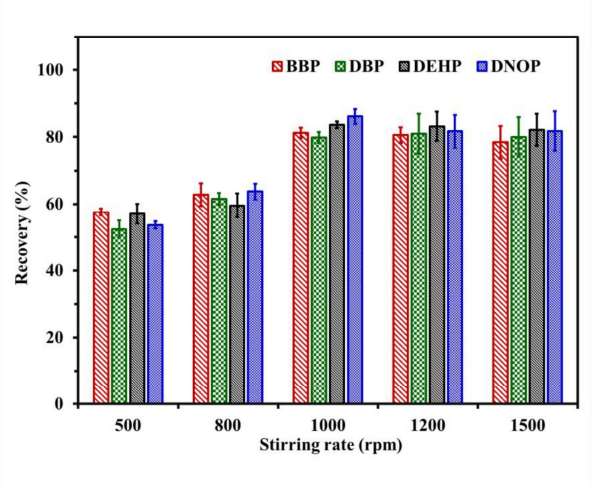

Fig. S11 The effect of stirring rate on the extraction of phthalate esters was investigated for 20 min using 0.30 g of the composite GOx/MIL-101/Fe_3O_4-SiO_2 alginate fiber in a sample volume of 10.0 mL.

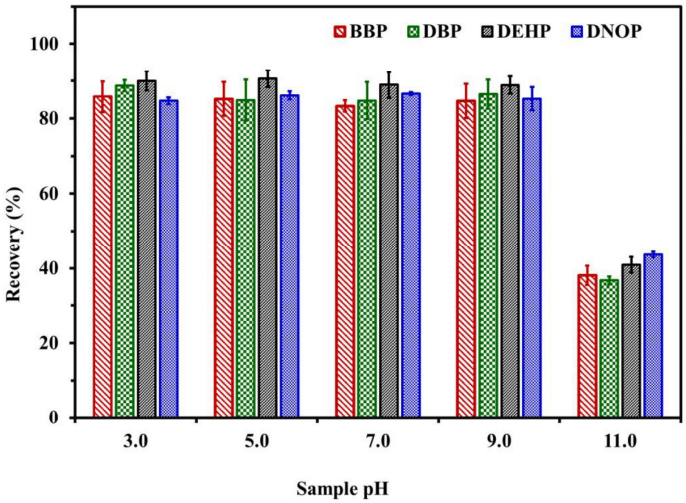

Fig. S12 The chart shows the effect of sample pH on the extraction of phthalate esters using the composite GOx/MIL-101/Fe_3O_4-SiO_2 alginate fiber.

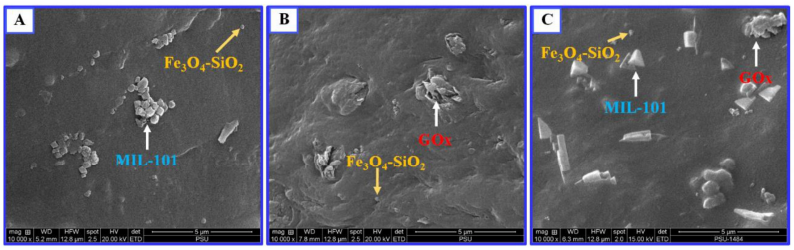

Fig. S13 SEM images of composite MIL-101/Fe_3O_4-SiO_2 (A), GOx/Fe_3O_4-SiO_2 (B) and GOx/MIL-101/Fe_3O_4-SiO_2 hydrogel fiber adsorbents (C)

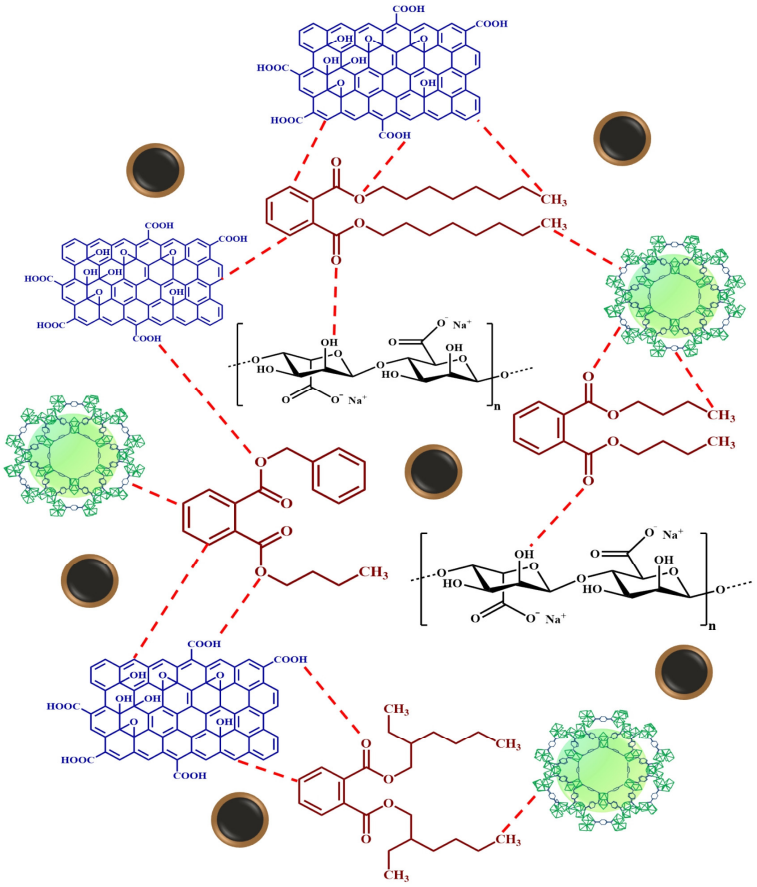

Fig. S14 The illustration shows the possible interaction between PAEs and the composite GOx/MIL-101/Fe_3O_4-SiO_2 magnetic alginate hydrogel fiber.

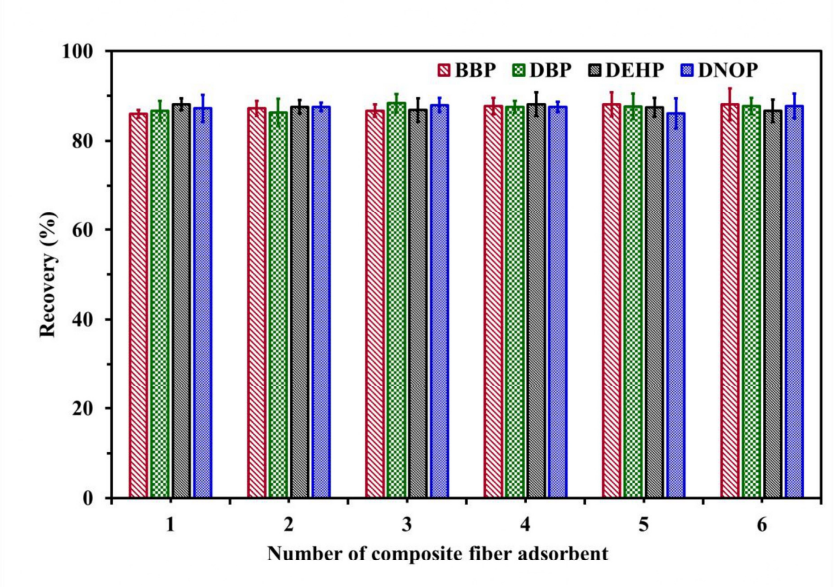

Fig. S15 The chart illustrates the reproducibility of the composite GOx/MIL-101/Fe_3O_4-SiO_2 alginate fiber for the extraction of phthalate esters. Six different batches of GOx/MIL-101/Fe_3O_4-SiO_2 alginate fiber adsorbents were fabricated at different times in the same condition and were used to extract four PAEs at 50.0 μg L^{-1}.

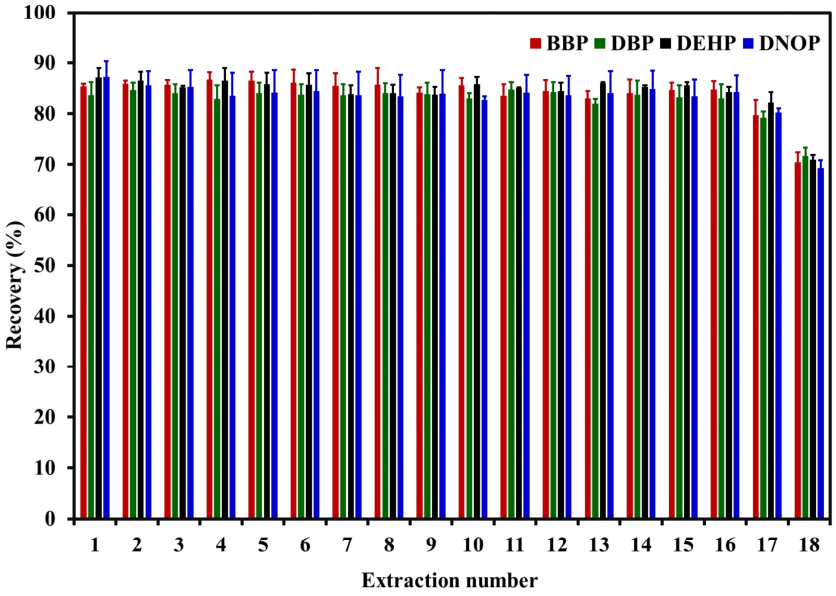

Fig. S16 The reusability of the composite GOx/MIL-101/Fe_3O_4-SiO_2 alginate fiber adsorbent for the determination of phthalate esters was demonstrated by using the same adsorbent to repeatedly extract four PAEs. After each extraction, the adsorbent was desorbed in acetonitrile and washed with DI water before being used to extract the PAEs again.

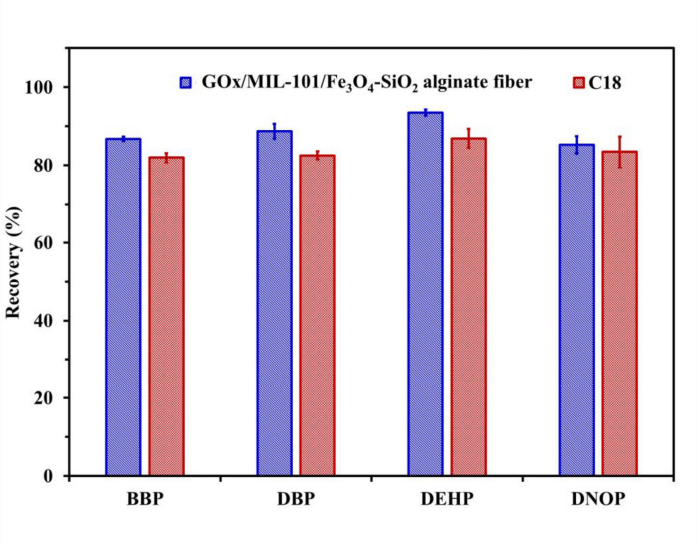

Fig. S17 Recoveries of phthalate esters with the composite GOx/MIL-101/Fe_3O_4-SiO_2 alginate fiber adsorbent were compared with recoveries achieved with a C18 SPE sorbent.

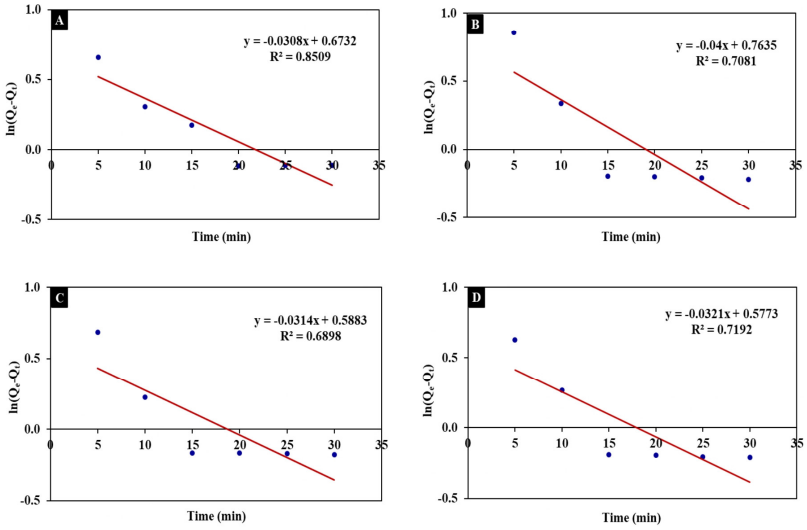

Fig. S18 The pseudo-first-order kinetics models of benzyl butyl phthalate (A), dibutyl phthalate (B), bis(2-ethylhexyl) phthalate (C) and di-n-octyl phthalate (D) adsorbed on the composite GOx/MIL-101/Fe_3O_4-SiO_2 alginate hydrogel fiber.

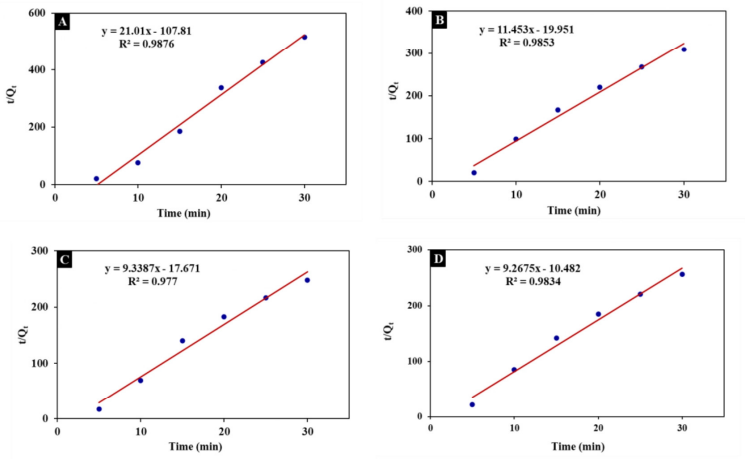

Fig. S19 The pseudo-second-order kinetics models of benzyl butyl phthalate (A), dibutyl phthalate (B), bis(2-ethylhexyl) phthalate (C) and di-n-octyl phthalate (D) adsorbed on the composite GOx/MIL-101/Fe_3O_4-SiO_2 alginate hydrogel fibers.

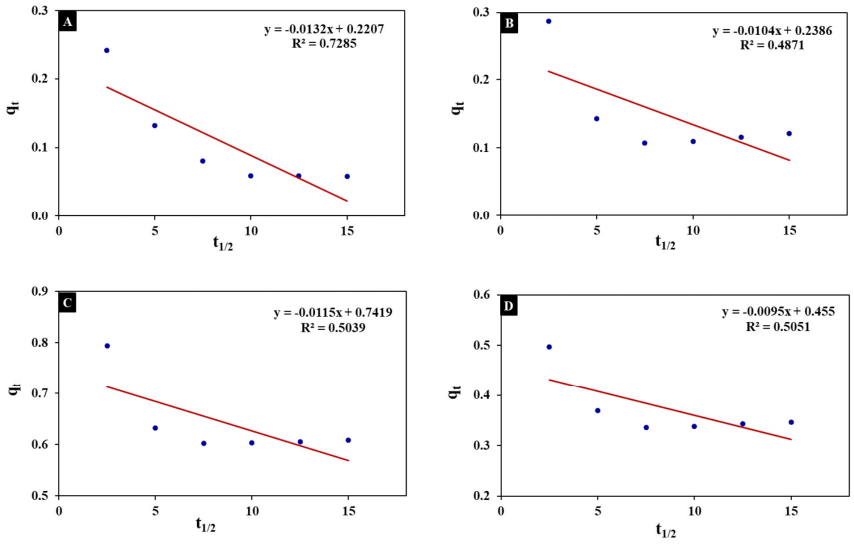

Fig. S20 The intraparticle diffusion models of benzyl butyl phthalate (A), dibutyl phthalate (B), bis(2-ethylhexyl) phthalate (C) and di-n-octyl phthalate (D) adsorbed on the composite GOx/MIL-101/Fe_3O_4-SiO_2 alginate hydrogel fibers.

Table S1 Analytical performances of the developed method.

Compounds	Linear range (μg L^{-1})	Regression linear equation	R^2	LOD (μg L^{-1})	LOQ (μg L^{-1})	Enrichment factor	Repeatability (%RSD)	
							Intra-day (n=6)	Inter-day (n=6)
Benzyl butyl phthalate	3.0-250.0	y = (0.1481±0.0030)x + (0.46±0.33)	0.9984	3.0	10.0	8.4	2.5	3.5
Dibutyl phthalate	3.0-250.0	y = (0.1275±0.0026)x + (0.48±0.29)	0.9984	3.0	10.0	8.3	2.0	4.6
Bis(2-ethylhexyl) phthalate	5.0-250.0	y − (0.0844±0.0022)x + (0.57±0.27)	0.9980	5.0	15.0	8.8	2.4	4.8
Di-n-octyl phthalate	5.0-250.0	y = (0.0776±0.0014)x + (0.29±0.18)	0.9990	5.0	15.0	8.6	3.1	4.2

Table S2 Concentration of phthalate esters in real samples.

Samples	Concentration (μg L^{-1})			
	BBP	DBP	DEHP	DNOP
Mineral water	ND	19.24±4.89	<LOQ	ND
Vitamin water	ND	16.27±7.95	<LOQ	ND
Juice	ND	10.67±5.66	<LOQ	ND
Tea	ND	<LOQ	<LOQ	ND

ND = Not detectable

Table S3 The kinetics equations and linear plots of the three different kinetics models considered.

Kinetics model	Equation	Linear plot
Pseudo-first-order	$\ln(Q_e - Q_t) = \ln Q_e - K_1 t$	$\ln(Q_e - Q_t)$ Vs. t
Pseudo-second-order	$\frac{t}{Q_t} = \frac{1}{K_2 Q^2_e} + \frac{t}{Q_e}$	$\frac{t}{Q_t}$ Vs. t
Intraparticle diffusion	$Q_t = K_3 t^{1/2} + c$	Q_t Vs. $t_{1/2}$

Q_t (μg g^{-1}) = the adsorption capacity at time t; K_1, K_2 and K_3 (min^{-1}) are the rate constants of the pseudo-first-order, pseudo-second-order and intraparticle diffusion models, respectively; c is the intercept.

Paper IV

Orachorn, N., Bunkoed, O., A composite adsorbent of graphene quantum dots, mesoporous carbon, and molecularly imprinted polymer to extract nonsteroidal anti-inflammatory drugs in milk. ***Microchimica Acta*** 189(12) (2022), 446.

Microchimica Acta (2022) 189:446
https://doi.org/10.1007/s00604-022-05550-9

ORIGINAL PAPER

A composite adsorbent of graphene quantum dots, mesoporous carbon, and molecularly imprinted polymer to extract nonsteroidal anti-inflammatory drugs in milk

Naphatsakorn Orachorn[1] · Opas Bunkoed[1]

Received: 13 July 2022 / Accepted: 25 October 2022

Abstract
A composite magnetic adsorbent was developed by embedding graphene quantum dots (GQDs), silica-modified magnetite (Fe_3O_4-SiO_2), and mesoporous carbon (MPC) into a molecularly imprinted polymer (GQDs/Fe_3O_4-SiO_2/MPC/MIP). The adsorbent was applied to extract nonsteroidal anti-inflammatory drugs (NSAIDs) in milk. The MIP was formed via a sol–gel copolymerization using flurbiprofen, diflunisal, and mefenamic acid as template molecules, 3-aminopropyltriethoxysilane as a monomer, and tetraethyl orthosilicate as a cross-linker. GQDs and MPC enhanced affinity binding between NSAIDs and the adsorbent through π-π stacking, hydrogen bonding, and hydrophobic interaction. The Fe_3O_4-SiO_2 nanoparticles embedded in the composite adsorbent enabled its rapid isolation from the sample solution. The extracted NSAIDs were quantified by high-performance liquid chromatography and exhibited good linearity from 1.0 to 100.0 μg L^{-1} for flurbiprofen and 0.5 to 100.0 μg L^{-1} for diflunisal and mefenamic acid, respectively. The limits of detection ranged from 0.5 to 1.0 μg L^{-1}. Recoveries of NSAIDs from spiked milk samples ranged from 81.4 to 93.7%, with RSDs below 7%. The reproducibility of the fabricated adsorbent was good and in the optimal conditions, the developed adsorbent could be used for up to six extraction-desorption cycles.

Keywords Flurbiprofen · Diflunisal · Mefenamic acid · Carbon-based nanomaterials · Graphene quantum dots · Mesoporous carbon · Sorbent extraction

Introduction

Nonsteroidal anti-inflammatory drugs (NSAIDs) possess broad-spectrum properties that reduce chronic pain and suppress inflammation and fever [1]. They are used in both human and veterinary medicine but high-dose or long-term use can lead to potential health hazards caused by the poor water solubility and slow degradation of NSAIDs [2]. These two properties promote the accumulation of NSAIDs in muscle tissue and can potentially cause kidney damage, cardiovascular problems, and gastrointestinal bleeding [3]. The European Union has established the limits of residual NSAIDs at 0.10 μg kg^{-1} in milk. Therefore, an effective method of determining NSAIDs would be a useful development.

NSAIDs are frequently separated and detected by high-performance liquid chromatography coupled with diode array detection (HPLC–DAD), which is a highly sensitive and reliable technique that has the useful ability to separate multiple target compounds at the same time [4, 5]. However, real samples normally present a variety of complex matrix components and NSAIDs at trace levels. Therefore, before chromatographic analysis, samples are normally treated with preparation procedures that reduce matrix interferences and pre-concentrate the target NSAIDs [6]. Sample preparation techniques that have been used to enrich NSAIDs include liquid–liquid microextraction (LLME) [7], stir bar sorptive extraction (SBSE) [2], micro solid-phase extraction (μ-SPE) [8, 9], and dispersive magnetic solid-phase extraction (D-MSPE) [1, 10]. D-MSPE attracts great interest. It is simple to operate, the adsorbent can be quickly isolated from the sample solution.

Composite D-MSPE adsorbents frequently make use of the magnetic properties of ferrous oxide nanoparticles

✉ Opas Bunkoed
opas.b@psu.ac.th

[1] Center of Excellence for Innovation in Chemistry, Division of Physical Science, Faculty of Science, Prince of Songkla University, Hat Yai, Songkhla 90110, Thailand

Published online: 12 November 2022

(Fe_3O_4) because they enable the rapid separation from the complex solution using a magnet [11, 12]. The surface of Fe_3O_4 nanoparticles is normally decorated or coated with a supporting material such as silica (SiO_2) [13], dextran [14], polydopamine [15], or polyethylene glycol [16]. The selectivity of D-MSPE adsorbents can also be improved with molecularly imprinted polymer (MIP), which present specific cavities for target analytes [17–20]. Fe_3O_4 has been utilized as a core in an MIP layer to produce a magnetic molecularly imprinted polymer (MMIP) [21]. An MMIP can be further improved by incorporating affinity materials to enhance affinity binding between the MMIP-based adsorbent and NSAIDs. NSAIDs can be adsorbed by graphene quantum dots (GQDs), which are a carbon-based nanomaterial with a large surface area [22]. The chemical structure of GQDs comprises a π-conjugated ring and plenty of carboxyl and hydroxyl functional groups that can adsorb NSAIDs through π-π stacking and hydrogen bonding [23]. Moreover, GQDs have other advantages such as low environmental toxicity, good durability, simple synthesis [24], and good dispersibility in aqueous samples [25]. In addition, GQDs with modifiable structures and tunable properties can be prepared in large scale [26]. Mesoporous carbon (MPC) is another affinity material with has some extensive advantages such as high surface areas [27], hierarchical pore structure, and abundant natural sources [28]. MPC has a hydrophobic property that favors the adsorption of target analytes via hydrophobic interaction [29]. It is also chemically stable [30], rigid, and inexpensive [31].

We fabricated a hybrid composite magnetic adsorbent of graphene quantum dots, silica-modified magnetite, and mesoporous carbon incorporated into an MIP (GQDs/Fe_3O_4-SiO_2/MPC/MIP). The adsorbent was used to extract three NSAIDs, diflunisal, flurbiprofen, and mefenamic acid, in a D-MSPE procedure. The composite MMIP adsorbent adsorbed the target NSAIDs through π-π stacking, hydrophobic interaction, and hydrogen bonding. The extracted NSAIDs were determined by HPLC–DAD. The developed adsorbent was successfully applied to extract trace levels of the NSAIDs in milk samples.

Experimental

Chemical and reagents

Flurbiprofen, diflunisal, mefenamic acid, tetraethyl orthosilicate (TEOS), formic acid, citric acid, and 3-aminopropyltriethoxysilane (APTES) were purchased from Tokyo Chemical Industry Co. Ltd. (Tokyo, Japan, https://www.tcichemicals.com). Mesoporous carbon (MPC) was from XFNANO (Jiangsu, China, https://en.xfnano.com). Iron (III) chloride hexahydrate and iron (II) chloride tetrahydrate were obtained from Sigma-Aldrich (Steinheim, Germany, https://www.sigmaaldrich.com). Sodium hydroxide was from Loba Chemie Pvt. Ltd. (Mumbai, India, https://www.lobachemie.com). Dialysis membrane (12–14 kDa MWCO) was from Spectrum Laboratories, Inc. (CA, USA, http://www.spectrumlaboratoriesinc.com). Methanol, ammonia solution, and ethanol were from RCI Labscan (Bangkok, Thailand, https://www.rcilabscan.com).

Instrumental

HPLC was carried out using the Hewlett-Packard 1100 apparatus coupled with a diode array detector (Agilent Technologies Inc., USA, https://www.agilent.com). NSAIDs were separated by isocratic elution in a C18 analytical column (150 mm × 4.6 mm I.D., 5.0 µm particle size, Fortis Technologies Ltd., UK, https://fortis-technologies.com) using a mobile phase of 0.10% v/v formic acid (line A) and methanol (line B) (20%A: 80%B) at a flow rate of 0.90 mL min^{-1}. The detection wavelength for the quantitative analysis of the target NSAIDs was set at 230 nm. The functional groups of the GQDs/Fe_3O_4-SiO_2/MPC/MIP adsorbent and its component materials were examined by Fourier transform infrared spectroscopy (FTIR) (PerkinElmer, USA, https://www.perkinelmer.com). The stability of the adsorbent was investigated by thermogravimetric analysis (TGA) (TGA8000, PerkinElmer, USA, https://www.perkinelmer.com). The surface area of the adsorbent was calculated with a surface area and porosity analyzer (ASAP2460, Micromeritics, USA, https://www.micromeritics.com). Carbon, hydrogen, nitrogen, and oxygen contents in the adsorbent were determined by CHNS/O analyzer (Flash 2000, ThermoScientific, Italy, https://www.thermofisher.com). The magnetic property of the adsorbent was determined with a lab-built vibrating sample magnetometer (VSM). The morphology observation of the related materials was performed by field emission scanning electron microscopy (FESEM) (Apreo, FEI, the Netherlands,https://www.fei.com) and transmission electron microscope (TEM) (JEM 2010, JEOL, Japan, https://www.jeol.co.jp).

Synthesis of silica-modified magnetite nanoparticles(Fe_3O_4-SiO_2)

Magnetite nanoparticles (Fe_3O_4) were prepared in a co-precipitation synthesis [11] and the detail is provided in the electronic supporting material (ESM).

Synthesis of graphene quantum dots (GQDs)

The synthesis of GQDs was performed through the pyrolysis of citric acid [19]. Citric acid (2.0 g) was melted at 200 °C using a heating mantle until light-yellow liquid citric acid

was formed. The liquid citric acid was added dropwise into 100 mL of 0.25 M NaOH and continuously shaken for 30 min. The acquired solution was purified using dialysis bags (12 kDa cutoff) for 24 h to obtain GQDs.

Synthesis of the GQDs/Fe_3O_4-SiO_2/MPC/MIPadsorbent

The GQDs/Fe_3O_4-SiO_2/MPC/MIP adsorbent was prepared via a sol–gel copolymerization technique. Firstly, 100 mL of the synthesized GQDs was mixed with 7.50 mL of 3-aminopropyltriethoxysilane (APTES) under stirring at 40 °C for 30 min to obtain APTES-embedded GQDs. For the fabrication of the MIP, a solution containing the three templates was prepared by dissolving 4.9 mg of flurbiprofen, 5.0 mg of diflunisal, and 4.8 mg of mefenamic acid in 30 mL of ethanol. The solution was mixed under stirring at 400 rpm for 1 h with 358.0 µL of APTES, the functional monomer. Then, 10.0 mg of MPC, 3.0 g of Fe_3O_4-SiO_2, and 25.0 mL of APTES-embedded GQDs were added to the mixture solution. After stirring for 1 h, 1.50 mL of tetraethyl orthosilicate (cross-linker) and 1.0 mL of ammonia solution (25% w/v) were added, and the whole solution was stirred overnight to form the imprinted polymer. The next day, the three templates were removed from the polymer by washing three times with 10 mL of methanol. The GQDs/Fe_3O_4-SiO_2/MPC/MIP adsorbent was collected by centrifugation at 5000 rpm. A magnetic GQDs/Fe_3O_4-SiO_2/MPC/NIP adsorbent was also prepared using the identical procedure without the addition of the template. The synthesis procedure of the GQDs/Fe_3O_4-SiO_2/MPC/MIP magnetic adsorbent is shown in Fig. 1A.

Dispersive magnetic solid-phase extraction (D-MSPE)

The D-MSPE procedure is demonstrated in Fig. 1B. Initially, 0.10 g of the GQDs/Fe_3O_4-SiO_2/MPC/MIP adsorbent was dispersed in 10.0 mL of a spiked standard NSAIDs or a sample solution and magnetically stirred at 1000 rpm for 30 min to induce the mass transfer of target NSAIDs from the sample to the adsorbent. After extraction, the magnetic composite adsorbent was isolated from the sample with an external magnet. The adsorbed NSAIDs were then desorbed from the specific recognition cavities of the recovered adsorbent using 4.0 mL of methanol under sonication for 20 min. After complete desorption, a magnet was used to isolate the adsorbent from the desorption solution, which was then evaporated at 50 °C using a rotary evaporator. The residue was reconstituted with 1.0 mL of the mobile phase used for HPLC analysis and filtered through nylon syringe (0.22 µm of pore size) before analysis by HPLC–DAD. The used adsorbent was thoroughly washed with 2.0 mL of methanol and 5.0 mL of deionized (DI) water before being used for the next extraction. The extraction was performed at room temperature (28 ± 2 °C). Carry over was investigated to ensure that there were no residual target analytes on the washed used adsorbent.

Pretreatment of milk samples

Fat was removed from 10 mL of milk samples by centrifugation at 5000 rpm. After 10 min, the phase of de-fatted milk was separated, and 10 mL of acetonitrile was added to precipitate protein. The solution was then separated into two phases by centrifugation at 5000 rpm for 10 min. The supernatant was extracted by D-MSPE with the GQDs/Fe_3O_4-SiO_2/MPC/MIP adsorbent and then analyzed by HPLC–DAD.

Results and discussion

Characterization of the magnetic composite adsorbent

The functional groups of the component materials of the composite adsorbent were investigated by FTIR spectroscopy. The details are provided in the electronic supporting material ESM (Fig. S1a–i).

TEM images of MPC and GQDs/Fe_3O_4-SiO_2/MPC/MIP are shown in Fig. 2A and B. The surface morphology of MPC and GQDs/Fe_3O_4-SiO_2/MPC/MIP was examined by FESEM. MPC displayed uniformly arranged worm-like particles (Fig. 2C and D) whereas the morphology of GQDs/Fe_3O_4-SiO_2/MPC/MIP comprised irregular shapes with rough surfaces (Fig. 2E and F).

The BET surface areas of MPC, GQDs/Fe_3O_4-SiO_2/MPC/MIP, and GQDs/Fe_3O_4-SiO_2/MPC/NIP were 714.80, 34.03, and 19.08 $m^2 g^{-1}$, respectively. The large surface area of MPC helped to improve the adsorptive property of the composite adsorbent. The GQDs/Fe_3O_4-SiO_2/MPC/MIP adsorbent had a lower surface area than MPC due to the formation of specific binding sites for target NSAIDs. However, the surface area of MPC is non-specific for NSAIDs but the surface of composite GQDs/Fe_3O_4-SiO_2/MPC/MIP adsorbent is highly selective for NSAIDs. The GQDs/Fe_3O_4-SiO_2/MPC/MIP adsorbent had a larger surface area than the non-imprinted GQDs/Fe_3O_4-SiO_2/MPC/NIP, indicating the presence of recognition sites in the composite MIP adsorbent, which promoted the adsorption of NSAIDs. The N_2 adsorption–desorption isotherms of MPC, GQDs/Fe_3O_4-SiO_2/MPC/MIP, and GQDs/Fe_3O_4-SiO_2/MPC/NIP are depicted in Fig. S2A–C.

The thermal stability of the composite GQDs/Fe_3O_4-SiO_2/MPC/MIP adsorbent was determined by TGA. The

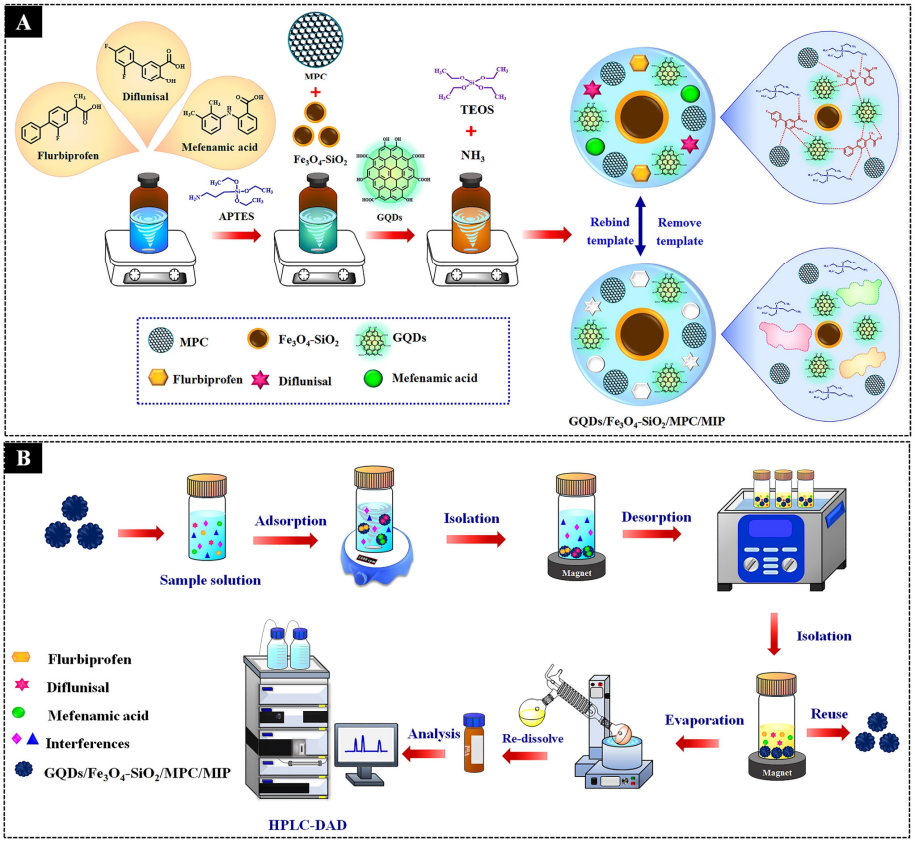

Fig. 1 The synthesis of a composite GQDs/Fe_3O_4-SiO_2/MPC/MIP adsorbent for the extraction of flurbiprofen, diflunisal, and mefenamic acid (**A**) and the dispersive magnetic solid phase extraction (D-MSPE) procedure used with the synthesized adsorbent (**B**)

TGA curve demonstrated that the weight of the adsorbent decreased above 100 °C because residual water in the adsorbent was eliminated (Fig. S2D). This result indicated that the fabricated adsorbent could be used to extract NSAIDs in the expected temperature condition (~ 30 °C) of use.

The magnetic property of the GQDs/Fe_3O_4-SiO_2/MPC/MIP adsorbent was inspected using a vibrating sample magnetometer (VSM). The VSM curve (Fig. S2E) demonstrated a maximum saturation of 8.014 emu g^{-1}, which indicated that the adsorbent could be easily isolated from the sample solution with an external magnet (Fig. S3).

A CHNS/O analyzer was used to determine carbon, hydrogen, nitrogen, and oxygen elements in the GQDs/Fe_3O_4-SiO_2/MPC/MIP adsorbent. The percentages of each element were 15.597 of C, 4.511 of H, 4.956 of N, and 11.863 of O.

Optimization of the composite adsorbent fabrication and D-MSPE conditions

The composite magnetic adsorbent was fabricated and utilized as D-MSPE for the extraction of NSAIDs. Graphene quantum dots and mesoporous carbon were incorporated

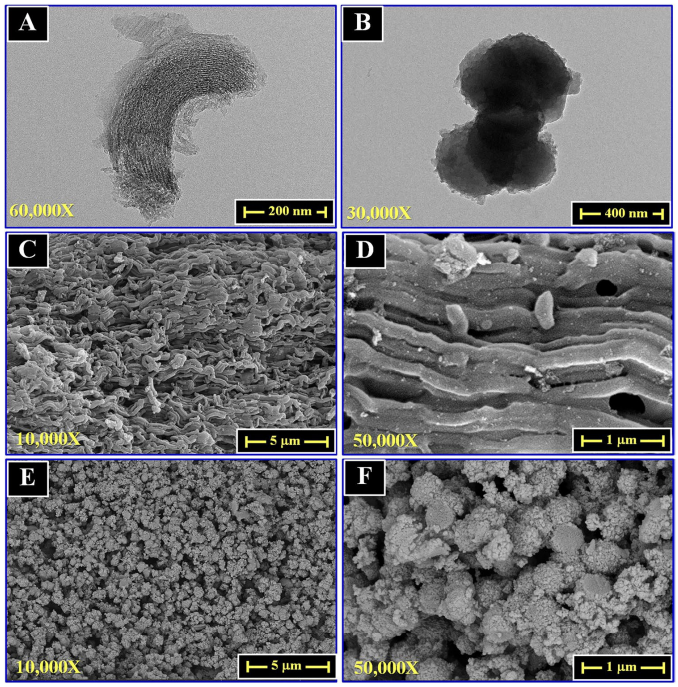

Fig. 2 TEM images are of mesoporous carbon (MPC) at 60,000 × (**A**) and GQDs/Fe_3O_4-SiO_2/MPC/MIP at 30,000 × (**B**). SEM images are of MPC at 10,000 × (**C**) and 50,000 × (**D**) and the GQDs/Fe_3O_4-SiO_2/MPC/MIP adsorbent at 10,000 × (**E**) and 50,000 × (**F**)

into molecularly imprinted polymer to improve the extraction efficiency of NSAIDs. They can enhance the extraction efficiency since they can adsorb NSAIDs via π-π interaction, hydrophobic interaction, and hydrogen bonding. MIP material can improve the selectivity of the adsorbent. While, magnetite nanoparticles incorporated in the composite adsorbent assisted a simple and rapid extraction procedure.

To obtain the highest extraction efficiency with a low solvent consumption and a short analysis time, the experimental conditions were optimized. These parameters were amount of adsorbent, amount of MPC, extraction time, desorption condition, sample stirring rate, sample volume, sample pH, and ionic strength. Respective results can be found in the electronic supporting material (Table S1). The following parameters were to give the best results: amount of adsorbent: 0.10 g (Fig. S4), amount of MPC: 10.0 mg (Fig. S5), extraction time: 30 min (Fig. S6), desorption condition: 4.0 mL of methanol for 20 min (Fig. S7, S8, and S9), sample stirring rate: 1000 rpm (Fig. S10), sample volume: 10.0 mL (Fig. S11), sample pH: 5–9 (Fig. S12), and ionic strength: 0.0% w/v (Fig. S13).

The optimal condition was considered to be the condition that achieved the best extraction recovery. Extraction recoveries were reported as means ± SD from three replicates ($n = 3$) and calculated from the equation

$$\text{Extraction recovery } (\%) = \left(C_f V_f / C_i V_i\right) \times 100$$

where C_f is the final NSAIDs concentration in the reconstituted solution (µg L^{-1}), C_i is the initial NSAIDs concentration spiked in water (µg L^{-1}), and V_f and V_i are the volume of the reconstituted solution and sample (mL), respectively. NSAIDs were spiked in at a concentration of 50.0 µg L^{-1}.

Extraction efficiency of different composite adsorbents

Four different fabricated adsorbents were evaluated for their capability to extract the target NSAIDs (Fig. 3). Adsorbents were fabricated with and without MPC and with imprinted and non-imprinted polymers. The adsorbents were therefore a GQDs/Fe_3O_4-SiO_2/NIP, GQDs/Fe_3O_4-SiO_2/MPC/NIP, a GQDs/Fe_3O_4-SiO_2/MIP, and a GQDs/Fe_3O_4-SiO_2/MPC/MIP. Since the MIP contains a

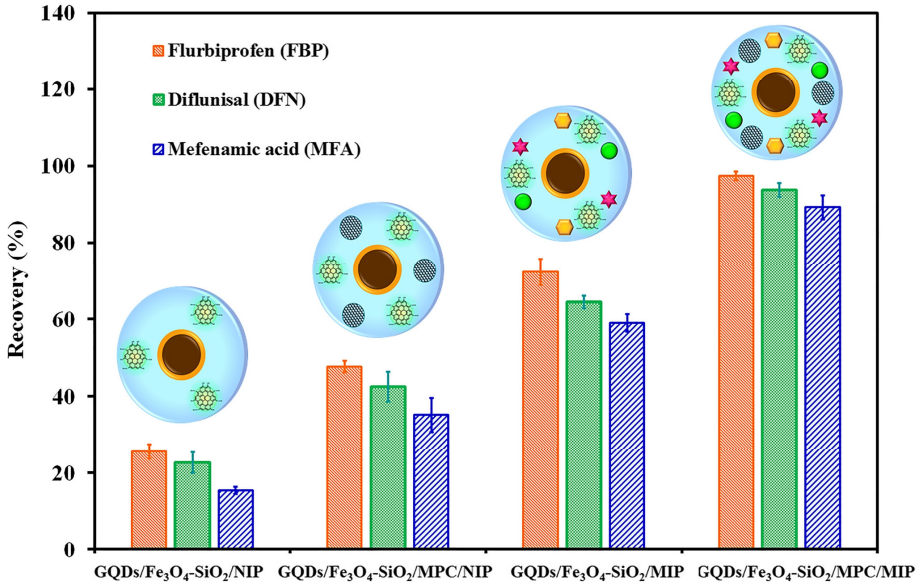

Fig. 3 The chart compares the recoveries of three nonsteroidal anti-inflammatory drugs extracted from aqueous solution by D-MSPE with different composite adsorbents ($n = 3$). Extraction condition: amount of adsorbent, 0.10 g; extraction time, 30 min; desorption condition, 4.0 mL of methanol for 20 min; sample stirring rate, 1000 rpm; sample volume, 10.0 mL

large number of imprinted recognition cavities for target NSAIDs, affinity and selectivity were better, and the extraction recoveries of both MIP adsorbents were higher than those of both NIP adsorbents. The GQDs/Fe_3O_4-SiO_2/NIP and GQDs/Fe_3O_4-SiO_2/MPC/NIP adsorbents could only adsorb the target molecules through hydrogen bonding and π-π stacking, so their extraction recoveries were lower. The extraction efficiency of the GQDs/Fe_3O_4-SiO_2/MPC/MIP adsorbent was better than that of the GQDs/Fe_3O_4-SiO_2/MIP. Thus, the composite GQDs/Fe_3O_4-SiO_2/MPC/MIP adsorbent was the most effective adsorbent for the extraction of the target NSAIDs.

Analytical performances

The performance of D-MSPE with the GQDs/Fe_3O_4-SiO_2/MPC/MIP adsorbent was investigated as demonstrated in Table 1. The three target NSAIDs were extracted from aqueous solution by D-MSPE in the optimal condition with the developed adsorbent and determined by HPLC–DAD. The

Table 1 The analytical performance of dispersive magnetic solid-phase extraction with a composite GQDs/Fe_3O_4-SiO_2/MPC/MIP adsorbent was evaluated from the determination by HPLC–DAD of three extracted nonsteroidal anti-inflammatory drugs (NSAID)

Target NSAID	Linear range (μg L^{-1})	Regression linear equation	R^2	LOD (μg L^{-1})	EF	Repeatability (%RSD)	
						Inter-day ($n = 6$)	Intra-day ($n = 6$)
Flurbiprofen	1.0–100.0	$y = (0.3247 \pm 0.0070)x + (0.23 \pm 0.32)$	0.9981	1.0	8.6	4.0	2.5
Diflunisal	0.5–100.0	$y = (0.3814 \pm 0.0036)x + (0.44 \pm 0.15)$	0.9996	0.5	8.9	4.6	2.9
Mefenamic acid	0.5–100.0	$y = (0.3974 \pm 0.0093)x + (0.62 \pm 0.39)$	0.9973	0.5	8.4	3.7	2.4

linearity of the developed method was evaluated by extracting various concentrations of the three target NSAIDs. The linear ranges were 1.0 to 100.0 μg L^{-1} for flurbiprofen and 0.5 to 100.0 μg L^{-1} for diflunisal and mefenamic acid with the coefficients of determination (R^2) were better than 0.997. The linear regression equations were calculated by Microsoft Excel software. The LODs based on S/N ≥ 3 were 1.0 μg L^{-1} for flurbiprofen, and 0.5 μg L^{-1} for diflunisal and mefenamic acid. These results implied that the developed strategy for the extraction of trace NSAIDs for determination by HPLC–DAD could be effectively applied. The enrichment factor (EF) was calculated from the equation $EF = C_f/C_i$, where C_f is the extracted NSAIDs calculated from calibration curves (μg L^{-1}), and C_i is the initial NSAID concentration in the sample (μg L^{-1}). The EF was evaluated using 10.0 mL of aqueous solution spiked with the three NSAIDs at 25.0 μg L^{-1}. EFs ranged from 8.4 to 8.9. The inter-day and intra-day precisions were used to evaluate the repeatability of the developed approach. The relative standard deviations (RSDs) were in the range of 3.7 to 4.6 for inter-day and 2.4 to 2.9 for intra-day precision.

Reproducibility and reusability

To evaluate the reproducibility of the fabrication procedure, six different batches of the GQDs/Fe_3O_4-SiO_2/MPC/MIP adsorbent were prepared in the same condition. The RSDs were lower than 5.0% (Fig. S14). The result confirmed the reproducibility of the preparation of the adsorbent.

The reusability of the adsorbent was investigated by repeated D-MSPE of the target NSAIDs. The used adsorbent was washed with 2.0 mL of methanol and 5.0 mL of DI water between each adsorption–desorption cycle. The developed adsorbent provided extraction recoveries better than 80% for up to 6 cycles (Fig. S15). The slightly lower recoveries after the sixth extraction cycle were perhaps due to damage caused to the specific imprinted cavities during the adsorption, desorption, and washing steps. The GQDs/Fe_3O_4-SiO_2/MPC/MIP adsorbent could be effectively used up to 6 times.

Adsorption kinetics

The mechanism of adsorption of the target NSAIDs on the GQDs/Fe_3O_4-SiO_2/MPC/MIP adsorbent was determined by fitting adsorption kinetics models to experimental data. The intraparticle diffusion and pseudo-first-order and pseudo-second-order models were applied, and the R^2 closest to unity was considered to indicate the most suitable model (Table S2). The R^2 value of the linear plot of the pseudo-second-order model was closest to 1 (Fig. S16, S17, and S18). This result indicated that the main adsorption process between the adsorbent and the three analytes was the chemical adsorption. The adsorption capacity of the adsorbent toward the target NSAIDs was estimated according to the equation

$$Qe = \frac{(C_0 - C_e)V}{m}$$

where Q_e is the adsorption capacity at equilibrium (μg g^{-1}), m is the mass of adsorbent (g), V is the sample volume (L), C_0 is the initial concentration of NSAIDs in a spiked solution (μg L^{-1}), and C_e is the equilibrium concentration of NSAIDs (μg L^{-1}).

Comparison with a commercial sorbent and other works

The extraction efficiency of the developed GQDs/Fe_3O_4-SiO_2/MPC/MIP adsorbent was compared with a C18 SPE sorbent. The results showed that both sorbents achieved recoveries over 80% (Fig. S19), but the proposed method can be performed without the need for an SPE manifold system. The recoveries of the three NSAIDs were also slightly better with the proposed adsorbent than with the commercial C18 sorbent.

The performances of D-MSPE with the proposed adsorbent were compared with those of previously published methods for the determination of NSAIDs (Table S3). The LOD, recovery, and RSD of the proposed adsorbent are either better than or comparable to those of other methods, and the developed adsorbent is superior in terms of selectivity toward the analytes, which can be an advantage when dealing with complex samples. In addition, the developed composite adsorbent can be reused up to six extraction-desorption cycles. Although the developed method has many advantages but the enrichment factor of this method is lower than some other works due to developed method used low sample volume, however, this volume is enough for the determination of NSAIDs in real sample.

Real sample analysis

The GQDs/Fe_3O_4-SiO_2/MPC/MIP adsorbent was utilized to extract the three NSAIDs from four bovine milk samples for determination by HPLC–DAD. Flurbiprofen was found in all four samples at concentrations that ranged from 5.5 to 12.6 μg L^{-1} (Table 2). The milk samples were then spiked with standard NSAIDs at 10.0, 25.0, and 50.0 μg L^{-1} to evaluate the accuracy of the developed strategy. Relative recoveries of the three NSAIDs ranged from 81.4 to 93.7% with RSDs below 7% (Table 2). HPLC chromatograms show detected compounds in a milk sample, and compounds extracted with the GQDs/Fe_3O_4-SiO_2/MPC/MIP adsorbent from a spiked milk sample, and a standard NSAIDs solution

Table 2 Analytical results from the determination by HPLC–DAD of NSAIDs recovered from four milk samples using D-MSPE with the developed GQDs/Fe_3O_4-SiO_2/MPC/MIP adsorbent ($n = 3$)

Sample	Added ($\mu g\ L^{-1}$)	FBP			DFN			MFA		
		Found ($\mu g\ L^{-1}$)	Recovery (%)	RSD (%)	Found ($\mu g\ L^{-1}$)	Recovery (%)	RSD (%)	Found ($\mu g\ L^{-1}$)	Recovery (%)	RSD (%)
Milk I	0.0	5.5	-	-	ND	-	-	ND	-	-
	10.0	13.9	83.3	2.9	8.9	89.1	5.7	9.2	92.0	4.2
	25.0	25.9	81.6	1.3	22.0	88.0	3.5	21.8	87.3	5.1
	50.0	48.2	85.4	1.4	46.6	93.2	2.0	42.8	85.6	1.3
Milk II	0.0	7.4	-	-	ND	-	-	ND	-	-
	10.0	15.7	83.2	1.6	8.9	88.6	3.5	8.2	82.2	2.1
	25.0	27.9	82.3	2.5	22.7	90.6	2.0	20.7	82.7	0.5
	50.0	50.7	86.7	1.3	46.9	93.7	2.9	45.0	90.1	2.7
Milk III	0.0	12.6	-	-	ND	-	-	ND	-	-
	10.0	21.1	84.8	4.3	8.8	87.9	5.1	8.1	81.4	1.9
	25.0	34.9	89.2	4.0	21.9	87.6	2.1	21.1	84.3	2.3
	50.0	56.1	86.9	4.2	44.1	88.2	3.5	40.8	81.6	2.9
Milk IV	0.0	11.6	-	-	ND	-	-	ND	-	-
	10.0	20.1	85.0	3.9	8.8	88.0	6.4	8.2	81.7	2.0
	25.0	34.0	89.6	2.7	22.3	89.3	5.6	20.6	82.6	1.3
	50.0	54.2	85.2	2.8	44.5	89.1	5.2	42.2	84.3	2.7

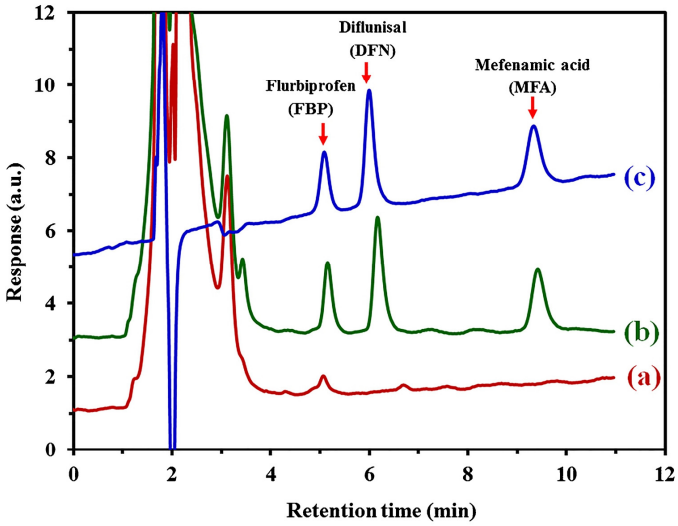

Fig. 4 The chromatograms were produced by a bovine milk sample (**a**), a spiked bovine milk sample (**b**) and a standard solution of three nonsteroidal anti-inflammatory drugs at 0.50 mg L^{-1} (**c**). Extraction condition: 0.10 mg of GQDs/Fe_3O_4-SiO_2/MPC/MIP adsorbent; extraction time, 30 min; desorption condition, 4.0 mL of methanol for 20 min; sample stirring rate, 1000 rpm; sample volume, 10.0 mL

at 0.50 mg L^{-1} (Fig. 4). The peaks of NSAIDs were clearly distinguished from peaks of interfering compounds. This result indicated that the GQDs/Fe_3O_4-SiO_2/MPC/MIP adsorbent is an effective and selective adsorbent for the extraction of NSAIDs in real sample. The accuracy of the developed adsorbent indicated that it can be effectively applied to determine NSAIDs in bovine milk.

Conclusion

A magnetic composite of GQDs/Fe_3O_4-SiO_2/MPC/MIP adsorbent was successfully fabricated using graphene quantum dots, silica-modified magnetite, and mesoporous carbon incorporated into molecularly imprinted polymer. The developed adsorbent was utilized for the D-MSPE of NSAIDs in milk samples. The developed adsorbent demonstrated a highly specific affinity toward flurbiprofen, diflunisal, and mefenamic acid. The integration of graphene quantum dots and mesoporous carbon with a MMIP increased the adsorption efficiency of the target molecules via strong π-π stacking, hydrophobic interaction, and hydrogen bonding. The fabricated composite adsorbent has good reproducibility and stability. The developed method can be adapted for the extraction and determination of NSAIDs in a variety of matrix samples.

Supplementary Information The online version contains supplementary material available at https://doi.org/10.1007/s00604-022-05550-9.

Acknowledgements The authors thank Mr. Thomas Duncan Coyne for English proofreading.

Funding This work was financially supported by the Prince of Songkla University (Grant No. SCI6502007S-0) and The Center of Excellence for Innovation in Chemistry (PERCH-CIC), Ministry of Higher Education, Science, Research and Innovation. Naphatsakorn Orachorn was supported by the Science Achievement Scholarship of Thailand (SAST).

The authors declare no competing interests.

References

1. Baile P, Vidal L, Canals A (2019) A modified zeolite/iron oxide composite as a sorbent for magnetic dispersive solid-phase extraction for the preconcentration of nonsteroidal anti-inflammatory drugs in water and urine samples. J Chromatogr A 1603:33–43. https://doi.org/10.1016/j.chroma.2019.06.039
2. Tanwar S, Di Carro M, Magi E (2015) Innovative sampling and extraction methods for the determination of nonsteroidal anti-inflammatory drugs in water. J Pharm Biomed Anal 106:100–106. https://doi.org/10.1016/j.jpba.2014.10.027
3. Golzari Aqda T, Behkami S, Bagheri H (2018) Porous eco-friendly fibers for on-line micro solid-phase extraction of non-steroidal anti-inflammatory drugs from urine and plasma samples. J Chromatogr A 1574:18–26. https://doi.org/10.1016/j.chroma.2018.08.055
4. Hassan M, Alshana U (2019) Switchable-hydrophilicity solvent liquid-liquid microextraction of non-steroidal anti-inflammatory drugs from biological fluids prior to HPLC-DAD determination. J Pharm Biomed Anal 174:509–517. https://doi.org/10.1016/j.jpba.2019.06.023
5. Medina GS, Acquaviva A, Reta M (2020) Development of monolithic sorbent cartridges (m-SPE) for the extraction of

non-steroidal anti-inflammatory drugs from surface waters and their determination by HPLC. Microchem J 159:105447. https://doi.org/10.1016/j.microc.2020.105447

6. Liang S, Jian N, Cao J, Zhang H, Li J, Xu Q, Wang C (2020) Rapid, simple and green solid phase extraction based on polyaniline nanofibers-mat for detecting non-steroidal anti-inflammatory drug residues in animal-origin food. Food Chem 328:127097. https://doi.org/10.1016/j.foodchem.2020.127097
7. Barfi B, Asghari A, Rajabi M, GoochaniMoghadam A, Mirkhani N, Ahmadi F (2015) Comparison of ultrasound-enhanced air-assisted liquid-liquid microextraction and low-density solvent-based dispersive liquid-liquid microextraction methods for determination of nonsteroidal anti-inflammatory drugs in human urine samples. J Pharm Biomed Anal 111:297–305. https://doi.org/10.1016/j.jpba.2015.03.034
8. Zhou Y, Xu J, Lu N, Wu X, Zhang Y, Hou X (2021) Development and application of metal-organic framework@GA based on solid-phase extraction coupling with UPLC-MS/MS for the determination of five NSAIDs in water. Talanta 225:121846. https://doi.org/10.1016/j.talanta.2020.121846
9. Peña-Velasco G, Hinojosa-Reyes L, Escamilla-Coronado M, Turnes-Palomino G, Palomino-Cabello C, Guzmán-Mar JL (2020) Iron metal-organic framework supported in a polymeric membrane for solid-phase extraction of anti-inflammatory drugs. Anal Chim Acta 1136:157–167. https://doi.org/10.1016/j.aca.2020.09.049
10. Ferrone V, Carlucci M, Ettorre V, Cotellese R, Palumbo P, Fontana A, Siani G, Carlucci G (2018) Dispersive magnetic solid phase extraction exploiting magnetic graphene nanocomposite coupled with UHPLC-PDA for simultaneous determination of NSAIDs in human plasma and urine. J Pharm Biomed Anal 161:280–288. https://doi.org/10.1016/j.jpba.2018.08.005
11. Kaewsuwan W, Kanatharana P, Bunkoed O (2017) Dispersive magnetic solid phase extraction using octadecyl coated silica magnetite nanoparticles for the extraction of tetracyclines in water samples. J Anal Chem 72(9):957–965. https://doi.org/10.1134/S1061934817090143
12. Bunkoed O, Nurerk P, Wannapob R, Kanatharana P (2016) Polypyrrole-coated alginate/magnetite nanoparticles composite sorbent for the extraction of endocrine-disrupting compounds. J Sep Sci 39(18):3602–3609. https://doi.org/10.1002/jssc.201600647
13. Orachorn N, Bunkoed O (2021) Nanohybrid magnetic composite optosensing probes for the enrichment and ultra-trace detection of mafenide and sulfisoxazole. Talanta 228:122237. https://doi.org/10.1016/j.talanta.2021.122237
14. Hong RY, Feng B, Chen LL, Liu GH, Li HZ, Zheng Y, Wei DG (2008) Synthesis, characterization and MRI application of dextran-coated Fe_3O_4 magnetic nanoparticles. Biochem Eng J 42(3):290–300. https://doi.org/10.1016/j.bej.2008.07.009
15. Socas-Rodríguez B, Hernández-Borges J, Salazar P, Martín M, Rodríguez-Delgado MÁ (2015) Core-shell polydopamine magnetic nanoparticles as sorbent in micro-dispersive solid-phase extraction for the determination of estrogenic compounds in water samples prior to high-performance liquid chromatography-mass spectrometry analysis. J Chromatogr A 1397:1–10. https://doi.org/10.1016/j.chroma.2015.04.010
16. Hu F, MacRenaris KW, Waters EA, Liang T, Schultz-Sikma EA, Eckermann AL, Meade TJ (2009) Ultrasmall, water-soluble magnetite nanoparticles with high relaxivity for magnetic resonance imaging. J Phys Chem C 113(49):20855–20860. https://doi.org/10.1021/jp907216g
17. Orachorn N, Bunkoed O (2019) A nanocomposite fluorescent probe of polyaniline, graphene oxide and quantum dots incorporated into highly selective polymer for lomefloxacin detection. Talanta 203:261–268. https://doi.org/10.1016/j.talanta.2019.05.082
18. Villa CC, Sánchez LT, Valencia GA, Ahmed S, Gutiérrez TJ (2021) Molecularly imprinted polymers for food applications: a review. Trends Food Sci Technol 111:642–669. https://doi.org/10.1016/j.tifs.2021.03.003
19. Chullasat K, Kanatharana P, Bunkoed O (2019) Nanocomposite optosensor of dual quantum dot fluorescence probes for simultaneous detection of cephalexin and ceftriaxone. Sens Actuators B Chem 281:689–697. https://doi.org/10.1016/j.snb.2018.11.003
20. Chullasat K, Nurerk P, Kanatharana P, Davis F, Bunkoed O (2018) A facile optosensing protocol based on molecularly imprinted polymer coated on CdTe quantum dots for highly sensitive and selective amoxicillin detection. Sens Actuators B Chem 254:255–263. https://doi.org/10.1016/j.snb.2017.07.062
21. Wei X, Yu M, Li C, Gong X, Qin F, Wang Z (2018) Magnetic nanoparticles coated with a molecularly imprinted polymer doped with manganese-doped ZnS quantum dots for the determination of 2,4,6-trichlorophenol. Microchim Acta 185(4):208. https://doi.org/10.1007/s00604-018-2742-5
22. Henna TK, Pramod K (2020) Graphene quantum dots redefine nanobiomedicine. Mater Sci Eng C 110:110651. https://doi.org/10.1016/j.msec.2020.110651
23. Mahmoudi-Moghaddam H, Tajik S, Beitollahi H (2019) A new electrochemical DNA biosensor based on modified carbon paste electrode using graphene quantum dots and ionic liquid for determination of topotecan. Microchem J 150:104085. https://doi.org/10.1016/j.microc.2019.104085
24. Li Y, Xiao Y, Tao Q, Yu M, Zheng L, Yang S, Ding G, Dong H, Xie X (2021) Selective coordination and localized polarization in graphene quantum dots: Detection of fluoride anions using ultra-low-field NMR relaxometry. Chin Chem Lett 32(12):3921–3926. https://doi.org/10.1016/j.cclet.2021.05.014
25. Nesakumar N, Srinivasan S, Alwarappan S (2022) Graphene quantum dots: Synthesis, properties, and applications to the development of optical and electrochemical sensors for chemical sensing. Microchim Acta 189(7):258. https://doi.org/10.1007/s00604-022-05353-y
26. Dong Y, Shao J, Chen C, Li H, Wang R, Chi Y, Lin X, Chen G (2012) Blue luminescent graphene quantum dots and graphene oxide prepared by tuning the carbonization degree of citric acid. Carbon 50(12):4738–4743. https://doi.org/10.1016/j.carbon.2012.06.002
27. Fu R-w, Li Z-h, Liang Y-r, Li F, Xu F, Wu D-c (2011) Hierarchical porous carbons: design, preparation, and performance in energy storage. New Carbon Mater 26(3):171–179. https://doi.org/10.1016/S1872-5805(11)60074-7
28. Ni J, Zhao T, Tang L, Qiu P, Jiang W, Wang L, Xu P, Luo W (2020) Solution-phase synthesis of ordered mesoporous carbon as resonant-gravimetric sensing material for room-temperature H_2S detection. Chin Chem Lett 31(6):1680–1685. https://doi.org/10.1016/j.cclet.2019.11.025
29. Fan G, Ge J, Kim H-Y, Ding B, Al-Deyab SS, El-Newehy M, Yu J (2015) Hierarchical porous carbon nanofibrous membranes with an enhanced shape memory property for effective adsorption of proteins. RSC Adv 5(79):64318–64325. https://doi.org/10.1039/C5RA11627A

30. Xu Z, Li L, Li K, Chen M-L, Tu J, Chen W, Zhu S-H, Cheng Y-H (2021) Peroxidase-mimetic activity of a nanozyme with uniformly dispersed Fe_3O_4 NPs supported by mesoporous graphitized carbon for determination of glucose. Microchim Acta 188(12):421. https://doi.org/10.1007/s00604-021-05035-1
31. Wu Y, Cao J-P, Zhuang Q-Q, Zhao X-Y, Zhou Z, Wei Y-L, Zhao M, Bai H-C (2021) Biomass-derived three-dimensional hierarchical porous carbon network for symmetric supercapacitors with ultra-high energy density in ionic liquid electrolyte. Electrochim Acta 371:137825. https://doi.org/10.1016/j.electacta.2021.137825

Electronic Supporting Material

for the Microchimica Acta publication entitled

A composite adsorbent of graphene quantum dots, mesoporous carbon and molecularly imprinted polymer to extract nonsteroidal anti-inflammatory drugs in milk

Naphatsakorn Orachorn and Opas Bunkoed*

Center of Excellence for Innovation in Chemistry, Division of Physical Science, Faculty of Science, Prince of Songkla University, Hat Yai, Songkhla 90110, Thailand

Corresponding author**:** opas.b@psu.ac.th

Synthesis of silica-coated magnetite nanoparticles (Fe_3O_4-SiO_2)

In a three-necked flask, 3.0 g of $FeCl_2 \cdot 4H_2O$ and 9.0 g of $FeCl_3 \cdot 6H_2O$ were mixed with 160 mL of deionized water and heated to 80 °C under N_2 gas. Ammonium hydroxide (20 mL) was then rapidly added into the mixture solution and refluxed for 1 h. The synthesized Fe_3O_4 nanoparticles were separated with an external magnet, washed with 40 mL of deionized water, and dried in an oven at 80 °C for 12 h. The dried, synthesized Fe_3O_4 nanoparticles were coated with silica via a sol-gel technique. A solution was prepared of 100 mL of deionized water, 200 mL of ethanol and 4.0 mL of ammonium hydroxide. Into this solution, 4.0 g of Fe_3O_4 nanoparticles were introduced and continuously stirred at 40 °C for 30 min. Then, 4.0 mL of tetraethyl orthosilicate were injected into the mixed solution and continuously stirred for 12 h. The silica-coated nanoparticles were isolated from the solution using a magnet, washed with ethanol and deionized water, and dried at 80 °C for 6 h to obtain Fe_3O_4-SiO_2 nanoparticles.

Characterization of the magnetic composite adsorbent

The spectrum of Fe_3O_4-SiO_2 (**Fig. S1a**) presented significant peaks at 585 and 1080 cm^{-1} that were attributed to Fe-O-Fe stretching of magnetite and Si-O-Si stretching of silica, respectively. In the FTIR spectrum of GQDs (**Fig. S1b**), an absorption band at approximately 3416 cm^{-1} was attributed to O-H stretching, and peaks at 2940, 1387 and 1581 cm^{-1} were respectively derived from *C*-H stretching, *C*-H bending and *C*=C stretching of graphene sheet. The spectrum of MPC (**Fig. S1c**) presented the same characteristic peaks at the same wavenumbers as the spectrum of GQDs with an additional peak at 1270 cm^{-1} that corresponded to C-O stretching. Flurbiprofen (**Fig. S1d**), diflunisal (**Fig. S1e**) and mefenamic acid (**Fig. S1f**) produced three strong peaks between 1800 and 1100 cm^{-1} in the spectrum of the GQDs/Fe_3O_4-SiO_2/MPC/MIP adsorbent before removal of the templates (**Fig. S1g**). The spectrum of GQDs/Fe_3O_4-SiO_2/MPC/MIP indicated that the polymerization of the MIP was complete and included the three templates. After the removal of the templates from the MIP, the peaks

attributed to flurbiprofen, diflunisal and mefenamic acid were no longer present in the spectrum (**Fig. S1h**). In addition, absorption peaks were present at the same wavenumbers found in the spectra of Fe_3O_4-SiO_2, GQDs and MPC. In the spectrum of GQDs/Fe_3O_4-SiO_2/MPC/MIP, a peak at 1051 cm^{-1} was due to Si-O-Si asymmetric stretching, and peaks at 780 and 460 cm^{-1} corresponded to the Si-O vibration band of the silica layer. Moreover, the spectrum of GQDs/Fe_3O_4-SiO_2/MPC/MIP after the removal of the templates was not significantly different from the spectrum of GQDs/Fe_3O_4-SiO_2/MPC/NIP (**Fig. S1i**). These results confirmed that the GQDs/Fe_3O_4-SiO_2/MPC/MIP adsorbent was successfully fabricated.

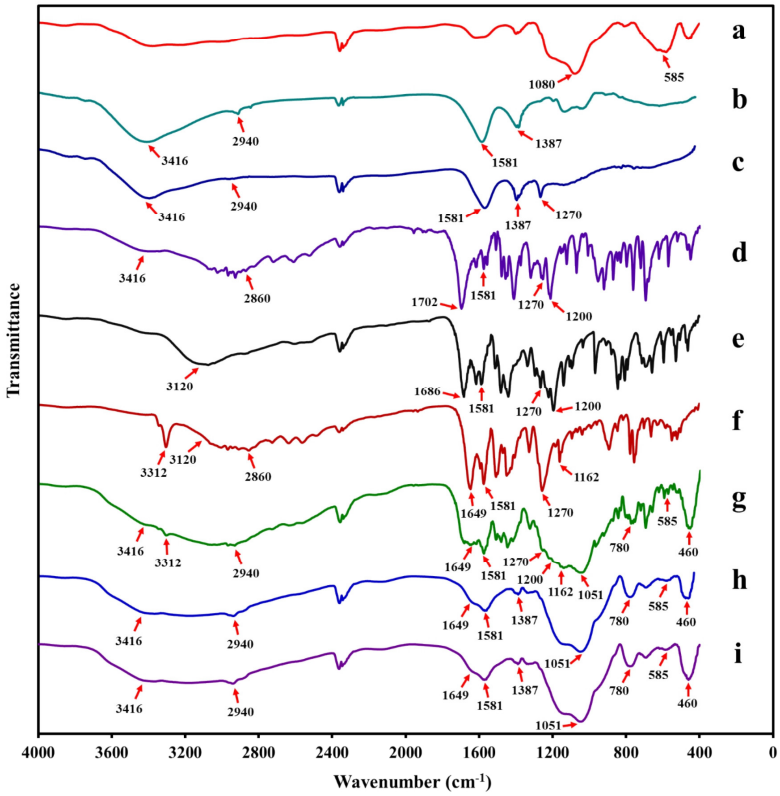

Fig. S1 FTIR spectra are of silica-coated magnetite nanoparticles (Fe_3O_4-SiO_2) (a), graphene quantum dots (GQDs) (b), mesoporous carbon (MPC) (c), flurbiprofen (d), diflunisal (e), mefenamic acid (f), GQDs/Fe_3O_4-SiO_2/MPC/MIP with templates (g), GQDs/Fe_3O_4-SiO_2/MPC/MIP without templates (h) and GQDs/Fe_3O_4-SiO_2/MPC/NIP (i).

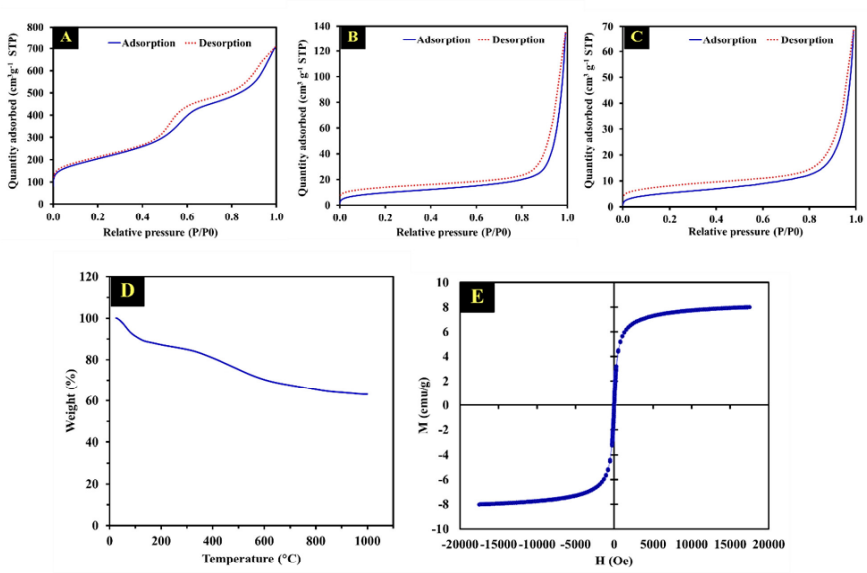

Fig. S2 The adsorption and desorption isotherms are for mesoporous carbon (MPC) (A), the GQDs/Fe_3O_4-SiO_2/MPC/MIP adsorbent (B), the GQDs/Fe_3O_4-SiO_2/MPC/NIP adsorbent (C), the thermogravimetric analysis curve (D) and vibrating sample magnetometer curve (E) were produced by the GQDs/Fe_3O_4-SiO_2/MPC/MIP adsorbent

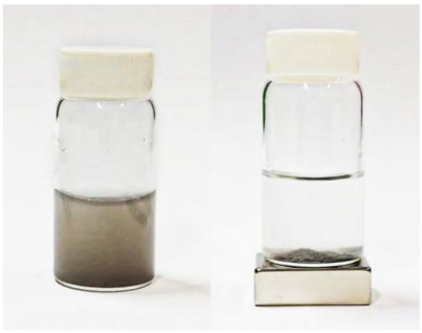

Fig. S3 The photograph shows the dispersed GQDs/Fe_3O_4-SiO_2/MPC/MIP adsorbent and the adsorbent isolated from the solution by a magnet.

Effect of amount of adsorbent

The amount of adsorbent used in the D-MSPE extraction process could influence the extraction of the NSAIDs. The dosage of the adsorbent was varied at 0.050, 0.075, 0.10, 0.25 and 0.50 g. Extraction recoveries increased with increments of adsorbent dose from 0.050 to 0.10 g, and remained almost constant to 0.50 g (**Fig. S4**). The dosage of 0.10 g was selected as the smallest amount of adsorbent that produced the highest recoveries of the target molecules.

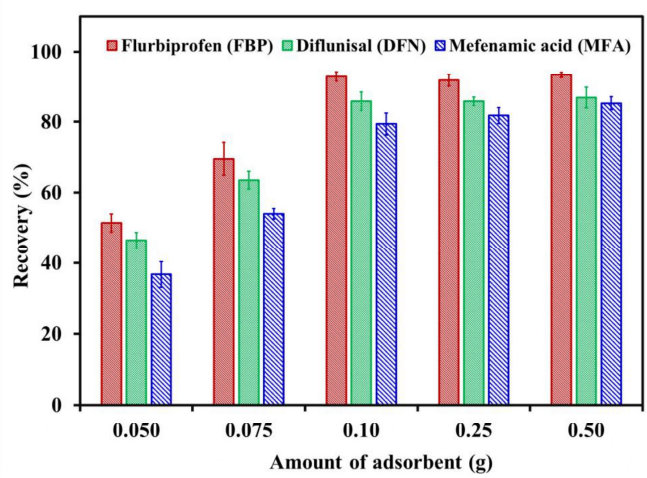

Fig. S4 Effect of adsorbent dosage on the recoveries of three nonsteroidal anti-inflammatory drugs extracted by dispersive magnetic solid-phase extraction with a GQDs/Fe_3O_4-SiO_2/MPC/MIP adsorbent (n=3)

Effect of amount of MPC

The amount of MPC incorporated into the composite adsorbent was optimized to improve the binding ability of the adsorbent toward the target NSAIDs. The effect of MPC was investigated at loadings of 3.0, 5.0, 7.0, 10.0 and 15.0 mg. The MPC loading that achieved the highest extraction recovery was 10.0 mg (**Fig. S5**). Lower recoveries were obtained at 3.0, 5.0, and 7.0 mg of MPC because the number of accessible adsorption sites for the three NSAIDs

was low. The higher loading of 15.0 mg of MPC provided slightly lower recoveries because the imprinted recognition cavities that bind NSAIDs were blocked. Thus, 10.0 mg of MPC was used to fabricate the composite adsorbent.

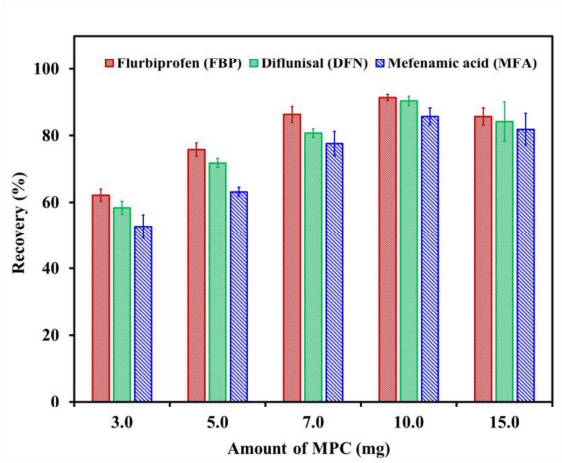

Fig. S5 Effect of MPC loading on the recoveries of three nonsteroidal anti-inflammatory drugs extracted using dispersive magnetic solid-phase extraction with a GQDs/Fe_3O_4-SiO_2/MPC/MIP adsorbent (n=3)

Effect of extraction time

The adsorption of target molecules requires an appropriate binding time to acquire the highest extraction efficiency. Here, extraction time was determined from 10 to 50 min. The shortest extraction time that produced the highest recoveries of the target NSAIDs was 30 min (**Fig. S6**). D-MSPE of the target NSAIDs was therefore performed with a 30 min adsorption period.

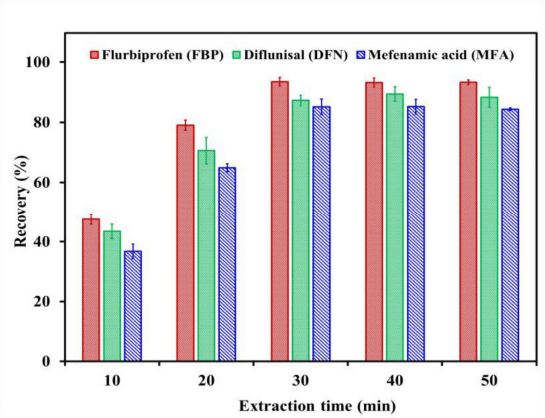

Fig. S6 Effect of extraction time on the recoveries of three nonsteroidal anti-inflammatory drugs extracted by dispersive magnetic solid-phase extraction with a GQDs/Fe_3O_4-SiO_2/MPC/MIP adsorbent (n=3)

Desorption condition

The selection of an appropriate desorption solvent is a significant factor for the elution of adsorbed analytes from an adsorbent. Desorption solvents of different polarities were evaluated in this study. The solvents were methanol, ethanol, acetonitrile, acetone and ethyl acetate. Methanol produced the highest extraction recoveries of all three target NSAIDs (**Fig. S7**). To avoid excessive solvent consumption, the volume of methanol used to desorb the adsorbed target molecules was then varied from 1.0 to 6.0 mL. The results showed that 4.0 mL of methanol was adequate for the elution of the three NSAIDs (**Fig. S8**). Desorption time was then optimized from 10 to 50 min. The target NSAIDs could be completely eluted from the adsorbent within 20 min (**Fig. S9**). Therefore, 20 min was selected as the optimal desorption times.

9

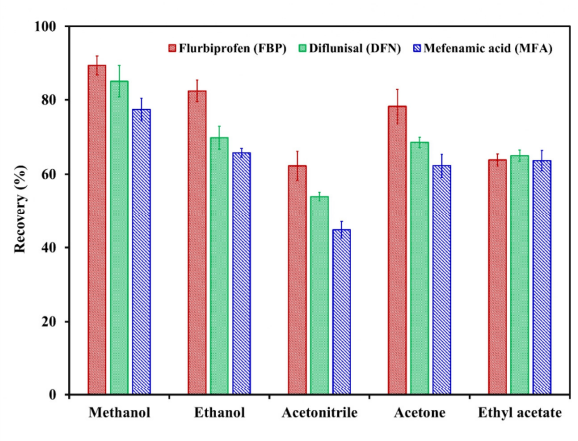

Fig. S7 Effect of desorption solvent type on the recoveries of three nonsteroidal anti-inflammatory drugs extracted using dispersive magnetic solid-phase extraction with a GQDs/Fe_3O_4-SiO_2/MPC/MIP adsorbent (n=3)

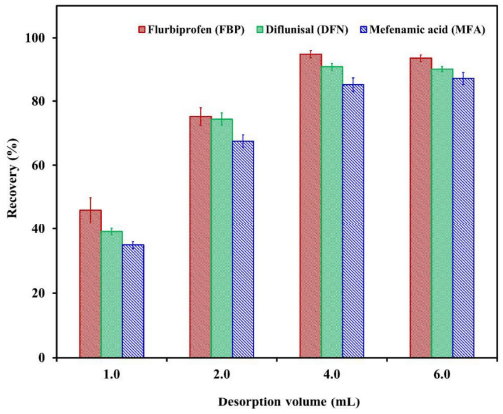

Fig. S8 Effect of desorption solvent volume on the recoveries of three nonsteroidal anti-inflammatory drugs extracted by dispersive magnetic solid-phase extraction with a GQDs/Fe_3O_4-SiO_2/MPC/MIP adsorbent (n=3)

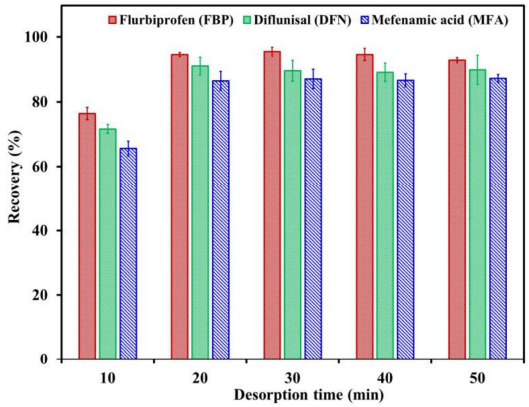

Fig. S9 Effect of desorption time on the recoveries of three nonsteroidal anti-inflammatory drugs extracted using dispersive magnetic solid-phase extraction with a GQDs/Fe_3O_4-SiO_2/MPC/MIP adsorbent (n=3)

Effect of sample solution stirring rate

During the adsorption step of D-MSPE, the mass transfer of target molecules from the sample to the adsorbent can be affected by the stirring rate. The stirring rate in this study was varied at 500, 1000, 1200 and 1500 rpm. Recoveries were higher at a stirring speed of 1000 rpm than 500 rpm and recoveries were lower at rates above 1000 rpm. At 500 rpm, recoveries were low because the stirring rate was insufficient to disperse the adsorbent throughout the sample solution. At 1200 and 1500 rpm, the adsorbent made strong contact with the wall of the container and was damaged. The highest extraction efficiency was achieved at a stirring rate of 1000 rpm (**Fig. S10**), which was the speed used to stir the sample solution during the D-MSPE of the analytes of interest.

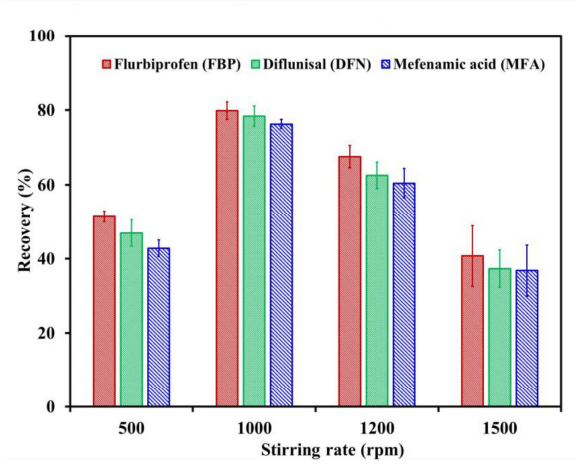

Fig. S10 Effect of sample solution stirring rate on the recoveries of three nonsteroidal anti-inflammatory drugs extracted using dispersive magnetic solid-phase extraction with a GQDs/Fe_3O_4-SiO_2/MPC/MIP adsorbent (n=3)

Effect of sample volume

The effect of sample volume was a significant parameter that could improve the enrichment factor and extraction efficiency. The volume of the spiked sample was examined from 5.0 to 20.0 mL. The results showed that sample volumes of 5.0 mL and 10.0 mL both provided extraction recoveries above 80 %, but the enrichment factor was higher at 10.0 mL than at 5.0 mL (**Fig. S11**). Extraction recoveries decreased when the sample volume was higher than 10.0 mL since the amount of adsorbent in dispersion was insufficient to adsorb the target analytes. Thus, the optimal sample volume was 10.0 mL for the extraction of target NSAIDs with the composite adsorbent.

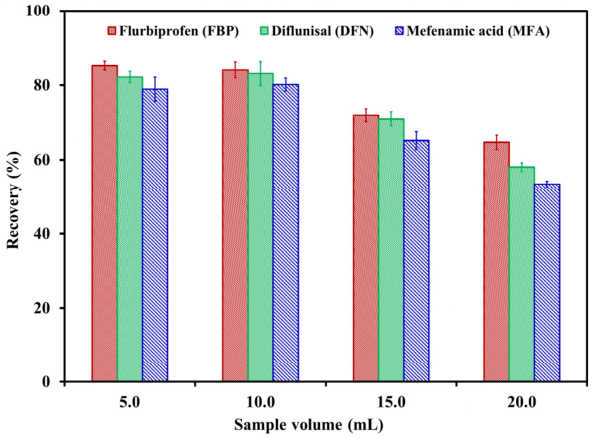

Fig. S11 Effect of sample volume on the recoveries of three nonsteroidal anti-inflammatory drugs extracted by dispersive magnetic solid-phase extraction with a GQDs/Fe_3O_4-SiO_2/MPC/MIP adsorbent (n=3)

Effect of sample pH

Sample solution pH can affect the stability of an adsorbent and its interactions with the analytes. In this work, sample solution pH was adjusted with HCl and NaOH to 3.0, 5.0, 7.0, 9.0 and 11.0. Sample solution pH from 5.0 to 9.0 produced good recoveries, but pH 3.0 and 11.0 produced low recoveries (**Fig. S12**). At a sample solution pH of 3.0, recoveries were low because the structure of the three NSAIDs became cationic in the strong acidic condition, reducing binding between the NSAIDs and the adsorbent. At a sample solution pH of 11.0, the NSAIDs were deprotonated to anionic form, and the silica component of the adsorbent was not stable in the elevated basic condition, which affected adsorption. However, the pH of milk is normally in the range of 6.0 to 8.0, and thus the sample solution pH did not need to be adjusted.

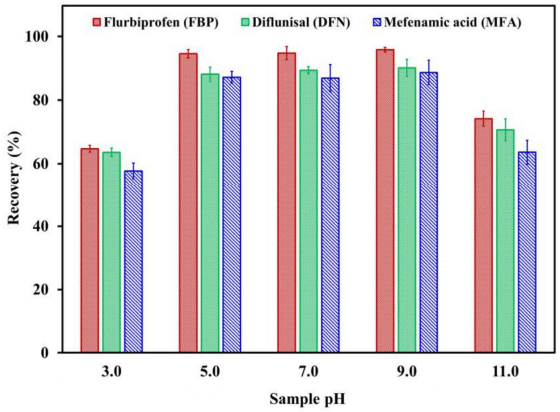

Fig. S12 Effect of sample solution pH on the recoveries of three nonsteroidal anti-inflammatory drugs extracted by dispersive magnetic solid-phase extraction with a GQDs/Fe_3O_4-SiO_2/MPC/MIP adsorbent (n=3)

Effect of ionic strength

The ionic strength of the sample can also influence the mass transfer of analytes to the adsorbent during the adsorption process. In this work, the ionic strength of the sample was boosted with sodium chloride (NaCl) at concentrations of 0.0, 1.0, 2.0, 5.0 and 10.0 %w/v. Extraction recoveries were not significantly different at 0.0 and 1.0 %w/v NaCl but were lower with additions of NaCl at 2.0, 5.0 and 10.0 %w/v (**Fig. S13**). The reduced extraction efficiency was due to the increased the viscosity of the sample solution which disturbed the adsorption between the NSAIDs and the adsorbent. Therefore, the extraction was performed without adding salt to the sample.

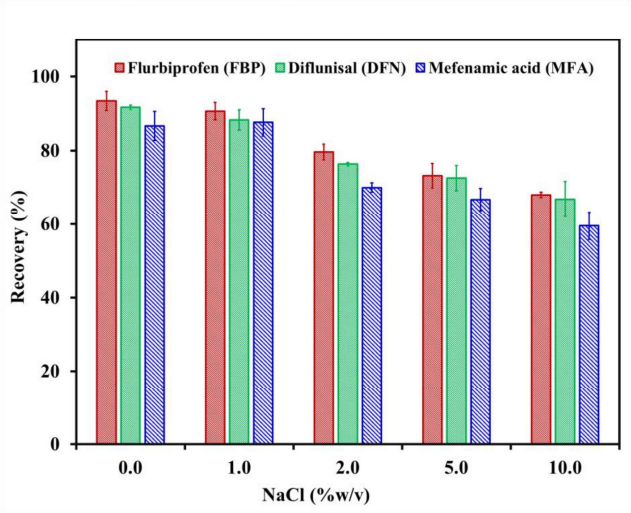

Fig. S13 Effect of sample solution ionic strength on the recoveries of three nonsteroidal anti-inflammatory drugs extracted using dispersive magnetic solid-phase extraction with a GQDs/Fe_3O_4-SiO_2/MPC/MIP adsorbent (n=3)

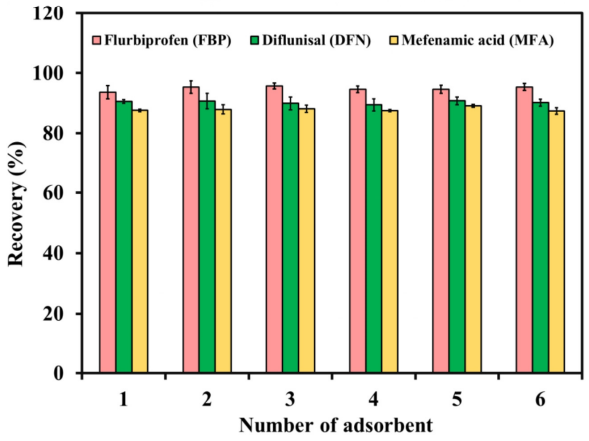

Fig. S14 The reproducibility of the developed GQDs/Fe_3O_4-SiO_2/MPC/MIP adsorbent for the extraction of nonsteroidal anti-inflammatory drugs (n=3)

15

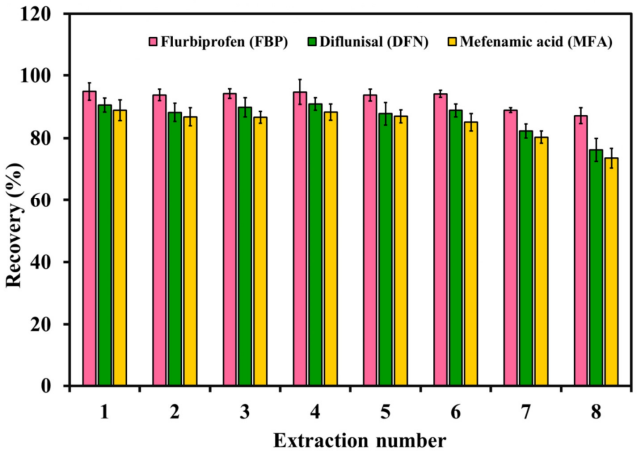

Fig. S15 The reusability of the developed composite GQDs/Fe_3O_4-SiO_2/MPC/MIP adsorbent was evaluated by repeated extractions of three nonsteroidal anti-inflammatory drugs (n=3).

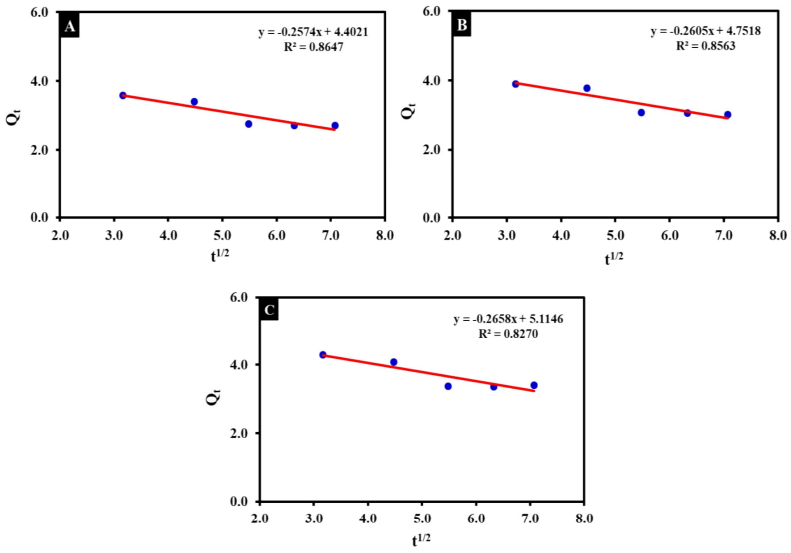

Fig. S16 The intraparticle diffusion models of flurbiprofen (A), diflunisal (B) and mefenamic acid (C) adsorbed on the composite GQDs/Fe_3O_4-SiO_2/MPC/MIP adsorbent.

17

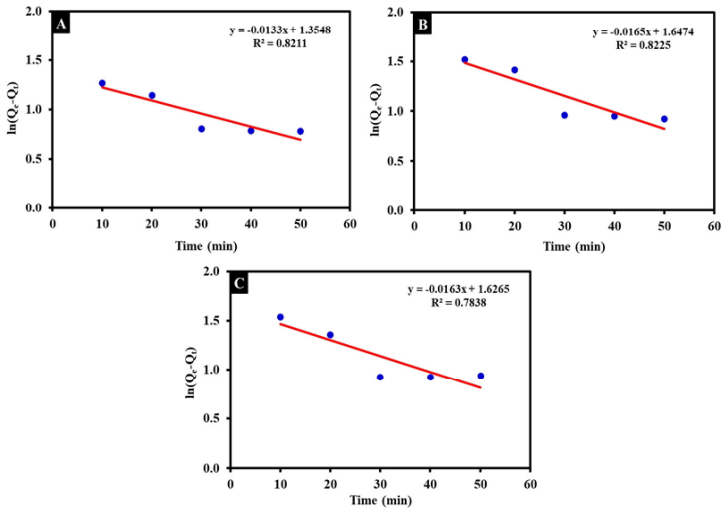

Fig. S17 The pseudo-first-order models of flurbiprofen (A), diflunisal (B) and mefenamic acid (C) adsorbed on the composite GQDs/Fe_3O_4-SiO_2/MPC/MIP adsorbent.

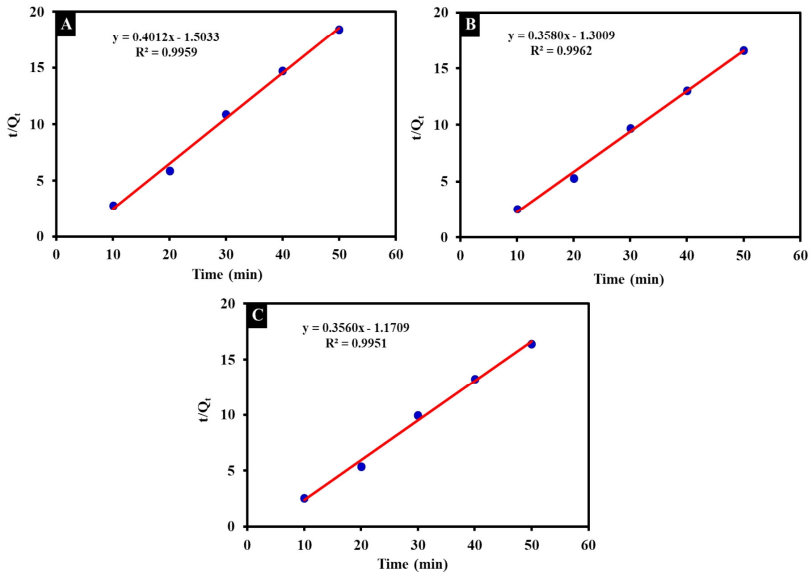

Fig. S18 The pseudo-second-order models of flurbiprofen (A), diflunisal (B) and mefenamic acid (C) adsorbed on the composite GQDs/Fe_3O_4-SiO_2/MPC/MIP adsorbent.

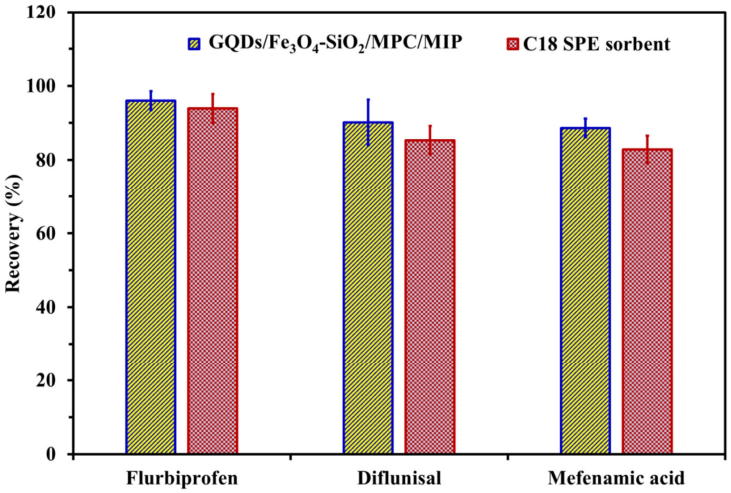

Fig. S19 The chart compares the extraction recoveries of three nonsteroidal anti-inflammatory drugs achieved with a developed GQDs/Fe_3O_4-SiO_2/MPC/MIP adsorbent and a C18 SPE sorbent (n=3).

Table S1 Optimization of dispersive magnetic-solid phase extraction (D-MSPE) using the GQDs/Fe_3O_4-SiO_2/MPC/MIP adsorbent for the extraction and determination of NSAIDs

Optimization parameter	Optimization value	Optimum condition
Amount of adsorbent (g)	0.050, 0.075, 0.10, 0.25, 0.50	0.10
Amount of MPC (mg)	3.0, 5.0, 7.0, 10.0, 15.0	10.0
Extraction time (min)	10, 20, 30, 40, 50	30
Desorption solvent	Methanol, ethanol, acetonitrile, acetone, ethyl acetate	Methanol
Volume of desorption solvent (mL)	1.0, 2.0, 4.0, 6.0	4.0
Desorption time (min)	10, 20, 30, 40, 50	20
Sample stirring rate (rpm)	500, 1000, 1200, 1500	1000
Sample volume (mL)	5.0, 10.0, 15.0, 20.0	10.0
Sample pH	3.0, 5.0, 7.0, 9.0, 11.0	5.0-9.0
Ionic strength (% w/v)	0.0, 1.0, 2.0, 5.0, 10.0	0.0

Table S2 The kinetics equations and linear plots of three adsorption kinetics models

Kinetics model	Equation	Linear plot
Intraparticle diffusion	$Q_t = K_1 t^{1/2} + c$	Q_t Vs. $t^{1/2}$
Pseudo-first-order	$In(Q_e - Q_t) = InQ_e - K_2 t$	$In(Q_e - Q_t)$ Vs. t
Pseudo-second-order	$\frac{t}{Q_t} = \frac{1}{K_3 Q^2_e} + \frac{t}{Q_e}$	$\frac{t}{Q_t}$ Vs. t

Q_t (μg g^{-1}) = the adsorption capacity at time t; K_1, K_2 and K_3 (min^{-1}) are rate constants of the intraparticle diffusion, pseudo-first-order and pseudo-second-order models, respectively; c is the intercept.

Table S3 The analytical performances of the developed method are compared with the performances of reported methods of extracting nonsteroidal anti-inflammatory drugs.

Analytical method	Sample preparation method	Analyte	Sample matrix	Sample volume (mL)	LOD (μg L^{-1} or μg kg^{-1})	Recovery (%)	RSD (%)	Reference
HPLC-MS/MS	LLME	MFA, DIC, KTP, FBP	Bovine milk	5	0.01-0.03	96-107	< 7	[S1]
HPLC-UV	Co_3O_4@GO (HF-SPME)	MFA, IND, DIC, IBP	Human urine	10	0.18-1.1	93-102	3.2-10.1	[S2]
HPLC-UV	SPE-SUPRASF	DIC, MFA	Urine and water	30	0.7-4.0	90-104	4.9-7.2	[S3]
HPLC-UV	Co@CNTs (MSPE)	FBP, KTP	Human serum	200	0.0006-0.0007	87-97	0.8-6.6	[S4]
HPLC-UV	MOFs@GA (SPE)	NPX, FBN, CPF, FBP, IBP	Tap and river water	100	0.01-0.10	81-107	2.5-8.7	[S5]
HPLC-UV	MICOF@SiO_2 (SPE)	KTP, NPX, FBP, IND, DIC, IBP	River and lake water	10	0.2-1.4	77-112	4.1-9.4	[S6]
HPLC-DAD	Fe_3O_4@TCVA (MSPE)	DIC, IBP, MFA	Water and urine	50	0.014-0.11	80-120	0.5-9.9	[S7]
HPLC-DAD	SOE-SHS-LLME	KTP, ET, FBP, IBP	Human urine, saliva and milk	-	40-180	96-109	0.9-7.7	[S8]
HPLC-DAD	UAE-SPE	AMT, ATN, CMT, DTZ, MFA, RNT	Freshwater sediment	-	15,000-58,500	70-125	1.6-15.8	[S9]
HPLC-DAD	Oasis HLB (SPE)	KTP, DFN, FNP, OXP, FBP, DIC, IND, IBP, PBZ, MFA, MCA	Wastewater	100	3-15	73-94	1.7-9.3	[S10]
HPLC-DAD	Poly(GMA-*co*-EDMA) monolith MOF functionalized (MSCME)	KTP, IBP, FBP	Human urine	0.2	0.2-6.2	71-78	0.8-14.0	[S11]

HPLC-DAD	Poly(GMA-*co*-EDMA-*co*-o-SWNHs) monolith (MSCME)	NPX, FBF, FBP, IBP	Human urine	0.6	0.1-10	81-106	3.5-11.8	[S12]
HPLC-UV	Fe_3O_4/C (MSPE)	IND, KTP, FBP, IBP	Plasma, urine and lake	25	0.25-0.50	90-108	2.9-7.2	[S13]
UPLC-PDA	CF@UiO-66-NH_2 (SPE)	KTP, NPX, FBP, DIC, IBP	Shrimp and fish muscle tissues	20	0.12-3.5	73-117	0.7-9.8	[S14]
UPLC-DAD	UiO-66@FGR (BSE)	KTP, FBP, IBP, NPX, DIC	Sheep muscle, chicken wing and milk	20	0.92-5.13	81-117	1.4-6.5	[S15]
UPLC/MS-MS	TiONts-CTAB (SPE)	KTP, PIR, DFN, CEL	Environmental water	25	3.0-4.5	81-98	0.4-5.7	[S16]
HPLC-UV	DSBC (SPE)	KTP, CEL, MFA	Environmental water	30	1.0-2.0	87-101	4.2-8.2	[S17]
HPLC-DAD	GQDs/Fe_3O_4-SiO_2/MPC/MIP (D-MSPE)	FBP, DFN, MFA	Bovine milk	10	0.5-1.0	81-94	0.5-6.4	This work

LLME = Liquid-liquid microextraction; Co_3O_4@GO = Nanocubic Co_3O_4-coated graphene oxide; HF-SPME = Hollow fiber solid-phase microextraction; SPE = Solid-phase extraction; SUPRASF = Supramolecular solvent formation; Co@CNTs = Magnetic carbon nanotubes with encapsulated Co nanoparticles; MSPE = Magnetic solid-phase extraction; MOFs@GA = Graphene hybrid aerogel-supported metal–organic frameworks; MICOF@SiO_2 = Molecular imprinted covalent organic framework nanocomposite; TCVA = Triethyl-(4-vinylbenzyl)ammonium chloride and 4-vinylbenzeneboronic acid; SOE = Salting-out extraction; SHS = Switchable-hydrophilicity solvent; UAE = Ultrasonic-assisted extraction; HLB = Hydrophilic–lipophilic balance; Poly(GMA-*co*-EDMA) = (glycidyl methacrylate)-*co*-(ethylene glycol dimethacrylate) polymer; MSCME = Monolithic spin column microextraction; o-SWNHs = oxidized-single-walled carbon nanohorns; Fe_3O_4/C = Magnetic carbon;

UPLC = Ultra-high performance liquid chromatography; CF@UiO-66-NH_2 = Zirconium-based metal-organic framework UiO-66-NH_2 modified cotton fiber; UiO-66@FGR = Zirconium-based metal-organic framework UiO-66 coated frosted glass rod; BSE = Bar sorptive extraction; TiONts-CTAB = Titanate nanotubes modified with cetyltrimethylammonium bromide; DSBC = Biochar produced from date stones; MFA = Mefenamic acid; DIC = Diclofenac; KTP = Ketoprofen; FBP = Flurbiprofen; IND = Indomethacin; IBP = Ibuprofen; NPX = Naproxen; FBN = Felbinac; CPF = Carprofen; ET = Etodolac; AMT = Amitriptyline; ATN = Atenolol; CMT = Cimetidine; DTZ = Diltiazem; RNT = Ranitidine; DFN = Diflunisal; FNP = Fenoprofen; OXP = Oxaprozin; PBZ = Phenyl butazone; MCA = Meclofenamic acid; FBF = Fenbufen; PIR = Piroxicam; CEL = Celecoxib

References

[S1] Shishov A, Nechaeva D, Bulatov A (2019) HPLC-MS/MS determination of non-steroidal anti-inflammatory drugs in bovine milk based on simultaneous deep eutectic solvents formation and its solidification. Microchem J 150:104080. https://doi.org/10.1016/j.microc.2019.104080

[S2] Darvishnejad F, Raoof JB, Ghani M (2021) In-situ synthesis of nanocubic cobalt oxide @ graphene oxide nanocomposite reinforced hollow fiber-solid phase microextraction for enrichment of non-steroidal anti-inflammatory drugs from human urine prior to their quantification via high-performance liquid chromatography-ultraviolet detection. J Chromatogr A 1641:461984. https://doi.org/10.1016/j.chroma.2021.461984

[S3] Rezaei F, Yamini Y, Moradi M, Ebrahimpour B (2013) Solid phase extraction as a cleanup step before microextraction of diclofenac and mefenamic acid using nanostructured solvent. Talanta 105:173-178. https://doi.org/10.1016/j.talanta.2012.11.035

[S4] Wu W, Lin F, Yang X, Wang B, Lu X, Chen Q, Ye F, Zhao S (2020) Facile synthesis of magnetic carbon nanotubes derived from ZIF-67 and application to magnetic solid-phase extraction of profens from human serum. Talanta 207:120284. https://doi.org/10.1016/j.talanta.2019.120284

[S5] Zhang X, Liang Q, Han Q, Wan W, Ding M (2016) Metal-organic frameworks@graphene hybrid aerogels for solid-phase extraction of non-steroidal anti-inflammatory drugs and selective enrichment of proteins. Analyst 141(13):4219-4226. https://doi.org/10.1039/C6AN00353B

[S6] Li W, Chen N, Zhu Y, Shou D, Zhi M, Zeng X (2019) A nanocomposite consisting of an amorphous seed and a molecularly imprinted covalent organic framework shell for extraction and HPLC determination of nonsteroidal anti-inflammatory drugs. Microchim Acta 186(2):76. https://doi.org/10.1007/s00604-018-3187-6

[S7] Li Y, Liao Y, Huang Y, Ye Z, Huang X (2019) Dual functional monomers modified magnetic adsorbent for the enrichment of non-steroidal anti-inflammatory drugs in water and urine samples. Talanta 201:496-502. https://doi.org/10.1016/j.talanta.2019.04.043

[S8] Hassan M, Alshana U (2019) Switchable-hydrophilicity solvent liquid-liquid microextraction of non-steroidal anti-inflammatory drugs from biological fluids prior to HPLC-DAD determination. J Pharm Biomed Anal 174:509-517. https://doi.org/10.1016/j.jpba.2019.06.023

[S9] Al-Khazrajy OSA, Boxall ABA (2017) Determination of pharmaceuticals in freshwater sediments using ultrasonic-assisted extraction with SPE clean-up and HPLC-DAD or LC-ESI-MS/MS detection. Anal Methods 9(28):4190-4200. https://doi.org/10.1039/C7AY00650K

[S10] Shaaban H, Górecki T (2011) High temperature-high efficiency liquid chromatography using sub-2μm coupled columns for the analysis of selected non-steroidal anti-inflammatory drugs and veterinary antibiotics in environmental samples. Anal Chim Acta 702(1):136-143. https://doi.org/10.1016/j.aca.2011.06.040

[S11] Giesbers M, Carrasco-Correa EJ, Simó-Alfonso EF, Herrero-Martínez JM (2019) Hybrid monoliths with metal-organic frameworks in spin columns for extraction of non-steroidal drugs prior to their quantitation by reversed-phase HPLC. Microchim Acta 186(12):759. https://doi.org/10.1007/s00604-019-3923-6

[S12] Fresco-Cala B, Cárdenas S, Herrero-Martínez JM (2017) Preparation of porous methacrylate monoliths with oxidized single-walled carbon nanohorns for the extraction of nonsteroidal anti-inflammatory drugs from urine samples. Microchim Acta 184(6):1863-1871. https://doi.org/10.1007/s00604-017-2203-6

[S13] Xu X, Feng X, Liu Z, Xue S, Zhang L (2021) 3D flower-liked Fe_3O_4/C for highly sensitive magnetic dispersive solid-phase extraction of four trace non-steroidal anti-inflammatory drugs. Microchim Acta 188(2):52. https://doi.org/10.1007/s00604-021-04708-1

[S14] Gao Y, Wang S, Zhang N, Xu X, Bao T (2021) Novel solid-phase extraction filter based on a zirconium meta-organic framework for determination of non-steroidal anti-inflammatory drugs residues. J Chromatogr A 1652:462349. https://doi.org/10.1016/j.chroma.2021.462349

[S15] Zhang N, Gao Y, Xu X, Bao T, Wang S (2021) Hydrophilic carboxyl supported immobilization of uio-66 for novel bar sorptive extraction of non-steroidal anti-inflammatory drugs in food samples. Food Chem 355:129623. https://doi.org/10.1016/j.foodchem.2021.129623

[S16] Hsen EB, Latrous L (2022) A SPE/LC-MS method for the simultaneous determination of non-steroidal anti-inflammatory drugs using TiO_2 nanotubes coated with cetyltrimethylammonium bromide as adsorbent. Chemistry Africa. https://doi.org/10.1007/s42250-022-00442-0

[S17] Bensghaier R, Tlili I, Latrous L, Megriche A (2022) A new date stone biochar for effective solid phase extraction of non-steroidal anti-inflammatory drugs in water. Chemistry Africa. https://doi.org/10.1007/s42250-022-00405-5

VITAE

Name Miss Naphatsakorn Orachorn

Student ID 6110230013

Education Attainment

Degree	Name of Institution	Year of Graduation
Bachelor of Science (Chemistry)	Prince of Songkla University	2018

Scholarship Awards during Enrolment

Naphatsakorn Orachorn was supported by Science Achievement Scholarship of Thailand (SAST). This work was supported by Division of Physical Science, Faculty of Science, Prince of Songkla University and Center of Excellence for Innovation in Chemistry (PERCH-CIC), Ministry of Higher Education, Science, Research and Innovation.

List of Publication

Orachorn, N., Bunkoed, O., A nanocomposite fluorescent probe of polyaniline, graphene oxide and quantum dots incorporated into highly selective polymer for lomefloxacin detection. ***Talanta*** 203 (2019), 261-268.

Orachorn, N., Bunkoed, O., Nanohybrid magnetic composite optosensing probes for the enrichment and ultra-trace detection of mafenide and sulfisoxazole. ***Talanta*** 228 (2021), 122237.

Orachorn, N., Klongklaew, P., Bunkoed, O., A composite of magnetic GOx@MOF incorporated in alginate hydrogel fiber adsorbent for the extraction of phthalate esters. ***Microchemical Journal*** 171 (2021), 106827.

Chaitong, N., Chansud, N., **Orachorn, N.**, Limbut, W., Bunkoed, O., A magnetic nanocomposite optosensing probe based on porous graphene, selective polymer and quantum dots for the detection of cefoperazone in milk. ***Microchemical Journal*** 171 (2021), 106838.

Orachorn, N., Bunkoed, O., A composite adsorbent of graphene quantum dots, mesoporous carbon, and molecularly imprinted polymer to extract nonsteroidal anti-inflammatory drugs in milk. ***Microchimica Acta*** 189(12) (2022), 446.

Oral Presentation

Orachorn, N., Bunkoed, O., A nanocomposite fluorescence probe of quantum dots incorporated into molecularly imprinted polymer for lomefloxacin detection, Japan-Thailand Joint Symposium on Advanced Nanomaterials and Devices for Electronics and Photonics (JT-AND 2020), 22-23 January 2020, Faculty of Science, Prince of Songkla University, Songkhla, Thailand.

Poster Presentation

Orachorn, N., Bunkoed, O., A nanocomposite fluorescence probe for highly sensitive and selective lomefloxacin detection, Pure and Applied Chemistry International Conference 2020 (PACCON 2020), 13-14 February 2020, IMPACT Forum, Muang Thong Thani, Nonthaburi, Thailand.

Orachorn, N., Bunkoed, O., Optosensor based on molecularly imprinted polymer composited with quantum dots and development of composite adsorbents for the determination of trace organic compounds in food and beverage, Thailand Research Expo 2022, 2-5 August 2022, Centara Grand & Bangkok Convention Centre at CentralWorld, Bangkok, Thailand